

IFIC

INSTITUT DE FÍSICA
CORPUSCULAR



VNIVERSITAT
DE VALÈNCIA



GENERALITAT
VALENCIANA

Conselleria de Educació, Cultura,
Universitats y Empleo

Gen-T

ASTRO PARTICLES
Astroparticles and High Energy Physics Group



MINISTERIO
DE CIENCIA, INNOVACIÓN
Y UNIVERSIDADES



Financiado por
la Unión Europea
NextGenerationEU



Plan de Recuperación,
Transformación y
Resiliencia



AGENCIA
ESTATAL DE
INVESTIGACIÓN

Valentina De Romeri
(IFIC Valencia - UV/CSIC)

COHERENT ELASTIC NEUTRINO-NUCLEUS SCATTERING



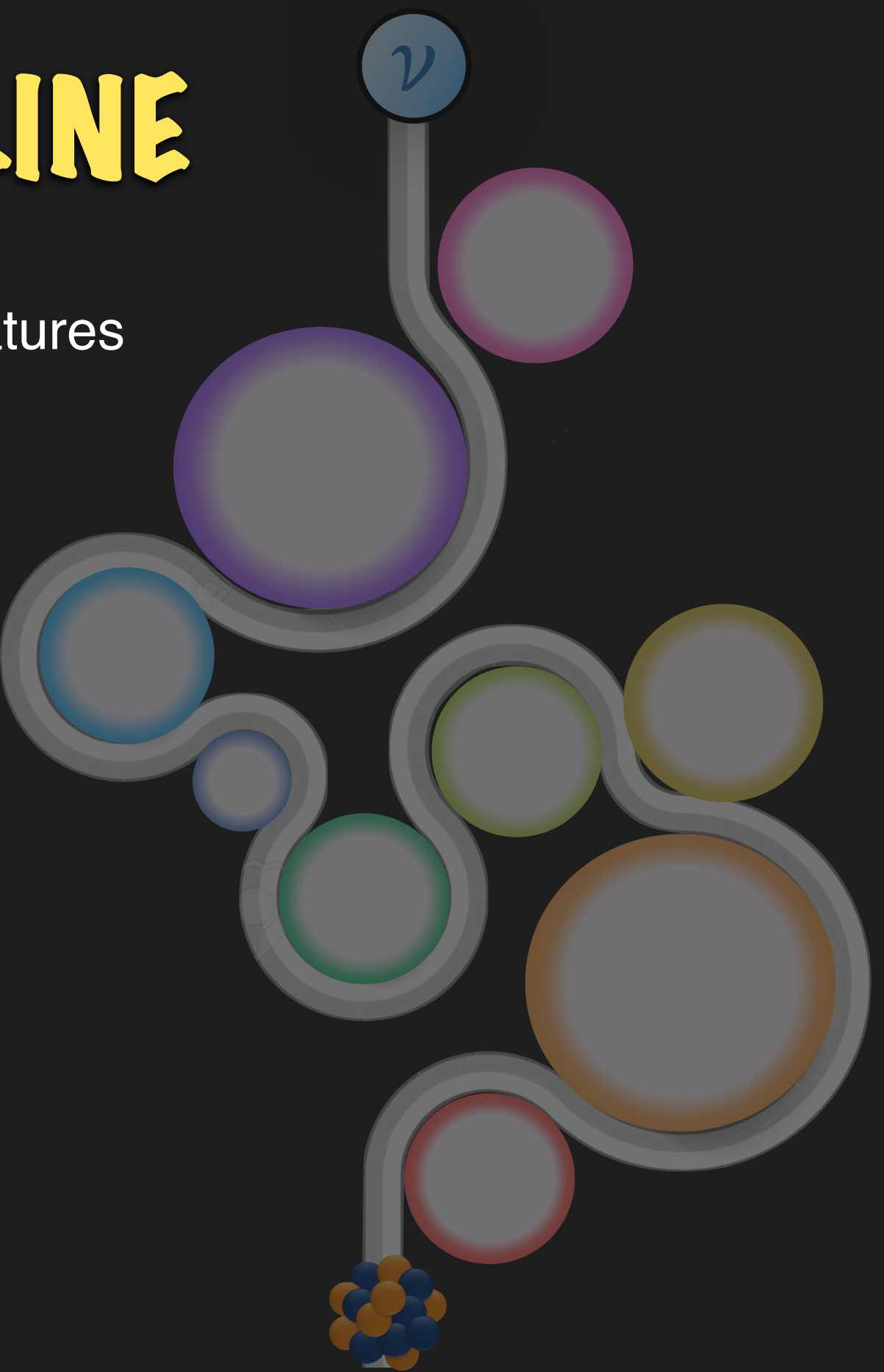
2nd EuCAPT Astroneutrino Theory Workshop
IEAP CTU in Prague
16-27 September 2024

A FEW USEFUL REFERENCES

- ▶ Papers/Reviews:
 - [Coherent elastic neutrino-nucleus scattering: Terrestrial and astrophysical applications](#) M. Abdullah et al.
 - [A view of Coherent Elastic Neutrino-Nucleus Scattering](#), M. Cadeddu, F. Dordei, C. Giunti
 - [Recent Probes of Standard and Non-standard Neutrino Physics With Nuclei](#), Papoulias, Kosmas, Kuno
 - [Probing new physics with coherent neutrino scattering off nuclei](#), Barranco, Miranda, Rashba
 - Walecka and Donnelly [https://doi.org/10.1016/0375-9474\(76\)90209-8](https://doi.org/10.1016/0375-9474(76)90209-8)
- ▶ Dark Matter Direct detection:
 - [The Theory of Direct Dark Matter Detection](#)
 - <https://arxiv.org/pdf/1904.07915>
 - <https://arxiv.org/pdf/1002.1912>
- ▶ Books:
 - Walecka Theoretical Nuclear and Subnuclear Physics, Oxford Stud.Nucl.Phys. 16 (1995) 1-610
 - Giunti & Kim: <https://oxford.universitypressscholarship.com/view/10.1093/acprof:oso/9780198508717.001.0001/acprof-9780198508717>
- ▶ Webpage:
 - http://www.nu.to.infn.it/Neutrino_Lectures
- ▶ Magnificent CEvNS workshop talks

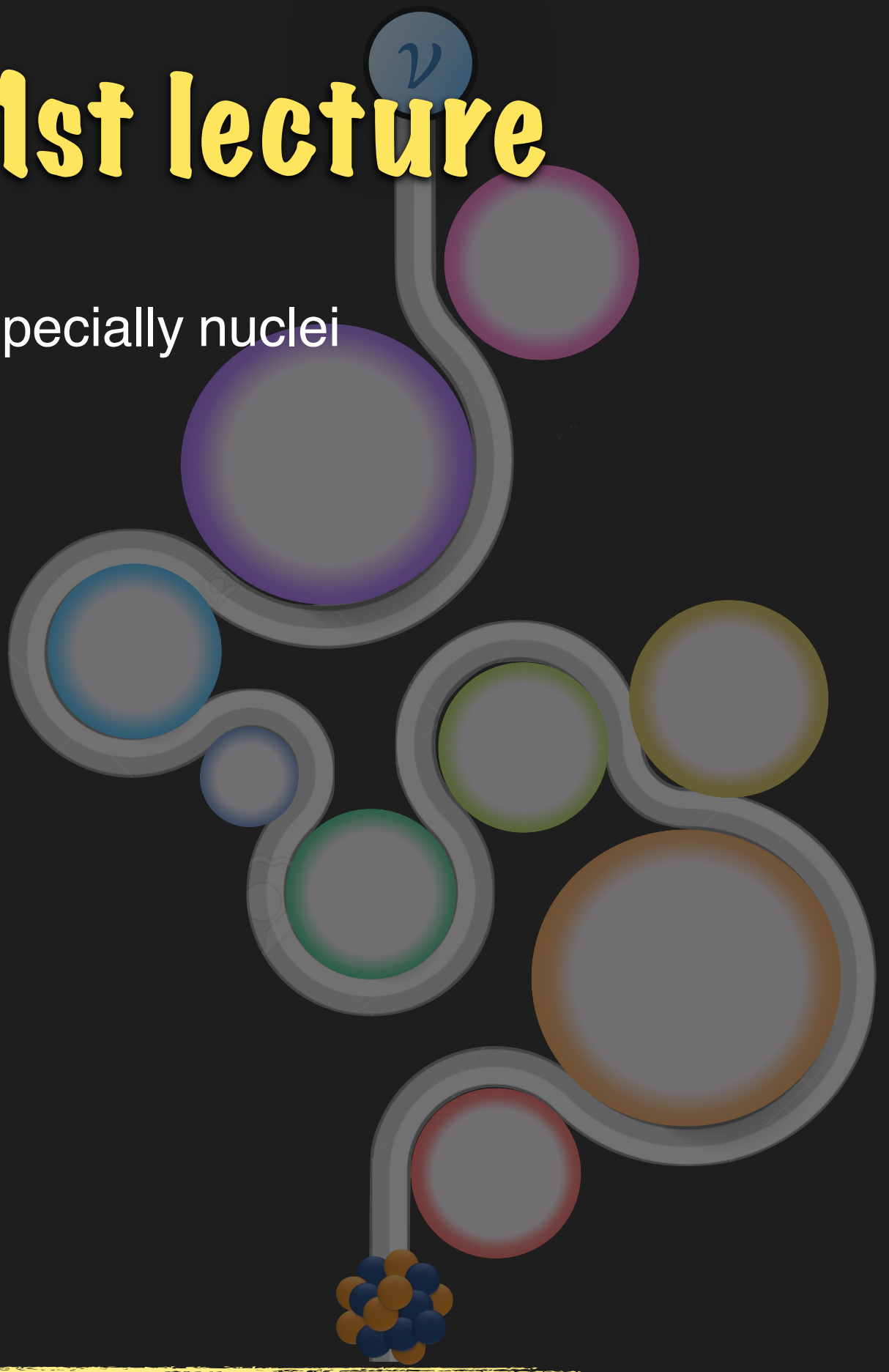
OUTLINE

1. Introduction to CE ν NS and main features
2. CE ν NS physics implications: SM
3. CE ν NS physics implications: BSM



OUTLINE - 1st lecture

- ▶ Neutrino interactions with matter, especially nuclei
- ▶ CEvNS: introduction and features
- ▶ CEvNS: neutrino sources
- ▶ CEvNS: experiments and detection
- ▶ CEvNS: observations
- ▶ CEvNS cross section in the SM

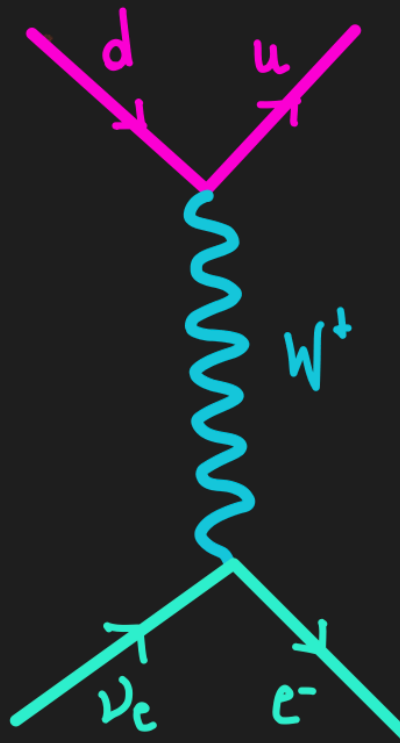


NEUTRINO INTERACTIONS WITH MATTER

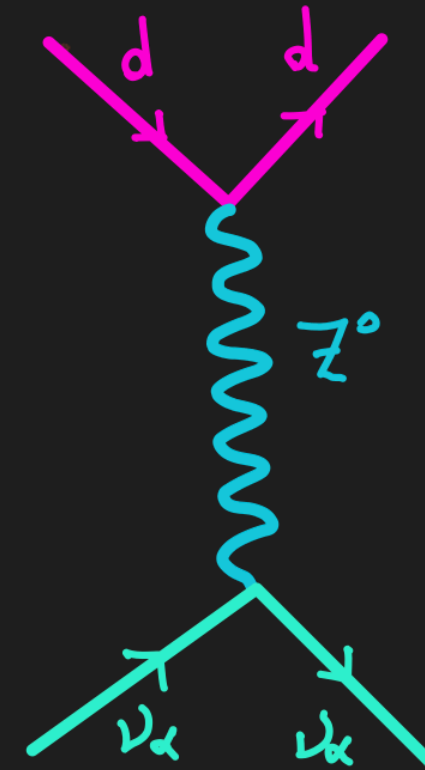
Neutrinos are elusive particles but not completely unfriendly

$$\mathcal{L}_{\text{SM}} = -\frac{g}{\sqrt{2}} \sum_{\alpha=e,\mu,\tau} \bar{\nu}_{\alpha L} \gamma^\mu \ell_{\alpha L} W_\mu - \frac{g}{2\cos\theta_W} \sum_{\alpha=e,\mu,\tau} \bar{\nu}_{\alpha L} \gamma^\mu \ell_{\alpha L} Z_\mu + h.c.$$

Charged Current (CC)



Neutral Current (NC)



Produces lepton with flavor corresponding to the neutrino flavor

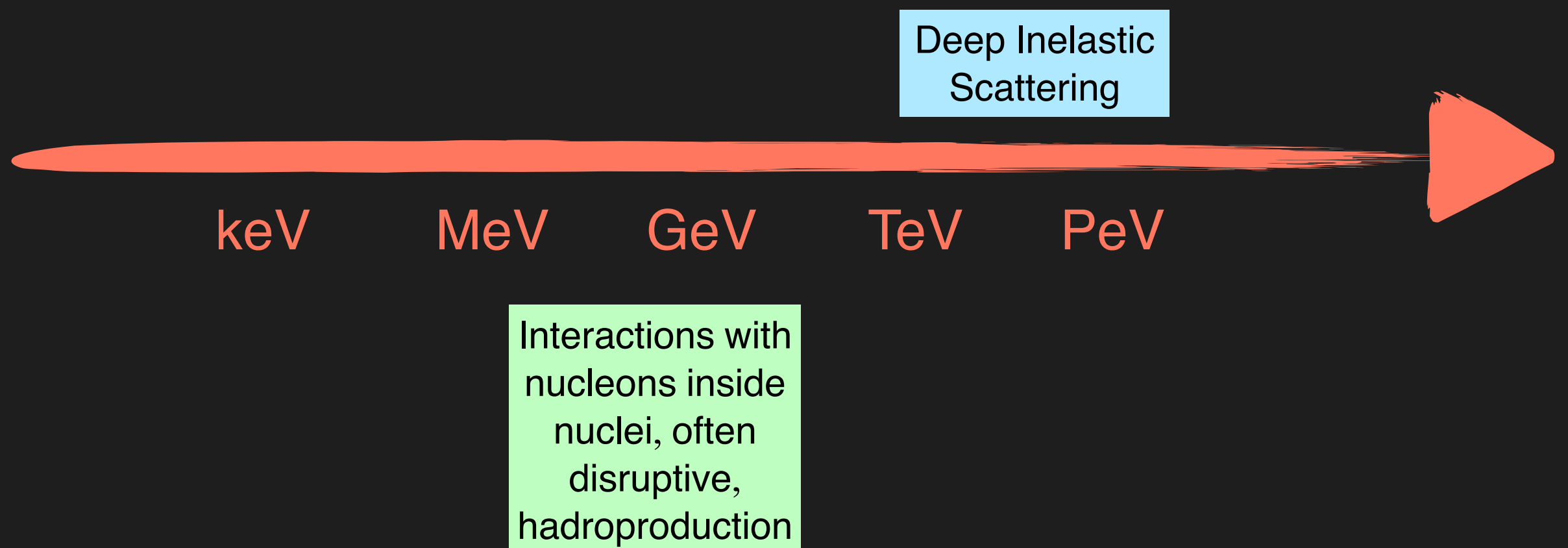
Flavor blind

NEUTRINO INTERACTIONS WITH NUCLEI



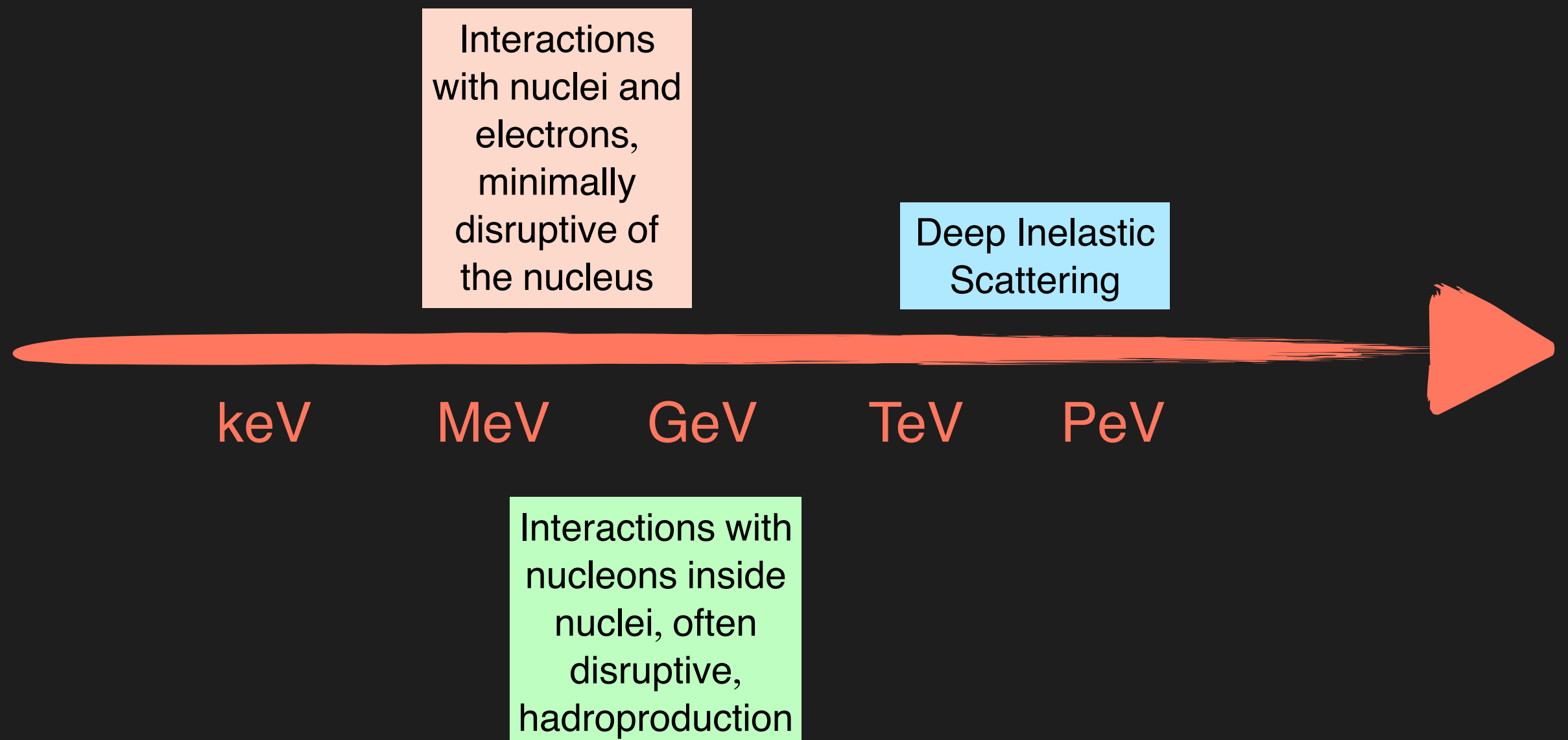
Adapted from Kate Scholberg

NEUTRINO INTERACTIONS WITH NUCLEI



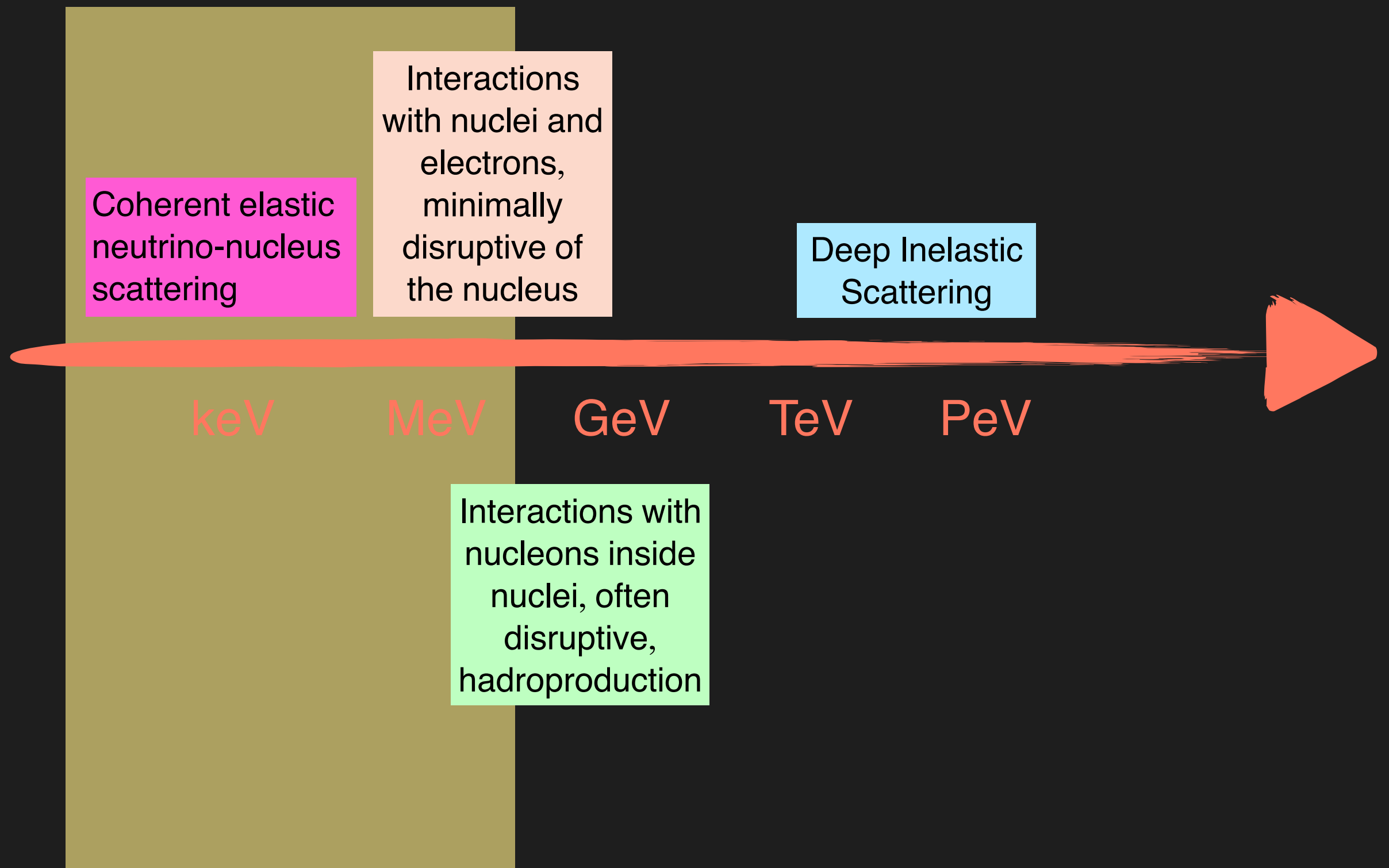
Adapted from Kate Scholberg

NEUTRINO INTERACTIONS WITH NUCLEI



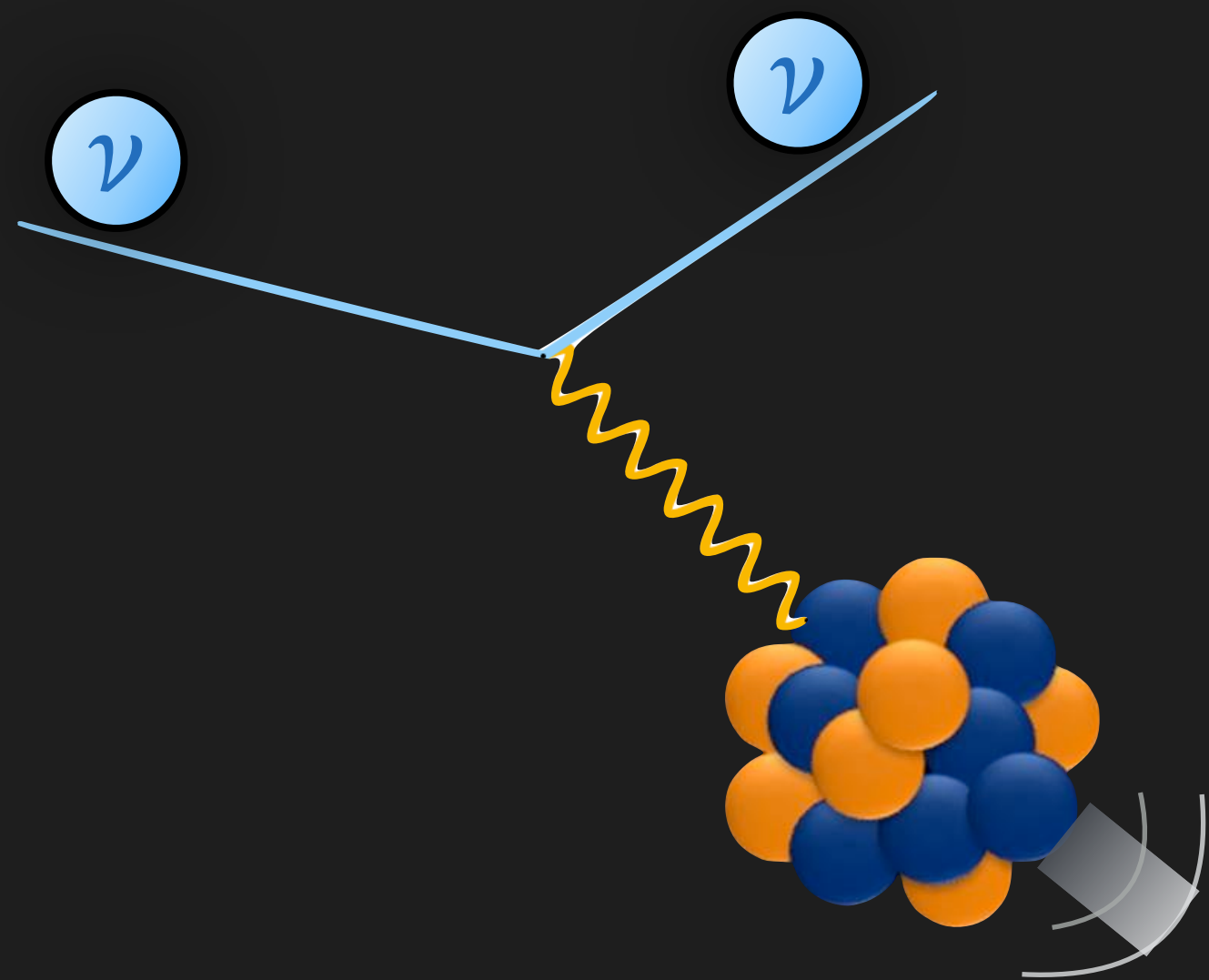
Adapted from Kate Scholberg

NEUTRINO INTERACTIONS WITH NUCLEI



Adapted from Kate Scholberg

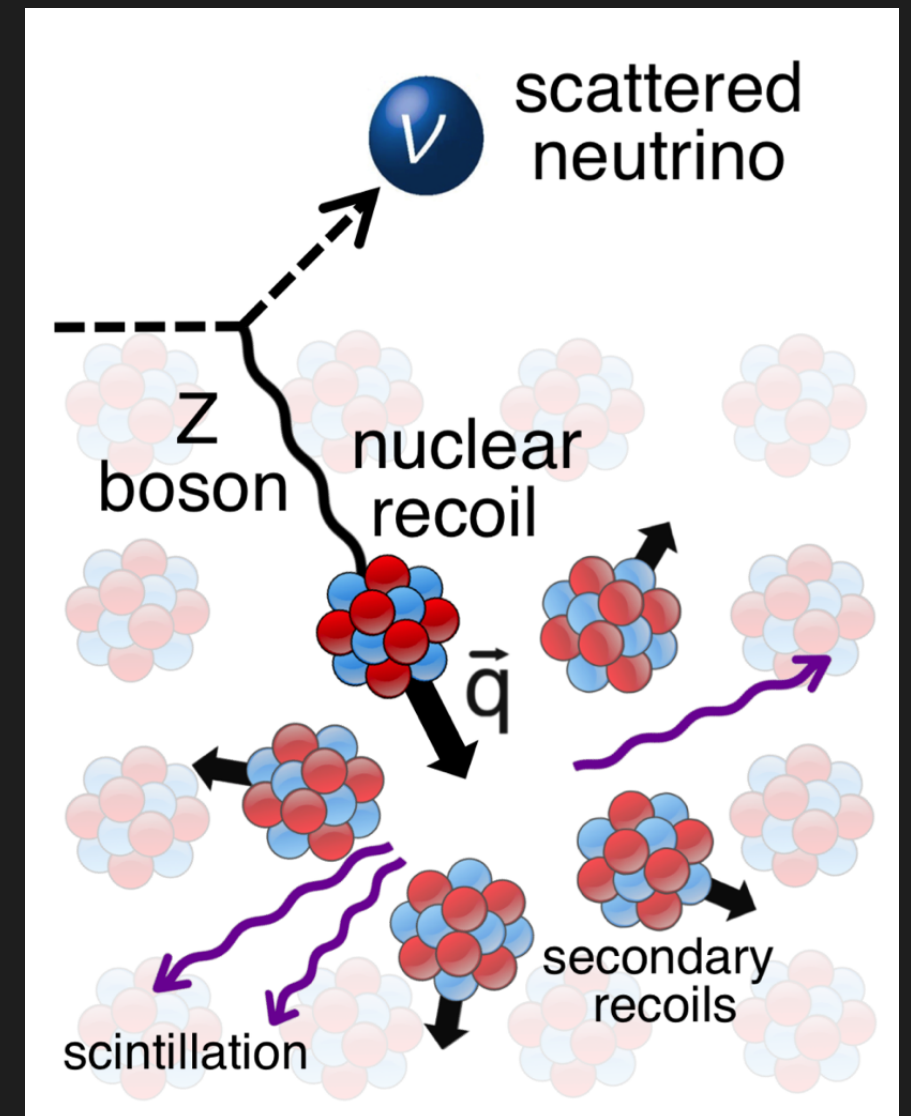
CEvNS: INTRODUCTION AND FEATURES



COHERENT ELASTIC NEUTRINO-NUCLEUS SCATTERING (CEvNS)

- Neutral-current process: $\nu + N(A,Z) \rightarrow \nu + N(A,Z)$
- Coherent: target nucleon wave functions remain in phase with each other before and after the collision. Amplitudes of scattering on individual nucleons add
- Elastic: no new particles are created and nuclear target remains in the same energy state
- The neutrino sees the nucleus as a whole:
 - => cross section enhancement $\sigma \sim (\# \text{scatter targets})^2$
 - => upper limit on neutrino energy (up to $E_\nu \sim 100 \text{ MeV}$)
- Total cross section scales approximately like N^2

$$\frac{d\sigma}{dE_R} \propto N^2$$



D. Akimov et al, Science 357 (2017)

- Can be ~ 2 orders of magnitude larger than inverse beta decay process used first to observe neutrinos.

INCOHERENT/INELASTIC SCATTERING

Incoherent scattering: $\sigma_{\text{NC}}(\nu \mathcal{N}) \propto \sum_i |\mathcal{A}(\nu n_i)|^2 \propto N$ (Probabilities of scattering on individual nucleons add)

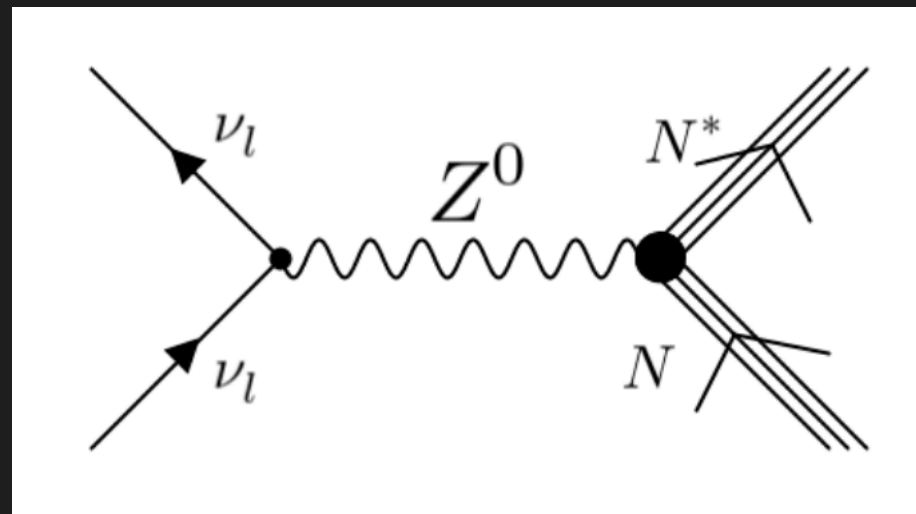
Coherent scattering: $\sigma_{\text{NC}}(\nu \mathcal{N}) \propto \left| \sum_i \mathcal{A}(\nu n_i) \right|^2 \propto N^2$ (Amplitudes of scattering on individual nucleons add)

$$\mathcal{A}(\vec{q}) = \sum_{j=1}^A a_j(\vec{q}) \exp^{i\vec{q}\vec{x}_j}$$

When the momentum transfer times the dimension of the nuclear target is very small, $qR \ll 1$, the phase factors are negligible: the amplitude is given by the **single constituent amplitude** multiplied by the constituents number A.

Bednyakov and Naumov Phys. Rev. D 98 no. 5, (2018) 053004
Pirinen+ Adv. High Energy Phys. 2018 (2018) 9163586,
Bednyakov and Naumov Phys. Part. Nucl. Lett. 16 no. 6, (2019) 638–646

INCOHERENT/INELASTIC SCATTERING

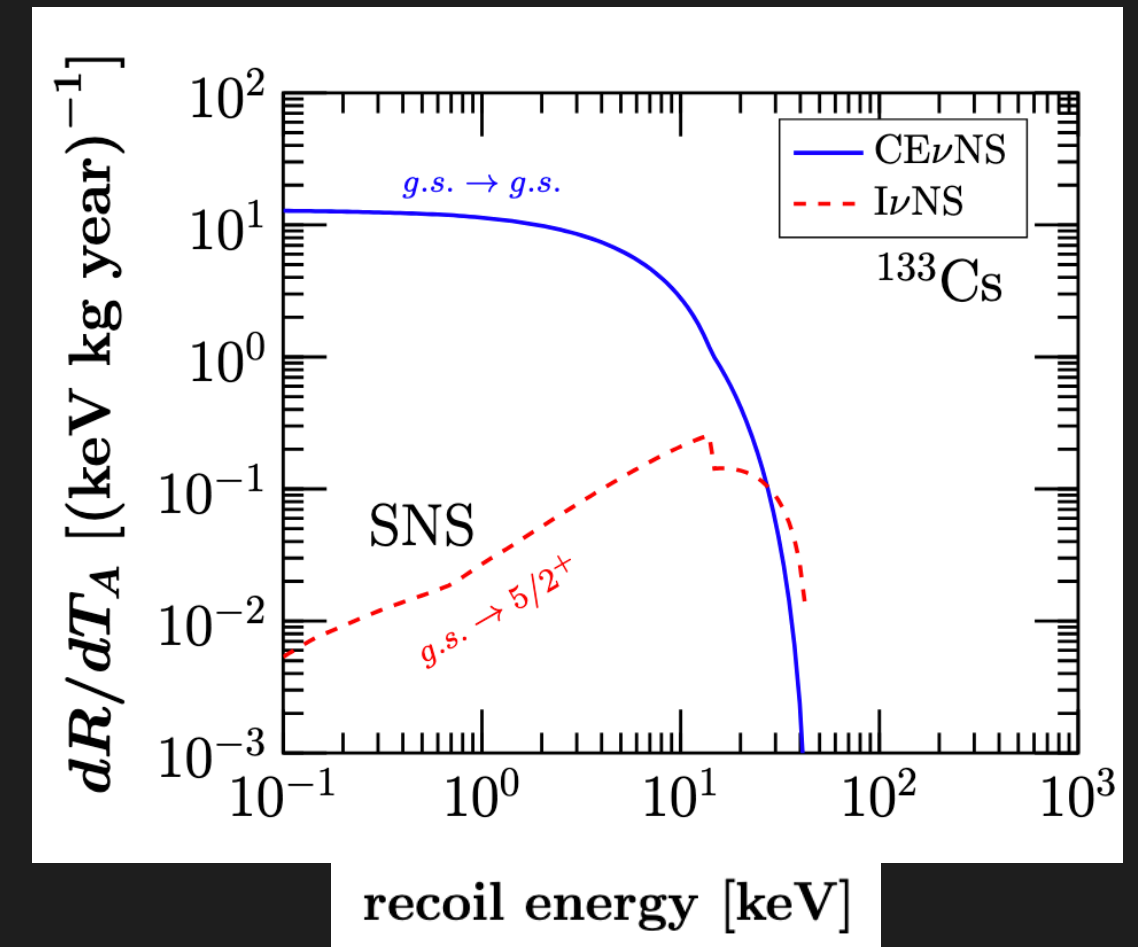


Going to higher neutrino energies, an approximation hints towards a smooth transition between the coherent and incoherent neutrino-nucleus scattering regime.

A correct treatment of both channels requires an accurate evaluation of the transition matrix elements describing the various interaction channels between the initial and final nuclear states.

Neutrinos with energies of tens of MeV can excite many states in the target nuclei used for CEvNS experiments.

This cross-section has a linear dependence on the number of nucleons.



Sahu+ Phys. Rev. C. 102 035501

Bednyakov+ Phys. Rev. D 98 (2018) 053004

Dutta+ Phys. Rev. D 106, 113006 (2022)

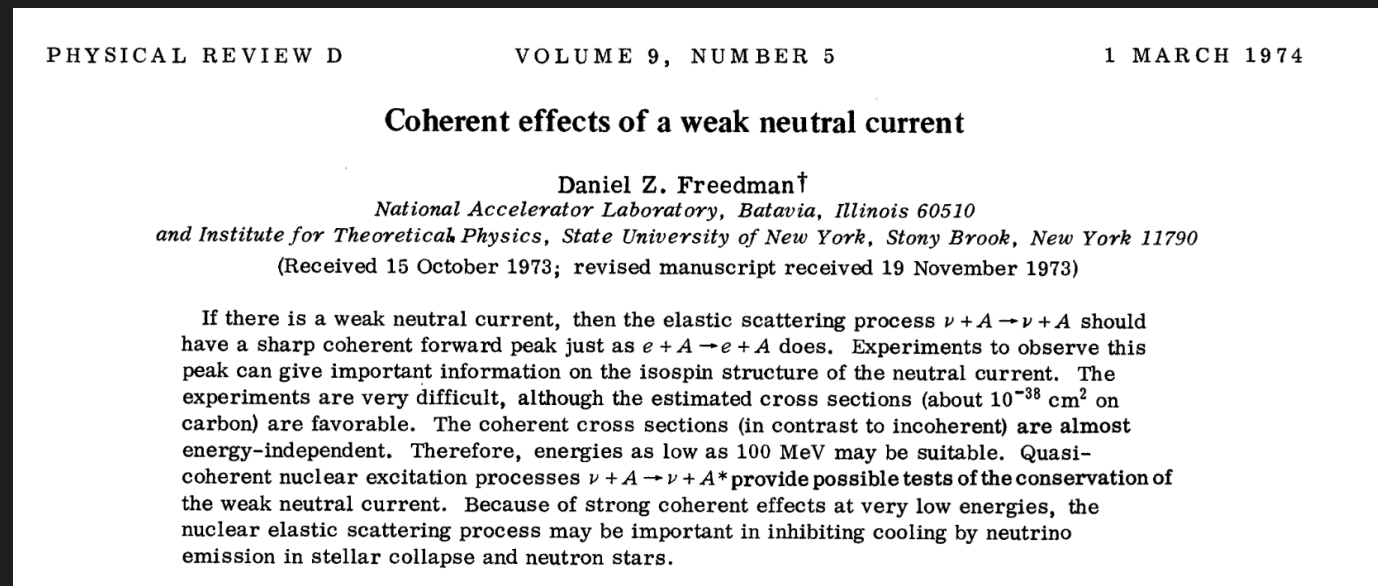
Sahu+ Phys. Rev. C. 102 035501

AN ACT OF HUBRIS

First theoretically predicted in 1974

D.Z. Freedman, Phys. Rev. D 9 (1974)

V.B. Kopeliovich and L.L. Frankfurt, JETP Lett. 19 4 236 (1974)



Our suggestion may be an act of hubris, because the inevitable constraints of interaction rate, resolution, and background pose grave experimental difficulties for elastic neutrino-nucleus scattering. We will discuss these problems at the end of this note, but first we wish to present the theoretical ideas relevant to the experiments.

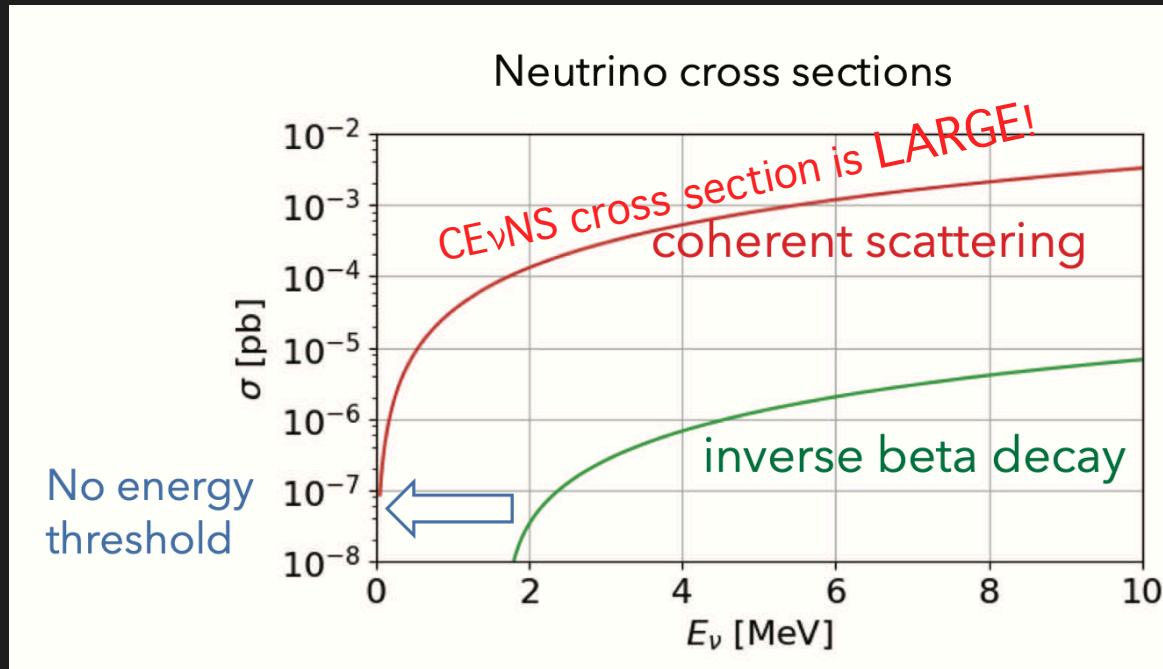
Experimentally the most conspicuous and most difficult feature of our process is that the only detectable reaction product is a recoil nucleus of low momentum. Ideally the apparatus should have sufficient resolution to identify and determine the momentum of the recoil nucleus and sufficient mass to achieve a reasonable interaction rate. Neutron background is a serious problem

CEvNS was observed for the first time ~40 years later, in 2017 by the COHERENT experiment at the Oak Ridge Spallation Neutron Source.

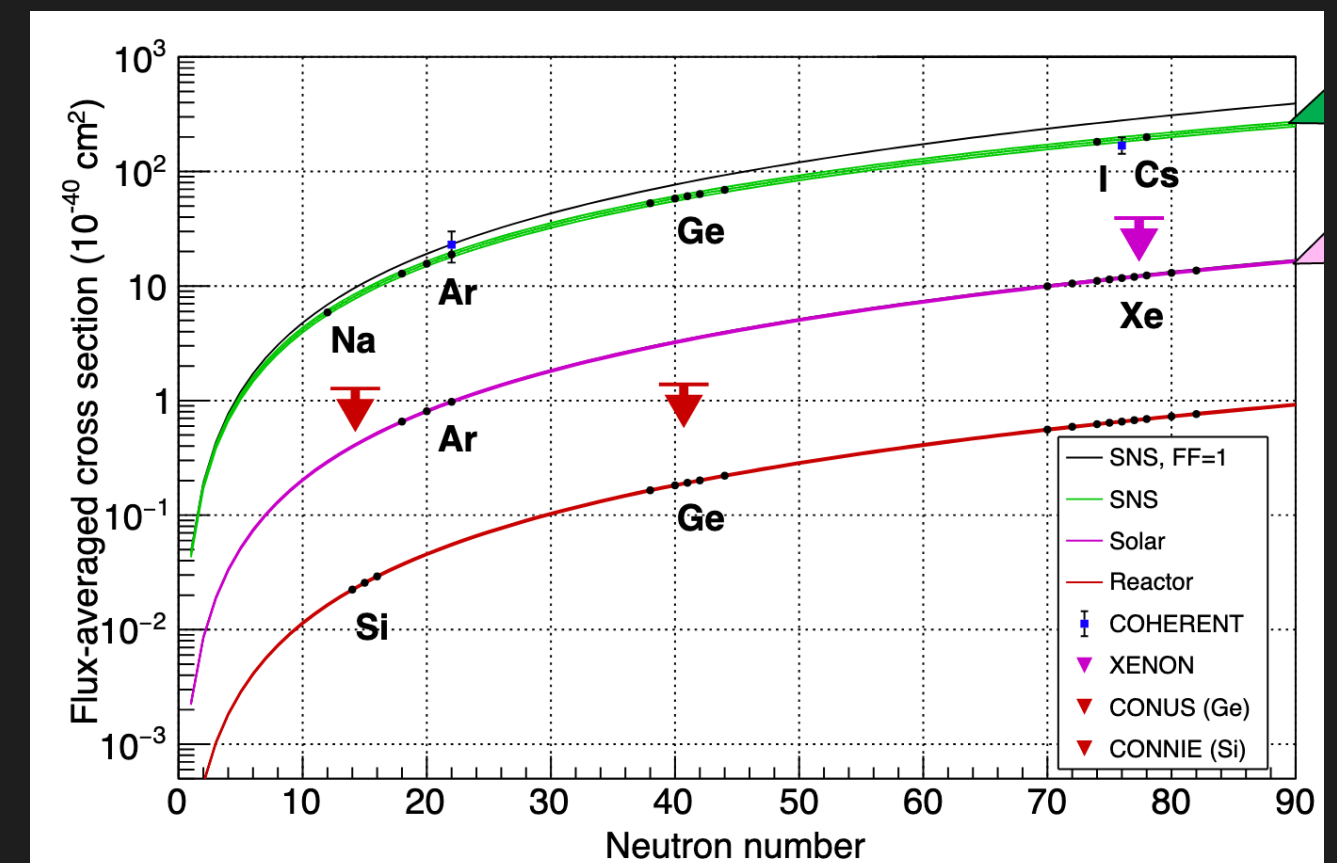
COHERENT ELASTIC NEUTRINO-NUCLEUS SCATTERING

CE ν NS is an exceptionally challenging process to observe

Despite its large cross section, not observed for years due to tiny nuclear recoil energies

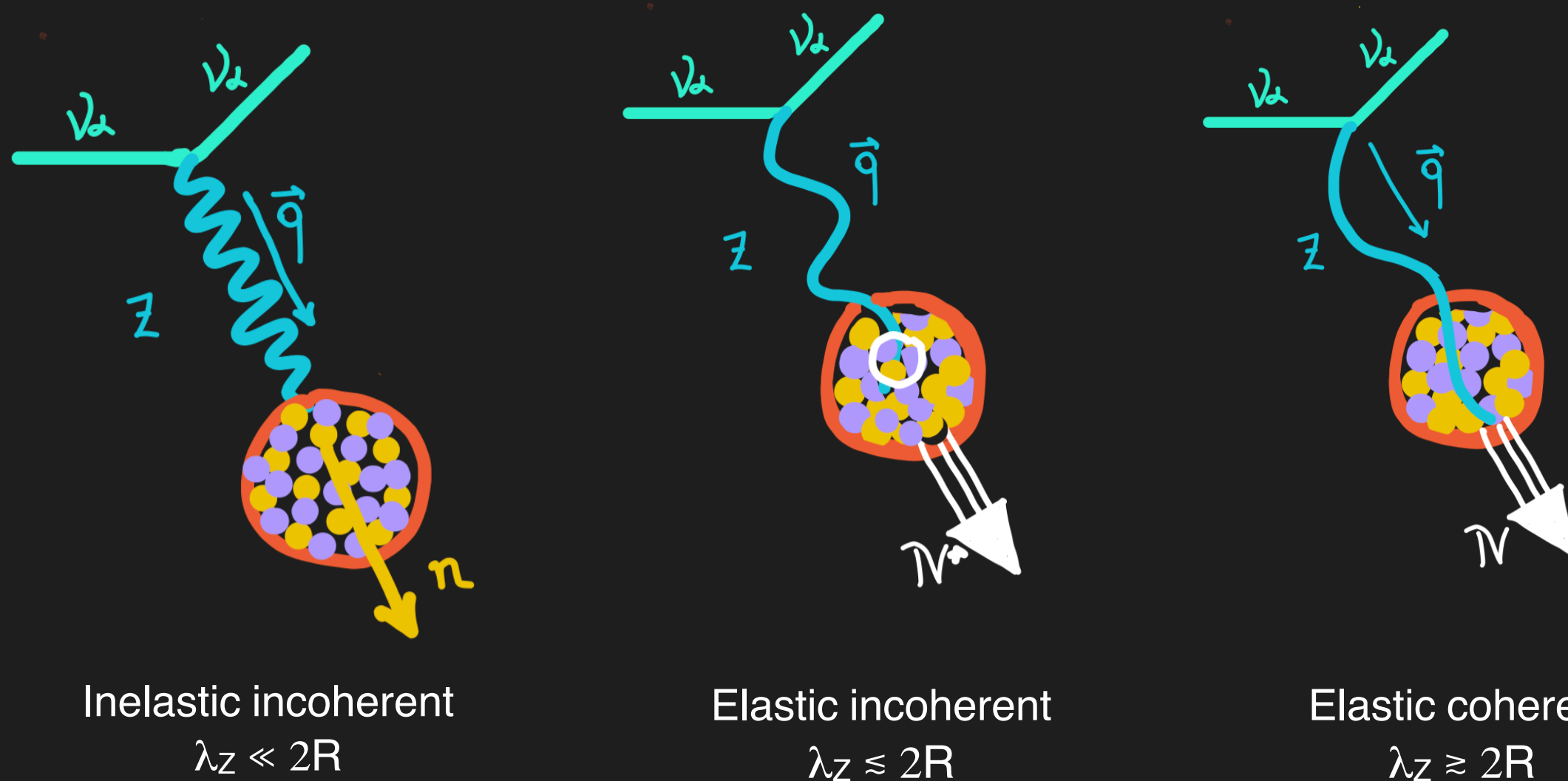


Credit: R. Strauss @ Magnificent CEvNS



Credit to K. Scholberg @ISAPP 2021

NEUTRINO-NUCLEUS SCATTERING

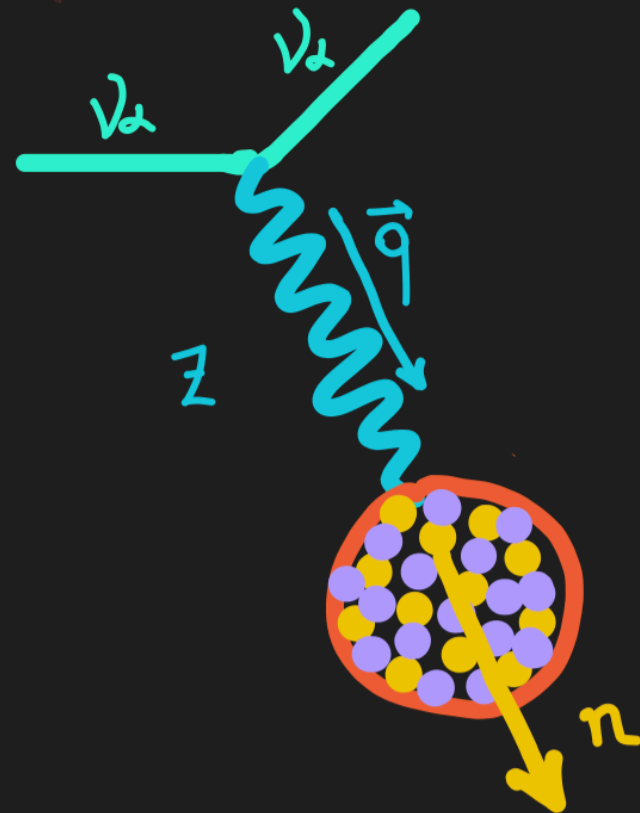


$$\lambda_Z = 2\pi \frac{\hbar}{|\vec{q}|}$$

Different types of interactions of a neutrino ν_α with a nucleus, depending on the wavelength of the mediator.

Adapted from Carlo Giunti

NEUTRINO-NUCLEUS SCATTERING



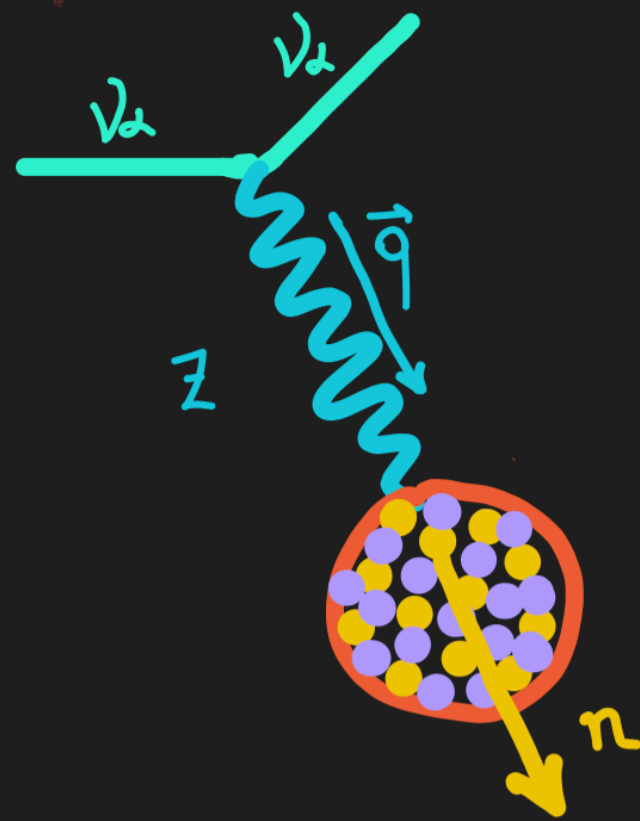
Inelastic incoherent

$$\lambda_Z \ll 2R$$

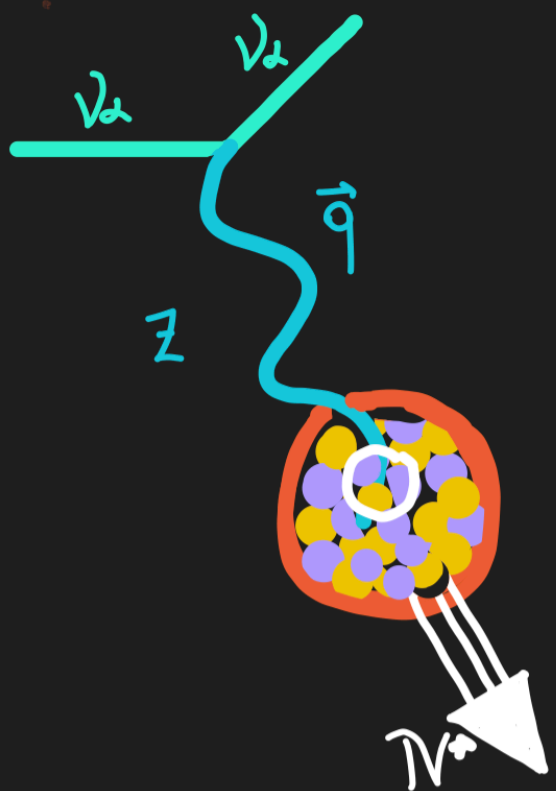
When $\lambda_Z \ll 2R$ the Z boson has a high probability of interacting with a single nucleon in the nucleus, ejecting it.

$$\lambda_Z = 2\pi \frac{\hbar}{|\vec{q}|}$$

NEUTRINO-NUCLEUS SCATTERING



Inelastic incoherent
 $\lambda_Z \ll 2R$

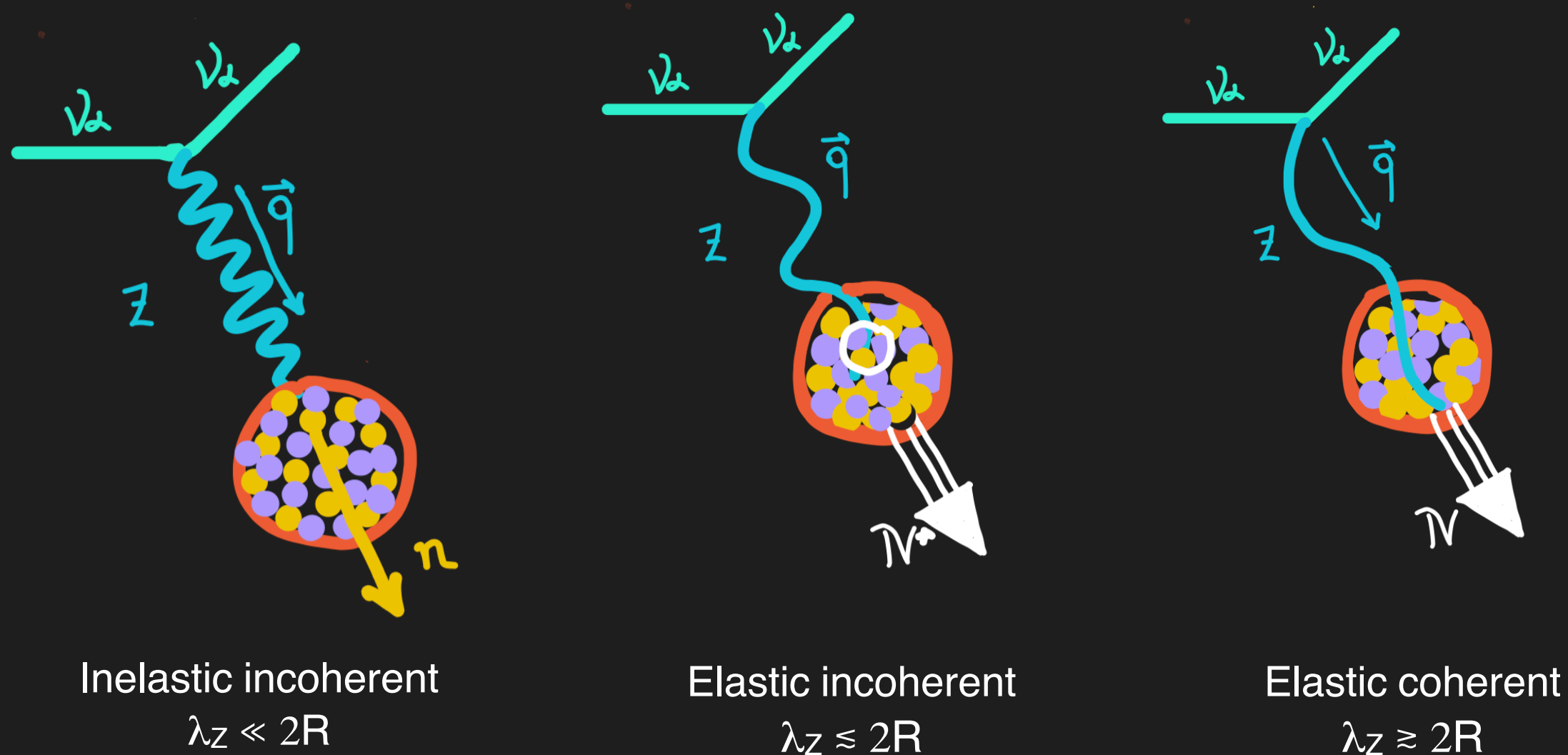


Elastic incoherent
 $\lambda_Z \lesssim 2R$

When $\lambda_Z \lesssim 2R$ the Z boson has a high probability of interacting with a group of nucleons inside the nucleus, exciting the latter to the state N^* .

$$\lambda_Z = 2\pi \frac{\hbar}{|\vec{q}|}$$

NEUTRINO-NUCLEUS SCATTERING



$$\lambda_Z = 2\pi \frac{\hbar}{|\vec{q}|}$$

CEvNS occurs when the neutrino energy E_ν is such that amplitudes sum up coherently: $|\vec{q}| \leq 1/R_{\text{nucleus}}$ (Natural units!)

COHERENT ELASTIC NEUTRINO-NUCLEUS SCATTERING

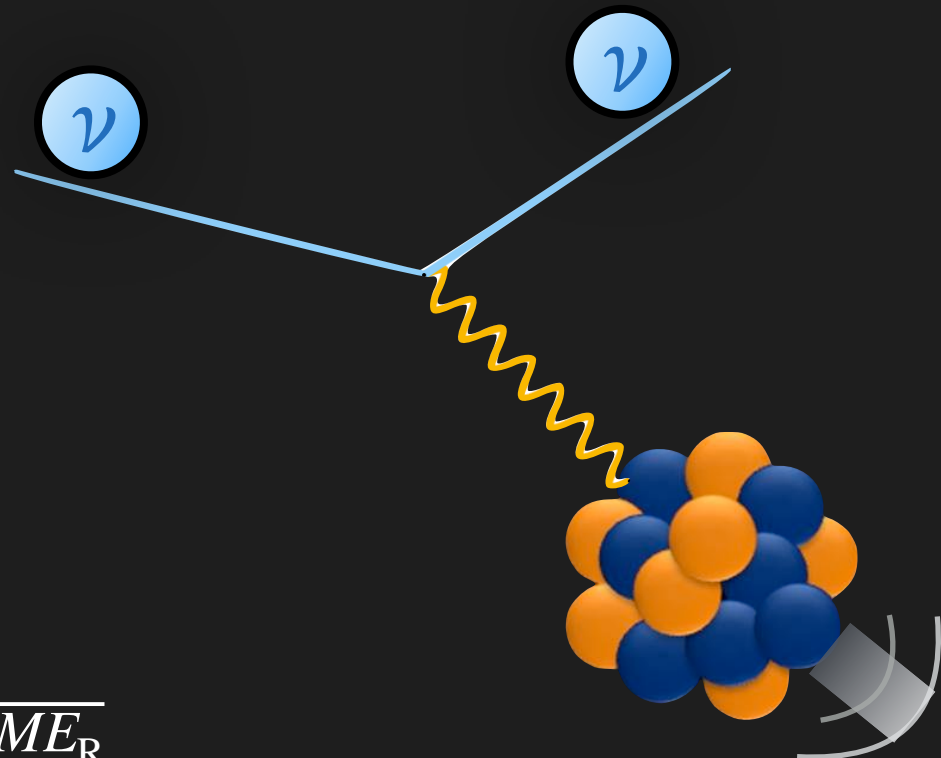
Heavy target nucleus:

$$A = 133, M \sim 133 \text{ GeV}$$

$$R = 1.2 A^{1/3} \sim 6 \text{ fm}$$

CE ν NS occurs for $|\vec{q}| \lesssim 35 \text{ MeV}$

Non-relativistic nuclear recoil: $|\vec{q}| \sim \sqrt{2ME_R}$



COHERENT ELASTIC NEUTRINO-NUCLEUS SCATTERING

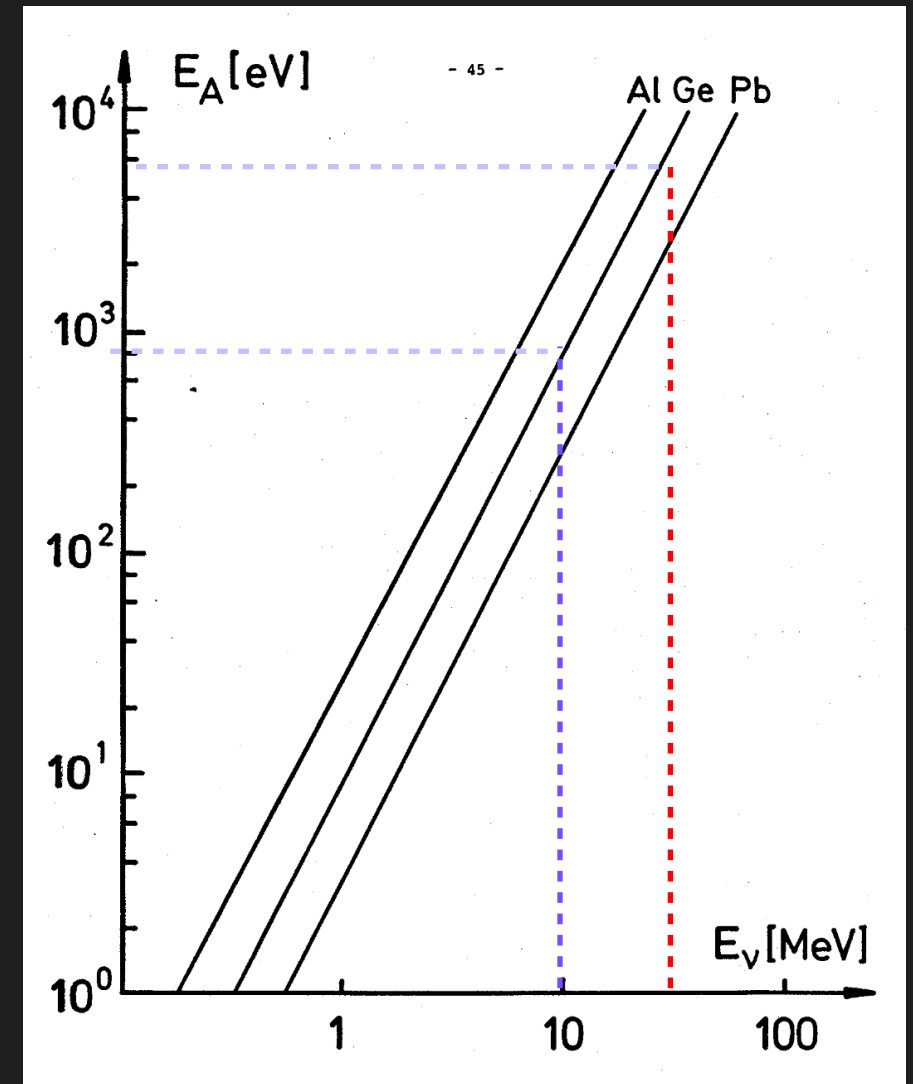
Maximum nuclear recoil is $E_R^{\max} = \frac{2E_{\nu}^2}{m_N}$

Accelerator neutrinos: $E_{\nu} \lesssim 50$ MeV $E_R \lesssim \mathcal{O}(10)$ keV

Close to decoherence

Reactor neutrinos: $E_{\nu} \lesssim 10$ MeV $E_R \lesssim \mathcal{O}(100)$ eV

Full coherence



Drukier, Stodolsky, PRD 30 (1984) 2295

- No threshold
- Heavier nuclei: higher cross section but lower recoil
- Both cross-section and maximum recoil energy increase with neutrino energy

BONUS SLIDE. WHAT HAPPENS AT EVEN LOWER E_R ?

The de Broglie wavelength of particles scales inversely with their momentum: $\lambda_{\text{DB}} \sim \frac{1}{p}$.

Particles scattering with lower momentum see a larger target and scatter with larger cross sections.

BONUS SLIDE. WHAT HAPPENS AT EVEN LOWER E_R ?

If $|\vec{q}| \leq 1/R_{\text{atom}}$ the reaction occurs with the whole atom.

Coherence would be visible for $|\vec{q}| \sim 2 \text{ keV}/R_{\text{atom}}$ with a corresponding recoil energy

$$E_R \approx 2 \text{ meV} / (A R_{\text{atom}}^2 [\text{\AA}])$$

For Helium, $R_{\text{atom}} = 0.5 \text{\AA}$ and $E_R \sim 2 \text{ meV}$.

Sehgal+ Phys.Lett.B 171 (1986) 107-112
Cadeddu+ Phys. Rev. D 100, 073014 (2019)
Donchenko+ FIELDS, PARTICLES, AND NUCLEI 117 (2023)

Electrons “screen” the nuclear weak charge as seen by an electron neutrino (destructive interference).

Observation requires:

- Sensitivity to tiny recoil energies
- neutrinos with energy of few keV

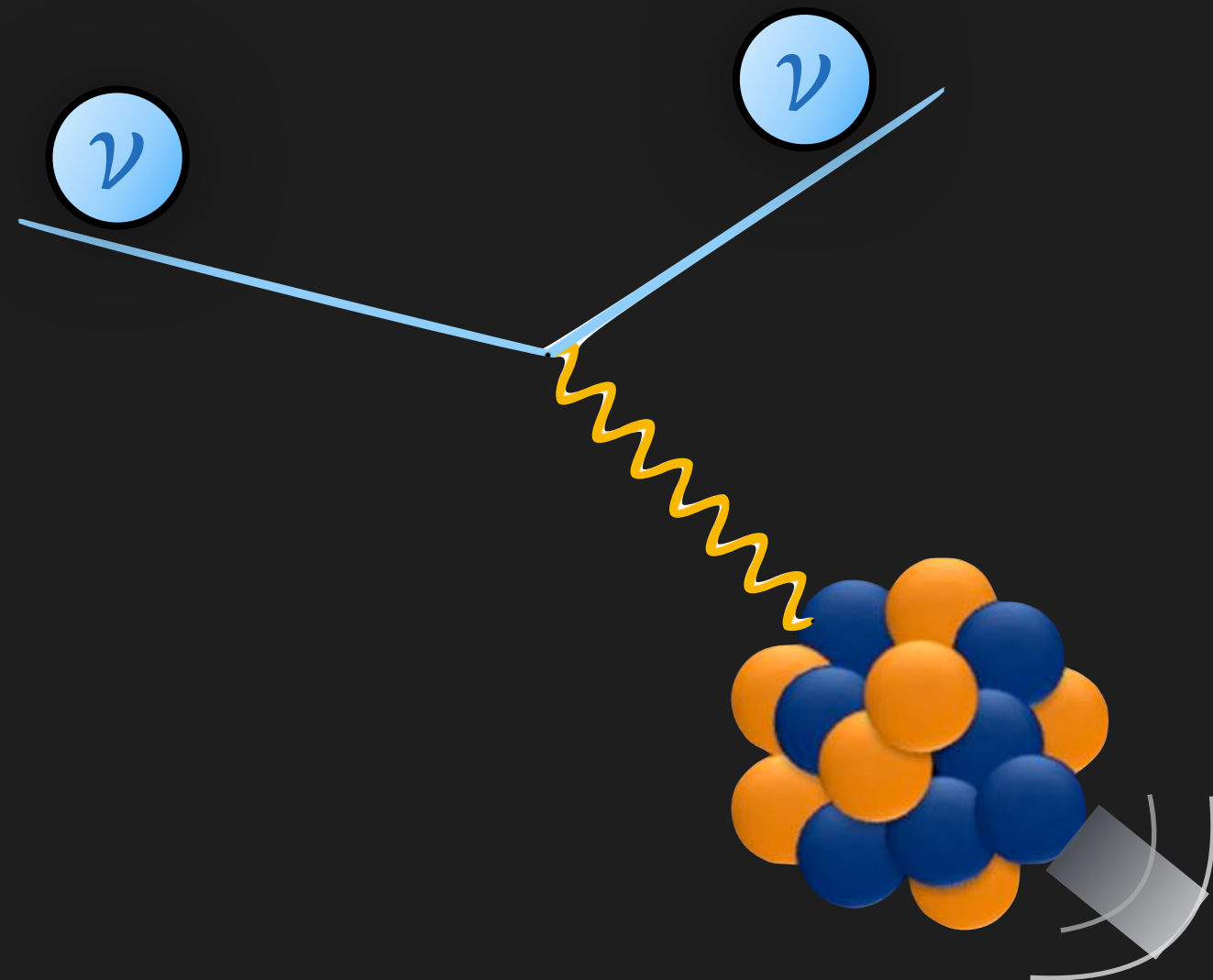
BONUS SLIDE. WHAT HAPPENS AT EVEN LOWER ER?

Observing relic neutrinos?

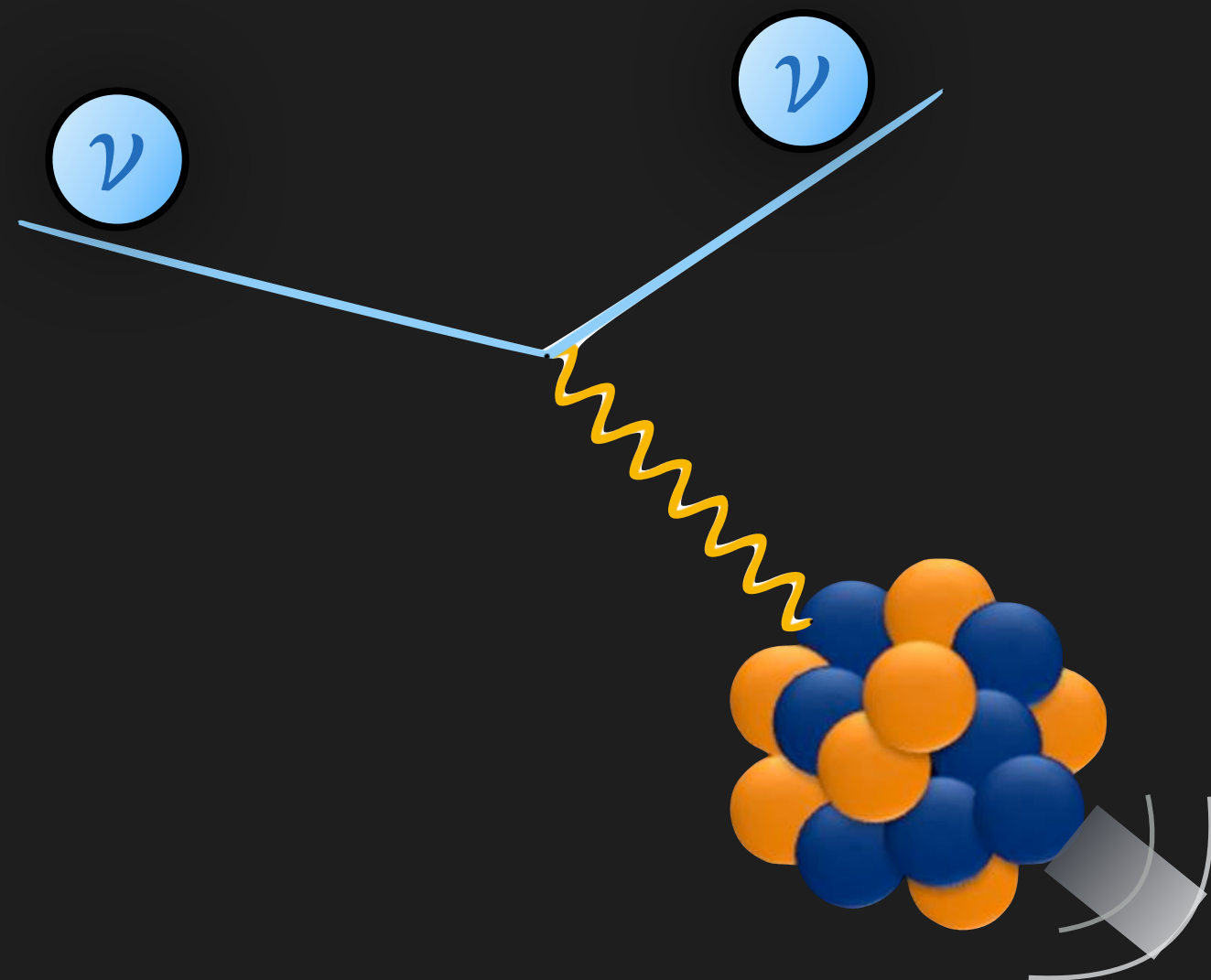
Relic neutrinos have momenta $p \sim 0.5$ meV, corresponding to macroscopic wavelengths $\lambda \sim \text{mm}$ and an enhancement factor of order the Avogadro number.

Opher, Astron. Astrophys. 37 (1974) no.1, 135-137
Lewis, PRD 21 (1980), 663
Shvartsman+, JETP Lett. 36 (1982), 277-279
Smith and Lewin, PLB 127 (1983), 185-190
Duda+ PRD 64 (2001), 122001
Domcke and Spinrath, JCAP 06 (2017), 055
Shergold JCAP 11 (2021), 052
...

CEvNS EXPERIMENTS AND DETECTION



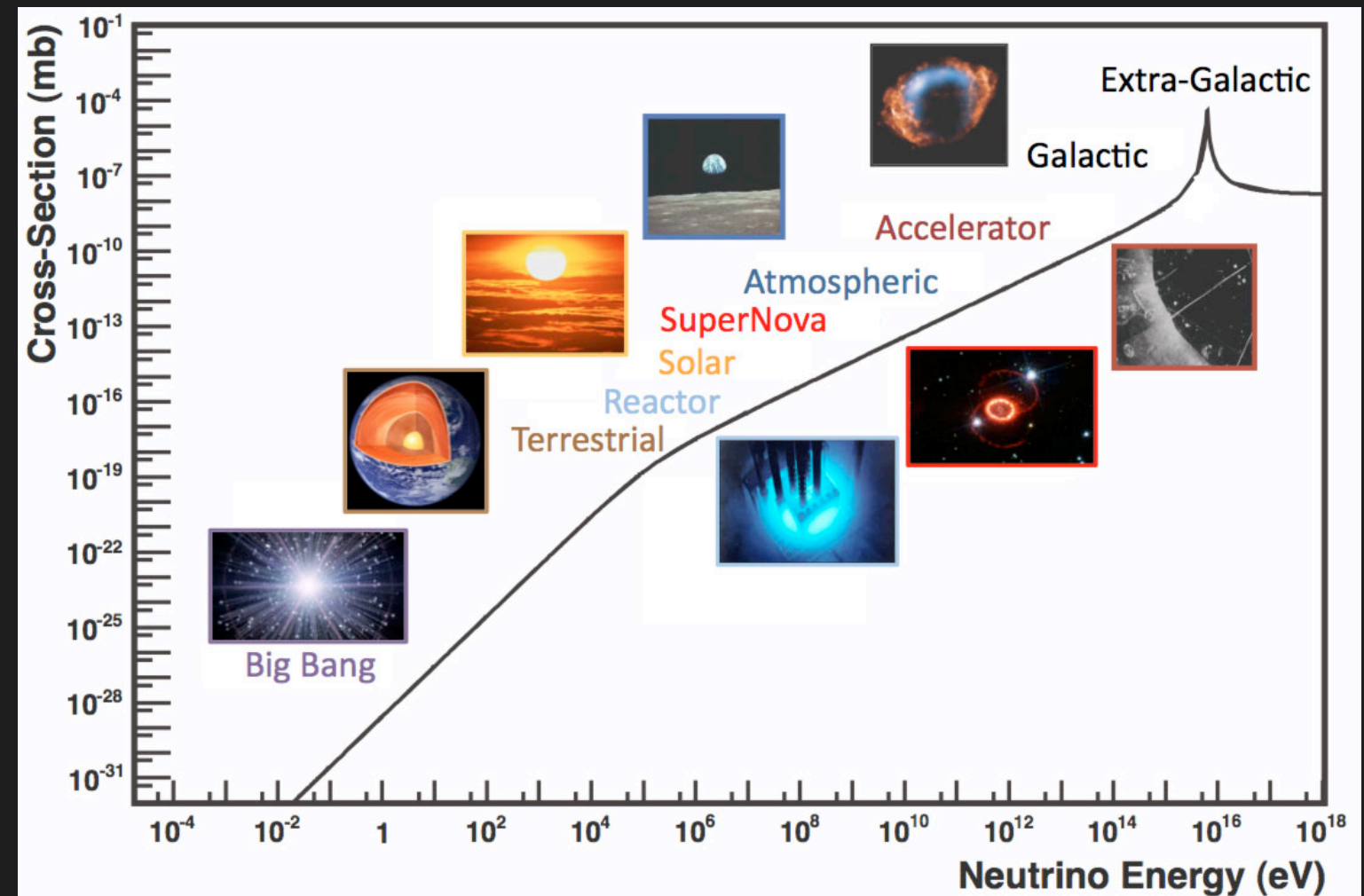
NEUTRINO SOURCES



NEUTRINO SOURCES

Preferable requisites:

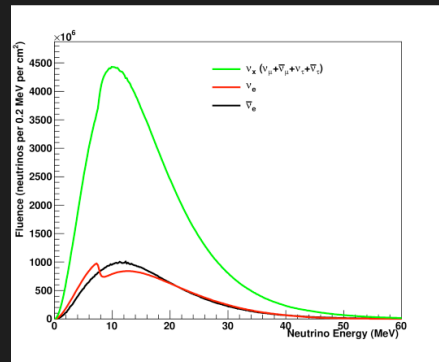
- High flux
- Well understood spectrum
- Multiple flavours
- Possibility of locating the detector close to the source
- Background rejection



Rev.Mod.Phys. 84 (2012) 1307-1341

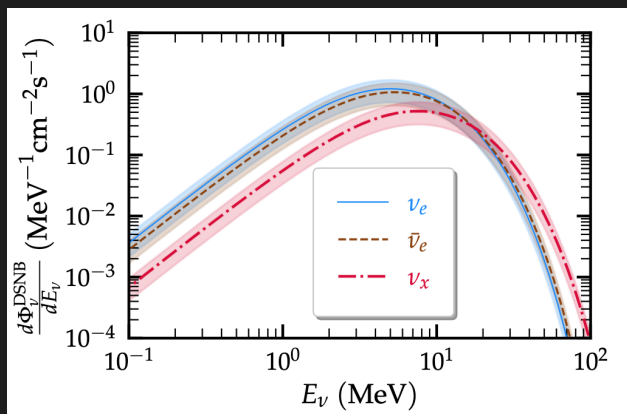
LOW-ENERGY NEUTRINOS FROM NATURAL SOURCES

Supernova
bursts neutrinos



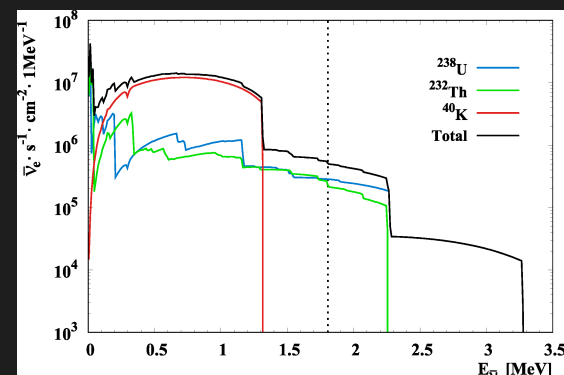
arXiv:1205.6003 [astro-ph.IM]

DSNB



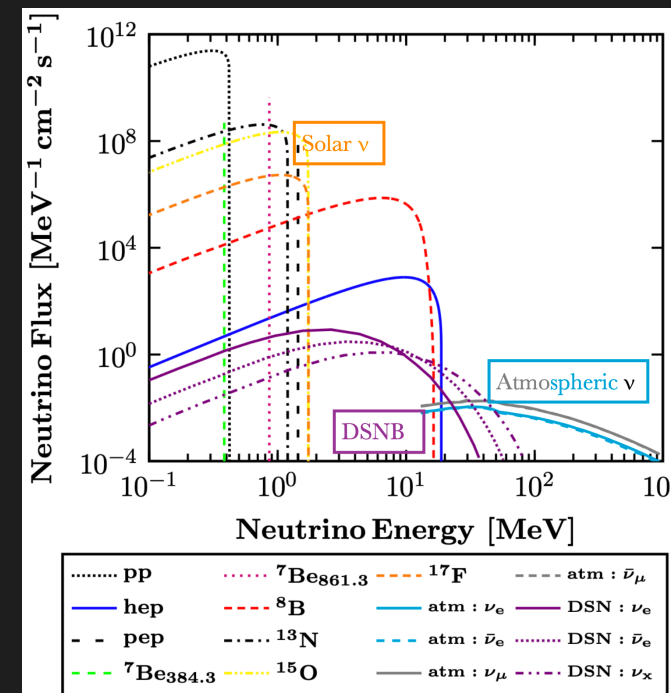
VDR, Majumdar+ 2309.04117 [hep-ph]

Geoneutrinos



Phys. Rev. D 101, 012009

Atmospheric neutrinos

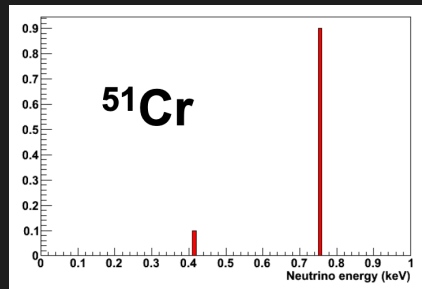


Aristizabal, VDR, Flores, Papoulias JCAP 01 (2022) 01, 055

Solar neutrinos

LOW-ENERGY NEUTRINOS FROM ARTIFICIAL SOURCES

Radioactive source
 ^{51}Cr

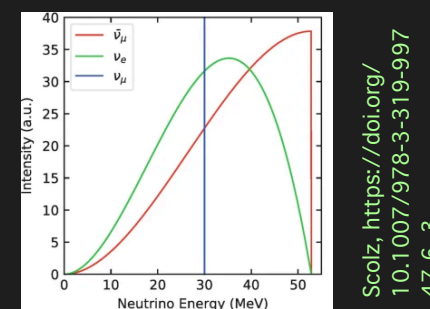


Electron-capture decaying isotope
4 monochromatic lines
very short baseline
low energy challenging

Beam induced radioactive sources (IsoDAR)

Higher energy than reactors
Does not exist yet

Stopped pions
(Decay at rest)
High energy, pulsed beam



Scolz, https://doi.org/10.1007/978-3-319-99747-6_3

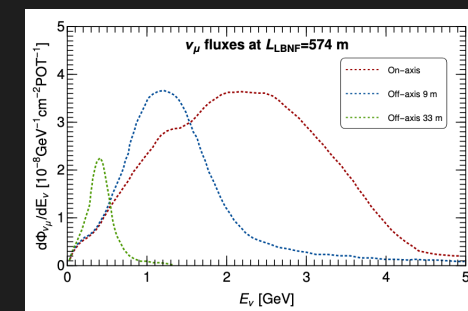


Reactors
Low energy, but high fluxes possible



Next-generation neutrino beams

Low-energy tail of the neutrino spectrum of LBNF

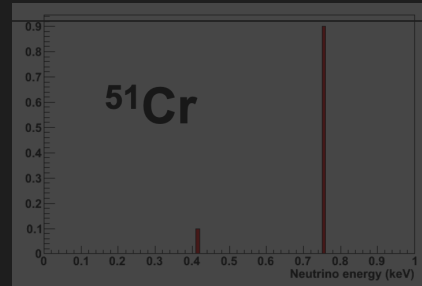


Aristizabal+ PRD 104, 033004 (2021)

Adapted from K. Scholberg @ CNNP2017
and Snowmass 2021 2203.07361

LOW-ENERGY NEUTRINOS FROM ARTIFICIAL SOURCES

Radioactive source
 ^{51}Cr



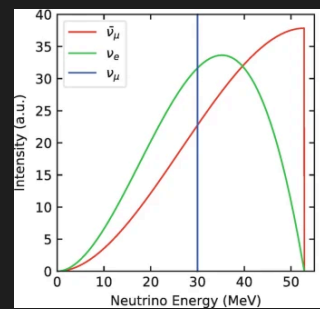
Electron-capture decaying isotope
4 monochromatic lines
very short baseline
low energy challenging

Beam induced radioactive sources (IsoDAR)

Higher energy than reactors
Does not exist yet

Adapted from K. Scholberg @ CNNP2017
and Snowmass 2021 2203.07361

Stopped pions
(Decay at rest)
High energy, pulsed beam



Scielo, https://doi.org/10.1007/978-3-319-99747-6_3

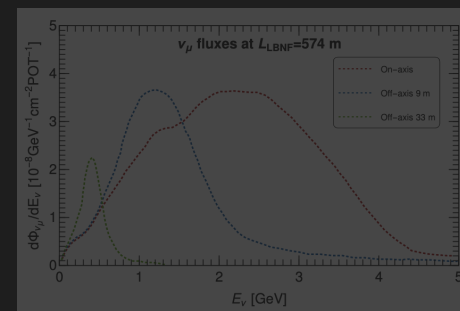


Credit: neutrinos.fnal.gov

Reactors
Low energy, but high fluxes possible

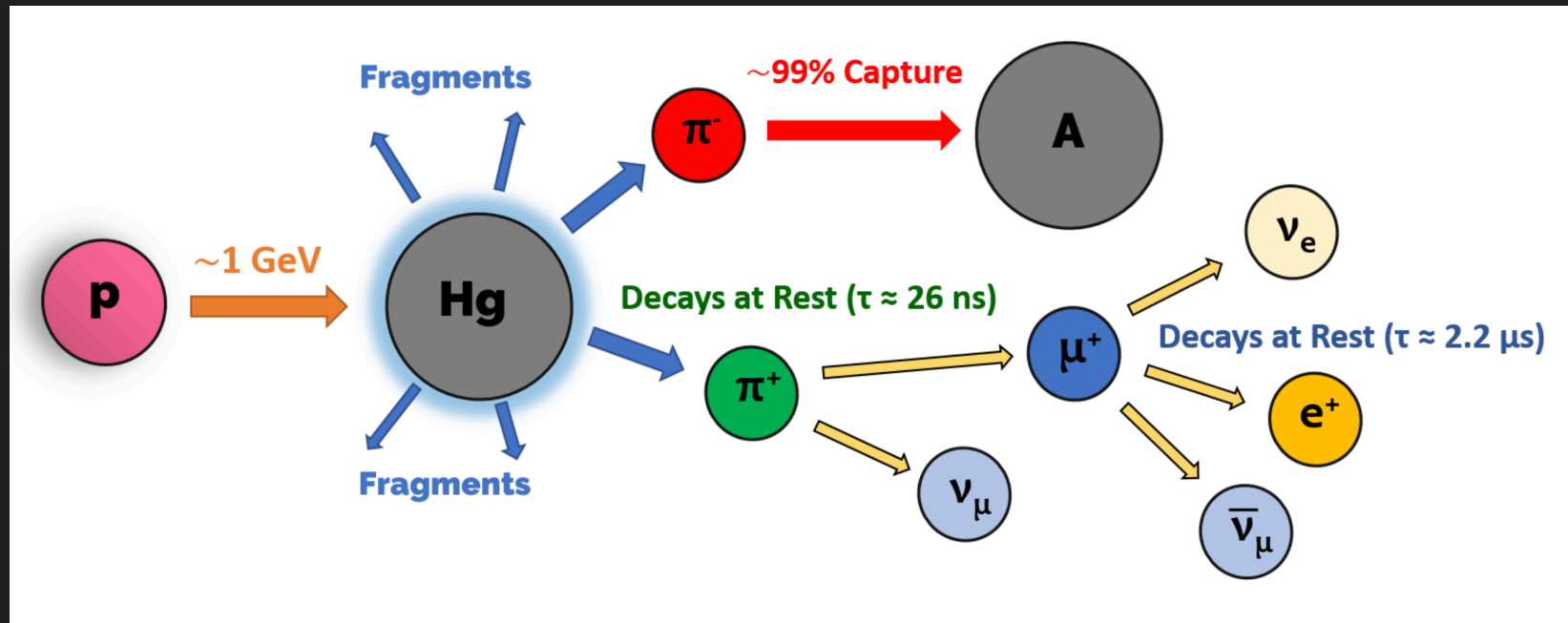


Next-generation neutrino beams
Low-energy tail of the neutrino spectrum of LBNF

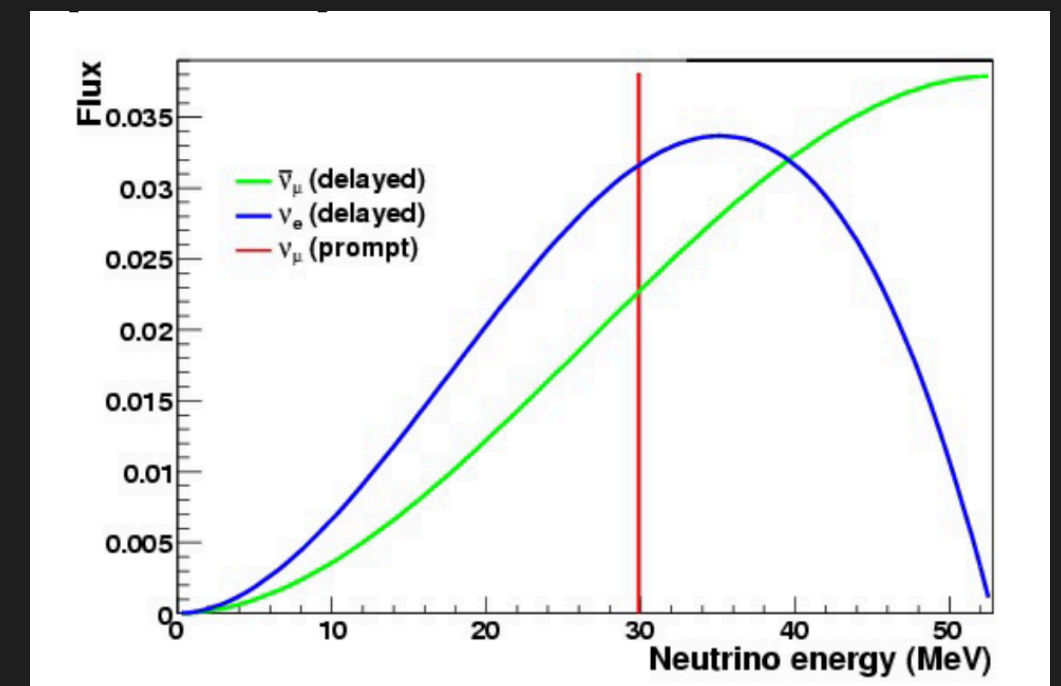
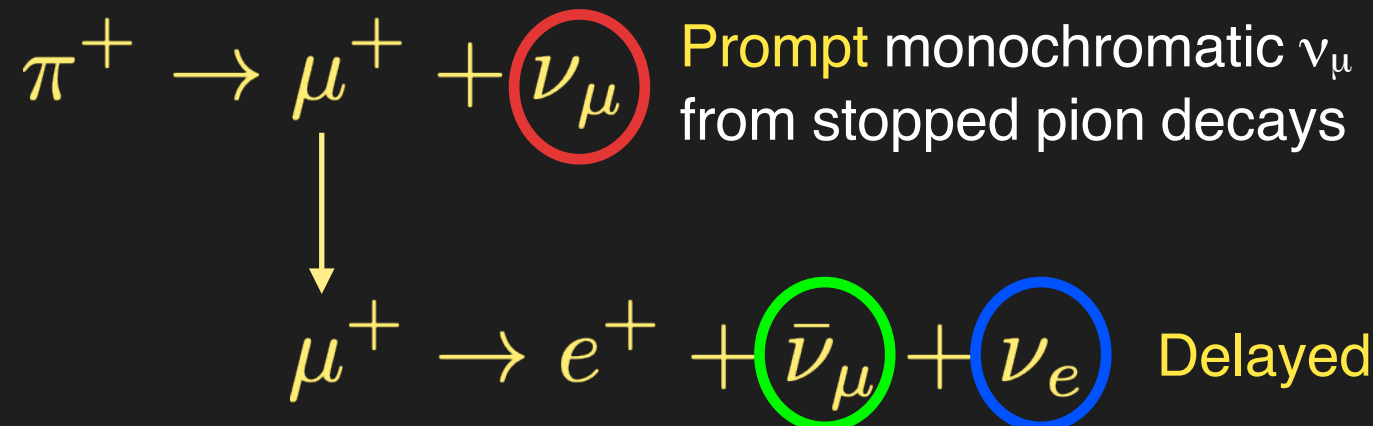


Aristizabal+ PRD 104, 033004 (2021)

STOPPED-PION (π -DAR) NEUTRINOS



Credit: M. Green @ Magnificent CEvNS 2019

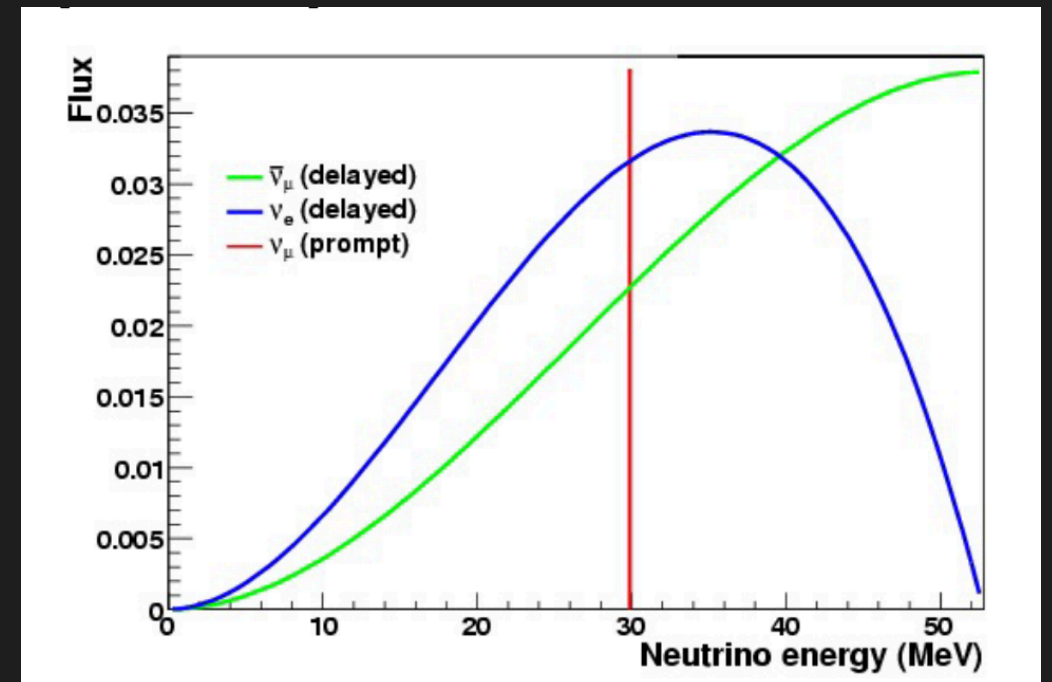


D. Akimov et al. (COHERENT). 2110.07730

STOPPED-PION (π -DAR) NEUTRINOS

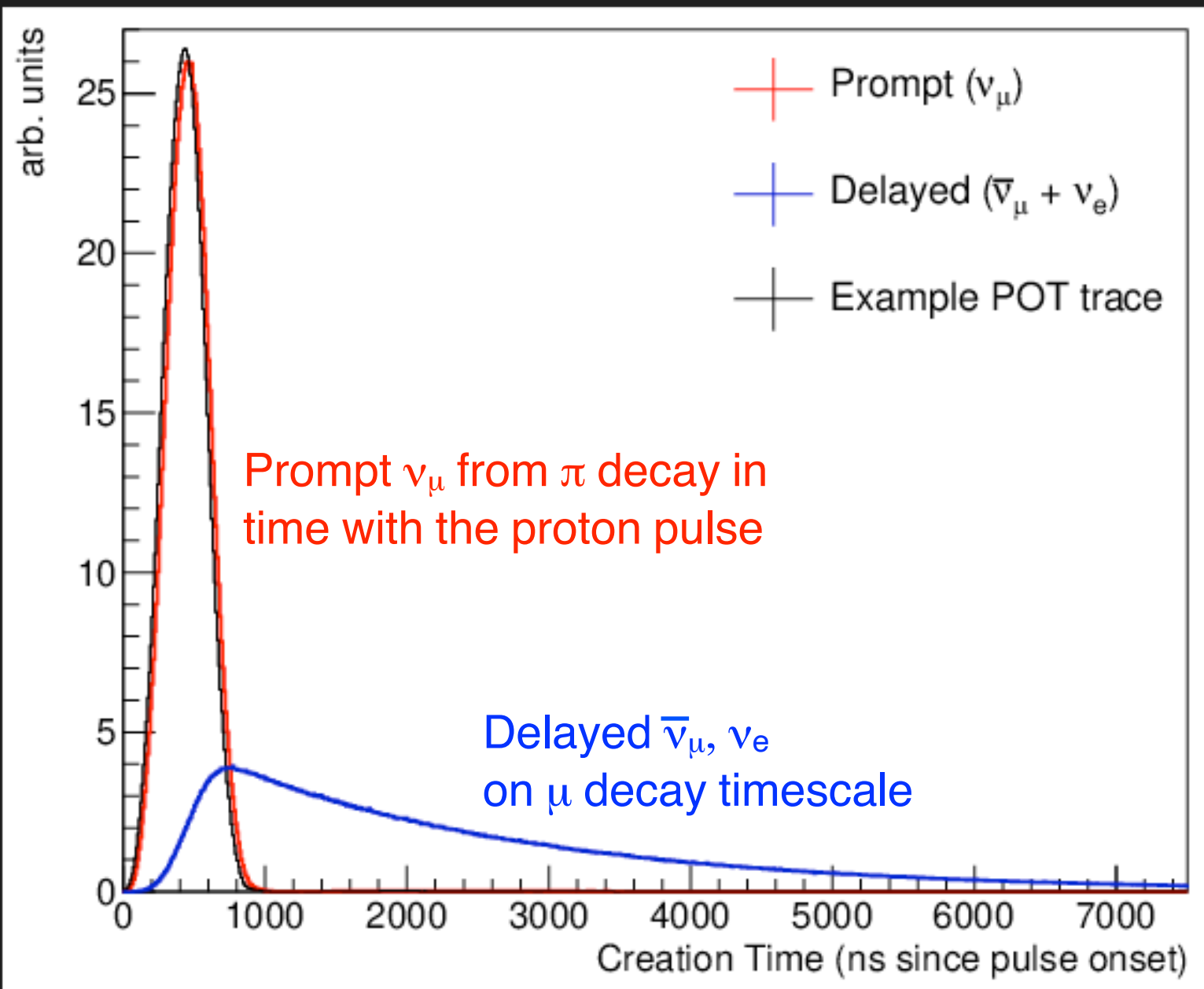
- Spallation Neutron Source (SNS) at Oak Ridge National Laboratory (USA).
- Lujan center at Los Alamos Neutron Science Center LANSCE (USA).
- China Spallation Neutron Source CSNS (China).
- European Spallation Source (ESS) under construction (Sweden)

- High energy
- Pulsed beam → good background rejection
- Neutron backgrounds



D. Akimov et al. (COHERENT). 2110.07730

TIME DISTRIBUTION OF A π -DAR NEUTRINO SOURCE (SNS)



NEUTRINOS FROM NUCLEAR REACTORS

PROs:

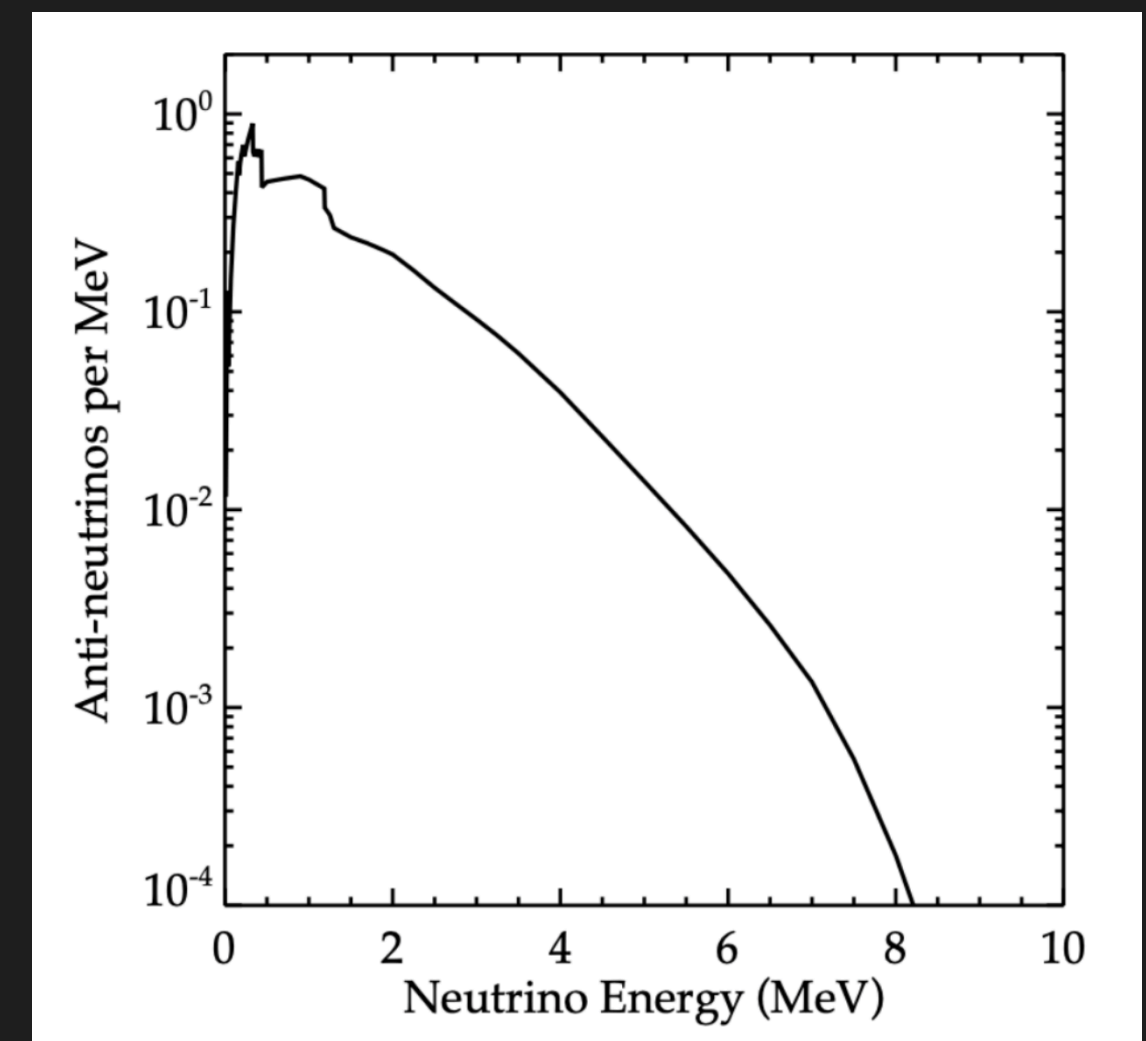
- Copious sources of electron antineutrinos
- Low energy (≤ 10 MeV): coherence condition for the recoil is largely preserved

CONs:

- Even smaller recoil energies
- Large backgrounds (although reactor-off allows to measure bckg)
- Only one flavor accessible

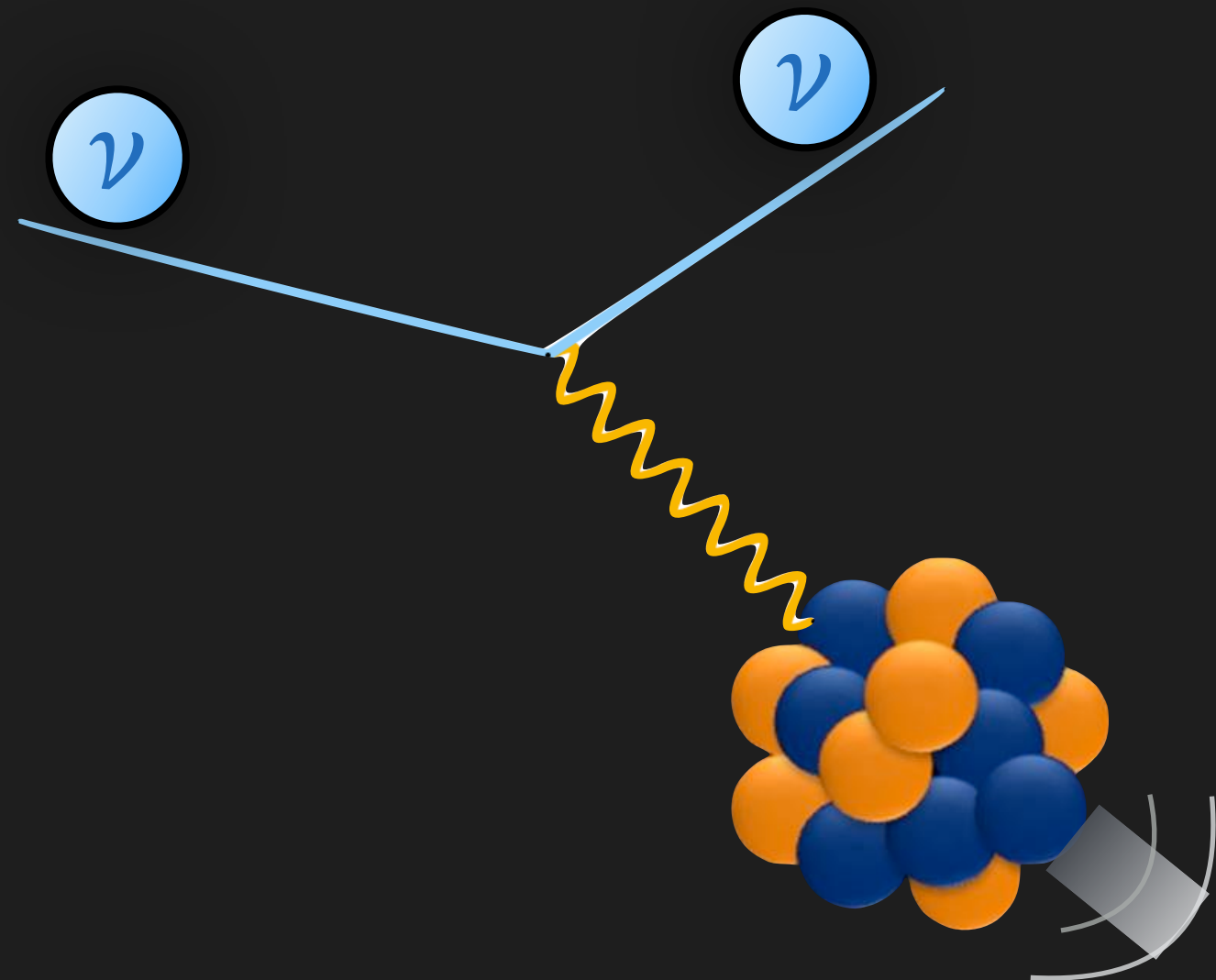


Credit: constellationenergy.com

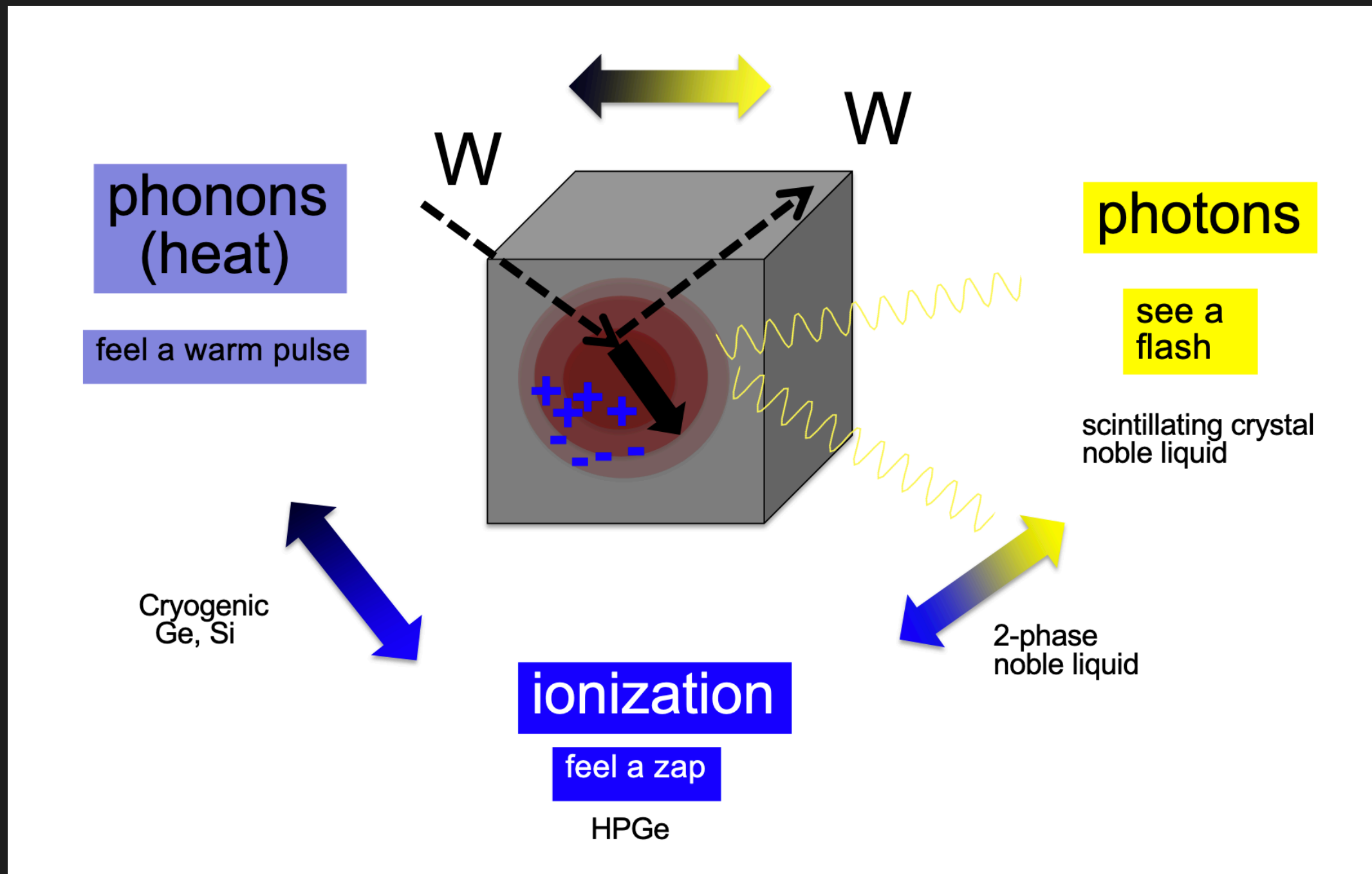


Snowmass 2021 2203.07361

EXPERIMENTS AND DETECTION

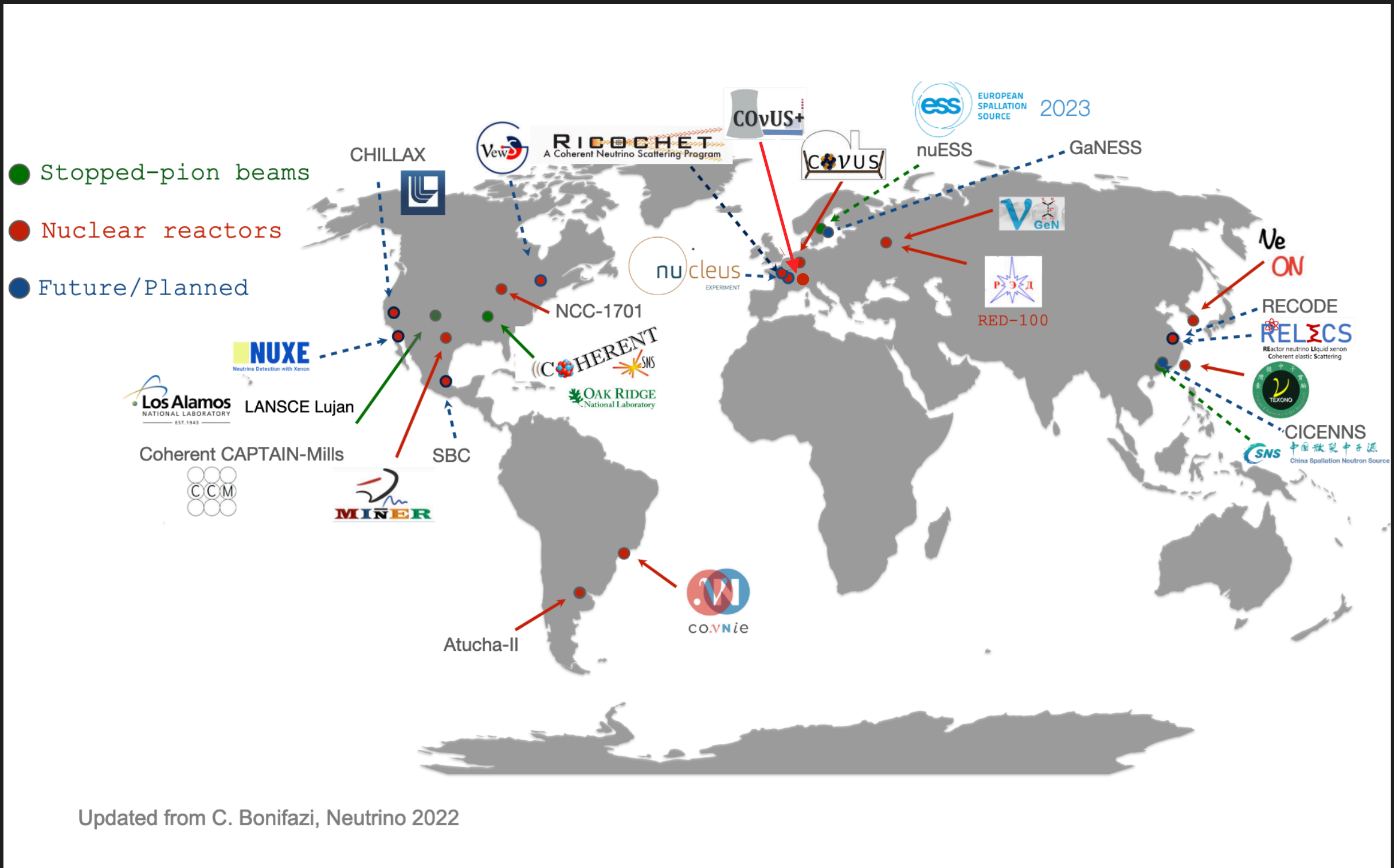


LOW-ENERGY NUCLEAR RECOIL DETECTION STRATEGIES



Credit to K. Scholberg @INSS 2021 and
<http://dmrc.snu.ac.kr/english/intro/intro1.html>

CEvNS EXPERIMENTS WORLDWIDE



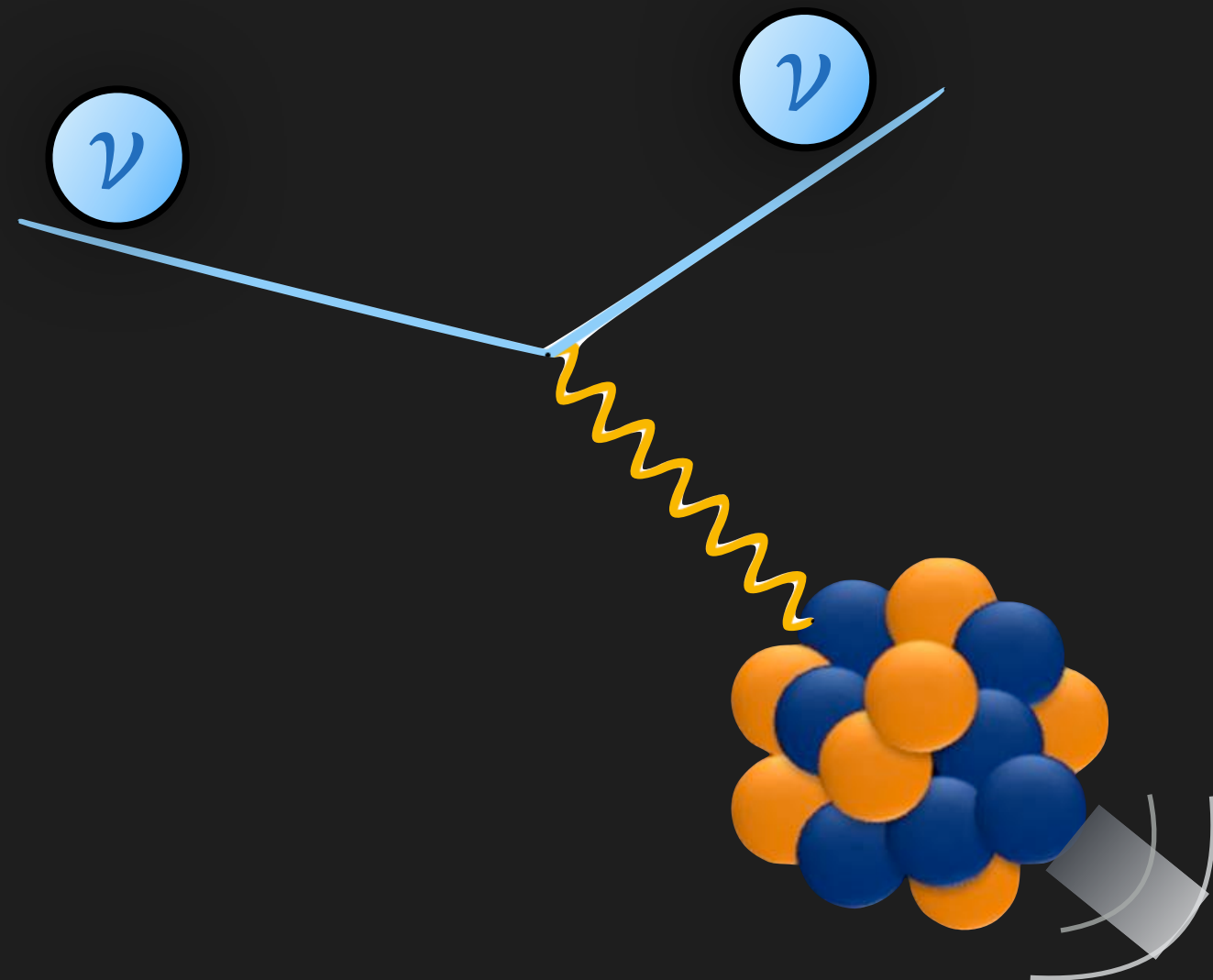
Updated from C. Bonifazi, Neutrino 2022

Credit to I. Nasteva @NEUTRINO 2024

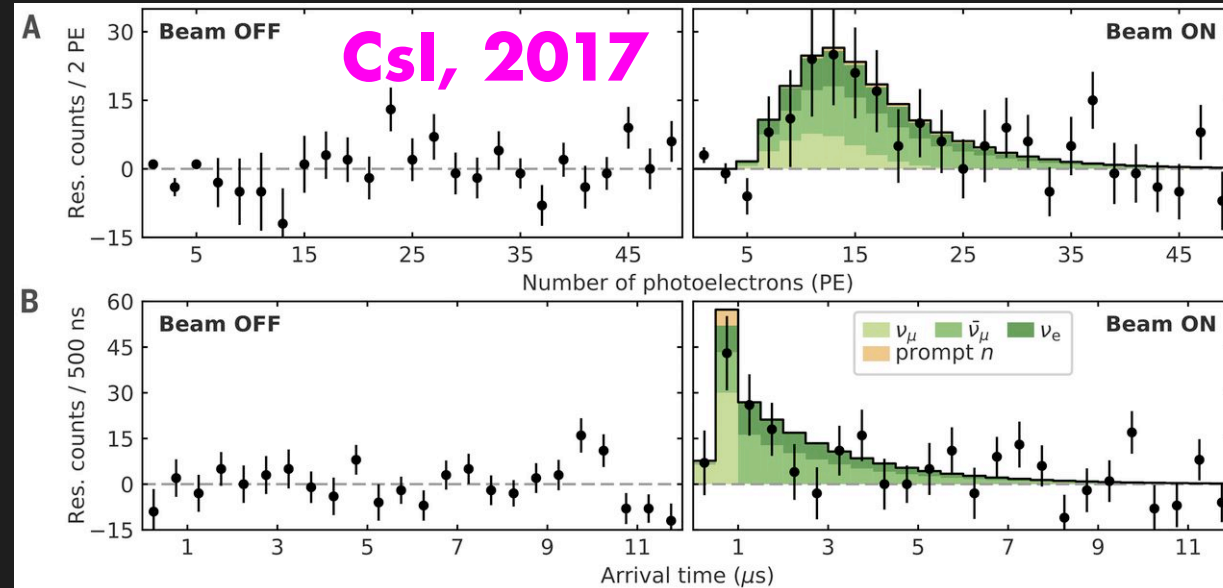
(INCOMPLETE! LIST OF) CEvNS EXPERIMENTS

Experiment	T_{th}	Baseline (m)	Target	Mass (kg)	Technology	Source	Neutrino flux ($\nu/cm^2/s$)
COHERENT	6.5 keV _{nr}	19.3	CsI[Na]	14.57	Scintillating crystal	π -DAR SNS	4.3×10^7
	1.5 keV _{ee}	22	Ge	10.66	HPGe PPC		
	20 keV _{nr}	29	LAr	2×10^3	Single phase		
	13 keV _{nr}	28	NaI[Tl]	185*/3388	Scintillating crystal		
CCM	10-20 keV	20-40	LAr	10^4	Scintillation	π -DAR Lujan	
ESS*			CsI, Ge, Xe, Ar			π -DAR	
CICENNS*	2 keV _{nr}	10.5	CsI(Na)	300	Scintillation	π -DAR	2×10^7
NCC-1701 (DRESDEN-II)	200 eV _{ee}	8	Ge	3	HPGe	NPP 2.9 GW	8.1×10^{13}
CONUS	210 eV _{ee}	17	Ge	4	HPGe	NPP 3.9 GW	2×10^{13}
CONUS+	150 eV _{ee}	20.7	Ge	4	HPGe	NPP 3.6 GW	1.45×10^{13}
MINER	100 eV _{nr}	1	Ge/Si/Al ₂ O ₃	2-10	cryogenic	NPP 1 MW	1×10^{12}
CONNIE	15 eV _{ee}	30	Si	0.5×10^{-3}	Si CCDs	NPP 3.9 GW	7.8×10^{12}
Ricochet	300 eV _{nr}	8.8	Ge,Zn,Al, Sn	0.68	cryogenic	NPP 58 MW	1.6×10^{12}
NUCLEUS	200 eV _{ee}	77, 102	CaWO ₄ Al ₂ O ₃	10^{-2}	Cryogenic CaWO ₄ Al ₂ O ₃ calorimeter array	NPP 8.54 GW	1.7×10^{12}
RED100	500 eV	19	Xe	200	LXe dual phase	NPP 3.1 GW	1.35×10^{13}
vGEN	200 eV _{ee}	11-12	Ge	1.4	HPGe	NPP 3.1 GW	5.4×10^{13}
TEXONO	200 eV _{ee}	28	Ge	1.43	p-PCGe	NPP 2×2.9 GW	6.4×10^{12}
NEON	200 eV _{ee}	23.7	Na(Tl)	16.7	scintillator	NPP 2×2.8 GW	$\sim \times 10^{13}$
SBC*	100 eV _{ee}		Ar	10		NPP 2×2.9 GW	

WHICH EXPERIMENTS HAVE OBSERVED CEvNS?

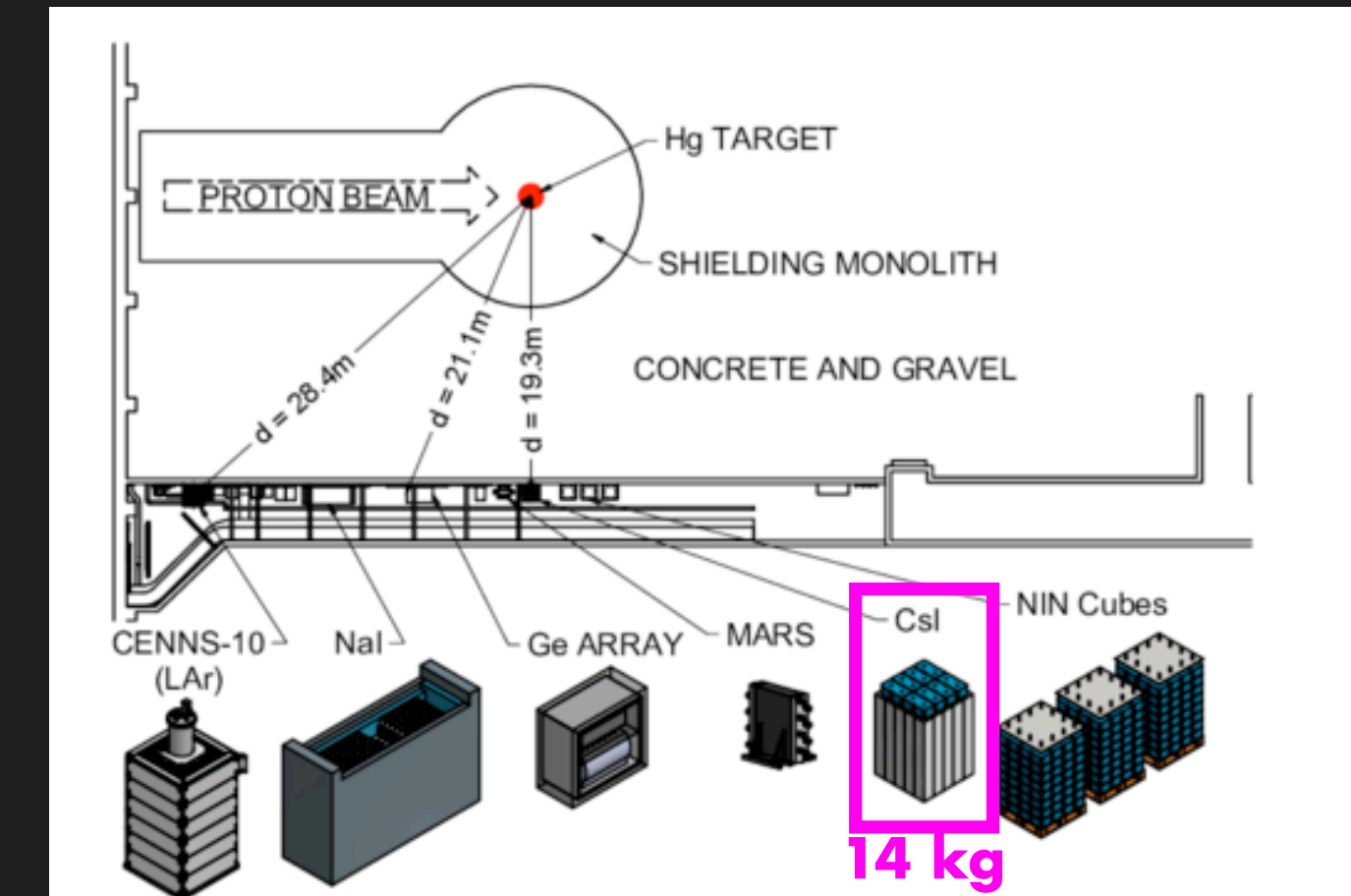


1st OBSERVATION OF CEvNS BY COHERENT



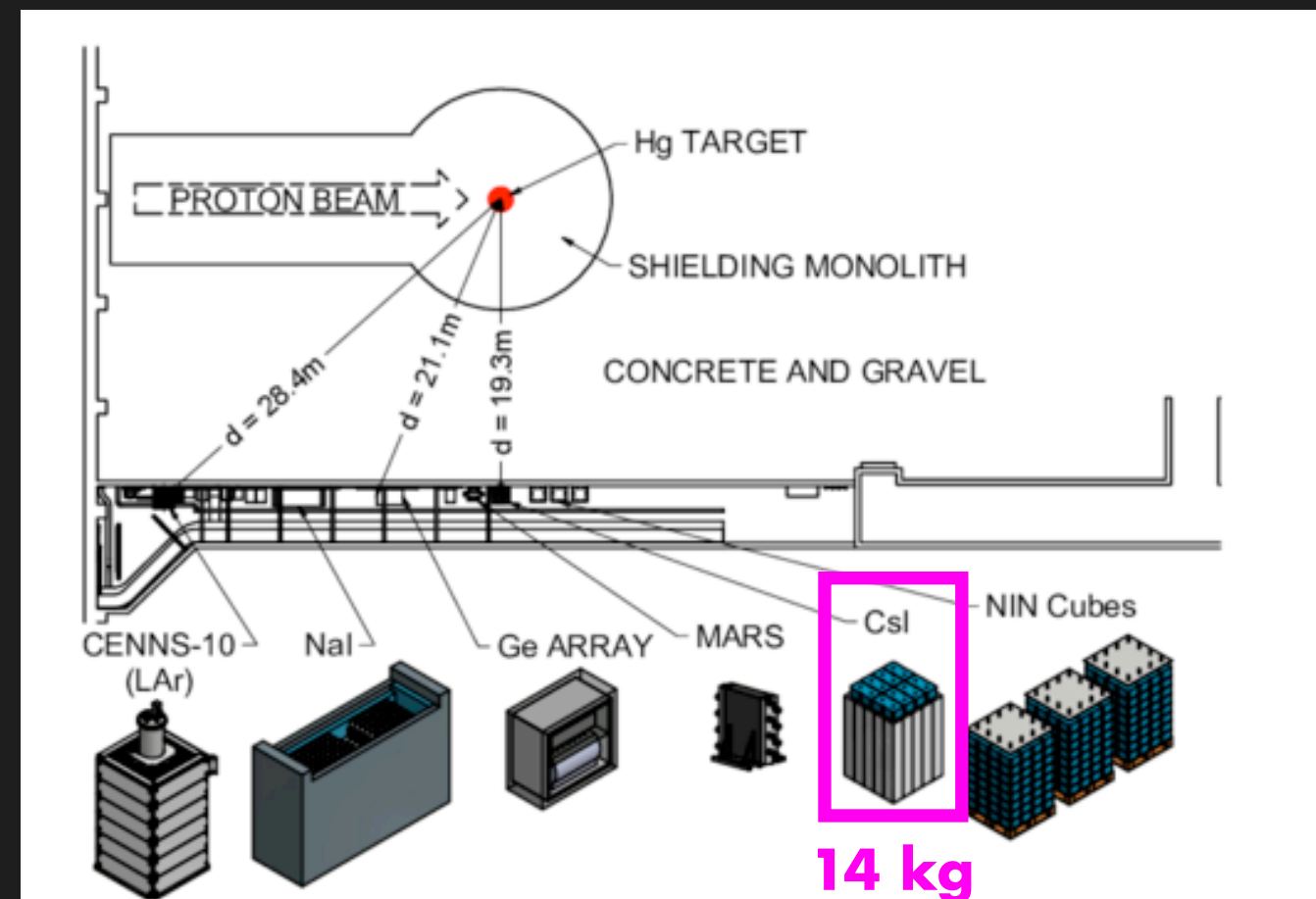
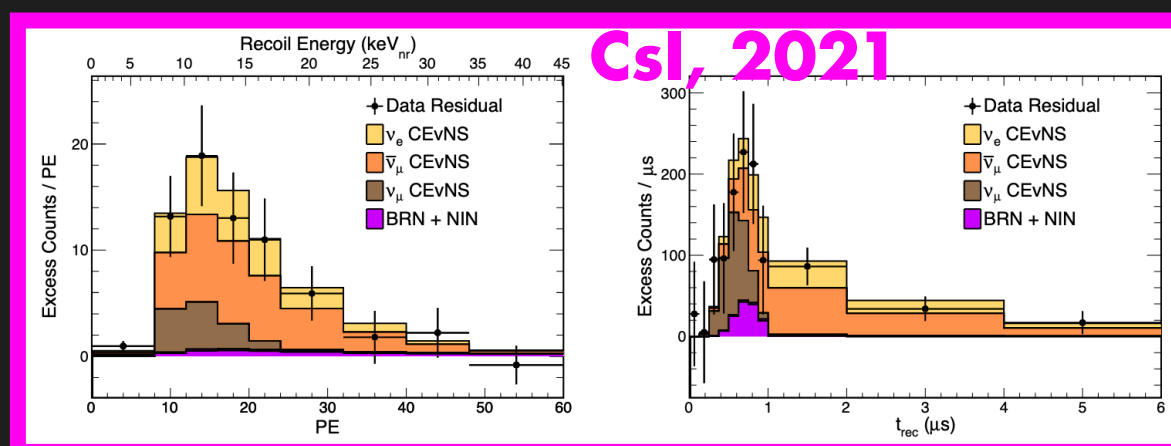
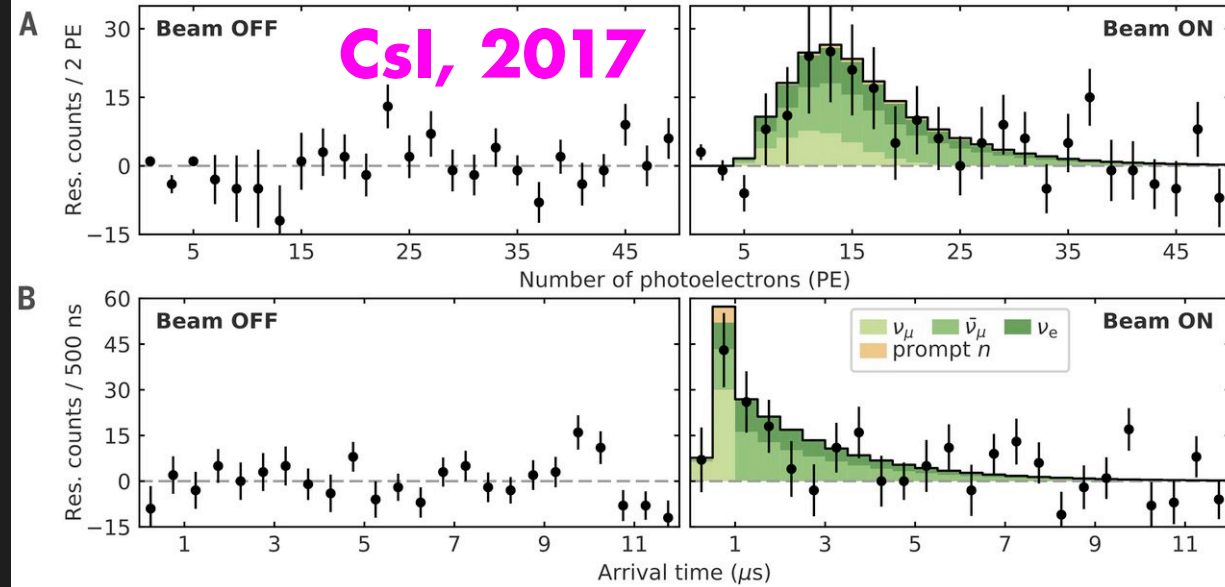
Observation at 6.7σ confidence level
 ~130 events observed

COHERENT-CsI[Na] was the world's
 smallest working neutrino detector!



D. Akimov et al. (COHERENT) Science 357, 1123–1126 (2017)

COHERENT CsI MEASUREMENT

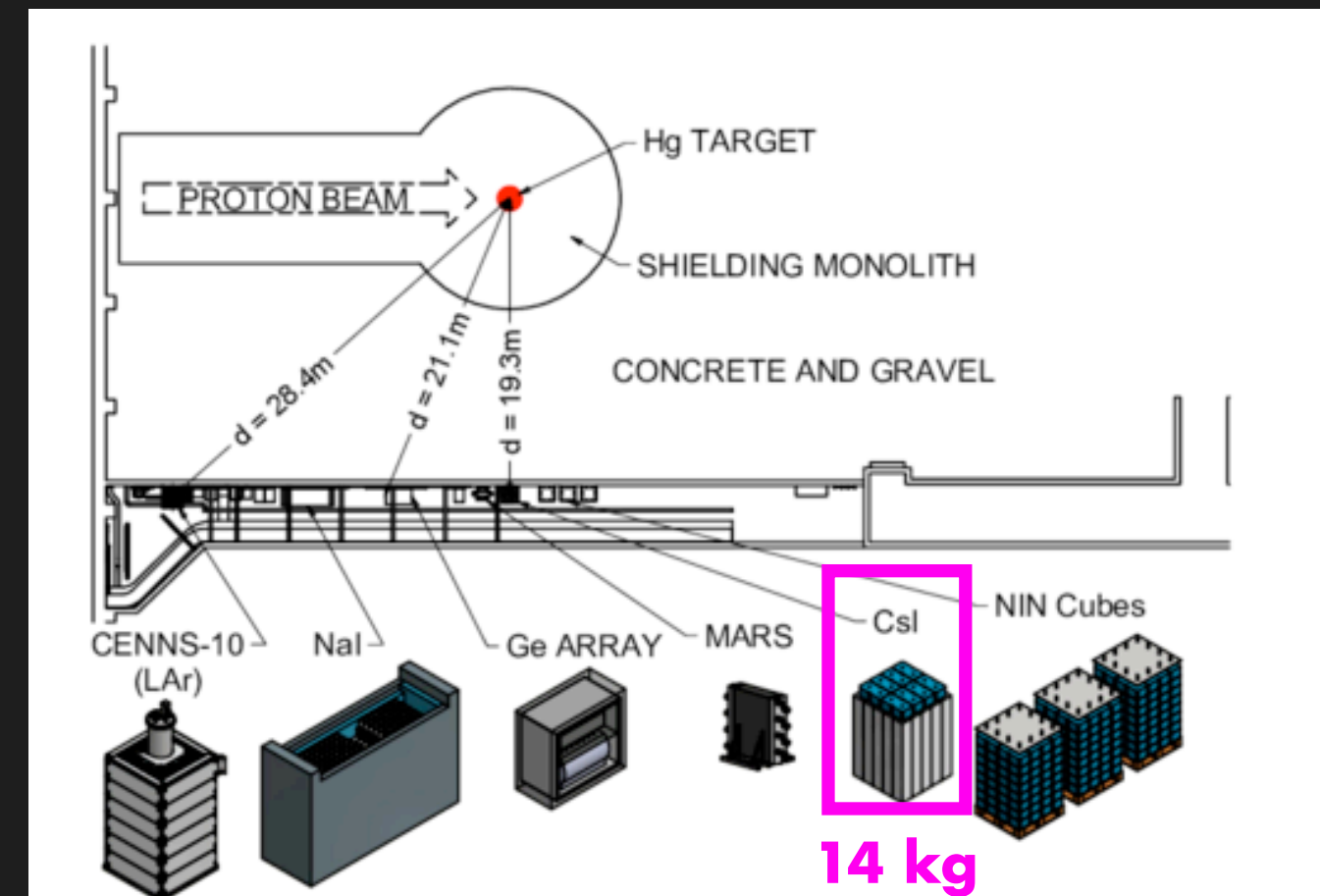
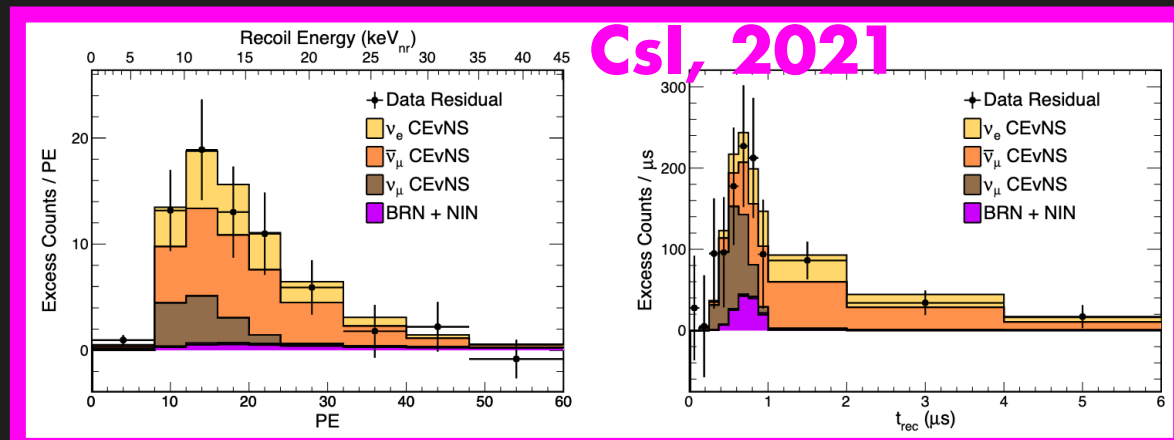


D. Akimov et al. (COHERENT) Science 357, 1123–1126 (2017)
 D. Akimov et al. (COHERENT) Phys. Rev. Lett. 129, 081801

COHERENT CsI MEASUREMENT

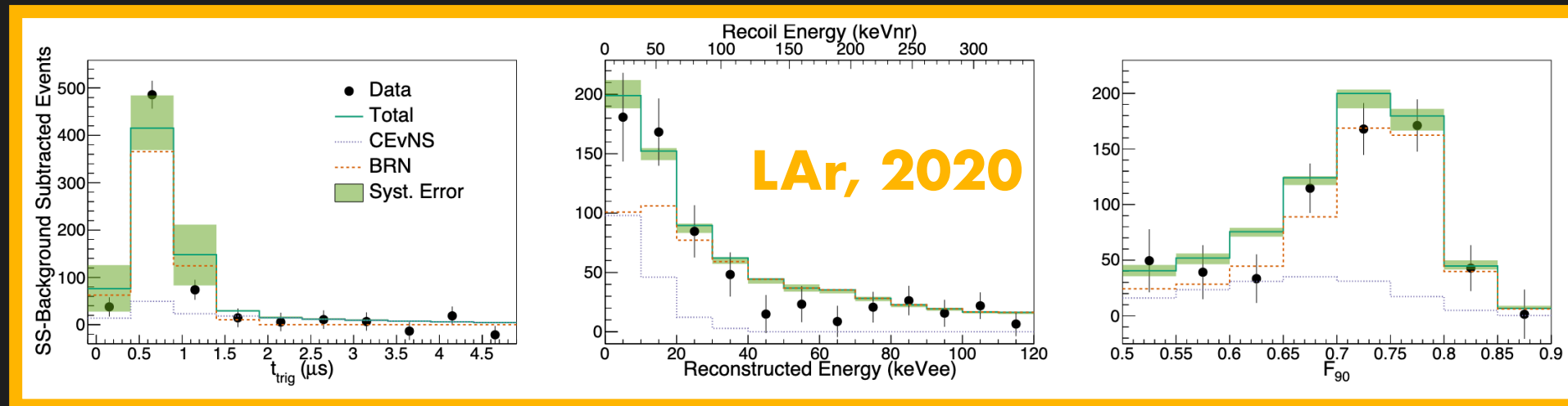
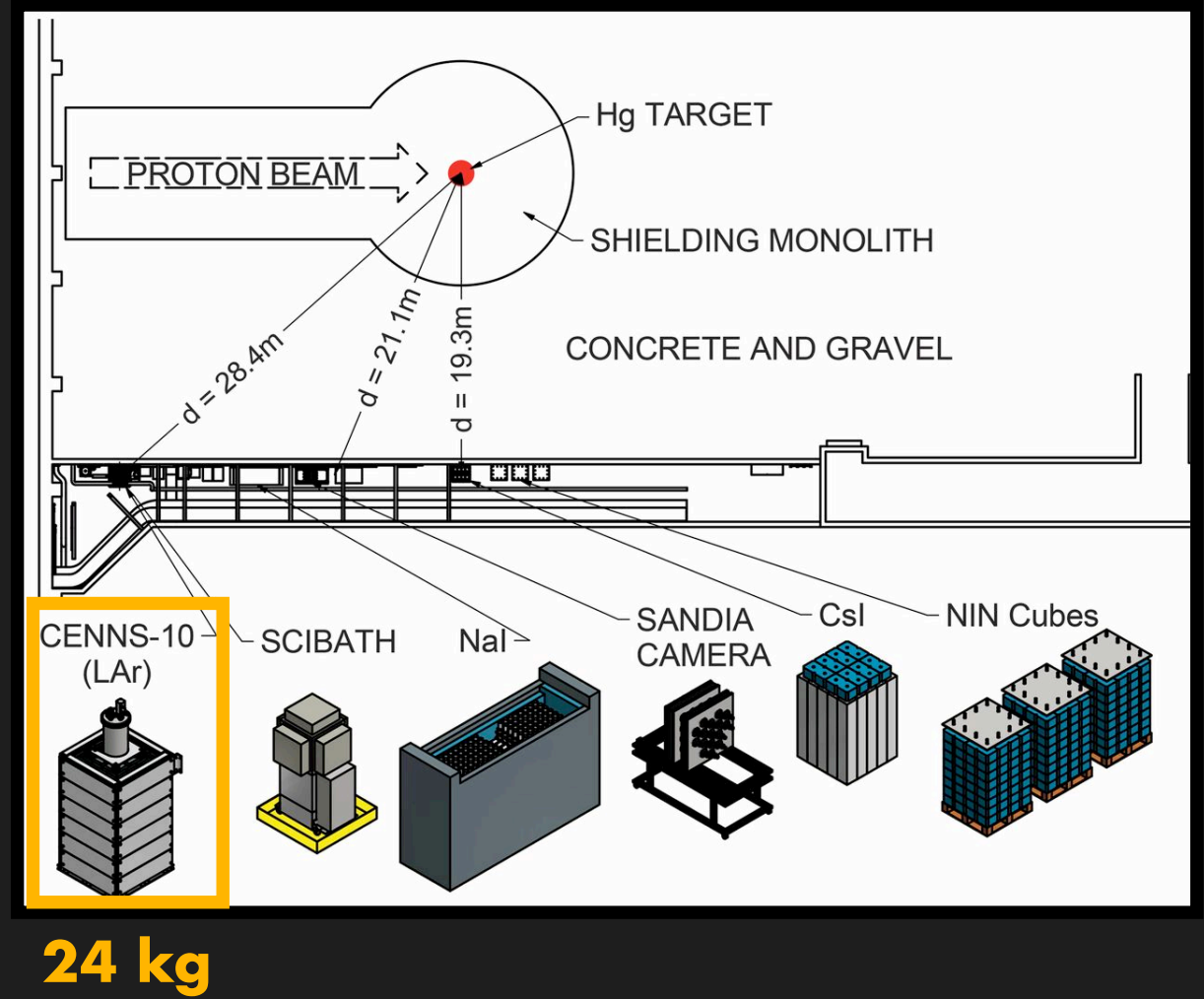
Full CsI[Na] dataset 2.2 times bigger, before decommissioning in 2019.
Updated scintillator response model, improved systematic uncertainties

Reject the no-CEvNS hypothesis at 11.6σ level
~300 events observed



D. Akimov et al. (COHERENT) Science 357, 1123–1126 (2017)
D. Akimov et al. (COHERENT) Phys. Rev. Lett. 129, 081801

COHERENT LAr MEASUREMENT

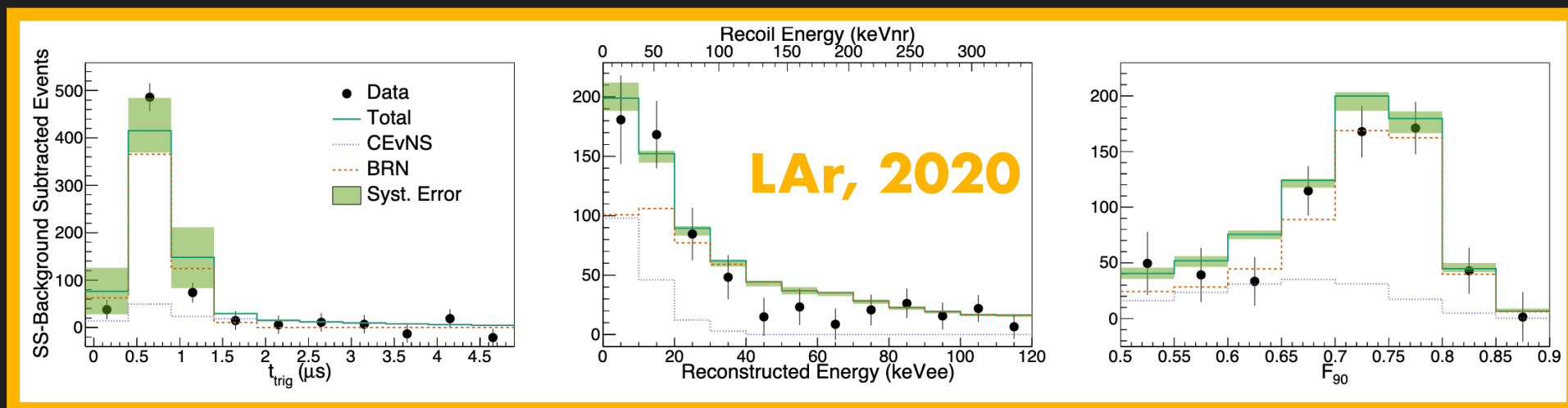


D. Akimov et al. (COHERENT). Phys. Rev. Lett. 126, 012002 (2021)

COHERENT LAr MEASUREMENT

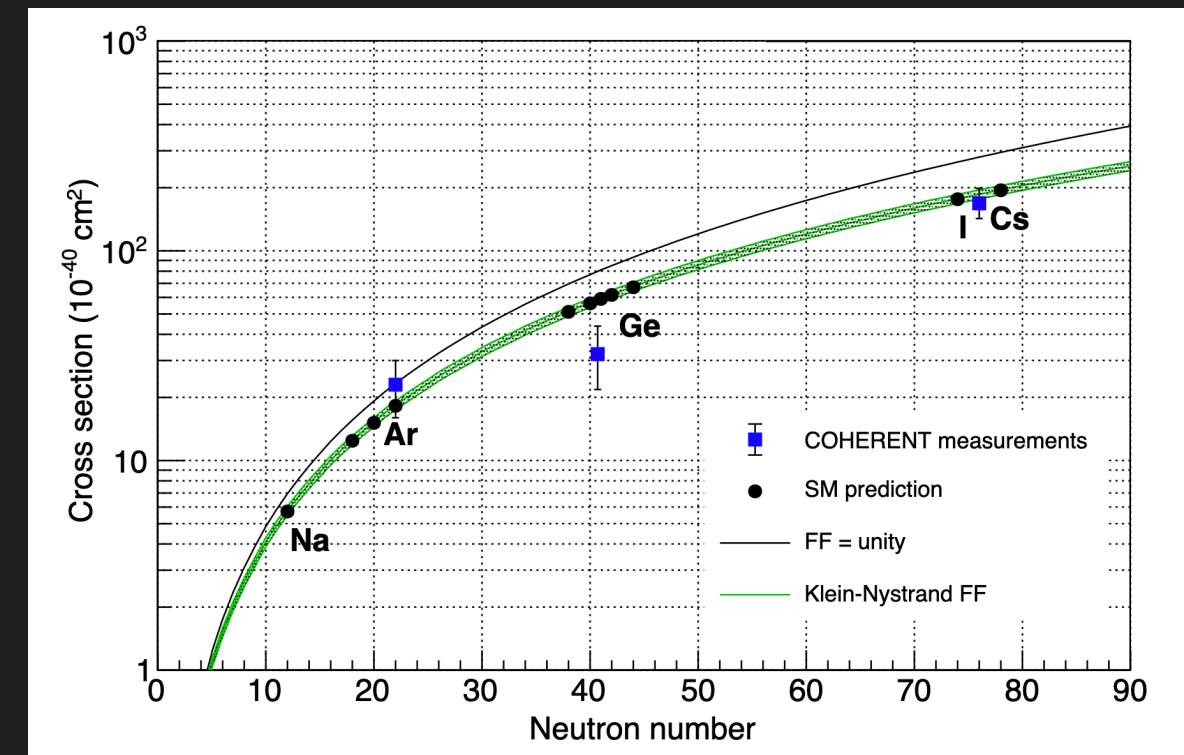
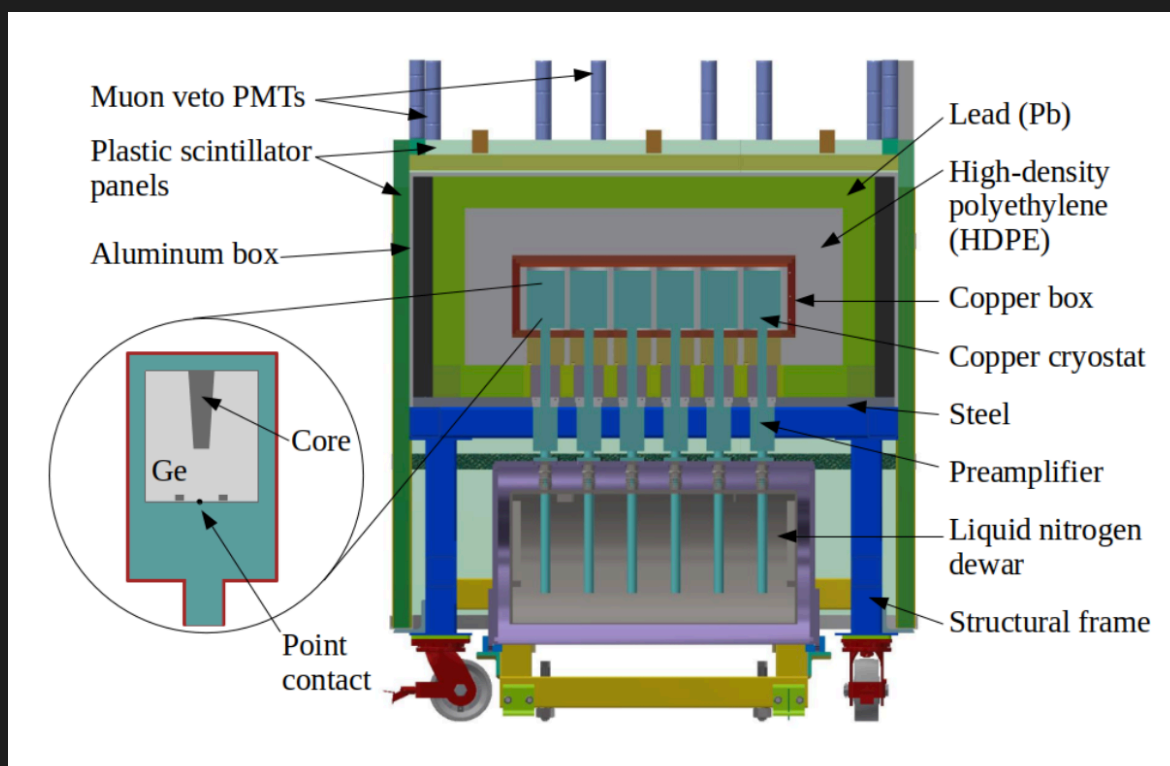


CENNS-10 Lar single-case (scintillation) detector.
Reject the no-CEvNS hypothesis at 3.9σ level
 ~ 150 events observed
First confirmation of its N^2 dependence



D. Akimov et al. (COHERENT). Phys. Rev. Lett. 126, 012002 (2021)

COHERENT-Ge MEASUREMENT

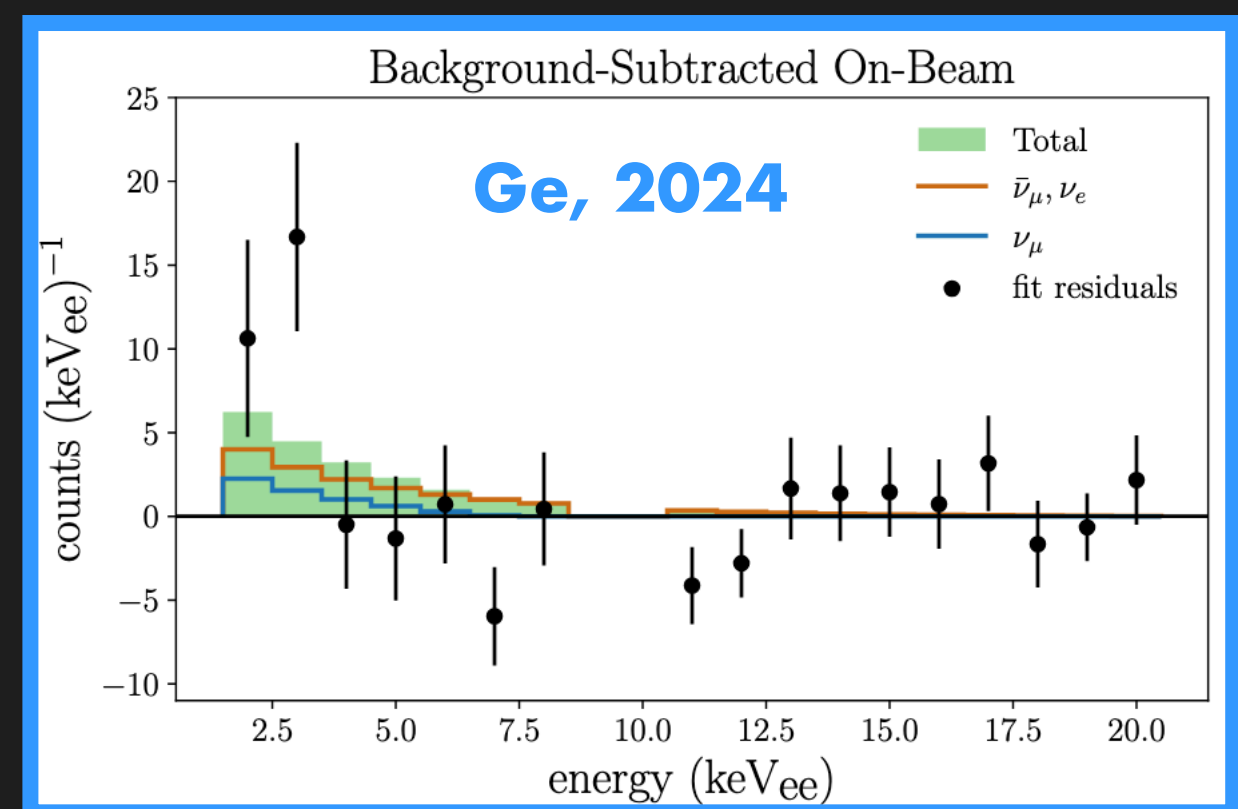


Ge-Mini detector system

~ 10 kg

Reject the no-CEvNS hypothesis at 3.9σ level
 ~ 20 events observed

S. Adamski et al. (COHERENT) arXiv: 2406.13806



EVIDENCE OF CEvNS ? AT NCC-1701 (DRESDEN-II REACTOR)

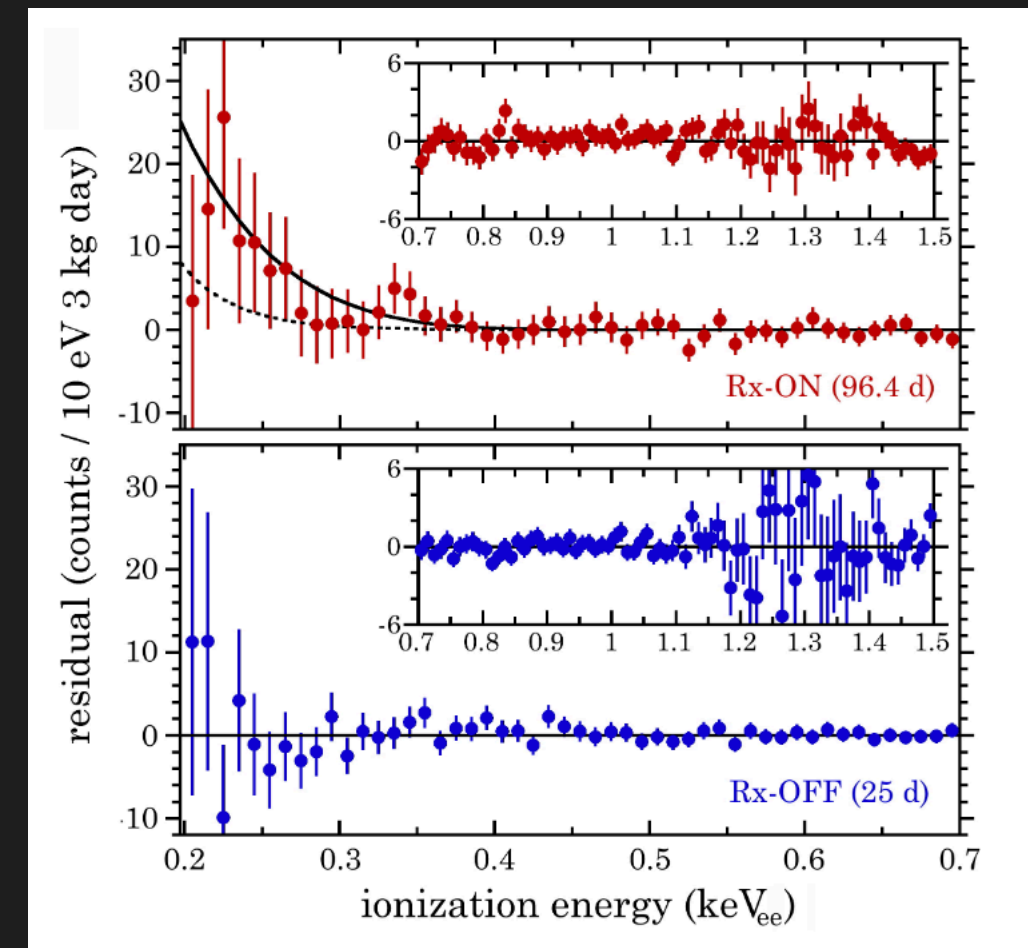
Neutrino source: Dresden-II boiling water reactor (USA) $2.96\text{GW} \rightarrow 4.8 \times 10^{13}$ neutrinos/sec/cm²

Detector: NCC-1701, a 2.924 kg ultra-low noise p-type point contact (PPC) Germanium detector

- low energy threshold (0.2 keV_{ee})
- distance to core: 10.39m
- 96.4-day exposure

CEvNS results: suggestive evidence of CEvNS is reported with strong preference (with respect to the background-only hypothesis)

- strongly dependent on quenching factor model

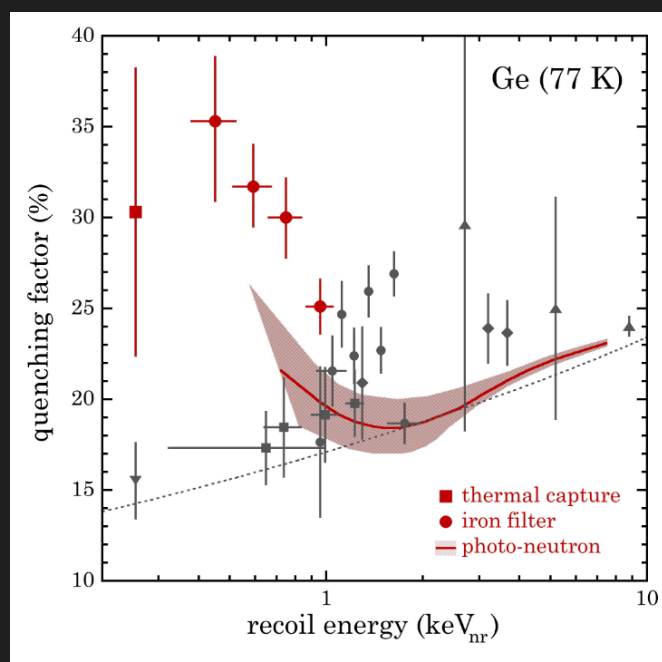


Colaresi, Collar et al. Phys. Rev. Lett. 129 (2022) 211802

EVIDENCE OF CEvNS? AT NCC-1701 (DRESDEN-II REACTOR)

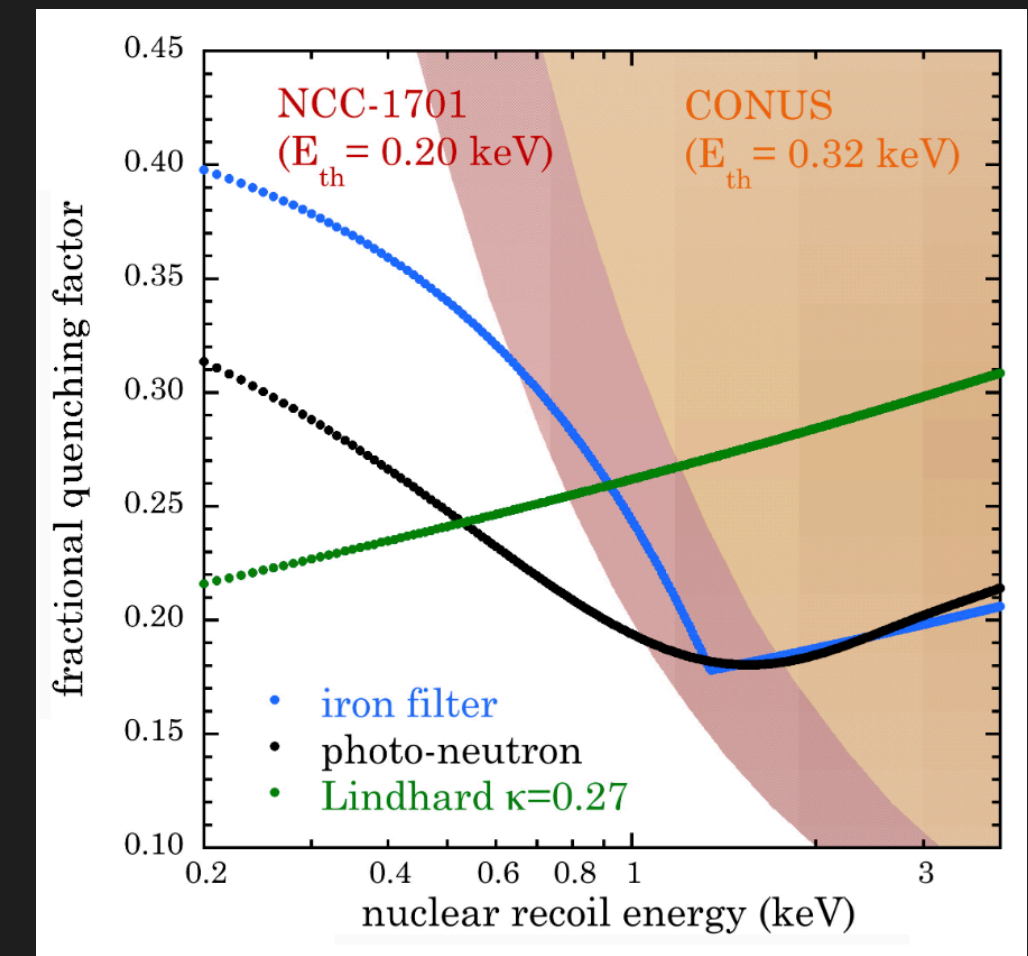
The quenching factor (QF) describes the observed reduction in ionization yield produced by a nuclear recoil when compared to an electron recoil of same energy

- often not (yet) well known at low recoil energies for CEvNS
- major uncertainty!



$$QF = E_{\text{meas}} / E_{\text{nuclear recoil}}$$

J.I. Collar et al, Phys. Rev. D 103, 122003

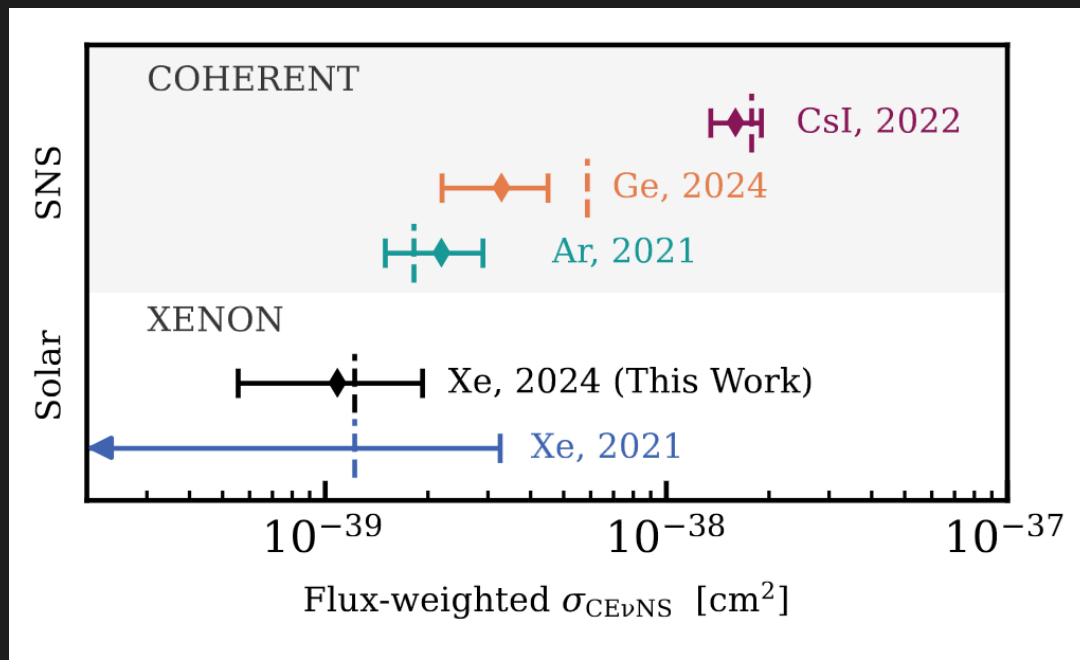


Colaresi et al., Phys. Rev. D 104, 072003 (2021)
Colaresi et al., 2202.09672 [hep-ex]

CONUS: Direct measurement of ionization quenching factor: $k=0.162 \pm 0.004$ (compatible with Lindhard)

CONUS Phys. Rev. Lett. 126, 041804

XENONnT

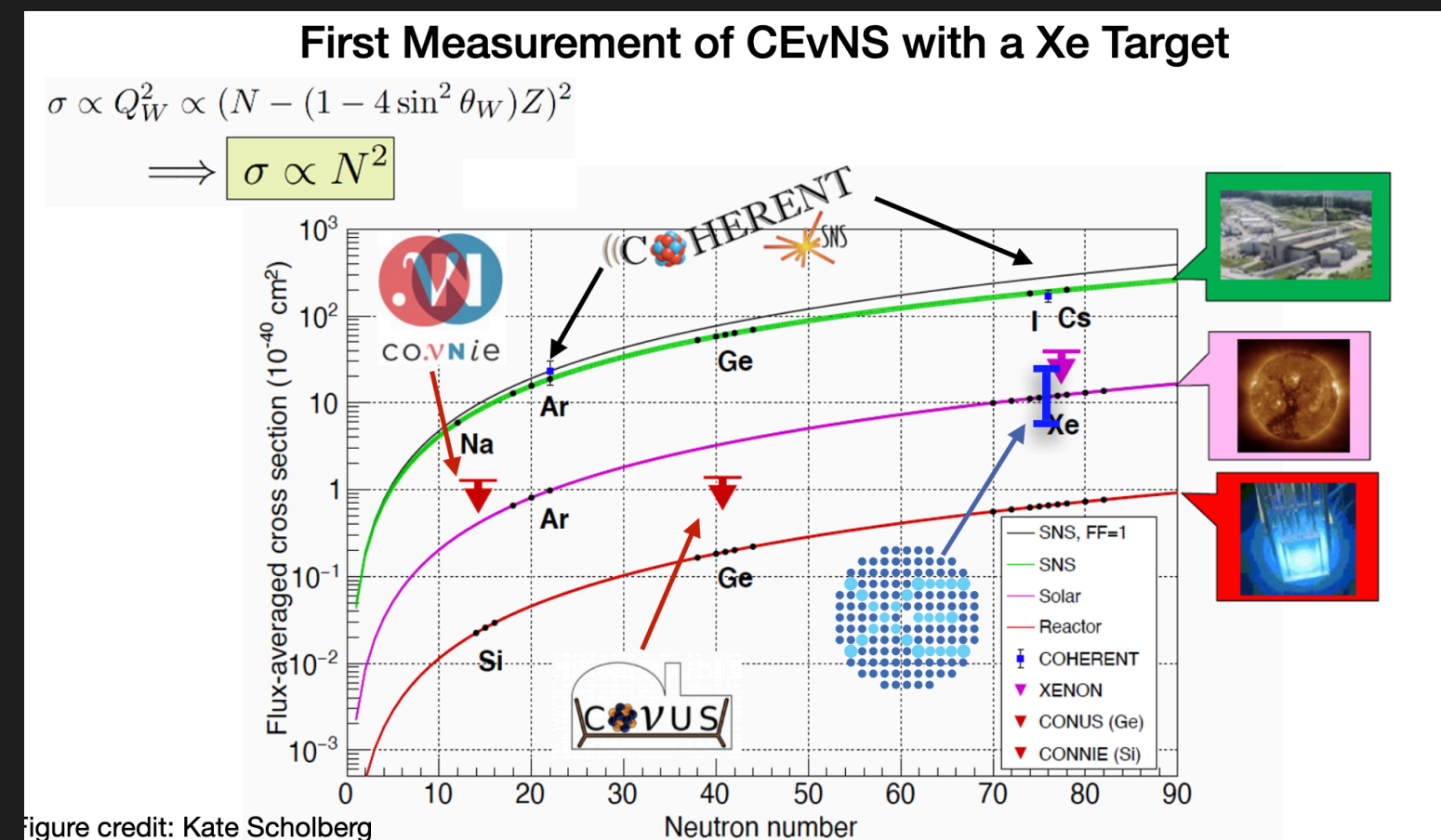


Aprile et al. arXiv:2408.02877v1

XENONnT “measures” the CEvNS signal in Xe from solar 8B neutrinos for the first time.

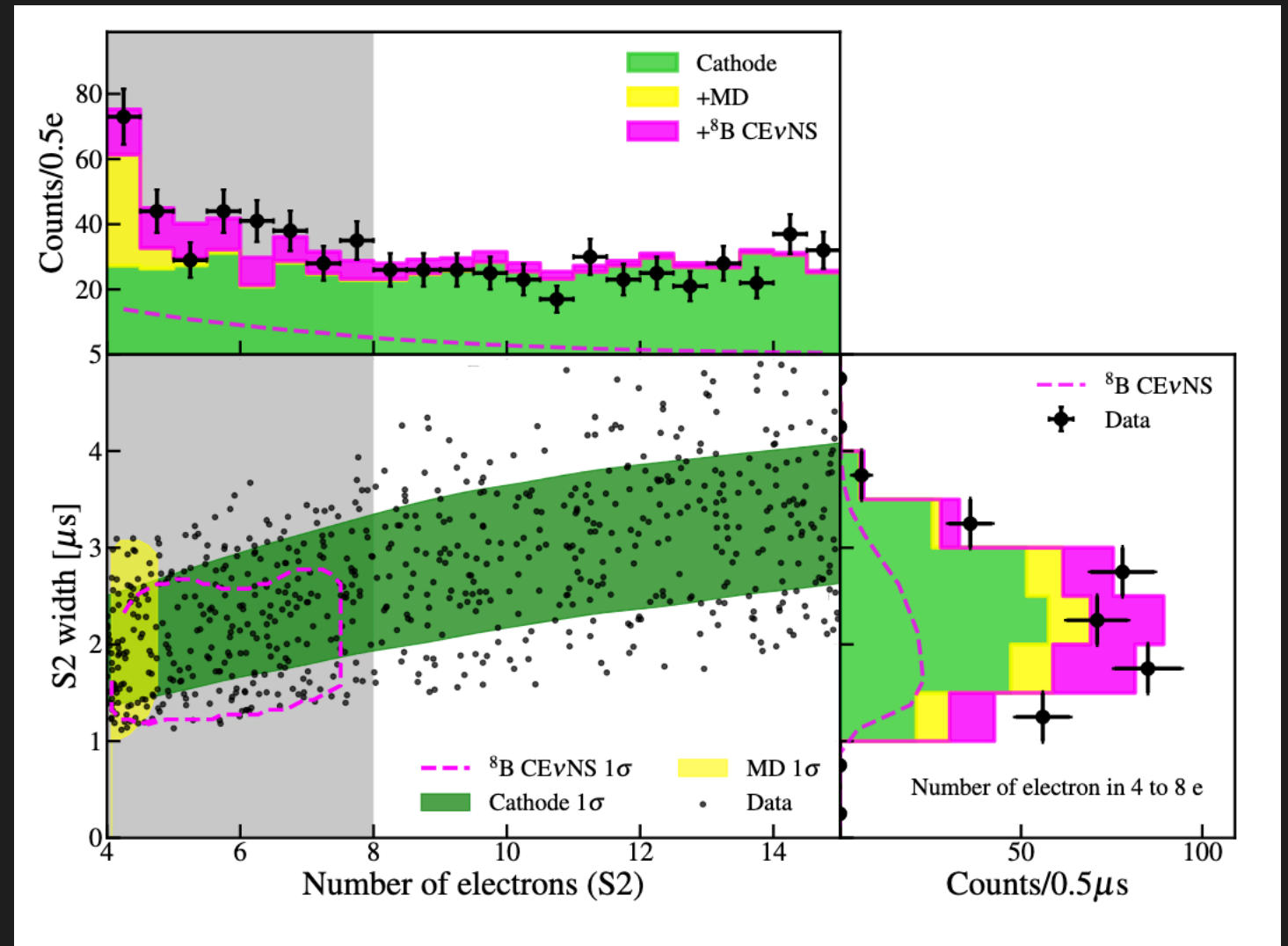
The background-only hypothesis is disfavored at 2.73σ

From Fei Gao’s talk @ IDM 2024



PandaX-4T

A combined analysis yields a best-fit ${}^8\text{B}$ neutrino signal of 3.5 (75) events from the scintillation and ionization (ionization-only) data sample.



Z. Bo et al. (PandaX collaboration) arXiv:2407.10892

The background-only hypothesis is disfavored at 2.64σ significance

LIST OF EXPERIMENTAL PAPERS

1. Coherent Elastic Neutrino-Nucleus Scattering Search in the ν GeN Experiment, Phys.Part.Nucl.Lett. 21 (2024) 4, 680-682
2. First Measurement of SolarB Neutrino Flux through Coherent Elastic Neutrino-Nucleus Scattering in PandaX-4T, Zihao Bo et al. (PandaX), [arXiv:2407.10892](#)
3. First detection of coherent elastic neutrino-nucleus scattering on germanium, S. Adamski et al. (COHERENT), [arXiv:2406.13806](#)
4. Final CONUS results on coherent elastic neutrino-nucleus scattering at the Brokdorf reactor, N. Ackermann et al. (CONUS), [arXiv:2401.07684](#)
5. First results of the nuGeN experiment on coherent elastic neutrino-nucleus scattering, I. Alekseev et al. (nuGeN), Phys.Rev.D 106 (2022) L051101, [arXiv:2205.04305](#).
6. Suggestive evidence for Coherent Elastic Neutrino-Nucleus Scattering from reactor antineutrinos, J. Colaresi, J.I. Collar, T.W. Hossbach, C.M. Lewis, K.M. Yocum, Phys.Rev.Lett. 129 (2022) 211802, [arXiv:2202.09672](#)
7. Search for coherent elastic neutrino-nucleus scattering at a nuclear reactor with CONNIE 2019 data, Alexis Aguilar-Arevalo et al. (CONNIE), JHEP 22 (2020) 017, [arXiv:2110.13033](#)
8. Measurement of the Coherent Elastic Neutrino-Nucleus Scattering Cross Section on CsI by COHERENT, D. Akimov et al. (COHERENT), Phys.Rev.Lett. 129 (2022) 081801, [arXiv:2110.07730](#)
9. First results from a search for coherent elastic neutrino-nucleus scattering (CEvNS) at a reactor site, J. Colaresi, J. I. Collar, T. W. Hossbach, A. R. L. Kavner, C. M. Lewis, A. E. Robinson, K. M. Yocum, Phys.Rev.D 104 (2021) 072003, [arXiv:2108.02880](#)
10. Search for coherent elastic scattering of solar 8B neutrinos in the XENON1T dark matter experiment, E. Aprile et al. (XENON), Phys.Rev.Lett. 126 (2021) 091301, [arXiv:2012.02846](#)
11. COHERENT Collaboration data release from the first detection of coherent elastic neutrino-nucleus scattering on argon, D. Akimov et al. (COHERENT), [arXiv:2006.12659](#)
12. First Detection of Coherent Elastic Neutrino-Nucleus Scattering on Argon, D. Akimov et al. (COHERENT), Phys.Rev.Lett. 126 (2021) 012002, [arXiv:2003.10630](#)
13. First Constraint on Coherent Elastic Neutrino-Nucleus Scattering in Argon, D. Akimov et al. (COHERENT), Phys.Rev. D100 (2019) 115020, [arXiv:1909.05913](#)
14. COHERENT Collaboration data release from the first observation of coherent elastic neutrino-nucleus scattering, D. Akimov et al. (COHERENT), [arXiv:1804.09459](#)
15. Observation of Coherent Elastic Neutrino-Nucleus Scattering, D. Akimov et al. (COHERENT), Science 357 (2017) 1123-1126, [arXiv:1708.01294](#)

CEVNS CROSS SECTION: STANDARD MODEL

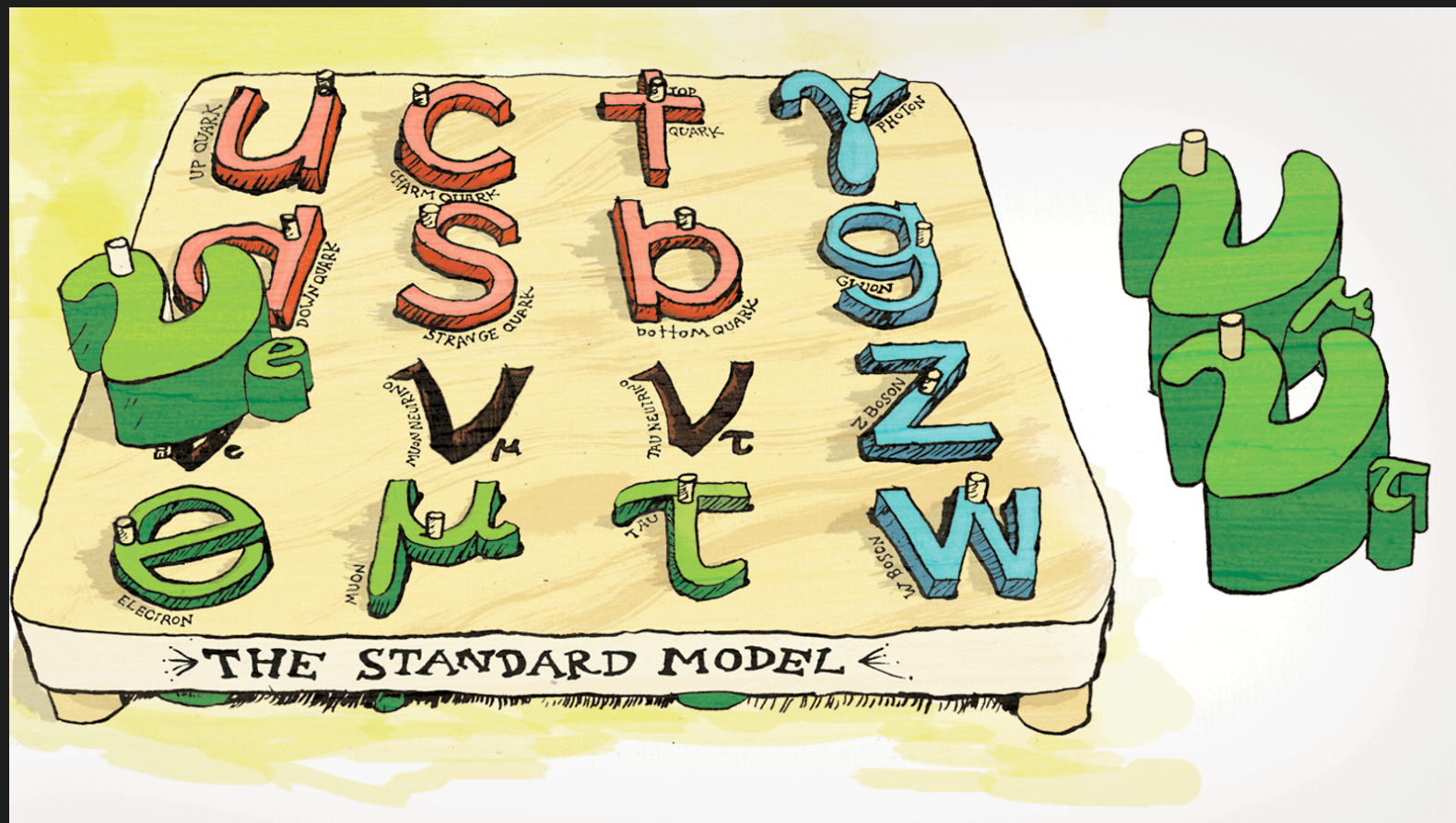


Illustration by Sandbox Studio, Chicago

CE ν NS CROSS SECTION IN THE SM

Interplay of particle, hadronic and nuclear physics

$$\frac{d\sigma_{\nu\mathcal{N}}}{dE_{\text{nr}}} \Big|_{\text{CE}\nu\text{NS}}^{\text{SM}} \propto \left| \sum_i c_i \text{kin}_i \mathcal{F}_i \right|^2$$

Kin_i : kinematics terms

C_i : particle physics coefficients (coupling neutrino-quarks)

\mathcal{F}_i : nuclear structure physics

In the Donnelly-Walecka approach any semi-leptonic nuclear process at low and intermediate energies can be described by an effective interaction Hamiltonian, written in terms of the leptonic and hadronic currents

$$\langle \text{final} | \mathcal{L} | \text{initial} \rangle = \langle \text{final} | \int d^3\mathbf{x} \hat{j}_\mu^{\text{lept}}(\mathbf{x}) \hat{J}^\mu(\mathbf{x}) | \text{initial} \rangle$$

The accurate evaluation of the required transition matrix elements is obtained on the basis of reliable nuclear wave functions.

CE ν NS CROSS SECTION IN THE SM

We follow a multi-step process:

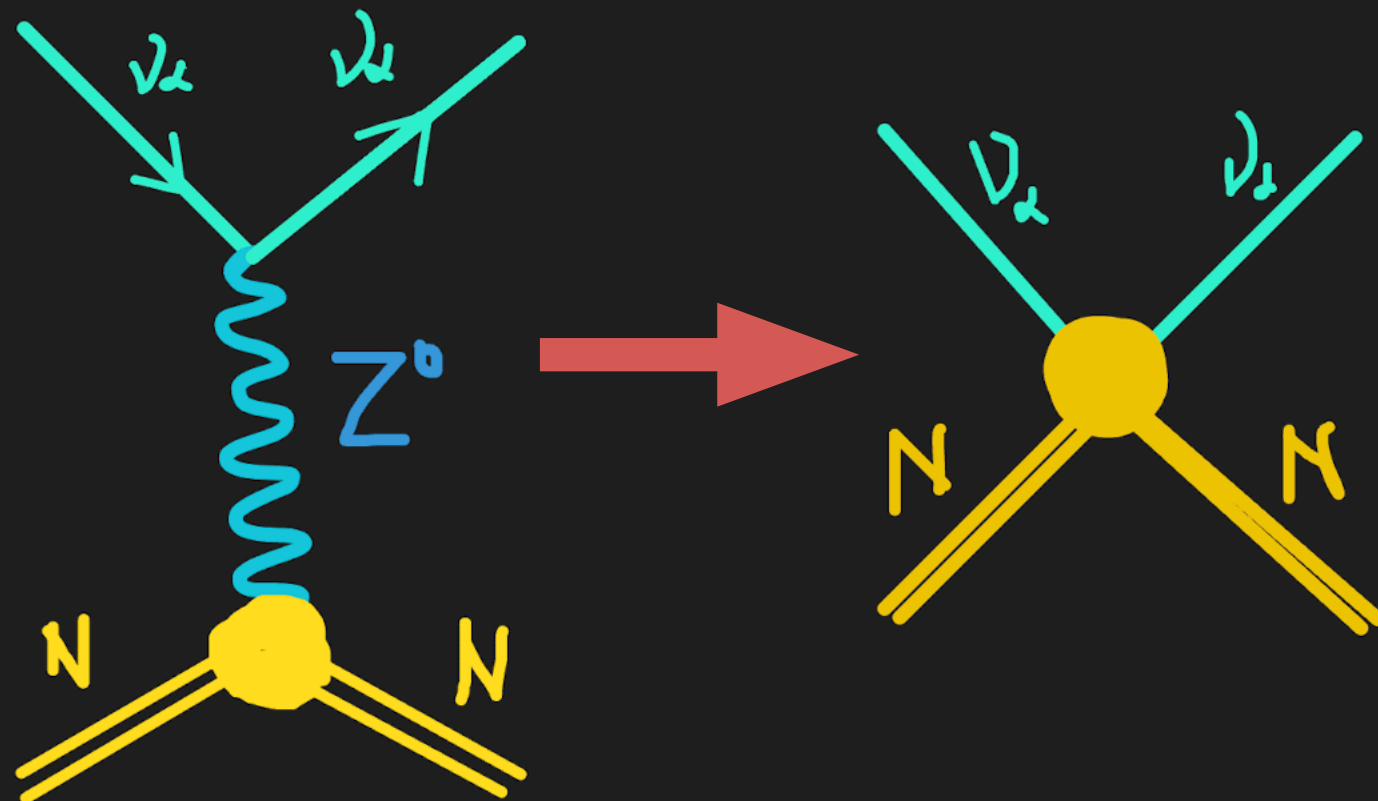
1. First, we define the **effective neutrino-quark interaction** in the non-relativistic limit (small momentum transfer) — same as going from the electroweak theory to the Fermi four-fermion theory
2. Second, we need to **account for the quark content of the nucleons**: we need to take the quark field operators and express them in terms of nucleon ones
3. Finally, we need to promote the operators at the nucleon level to the nuclear one. We need a **nuclear model**.

Freedman Phys. Rev. D 9, 1389-1392 (1974)
Drukier, Stodolsky, PRD 30 (1984) 2295
Amanik+ Astropart.Phys. 24 (2005) 160-182
J. Barranco+ JHEP 0512 (2005) 021
Papoulias+ Advances in High Energy Physics, vol. 2015, 763648
Lindner+ JHEP03(2017)097
Hoferichter+ Physical Review D 102, 074018 (2020)
Tomalak+ JHEP 2102, 097 (2021) (Radiative corrections)
Pandey Prog.Part.Nucl.Phys. (2023)
Khaleq+ arXiv:2405.20060

CEvNS CROSS SECTION IN THE SM

We want to compute the cross-section for the process $\nu_\ell \mathcal{N} \rightarrow \nu_\ell \mathcal{N}$.
Elastic process: final state nucleus remains unvaried.

The momentum transfer is much smaller than the mass of the mediator, so we can define an effective Lagrangian for the process.



CEvNS CROSS SECTION IN THE SM

$$\mathcal{L}_{\text{eff}}^{\text{NC}} = \frac{G_F}{\sqrt{2}} \sum_q [\bar{\nu} \gamma^\mu (g_V^\nu - g_A^\nu \gamma^5) \nu] [\bar{q} \gamma_\mu (g_V^q - g_A^q \gamma^5) q]$$

The Lagrangian is defined as a sum of the interactions at the quark level.
The vector and axial couplings at the tree level are:

$$g_V^\nu = 1/2 \quad g_V^q = \boxed{T_3^q} - 2Q^q \sin^2 \theta_W = \begin{cases} 1/2 - 1/3 \sin^2 \theta_W & q = u, c, t \\ -1/2 + 2/3 \sin^2 \theta_W & q = d, s, b \end{cases}$$

3rd component
Weak Isospin

The term $\bar{q} \gamma^\mu \gamma^5 q$ is the spin-dependent one. It is suppressed compared to the vector current. Only relevant for light nuclei with non-zero spin. Nuclei with even number of protons and neutrons have zero spin, so that axial terms vanish.

CEvNS CROSS SECTION IN THE SM

Promote the quark operators to the nucleon level.

Project the quark current on the initial and final nucleon states:

$$\langle \eta(p_f) | \mathcal{O}_q | \eta(p_i) \rangle = \langle \eta(p_f) | \bar{q} \gamma^\mu q | \eta(p_i) \rangle$$

$$= \bar{u}_N \left(\boxed{F_1^{q,\eta}(\mathbf{q}^2) \gamma^\mu} + F_2^{q,\eta}(\mathbf{q}^2) \frac{i\sigma^{\mu\nu} q_\nu}{2m_\eta} \gamma^\mu \right) u_N$$

The nucleon matrix element can be parametrized by means of its transformation properties under the Lorentz symmetry, spatial parity and time reversal. F_2 is suppressed (involves spin and goes as \mathbf{q}/m_η). At zero momentum transfer, vector currents ‘count’ the valence quarks in the nucleon.

$$\sum_{\eta=n,p} \sum_q \langle g_V^q \eta(p_f) | \bar{q} \gamma^\mu q | \eta(p_i) \rangle$$

$$= \boxed{g_v^u + 2g_v^d} \bar{n} \gamma^\mu n + \boxed{(2g_v^u + g_v^d)} \bar{p} \gamma^\mu p$$

g_v^p

g_v^n

CEvNS CROSS SECTION IN THE SM

Final step: we need to go from interaction with nucleons to interaction with the nucleus.
At non-zero momentum transfer there will be a form-factor suppression given by the specific nuclear wave.

Construct the nuclear operator:

$$\langle \mathcal{N}(k_f) | \bar{\eta} \gamma^\mu \eta | \mathcal{N}(k_i) \rangle = \boxed{N_\eta} \bar{\mathcal{N}} \gamma^\mu \mathcal{N} F_v^\eta(\mathbf{q}^2)$$

Counts
nucleons
inside nuclei

$$= [Zg_v^p F_v^p(\mathbf{q}^2) + Ng_v^n F_v^n(\mathbf{q}^2)] \bar{\mathcal{N}} \gamma^\mu \mathcal{N}$$

The weak form factor is defined as

$$\tilde{F}_w(\mathbf{q}^2) = [Zg_v^p F_v^p(\mathbf{q}^2) + Ng_v^n F_v^n(\mathbf{q}^2)]$$

And then normalized to one through (valid at $\mathbf{q} \rightarrow 0$)

$$Q_w = (Zg_v^p + Ng_v^n) = -N/2 + (1/2 - 2\sin^2\theta_w)Z \quad F_w(\mathbf{q}^2) = \frac{\tilde{F}_w(\mathbf{q}^2)}{Q_w}$$

CEvNS CROSS SECTION IN THE SM

$$\mathcal{L}_{\text{eff}}^{\text{NC}} = \frac{G_F}{\sqrt{2}} \sum_q [\bar{\nu} \gamma^\mu P_L \nu] \left[Q_w F_w(\mathbf{q}^2) \bar{\mathcal{N}} \gamma_\mu \mathcal{N} \right]$$

Assume the nucleus is in a fermionic ground state, we can compute the amplitude squared of the process, starting from the matrix element

$$\mathcal{M}^{ss'rr'} = \frac{G_F}{\sqrt{2}} Q_w F_w(\mathbf{q}^2) [\bar{u}^{s'}(p') \gamma^\mu P_L u^s(p)] [\bar{u}^{r'}(k') \gamma_\mu u^r(k)]$$

$$|\mathcal{M}|^2 = \frac{G_F^2}{4} Q_w^2 F_w^2(\mathbf{q}^2) \boxed{L^{\mu\nu}} \boxed{W_{\mu\nu}}$$

Lepton tensor Hadron tensor

CE ν NS CROSS SECTION IN THE SM

$$\frac{d\sigma_{\nu\mathcal{N}}}{dE_{\text{nr}}} \Big|_{\text{CE}\nu\text{NS}}^{\text{SM}} = \frac{G_F^2 m_N}{128\pi} \frac{Q_w^2 F_w^2(\mathbf{q}^2)}{E_\nu^2 m_N} L^{\mu\nu} W_{\mu\nu}$$

Performing all traces calculations one obtains

$$\boxed{\frac{d\sigma_{\nu\mathcal{N}}}{dE_{\text{nr}}} \Big|_{\text{CE}\nu\text{NS}}^{\text{SM}} = \frac{G_F^2 m_N}{\pi} F_w^2(\mathbf{q}^2) Q_w^2 \left(1 - \frac{m_N E_{\text{nr}}}{2E_\nu^2} - \frac{E_{\text{nr}}}{E_\nu} + \frac{E_{\text{nr}}^2}{2E_\nu^2} \right)}$$

$$Q_w = -N/2 + (1/2 - 2\sin^2\theta_w)Z$$

$\sin^2\theta_w = 0.23 \rightarrow$ protons unimportant
Neutron contribution dominates

FORM FACTORS

The form factor corrects for scattering that is not completely coherent at higher energies. It encodes information about the nuclear densities through a Fourier transform of the nuclear charge density distribution

$$F_{n,p}(q^2) = \frac{1}{Q_a} \int \rho_{p,n}(\vec{r}) e^{i\vec{q}\cdot\vec{r}} d^3\vec{r}$$

Q_a is the charge of the entire distribution.

Assuming a spherically symmetrical distribution:

$$F_{n,p}(q^2) = \frac{4\pi}{Q_a q} \int \rho_{p,n}(r) \sin(q \cdot r) r dr$$

- Patton et al, arXiv:1207.0693
Bednyakov, Naumov, arXiv:1806.08768
Papoulias et al, Phys.Lett. B800 (2020) 135133
Ciuffoli et al, arXiv:1801.02166
Canas et al, arXiv:1911.09831
Van Dessel et al, arXiv:2007.03658
Aristizabal-Sierra JHEP 1906:141 (2019)
Coloma+ JHEP 08 (2020) 08, 030
Aristizabal-Sierra Phys.Lett.B 845 (2023) 138140

FORM FACTORS

We can expand the form factor in terms of q:

$$F_{n,p}(q^2) \approx \int \rho_{p,n}(r) \left(1 - \frac{q^2}{3!} r^2 + \frac{q^4}{5!} r^4 - \frac{q^6}{7!} r^6 + \dots \right) r^2 dr$$
$$\approx 1 - \frac{q^2}{3!} \langle R_{p,n}^2 \rangle + \frac{q^4}{5!} \langle R_{p,n}^4 \rangle - \frac{q^6}{7!} \langle R_{p,n}^6 \rangle + \dots$$

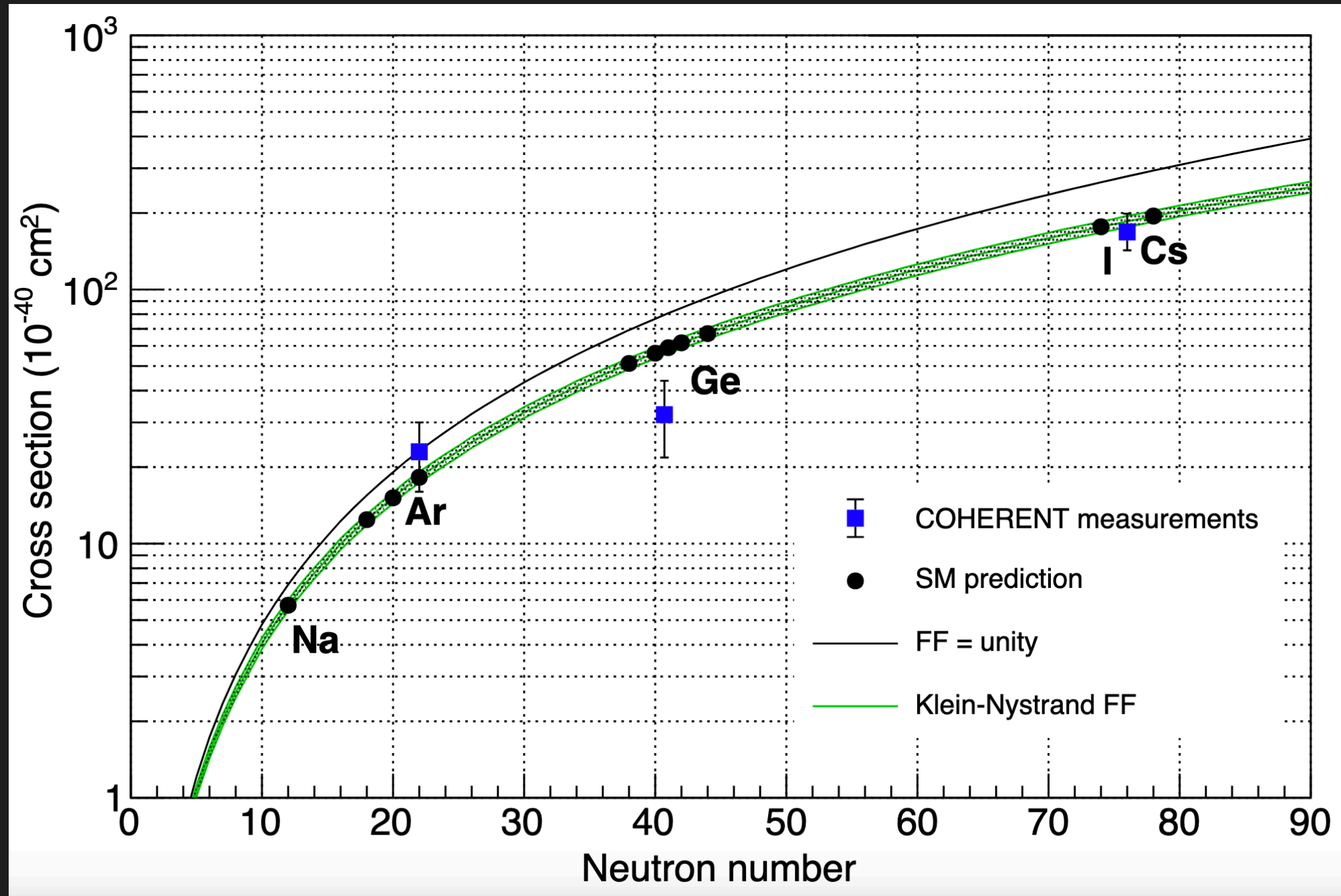
with the k-th radial moment defined as

Patton et al, arXiv:1207.0693
Papoulias et al, Phys.Lett. B800 (2020) 135133

$$\langle R_{p,n}^k \rangle = \frac{\int \rho_{p,n}(\vec{r}) r^k d^3\vec{r}}{\int \rho_{p,n}(\vec{r}) d^3\vec{r}}$$

In this way the form factor is a sum of the even moments of the neutron density distribution, that represent physically relevant and measurable quantities.

FORM FACTORS

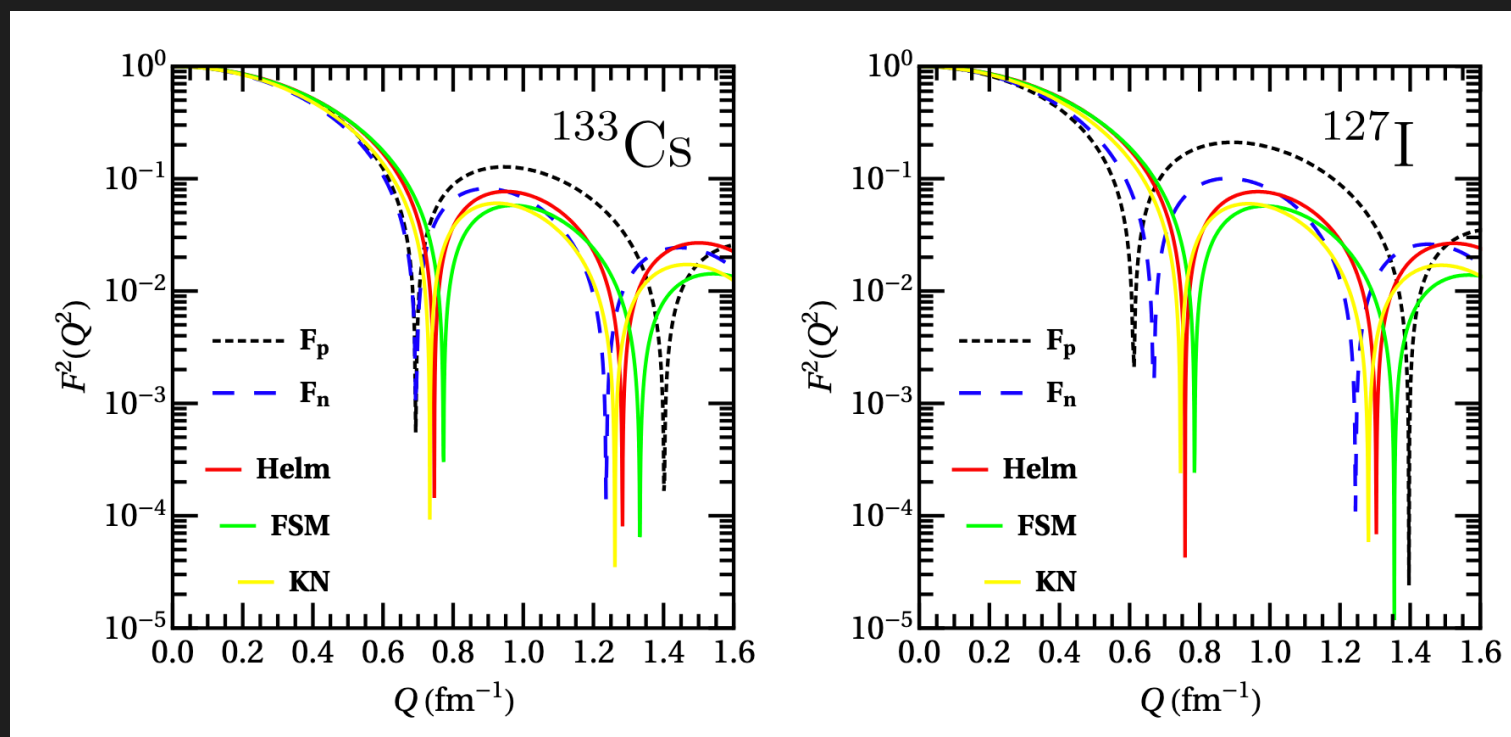


From Ryan Bouabid's talk @Magnificent CEvNS2024

FORM FACTORS

How to obtain the nuclear form factors:

- Nuclear structure calculations; S. Kosmas+ Nucl. Phys. A 570 (1994) 637
Papoulias+ Phys.Lett. B800 (2020) 135133
- Use of available experimental data: the proton nuclear form factors are computed by means of a model-independent analysis (using a Fourier-Bessel expansion model or others) of the electron scattering data for the proton charge density; De Vries+ Data and Nucl. Data Tables 36 (1987) 495536
- Use of analytical approximations for the nuclear form factors.



Papoulias+ Phys.Lett. B800 (2020) 135133

FORM FACTORS: PARAMETRIZATIONS

The basic properties of nucleonic distributions can be described by different parametrizations.

J. Engel, Phys.Lett. B 264 (1991) 114

In the Helm model, the nuclear form factor is given by the convolution of two nucleonic densities: a uniform-density one with a cut-off radius R_0 and a second one with a Gaussian profile, in terms of the surface thickness s .

$$F_{\text{Helm}}(q^2) = 3 \frac{j_1(qR_0)}{qR_0} e^{(-qs)^2/2}$$

Helm Phys. Rev. 104 (1956) 1466–1475

$j_1(x)$ denotes the 1st-order spherical Bessel function.

The root-mean-square (rms) radius $\langle R_n^2 \rangle = \frac{3}{5}R_0^2 + 3s^2$

$s = 0.9$ from muon spectroscopy data

Fricke Nucl.Data Tabl. 60 (1995) 177–285

FORM FACTORS: PARAMETRIZATIONS

The Klein-Nystrand form factor follows from the convolution of short-range Yukawa potential with $a_k = 0.7$ fm, over a distribution approximated as a hard sphere with radius R_A .

$$F_{\text{KN}}(q^2) = 3 \frac{j_1(qR_A)}{qR_A} [1 + (qa_k)^2]^{-1}$$

Klein, Nystrand Phys. Rev. C60 (1999) 014903

$j_1(x)$ denotes the 1st-order spherical Bessel function.

The root-mean-square (rms) radius $\langle R_n^2 \rangle = \frac{3}{5}R_A^2 + 6a_k^2$ semi-empirical formula
 $R_A \approx 1.2 \times A^{1/3}$ fm

NUCLEAR RMS RADIUS

The form factor parametrizations depend on two parameters that measure different nuclear properties and that are constrained by means of the rms radius of the distribution:

$$\langle R_{p,n}^2 \rangle = \frac{\int \rho_{p,n}(\vec{r}) r^2 d^3\vec{r}}{\int \rho_{p,n}(\vec{r}) d^3\vec{r}}$$

The rms radii of the proton density distributions are determined from different experimental sources: optical and X-ray isotope shifts, muonic spectra, and electronic scattering experiments.

Angeli+ Atom. Data Nucl. Data Tabl. 99, 69 (2013)

Neutron rms radii: their experimental values follow from hadronic experiments which are subject to large uncertainties.

CE ν NS CROSS SECTION: RECAP

CE ν NS has a well-calculable cross-section in the SM:
 (probability of kicking a nucleus with nuclear recoil energy T)

Fermi constant (SM parameter)	Kinematics	Nuclear Form Factor: $F=1$ full coherence
$\frac{d\sigma}{dT} = \frac{G_F^2 M}{4\pi} \left(1 - \frac{MT}{2E_\nu^2} - \frac{T}{E_\nu} \right) Q_w^2 [F_w(q^2)]^2 + \frac{G_F^2 M}{4\pi} \left(1 + \frac{MT}{2E_\nu^2} - \frac{T}{E_\nu} \right) F_A(q^2)$		
Weak nuclear charge		

$$Q_w = [Z(1 - 4 \sin^2 \theta_W) - N] \quad \begin{matrix} s w^2 = 0.23 \rightarrow \text{protons unimportant} \\ \text{Neutron contribution dominates} \end{matrix}$$

- $E\nu$: is the incident neutrino energy
- M : the nuclear mass of the detector material
- 3-momentum transfer $|\vec{q}|^2 = 2MT$
- (Q_A included in F_A)

Axial contribution is small for most nuclei, spin-dependent.
 It vanishes for nuclei with even number of protons and neutrons

Freedman, PRD 9 (1974) 1389; Drukier, Stodolsky, PRD 30 (1984) 2295; Barranco, Miranda, Rashba, hep-ph/0508299

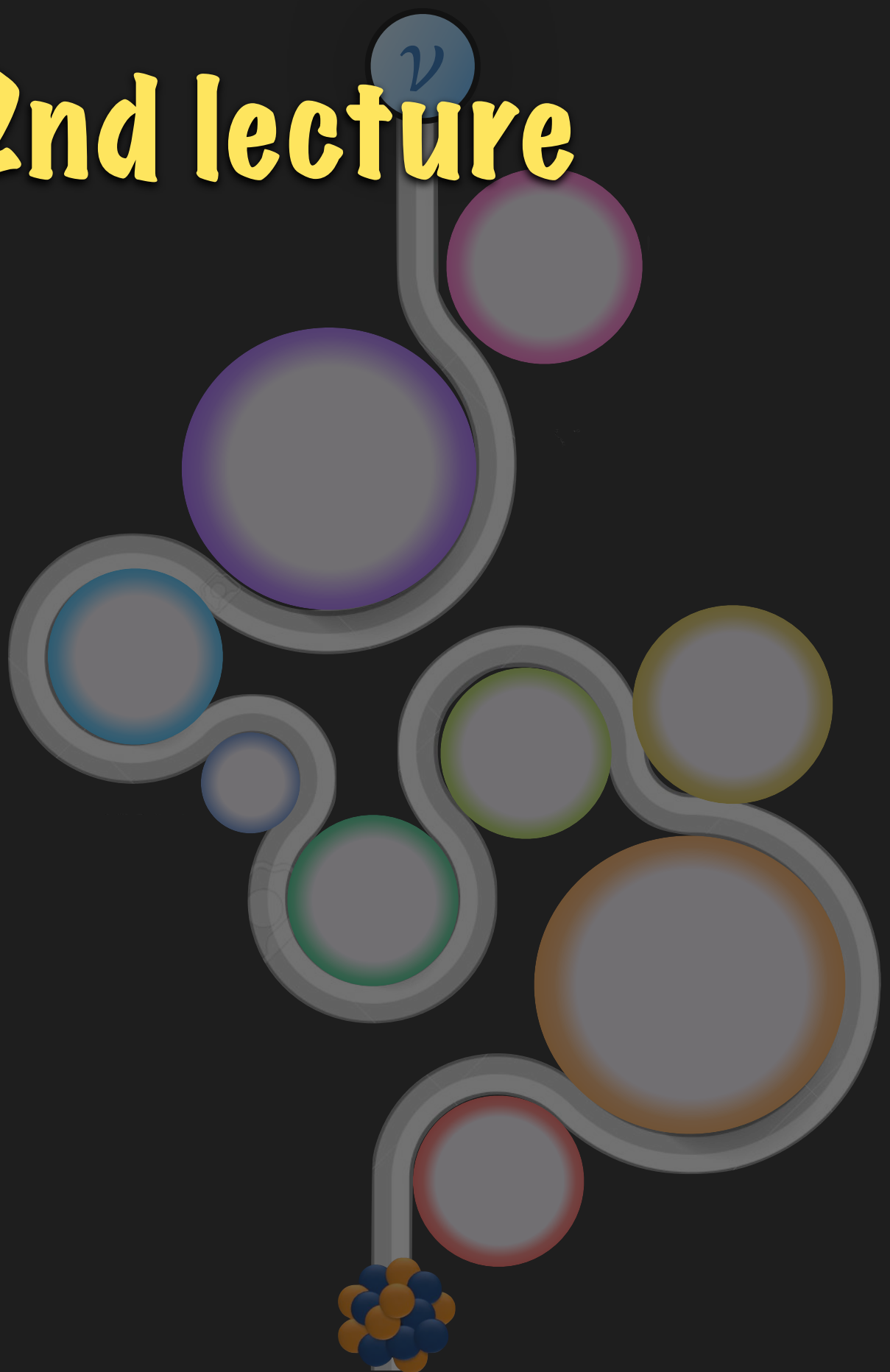
OUTLINE - 2nd lecture

► CEvNS physics potential in the SM:

- Weak mixing angle
- Neutron rms radii

► CEvNS physics potential BSM:

- Electromagnetic properties
- NSI
- NGI
- Light mediators



IMPLICATIONS OF CEvNS: STANDARD MODEL

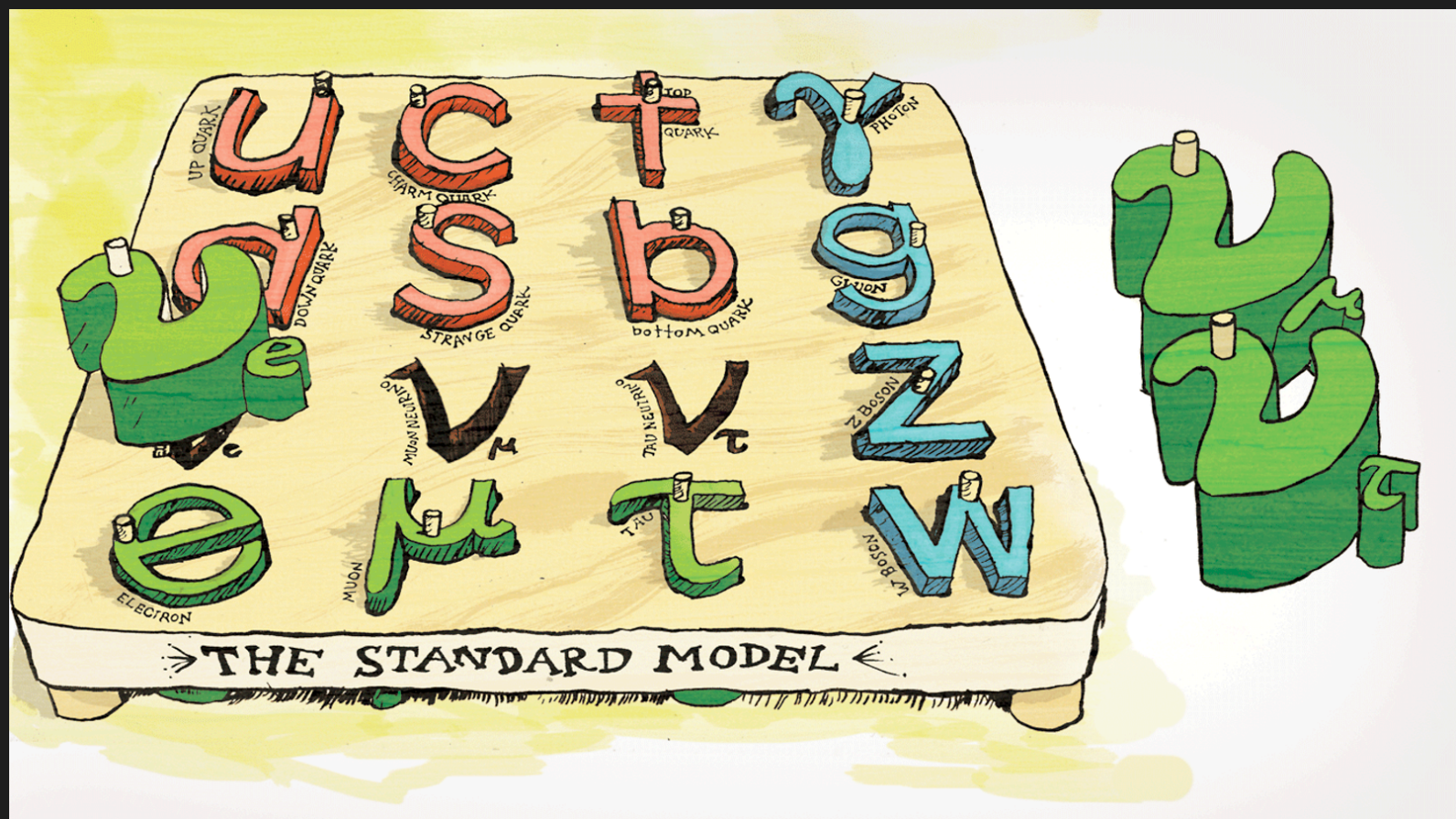
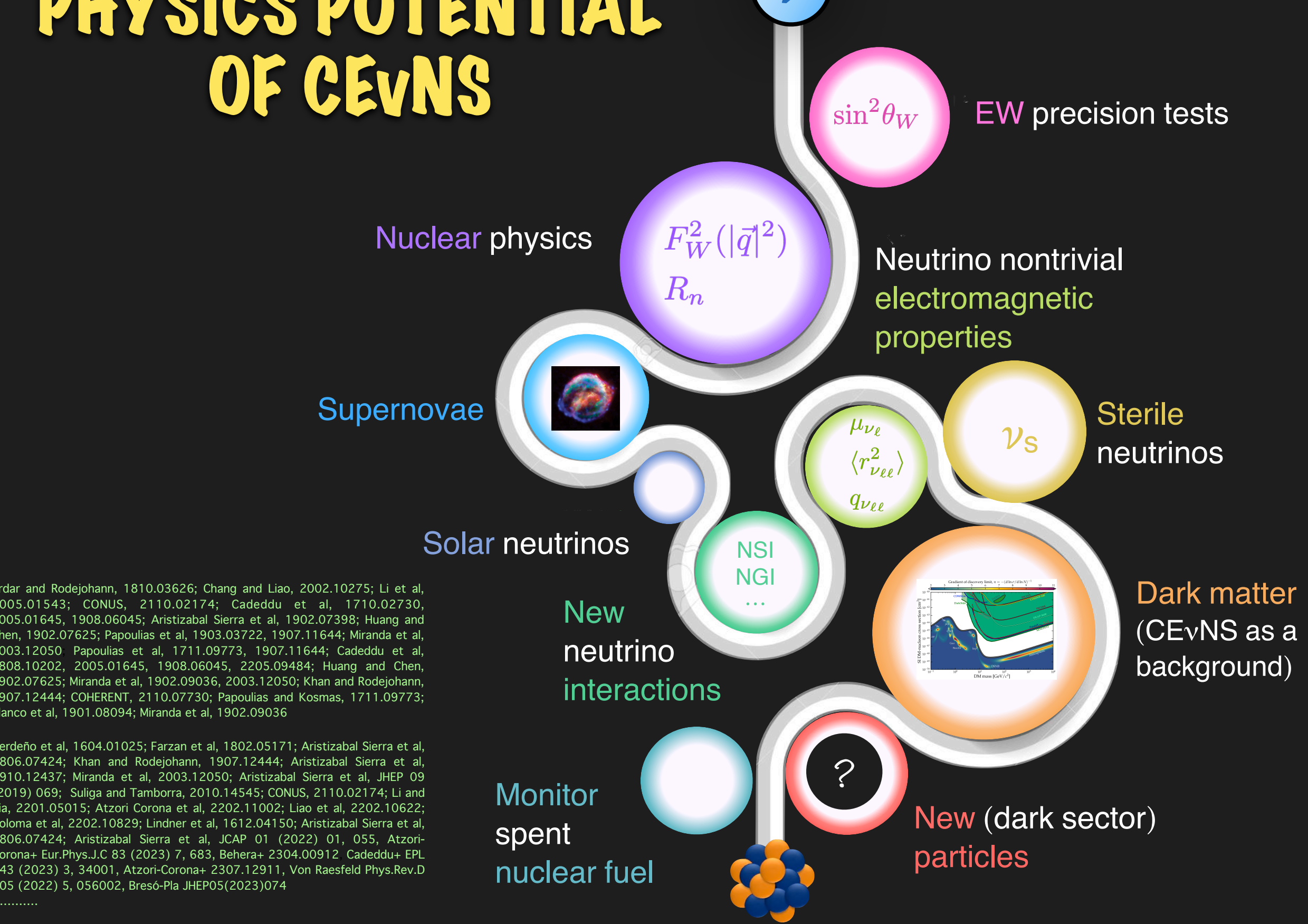
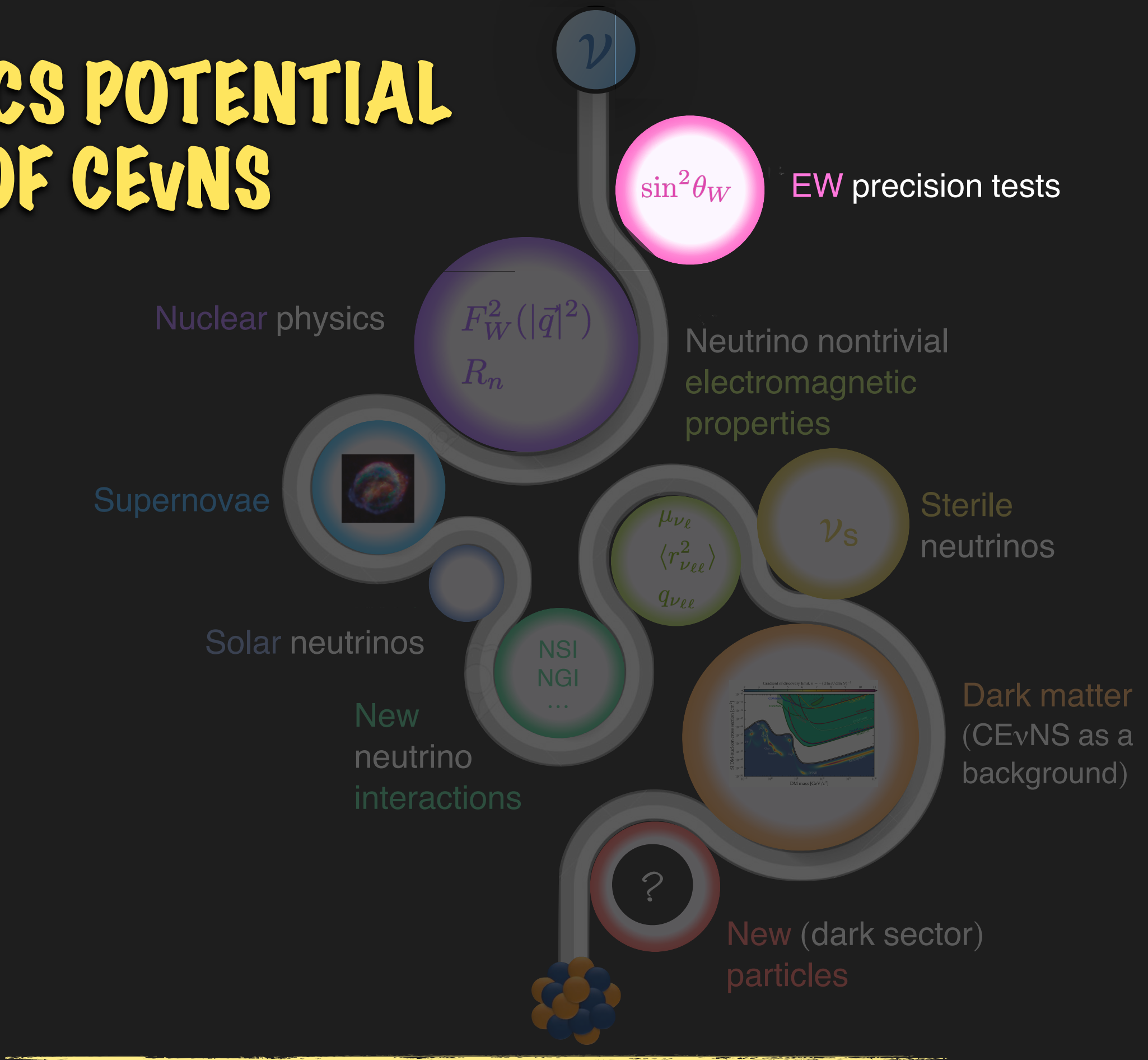


Illustration by Sandbox Studio, Chicago

PHYSICS POTENTIAL OF CEvNS



PHYSICS POTENTIAL OF CEvNS



STANDARD MODEL PHYSICS

$$\frac{d\sigma_{\nu N}}{dE_{\text{nr}}} \Big|_{\text{CE}\nu\text{NS}}^{\text{SM}} = \frac{G_F^2 m_N}{\pi} F_W^2(\mathbf{q}^2) Q_W^2 \left(1 - \frac{m_N E_{\text{nr}}}{2E_\nu^2} - \frac{E_{\text{nr}}}{E_\nu} + \frac{E_{\text{nr}}^2}{2E_\nu^2} \right)$$

$$Q_W = -N/2 + (1/2 - 2\sin^2\theta_w)Z \quad s w^2 = 0.23 \rightarrow \text{protons unimportant}$$

Neutron contribution dominates

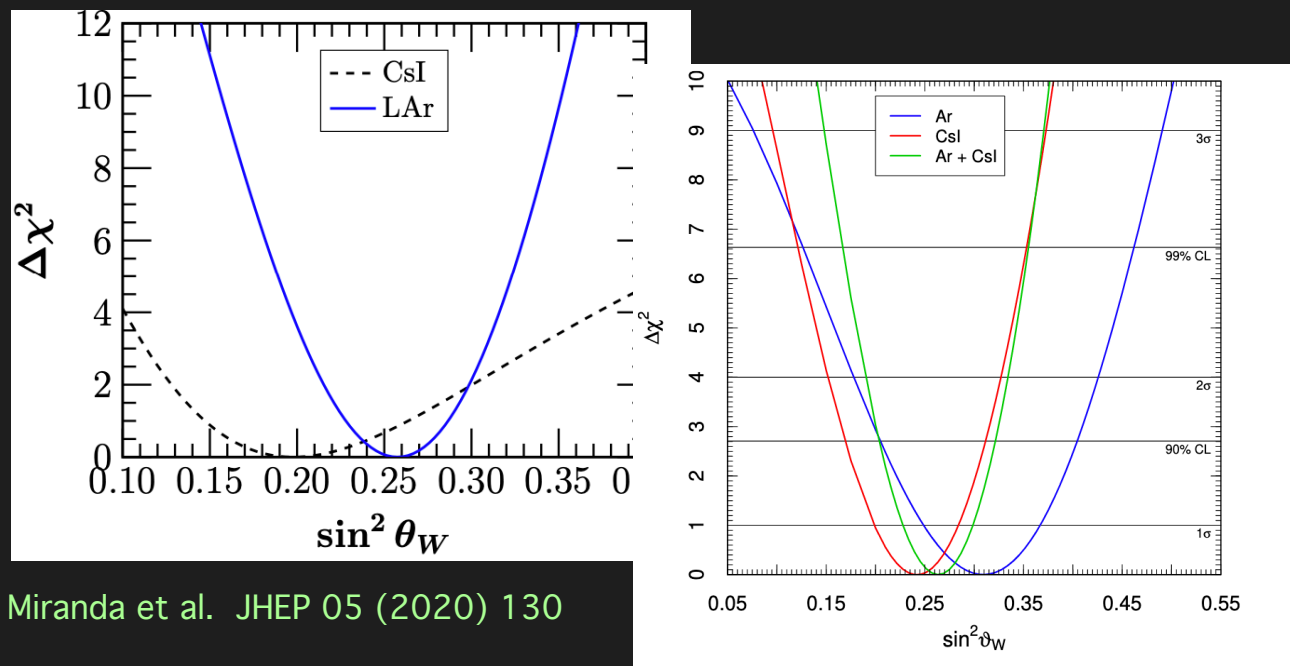
Information on the value of the neutrino neutral-current interaction at low energy:

- Observable: $\sin^2\theta_w$
- poorly measured at low energies
- Affects the normalization of CEvNS spectra



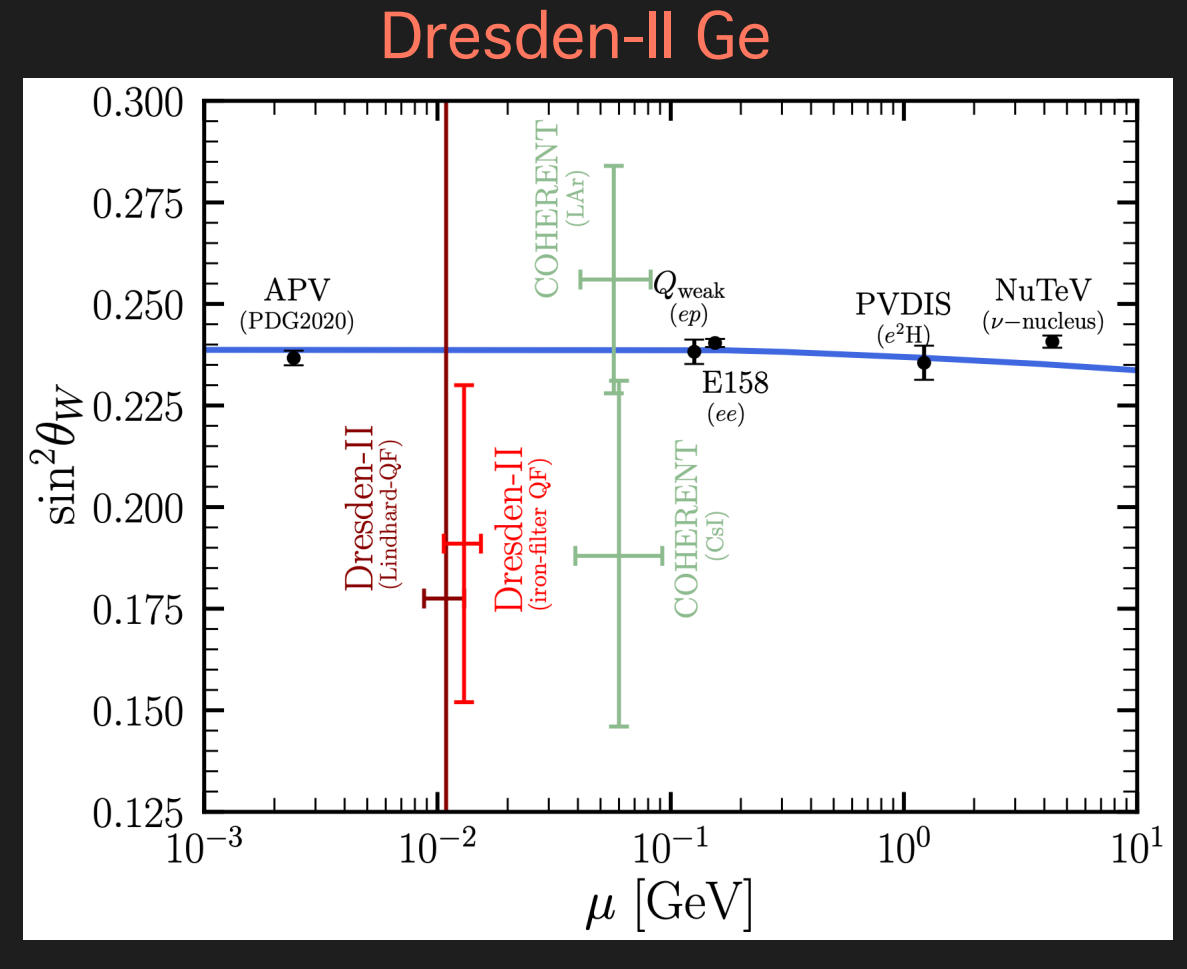
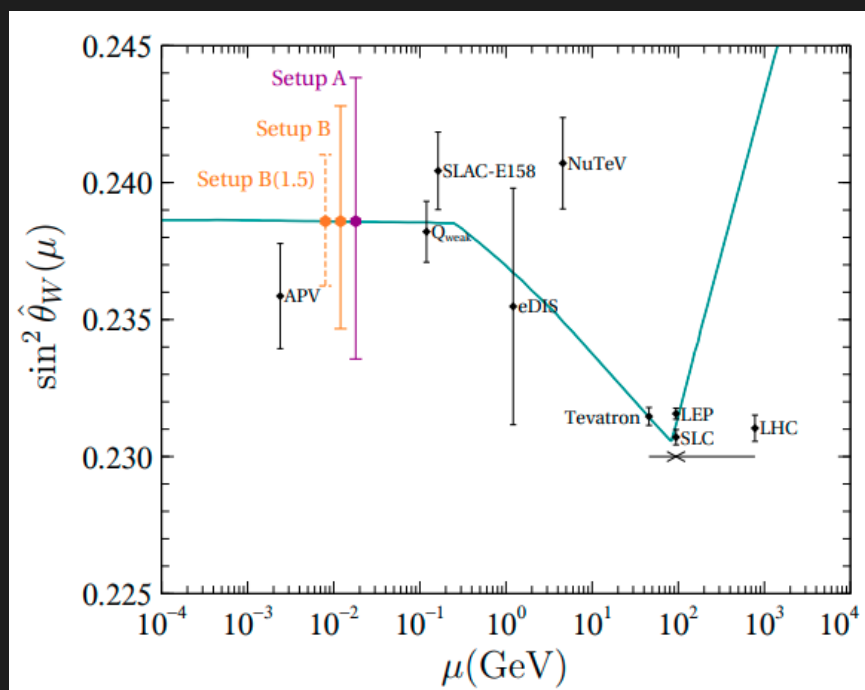
EW PRECISION TESTS: WEAK MIXING ANGLE

COHERENT CsI
(2017) + LAr



Miranda et al. JHEP 05 (2020) 130

Cadeddu et al. Phys. Rev. D 102, 015030 (2020)



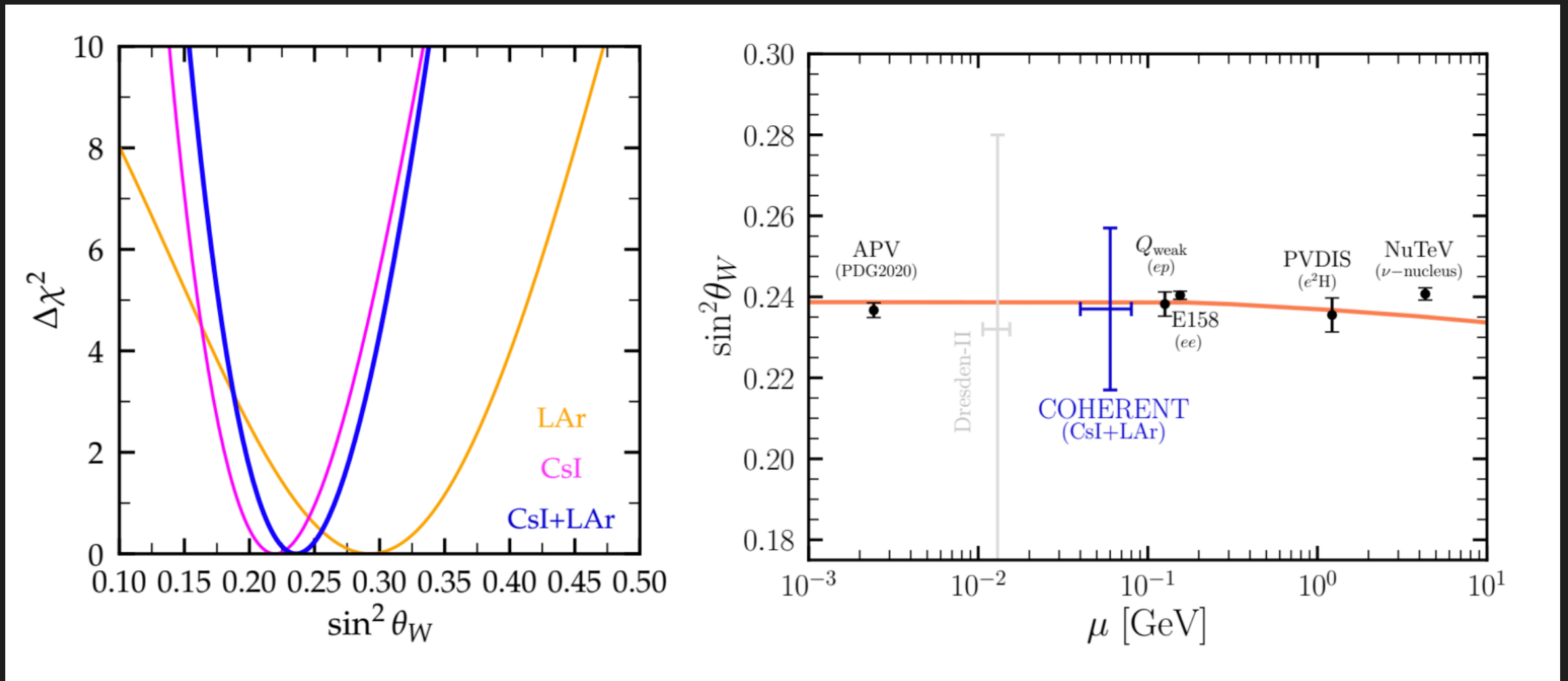
Aristizabal, VDR, Papoulias JHEP 09 (2022) 076

SBC LAr

[SBC Collaboration] L. J. Flores et al. Phys. Rev. D 103 (2021) 9, L091301

EW PRECISION TESTS: WEAK MIXING ANGLE

COHERENT CsI (2021) + LAr

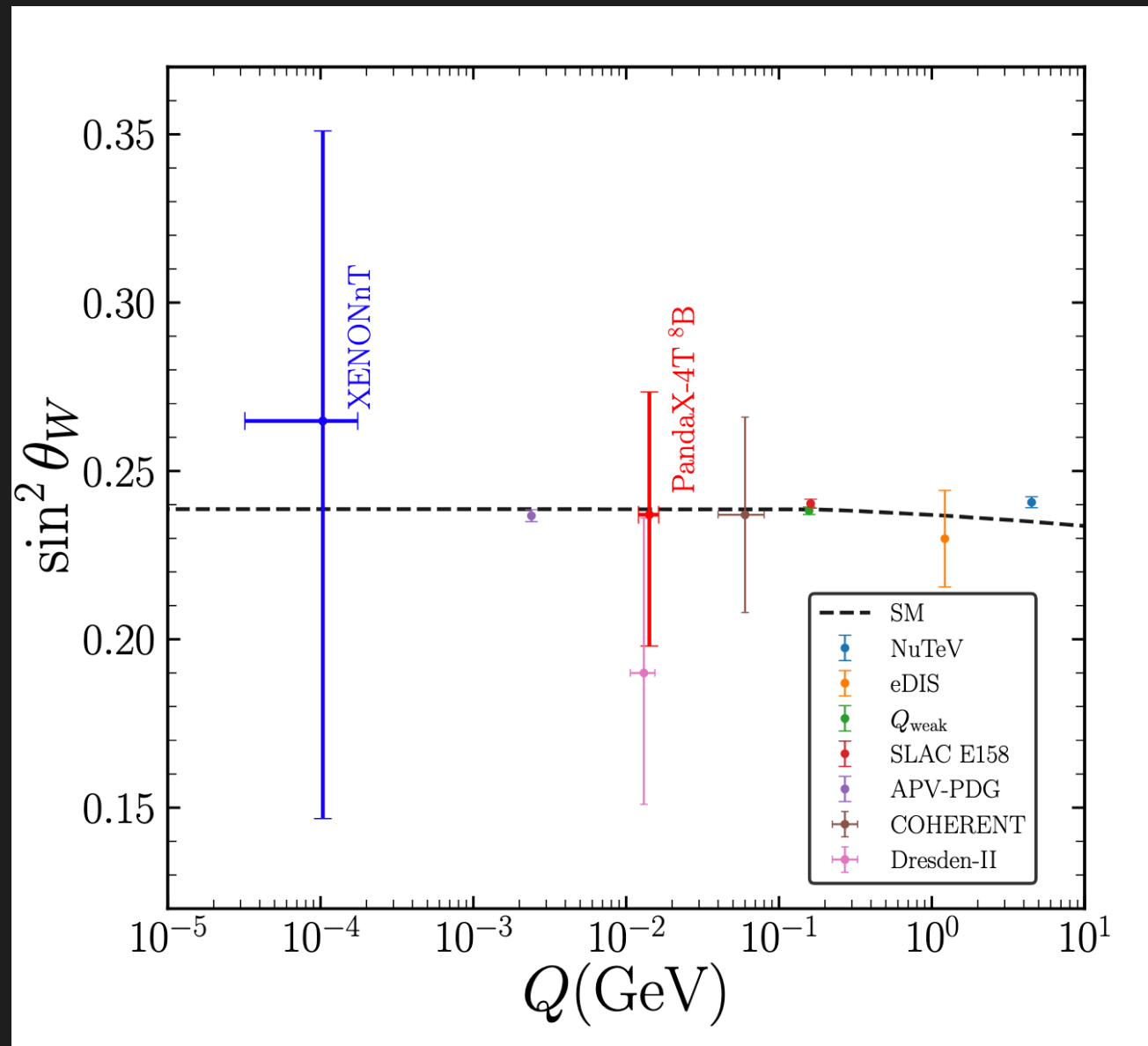


VDR, Miranda, Papoulias, Sanchez-García, Tórtola and Valle, JHEP 04 (2023) 035
 Majumdar, Papoulias, Srivastava and Valle, Phys.Rev.D 106 (2022) 9, 093010

$$\sin^2 \theta_W = 0.237 \pm 0.029 \quad (1\sigma)$$

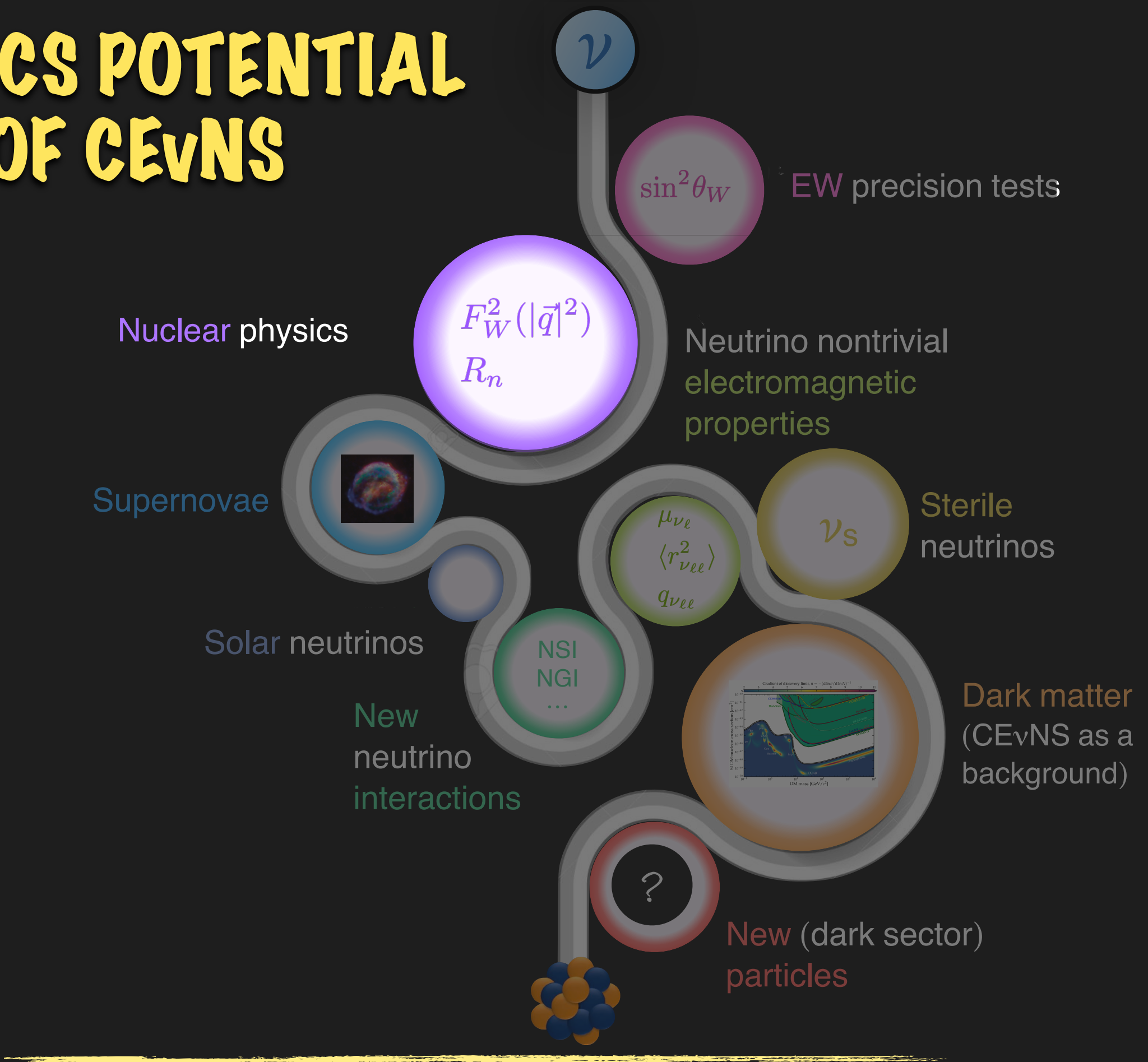
See also: Atzori-Corona+ JHEP 09 (2022) 164, Atzori-Corona+ Eur.Phys.J.C 83 (2023) 7, 683

EW PRECISION TESTS: WEAK MIXING ANGLE



Maity, Boehm 2409.04385

PHYSICS POTENTIAL OF CEvNS



NUCLEAR PHYSICS

$$\frac{d\sigma_{\nu N}}{dE_{\text{nr}}} \Big|_{\text{CEvNS}}^{\text{SM}} = \frac{G_F^2 m_N}{\pi} \boxed{F_W^2(\mathbf{q}^2)} Q_w^2 \left(1 - \frac{m_N E_{\text{nr}}}{2E_\nu^2} - \frac{E_{\text{nr}}}{E_\nu} + \frac{E_{\text{nr}}^2}{2E_\nu^2} \right)$$

Nuclear form factor $F_W^2(|\vec{q}|^2) = \int e^{-i\vec{q}\cdot\vec{r}} \rho(r) d^3r$
 $\rho(r)$ is the charge density distribution

is the Fourier transform of the neutron distribution in the nucleus

- Observable: nuclear rms radius
- Largest theoretical uncertainty
- Affects the shape of CEvNS spectra

Partial coherency gives information on the nuclear neutron form factor.

PROTON AND NEUTRON DENSITY DISTRIBUTIONS

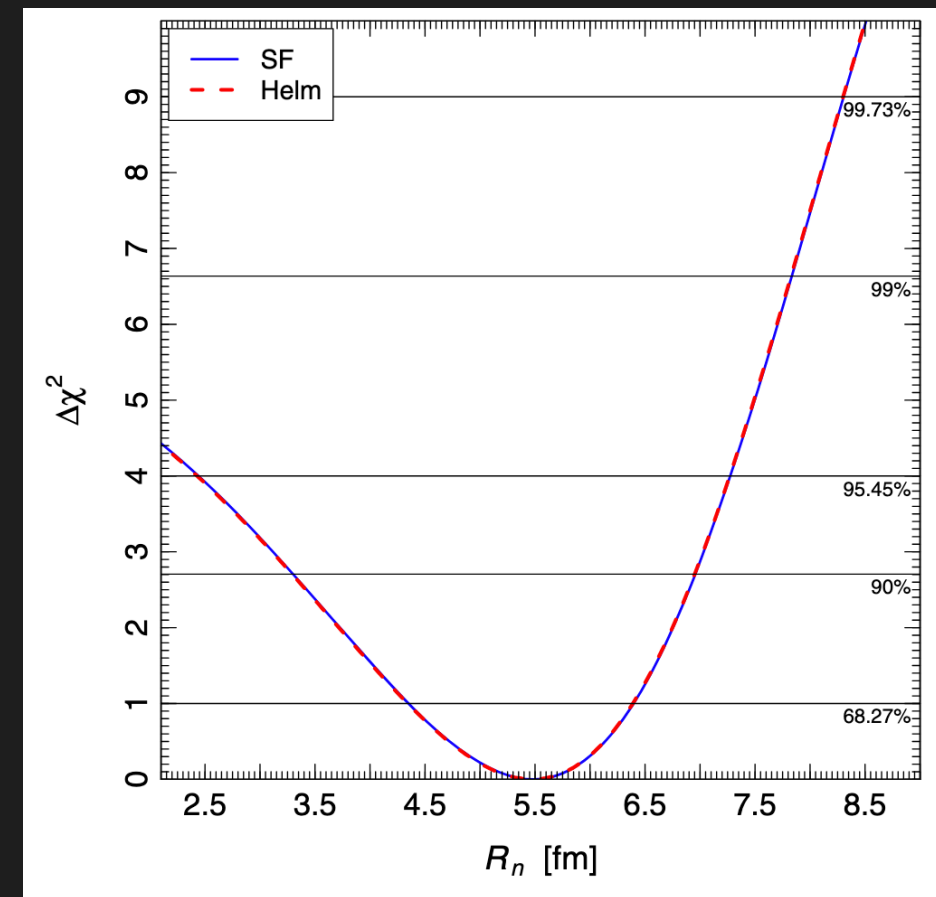
The nuclear proton distribution is probed with electromagnetic interactions.

What about neutron distributions? Hadron scattering experiments can give information, but their interpretation depends on the model used to describe non-perturbative strong interactions. Neutral-current weak interaction measurements are more reliable.

Before 2017 there was only one measurement of R_n with neutral-current weak interactions through parity-violating electron scattering (PREX).

The CEvNS process can be used to provide a model-independent measurement of the root-mean-square (rms) neutron distribution radius, R_n .

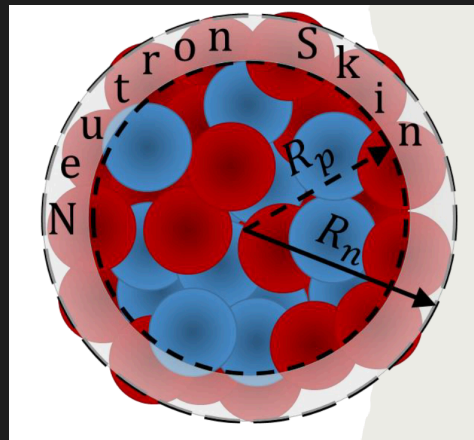
Determine for the first time the average neutron rms radius of ^{133}Cs and ^{127}I .



Cadeddu+ PRL 120, 072501 (2018)

NEUTRON DENSITY DISTRIBUTION

The CEvNS process can be used to provide a model-independent measurement of the root-mean-square (rms) neutron distribution radius, R_n .



Credit: M. Cadeddu

Proton rms radii are fixed

$$R_p(\text{I}) = 4.766 \text{ fm}$$

$$R_p(\text{Cs}) = 4.824 \text{ fm}$$

$$R_p(\text{Ar}) = 3.448 \text{ fm}$$

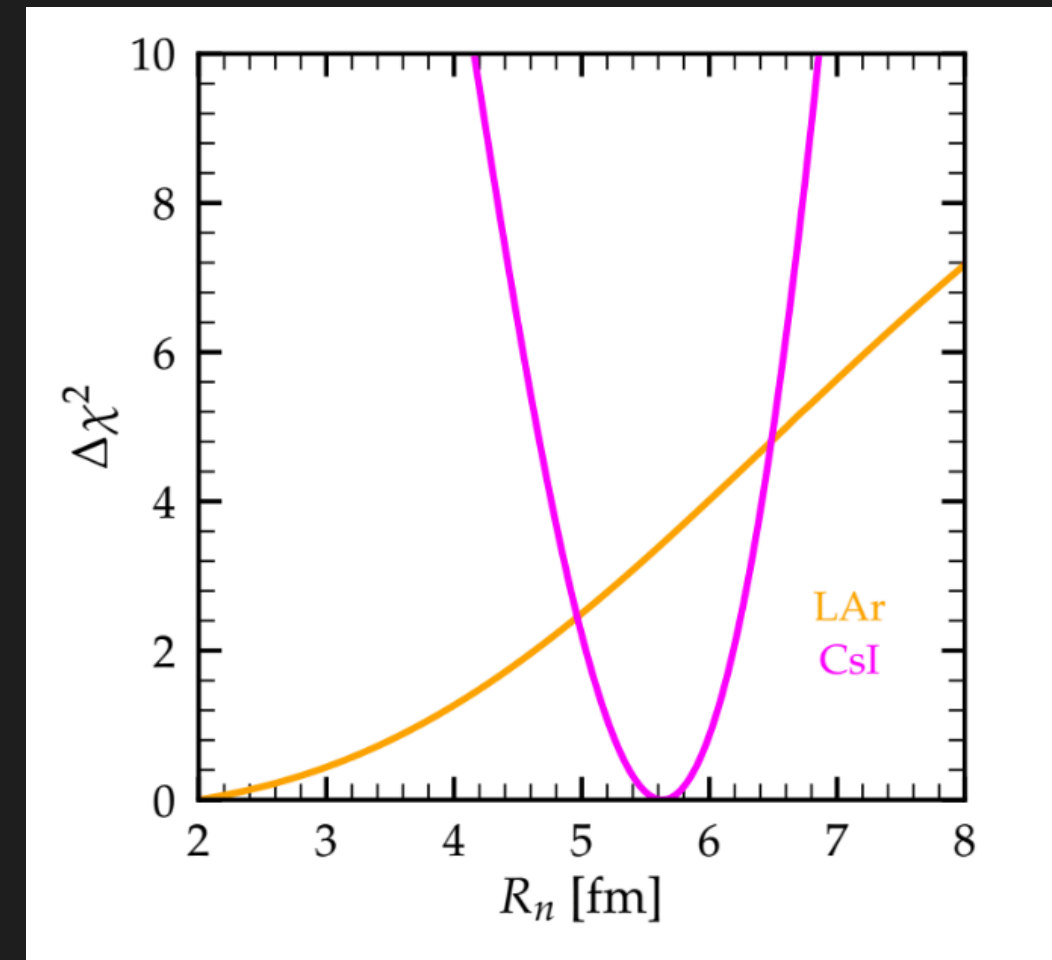
$$R_n = 1.23A^{1/3}(1 + \alpha_4)$$

See also: Aristizabal 2301.13249, Cadeddu+ Phys. Rev. D 101, 033004 (2020), Cadeddu+ Phys. Rev. D 102, 015030 (2020), Cadeddu-Dordei Phys. Rev. D 99, 033010 (2019), Cadeddu+ Phys. Rev. C 104, 065502 (2021), Atzori-Corona, Cadeddu, Cargioli, Giunti+, Cañas+ Phys. Lett. B 784, 159...

$$F_W(|\vec{q}|^2) = 3 \frac{j_1(|\vec{q}|R_A)}{|\vec{q}|R_A} \left(\frac{1}{1 + |\vec{q}|^2 a_k^2} \right)$$

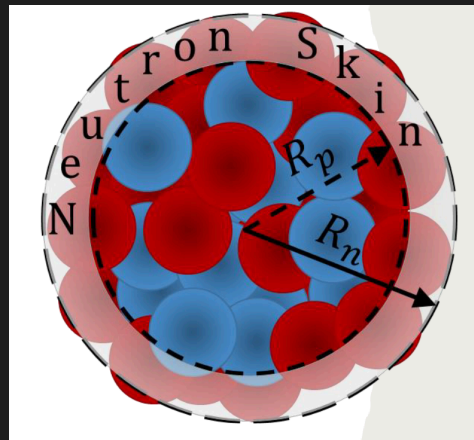
Klein-Nystrand parametrization

COHERENT CsI (2021) + LAr



NEUTRON DENSITY DISTRIBUTION

The CEvNS process can be used to provide a model-independent measurement of the root-mean-square (rms) neutron distribution radius, R_n .



Credit: M. Cadeddu

Proton rms radii are fixed

$$R_p(I) = 4.766 \text{ fm}$$

$$R_p(\text{Cs}) = 4.824 \text{ fm}$$

$$R_p(\text{Ar}) = 3.448 \text{ fm}$$

$$R_n = 1.23A^{1/3}(1 + \alpha_4)$$

$$R_n(\text{Ar}) \in [0.00, 3.72] \text{ fm}, \quad (1\sigma)$$

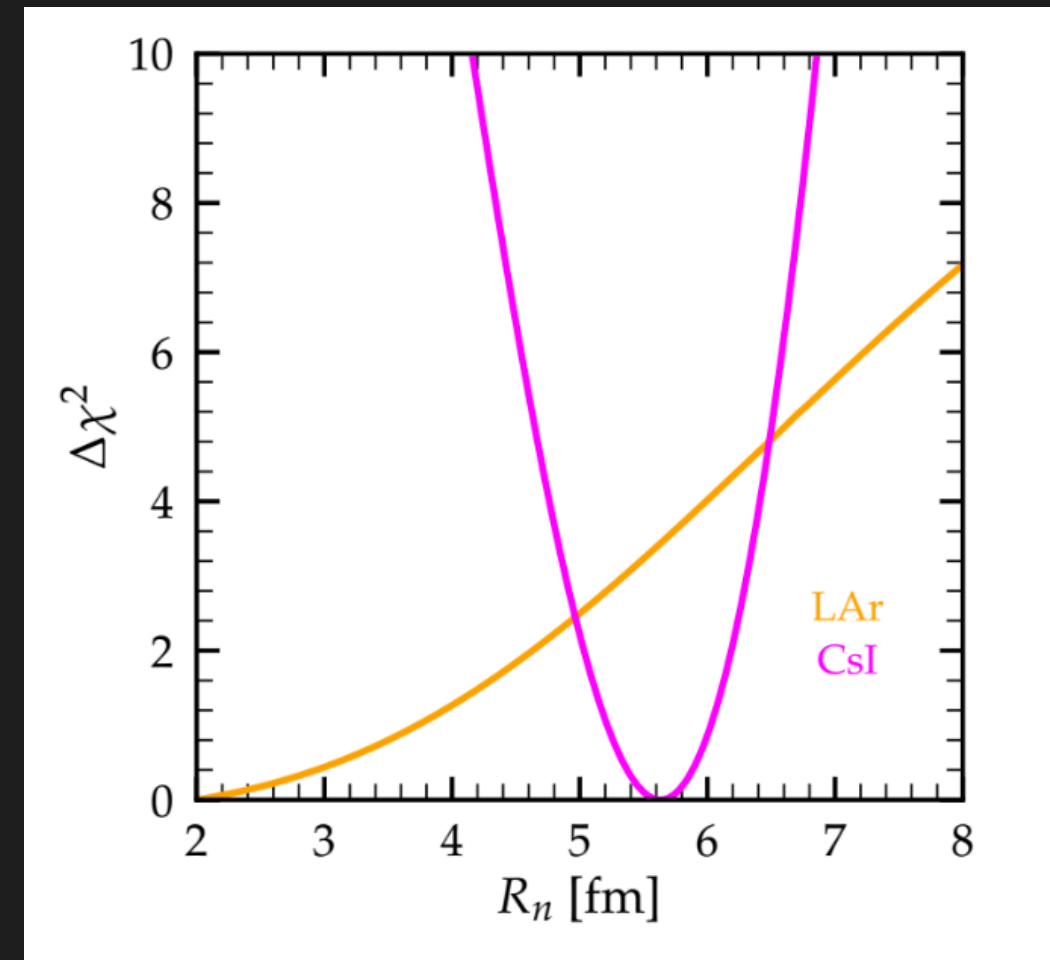
$$R_n(\text{CsI}) \in [5.22, 6.03] \text{ fm}$$

See also: Aristizabal 2301.13249, Cadeddu+ Phys. Rev. D 101, 033004 (2020), Cadeddu+ Phys. Rev. D 102, 015030 (2020), Cadeddu-Dordei Phys. Rev. D 99, 033010 (2019), Cadeddu+ Phys. Rev. C 104, 065502 (2021), Atzori-Corona, Cadeddu, Cargioli, Dordei, Giunti+ Eur.Phys.J.C 83 (2023) 7, 683, Cañas+ Phys. Lett. B 784, 159...

$$F_W(|\vec{q}|^2) = 3 \frac{j_1(|\vec{q}|R_A)}{|\vec{q}|R_A} \left(\frac{1}{1 + |\vec{q}|^2 a_k^2} \right)$$

Klein-Nystrand parametrization

COHERENT CsI (2021) + LAr



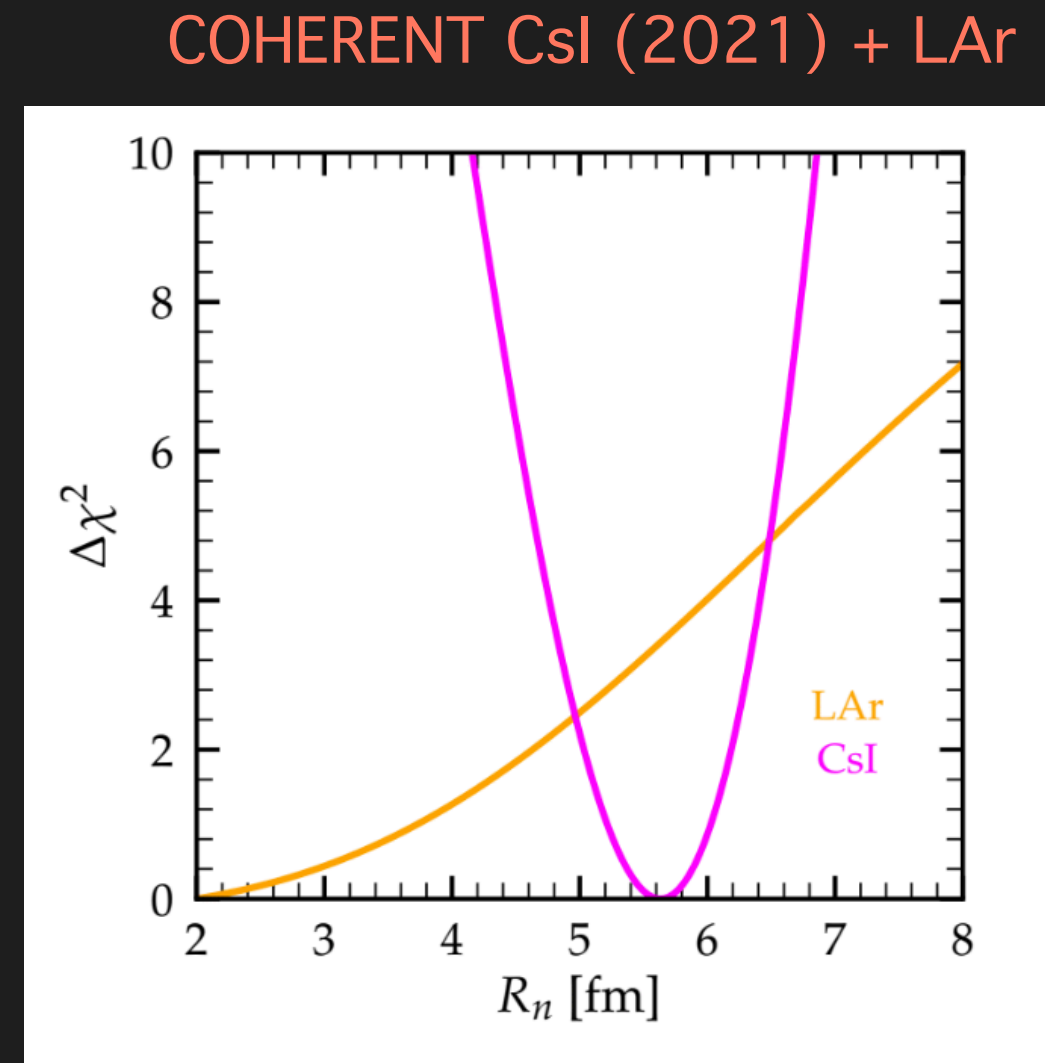
VDR, Miranda, Papoulias, Sanchez-García, Tórtola and Valle, JHEP 04 (2023) 035

NEUTRON DENSITY DISTRIBUTION

A large R_n has implications for:

- Nuclear physics → a larger pressure of neutrons, stability of nuclei
- Astrophysics → a larger size of neutron stars

$$R_n = 1.23A^{1/3}(1 + \alpha_4)$$
$$R_n(\text{Ar}) \in [0.00, 3.72] \text{ fm}, \quad (1\sigma)$$
$$R_n(\text{CsI}) \in [5.22, 6.03] \text{ fm}$$

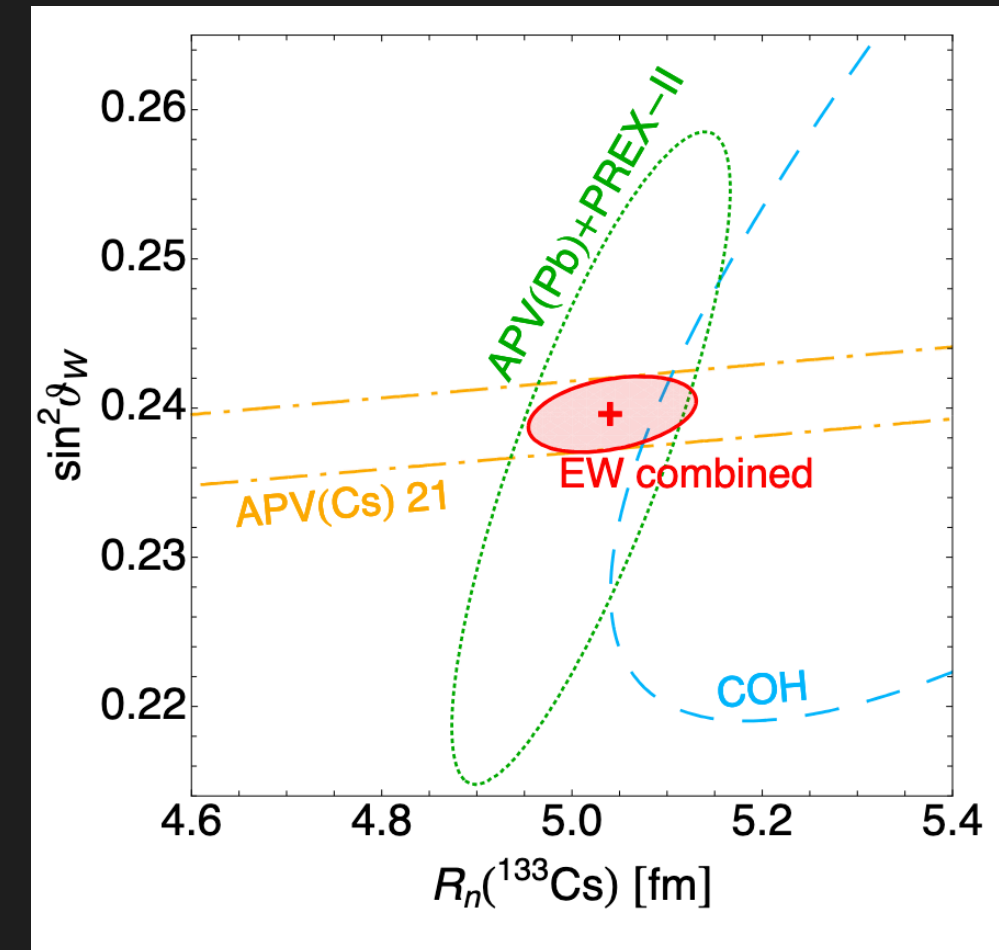


VDR, Miranda, Papoulias, Sanchez-García, Tórtola and Valle, JHEP 04 (2023) 035

COMBINING $\sin^2 \theta_W$ AND THE AVERAGE CsI NEUTRON RADIUS

Attempt to exploit correlations among different probes available in order to maximize the reliability and significance on $\sin^2 \theta_W$.

“Global fit” from atomic parity violation, coherent elastic neutrino-nucleus scattering and parity-violating electron scattering on different nuclei.

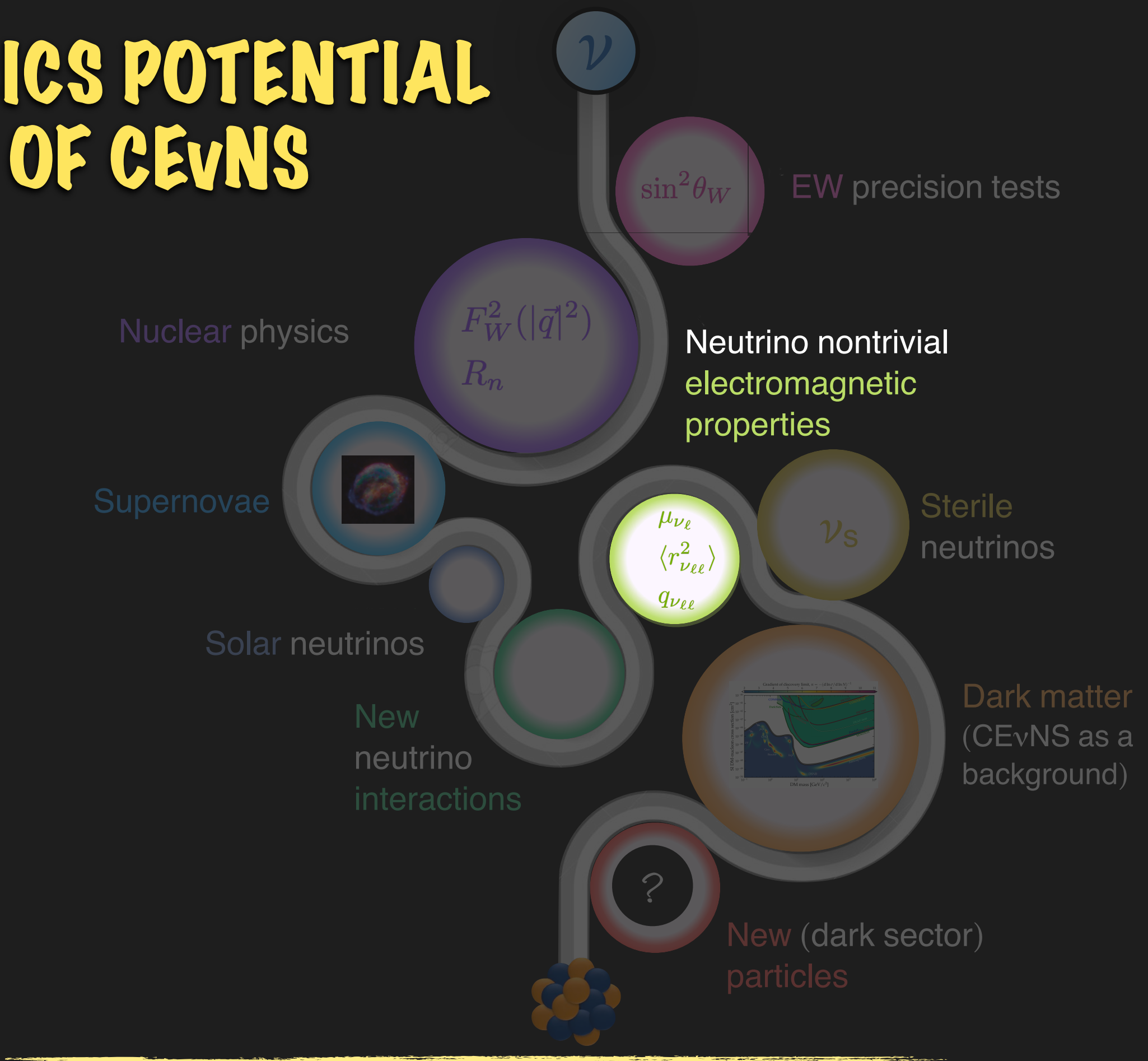


Atzori-Corona+ Eur.Phys.J.C 83 (2023) 7, 683
Atzori-Corona+ [2405.09416](#) [

IMPLICATIONS OF CEvNS: NEW PHYSICS



PHYSICS POTENTIAL OF CEvNS



NEUTRINO ELECTROMAGNETIC INTERACTIONS

Neutrino electromagnetic properties are important as they are connected to the fundamentals of particle physics.

They can be used to distinguish Dirac vs Majorana nature or to probe physics BSM.

The interaction of a fermionic field $f(x)$ with the electromagnetic field $A(x)$ is given by

$$\mathcal{H}_{\text{em}}^f(x) = j_\mu^f(x) A^\mu(x) = \mathbf{q}_f \gamma_\mu f(x) A^\mu(x)$$

Charge of the fermion f

C. Giunti, A. Studenikin, Rev Mod Phys, 87, 531 (2015)

NEUTRINO ELECTROMAGNETIC INTERACTIONS

Neutrino electromagnetic properties are important as they are connected to the fundamentals of particle physics.

They can be used to distinguish Dirac vs Majorana nature or to probe physics BSM.

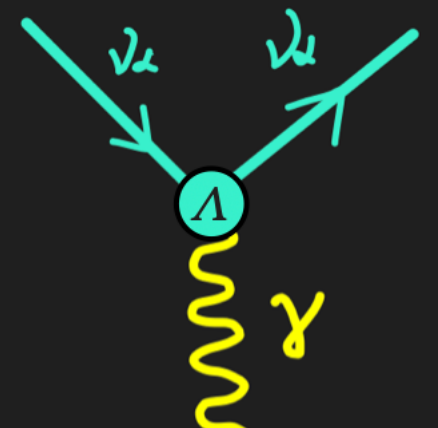
The interaction of a fermionic field $f(x)$ with the electromagnetic field $A(x)$ is given by

$$\mathcal{H}_{\text{em}}^f(x) = j_\mu^f(x) A^\mu(x) = \mathbf{q}_f \gamma_\mu f(x) A^\mu(x)$$

Charge of the fermion f

The electric charge of neutrinos in the SM is zero and there are no electromagnetic interactions at tree level.

Such interactions can arise from loop diagrams at higher order of the perturbative expansion of the interaction.



4x4 matrix in spinor space, can contain space/time derivatives

$$\mathcal{H}_{\text{em}}^\nu(x) = j_\mu^\nu(x) A^\mu(x) = \bar{\nu}(x) \mathbf{\Lambda}_\mu \nu(x) A^\mu(x)$$

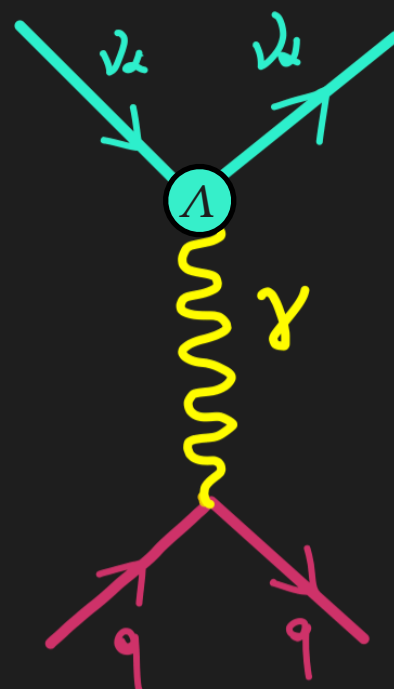
C. Giunti, A. Studenikin, Rev Mod Phys, 87, 531 (2015)

NEUTRINO ELECTROMAGNETIC INTERACTIONS

Effective electromagnetic vertex:

$$\langle \nu_f(p_f) | j_\mu^{(\nu)}(0) | \nu_i(p_i) \rangle = \bar{u}_f(p_f) \Lambda_\mu^{fi}(p) u_i(p_i)$$

Neutrinos are assumed to be free particles described by Dirac fields.



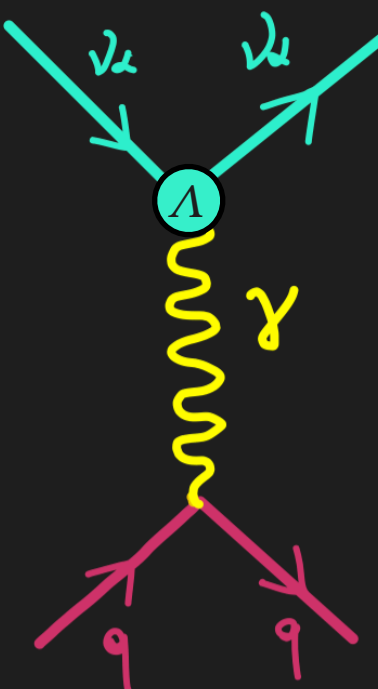
C. Giunti, A. Studenikin, Rev Mod Phys, 87, 531 (2015)

NEUTRINO ELECTROMAGNETIC INTERACTIONS

Effective electromagnetic vertex:

$$\langle \nu_f(p_f) | j_\mu^{(\nu)}(0) | \nu_i(p_i) \rangle = \bar{u}_f(p_f) \Lambda_\mu^{fi}(p) u_i(p_i)$$

Neutrinos are assumed to be free particles described by Dirac fields.



Lorentz and electromagnetic gauge invariance imply that the most general composition of the **vertex function**, in terms of linearly independent products of Dirac γ matrices and the available kinematical four-vector, is

$$\Lambda_\mu(p_f, p_i) = \mathbb{F}_1(q^2) q_\mu + \mathbb{F}_2(q^2) q_\mu \gamma_5 + \mathbb{F}_3(q^2) \gamma_\mu + \mathbb{F}_4(q^2) \gamma_\mu \gamma_5 + \mathbb{F}_5(q^2) \sigma_{\mu\nu} q^\nu + \mathbb{F}_6 \epsilon_{\mu\nu\rho\gamma}(q^2) q^\nu \sigma^{\rho\gamma}$$

\mathbb{F}_i are Lorentz-invariant form factors and q is the four-momentum of the photon.

NEUTRINO ELECTROMAGNETIC INTERACTIONS

Lorentz and electromagnetic gauge invariance imply that the most general composition of the **vertex function**, in terms of linearly independent products of Dirac γ matrices and the available kinematical four-vectors, is

$$\Lambda_\mu(p_f, p_i) = \mathbb{F}_1(q^2)q_\mu + \mathbb{F}_2(q^2)q_\mu\gamma_5 + \mathbb{F}_3(q^2)\gamma_\mu + \mathbb{F}_4(q^2)\gamma_\mu\gamma_5 + \mathbb{F}_5(q^2)\sigma_{\mu\nu}q^\nu + \mathbb{F}_6\epsilon_{\mu\nu\rho\gamma}(q^2)q^\nu\sigma^{\rho\gamma}$$

\mathbb{F}_i are Lorentz-invariant form factors and q is the four-momentum of the photon.

\mathbb{F}_i depend only on q^2 which is the only available Lorentz-invariant quantity.

Using the properties of Dirac matrices, one can find that

$\mathbb{F}_2, \mathbb{F}_3, \mathbb{F}_4$ are real
 $\mathbb{F}_1, \mathbb{F}_5, \mathbb{F}_6$ are imaginary

The number of independent form factors is further reduced by imposing current conservation

$$\partial^\mu j_\mu^\nu(x) = 0.$$

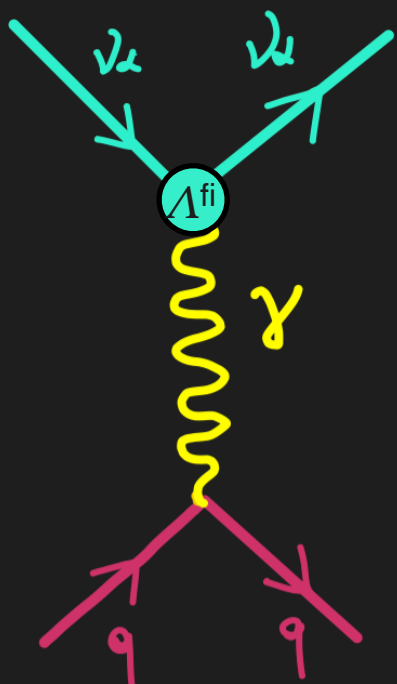
C. Giunti, A. Studenikin, Rev Mod Phys, 87, 531 (2015)

NEUTRINO ELECTROMAGNETIC INTERACTIONS

Lorentz and electromagnetic gauge invariance imply that the vertex functions is defined in terms of four form factors:

Kayser, Phys.Rev. D26 (1982) 1662
Nieves, Phys.Rev. D26 (1982) 3152

$$\Lambda_\mu(p_f, p_i) = \mathbb{F}_Q(q^2)\gamma_\mu - \mathbb{F}_M(q^2)i\sigma_{\mu\nu}q^\nu + \mathbb{F}_E\sigma_{\mu\nu}q^\nu\gamma_5 + \mathbb{F}_A(q^2)(q^2\gamma_\mu - q_\mu q)\gamma_5$$



Where $\mathbb{F}_Q = \mathbb{F}_3$, $\mathbb{F}_M = i\mathbb{F}_5$, $\mathbb{F}_E = -2i\mathbb{F}_6$, and $\mathbb{F}_A = -\mathbb{F}_2/2m$.

We can then generalise to the case of N massive neutrino fields, with masses m_k and take into account possible transitions among different massive neutrinos.

C. Giunti, A. Studenikin, Rev Mod Phys, 87, 531 (2015)

NEUTRINO ELECTROMAGNETIC INTERACTIONS

$\Lambda_\mu^{fi}(q)$ is a NxN matrix in the space of massive neutrinos expressed in terms of four Hermitian NxN form factors.

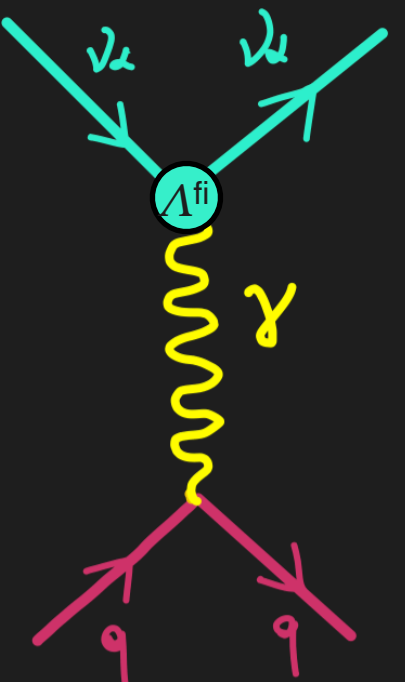
$$\Lambda_\mu^{fi}(q) = \left(\gamma_\mu - \frac{q_\mu q}{q^2} \right) \left[\mathbb{F}_Q^{fi}(q^2) + \mathbb{F}_A^{fi}(q^2)q^2\gamma_5 \right] - i\sigma_{\mu\nu}q^\nu \left[\mathbb{F}_M^{fi}(q^2) + i\mathbb{F}_E^{fi}(q^2)\gamma_5 \right]$$

Lorentz-invariant
form factors
 $(q^2 = 0$, coupling with
a real photon)

Charge (q)
Anapole (a)
Helicity conserving

Magnetic (μ)
Electric (ϵ)
Helicity flipping

The form factors with $f = i$ are called diagonal, if $f \neq i$, are called transition form factors.



C. Giunti, A. Studenikin, Rev Mod Phys, 87, 531 (2015)

NEUTRINO ELECTROMAGNETIC INTERACTIONS

$\Lambda_\mu^{fi}(q)$ is a NxN matrix in the space of massive neutrinos expressed in terms of four Hermitian NxN form factors.

$$\Lambda_\mu^{fi}(q) = \left(\gamma_\mu - \frac{q_\mu q}{q^2} \right) \left[\mathbb{F}_Q^{fi}(q^2) + \mathbb{F}_A^{fi}(q^2)q^2\gamma_5 \right] - i\sigma_{\mu\nu}q^\nu \left[\mathbb{F}_M^{fi}(q^2) + i\mathbb{F}_E^{fi}(q^2)\gamma_5 \right]$$

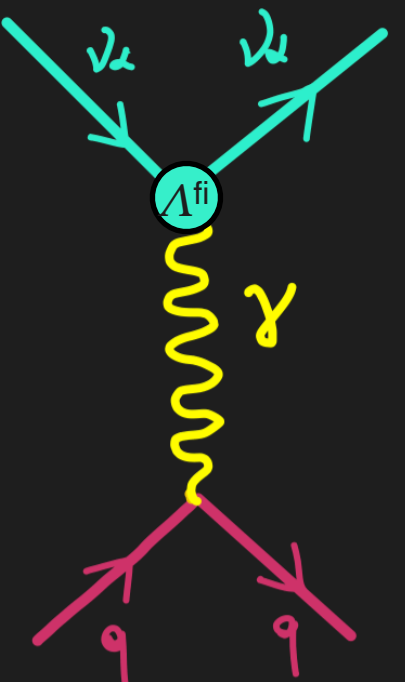
Lorentz-invariant
form factors
 $(q^2 = 0$, coupling with
a real photon)

Charge (q)
Anapole (a)
Helicity conserving

Magnetic (μ)
Electric (ϵ)
Helicity flipping

For Majorana neutrinos the charge, magnetic and electric form factors are antisymmetric matrices and the anapole one is symmetric.

Since \mathbb{F}_Q^M , \mathbb{F}_E^M and \mathbb{F}_M^M are antisymmetric, Majorana neutrinos cannot have diagonal charge and dipole magnetic and electric form factors.



Nieves Phys. Rev. D 26, 3152
Kayser Phys. Rev. D 26, 1662

C. Giunti, A. Studenikin, Rev Mod Phys, 87, 531 (2015)

NEUTRINO MAGNETIC MOMENT

The most studied neutrino electromagnetic moments are the dipole magnetic and electric moments:

$$\mu_{ij} = \mathbb{F}_M(0)_{ij}, \epsilon_{ij} = \mathbb{F}_E(0)_{ij}$$

The diagonal magnetic and electric moments of a Dirac neutrino in the minimally-extended SM with right-handed neutrinos are strongly suppressed:

$$\mu_{ii}^D = \frac{3eG_F m_i}{8\sqrt{2}\pi^2} \sim 3.2 \times 10^{-19} \left(\frac{m_i}{1\text{eV}} \right) \mu_B \quad \epsilon_{ii}^D = 0$$

$$\mu_{ij}^D, i\epsilon_{ij}^D \sim -3.9 \times 10^{-23} \left(\frac{m_i \pm m_j}{1\text{eV}} \right) \mu_B \sum_{\ell=e,\mu,\tau} U_{\ell i}^* U_{\ell j} \left(\frac{m_\ell}{m_\tau} \right)^2$$

Transition moments are GIM-suppressed

Fujikawa, Shrock, PRL 45 (1980) 963;
Pal, Wolfenstein, PRD 25 (1982) 766;
Shrock, NPB 206 (1982) 359;
Dvornikov, Studenikin, PRD 69 (2004)
073001, JETP 99 (2004) 254

NEUTRINO MAGNETIC MOMENT

Neutrino magnetic moment interactions flip chirality and do not interfere with the SM terms.
The differential cross section is incoherently added to the SM one:

$$\frac{d\sigma_{\nu_\ell N}}{dE_{\text{nr}}} \Big|_{\text{CE}\nu\text{NS}}^{\text{MM}} = \frac{\pi\alpha_{\text{EM}}^2}{m_e^2} \left(\frac{1}{E_{\text{nr}}} - \frac{1}{E_\nu} \right) Z^2 F_W^2(|\vec{q}|^2) \left| \frac{\mu_{\nu_\ell}}{\mu_B} \right|^2$$

Vogel, Engel. PRD 39 [1989] 3378

μ_ν^2 is an effective neutrino magnetic moment
dependent on a given neutrino beam (reactor,
SNS, etc.)

Transition magnetic moments

Schechter Valle, PhysRevD.24.1883

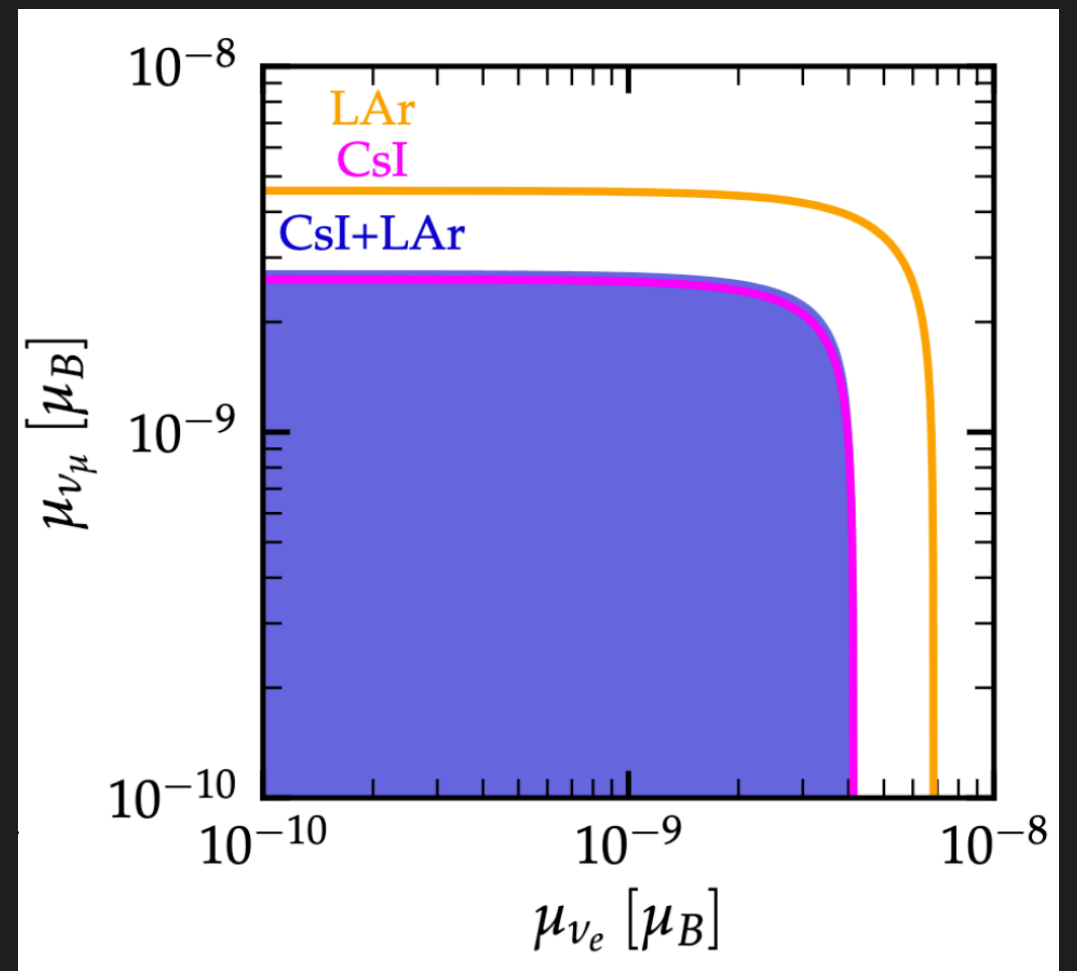
Canas+ Phys.Lett. B753 (2016) 191-198

Miranda+ JHEP 1907 (2019) 103,

Aristizabal-Sierra+ Phys.Rev.D 105 (2022) 035027

- can be dominant for sub-keV threshold experiments
- may lead to detectable distortions of the recoil spectrum

COHERENT CsI (2021) + LAr



VDR, Miranda, Papoulias, Sanchez-García, Tórtola and Valle, JHEP 04 (2023) 035

NEUTRINO CHARGE RADIUS

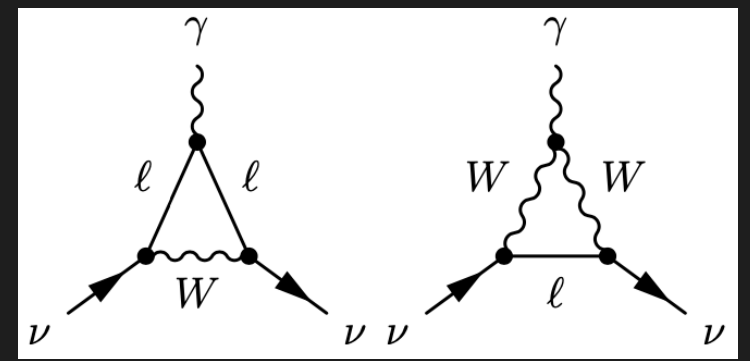
The neutrino charge radius is the only EM neutrino parameter different from zero within the SM framework.

A neutral particle can be characterized by a superposition of two charge distributions of opposite signs, so the particle form factor $\mathbb{F}_Q(q^2)$ can be nonzero for $q^2 \neq 0$.

Flavor-diagonal CR are generated via radiative corrections from the $\gamma - Z$ boson mixing and box diagrams involving W and Z boson.

The mean charge radius of an electrically neutral neutrino is given by the second term in the power-series expansion

$$\text{of the neutrino charge form factor } \langle r_\nu^2 \rangle = 6 \frac{d\mathbb{F}_Q(q^2)}{dq^2} \Big|_{q^2=0}$$



The SM values are $\left(\langle r_{\nu_{ee}}^2 \rangle, \langle r_{\nu_{\mu\mu}}^2 \rangle, \langle r_{\nu_{\tau\tau}}^2 \rangle \right) = (-0.83, -0.48, -0.30) \times 10^{-32} \text{ cm}^2$.

Bernabeu et al, PRD 62 (2000) 113012, NPB 680 (2004) 450
Giunti, Studenikin, Rev Mod Phys, 87, 531 (2015)
Kouzakov and Studenikin, PRD 95 (2017) 055013

NEUTRINO CHARGE RADIUS

The contribution to the CEvNS cross section due to flavor-diagonal charge radii is obtained through the substitution $g_V^p \rightarrow g_V^p - Q_{\ell\ell}^{\text{CR}}$

$$\langle r_{\nu_{\ell\ell}}^2 \rangle_{\text{SM}} = -\frac{G_F}{2\sqrt{2}\pi^2} \left[3 - 2 \ln \frac{m_\ell^2}{M_W^2} \right] \quad Q_{\ell\ell}^{\text{CR}} = \frac{\sqrt{2}\pi\alpha_{\text{EM}}}{3G_F} \left\langle r_{\nu_{\ell\ell}}^2 \right\rangle$$

Bernabeu et al, PRD 62 (2000) 113012, NPB 680 (2004) 450

In the SM there are only diagonal charge radii because lepton numbers are conserved.

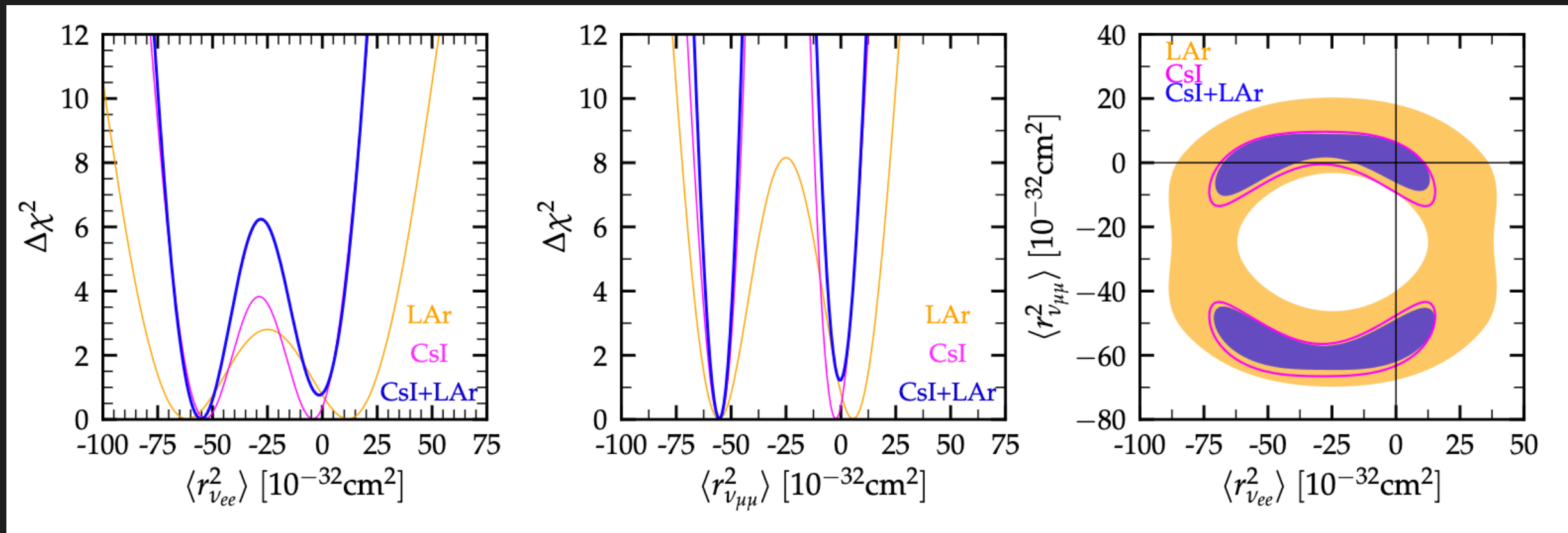
Transition charge radii can be generated via neutrino mixing and/or physics BSM and generate an incoherent contribution

$$\frac{d\sigma_{\nu_{\ell}\mathcal{N}}}{dE_{\text{nr}}} = \frac{G_F^2 m_N}{\pi} \left(1 - \frac{m_N E_{\text{nr}}}{2E_\nu^2} \right) \left[\left(g_V^n N F_N(\mathbf{q}^2) + g_V^p Z F_Z(\mathbf{q}^2) \right)^2 + 4/9 m_W^4 \sin^4 \theta_w Z^2 F_Z^2(\mathbf{q}^2) \sum_{\ell' \neq \ell} |\langle r_{\nu_{\ell'\ell}}^2 \rangle|^2 \right]$$

Kouzakov and Studenikin, PRD 95 (2017) 055013
Cadeddu+ PRD98 (2018) 113010

NEUTRINO CHARGE RADIUS

COHERENT CsI (2021) + LAr



VDR, Miranda, Papoulias, Sanchez-García, Tórtola and Valle, JHEP 04 (2023) 035

Bounds on flavor-diagonal neutrino charge radii.

The analysis of CsI data includes only CEvNS interactions, since the EvES events contribution on CsI is negligible. CsI data result in a more constrained allowed area, with two separate regions.

TEXONO (reactor ν_e - e^-) and BNL-E734 (accelerator ν_μ - e^-) bounds more stringent.

See also Atzori-Corona+ JHEP 09 (2022) 164, JHEP 05 (2024) 271

NEUTRINO MILlichARGE

In the SM the neutrality of neutrinos is a consequence of the quantization of electric charge.

Neutrinos can be millicharged particles in theories BSM that include right-handed neutrinos.

Babu and Mohapatra, PRL 63 (1989) 938

The contribution to the CEvNS cross section due to flavor-diagonal charge radii is obtained through the substitution $g_V^p \rightarrow g_V^p - Q_{\ell\ell}^{\text{EC}}$

$$Q_{\ell\ell}^{\text{EC}} = \frac{2\sqrt{2}\pi\alpha_{\text{EM}}}{G_F q^2} q_{\nu_{\ell\ell}}$$

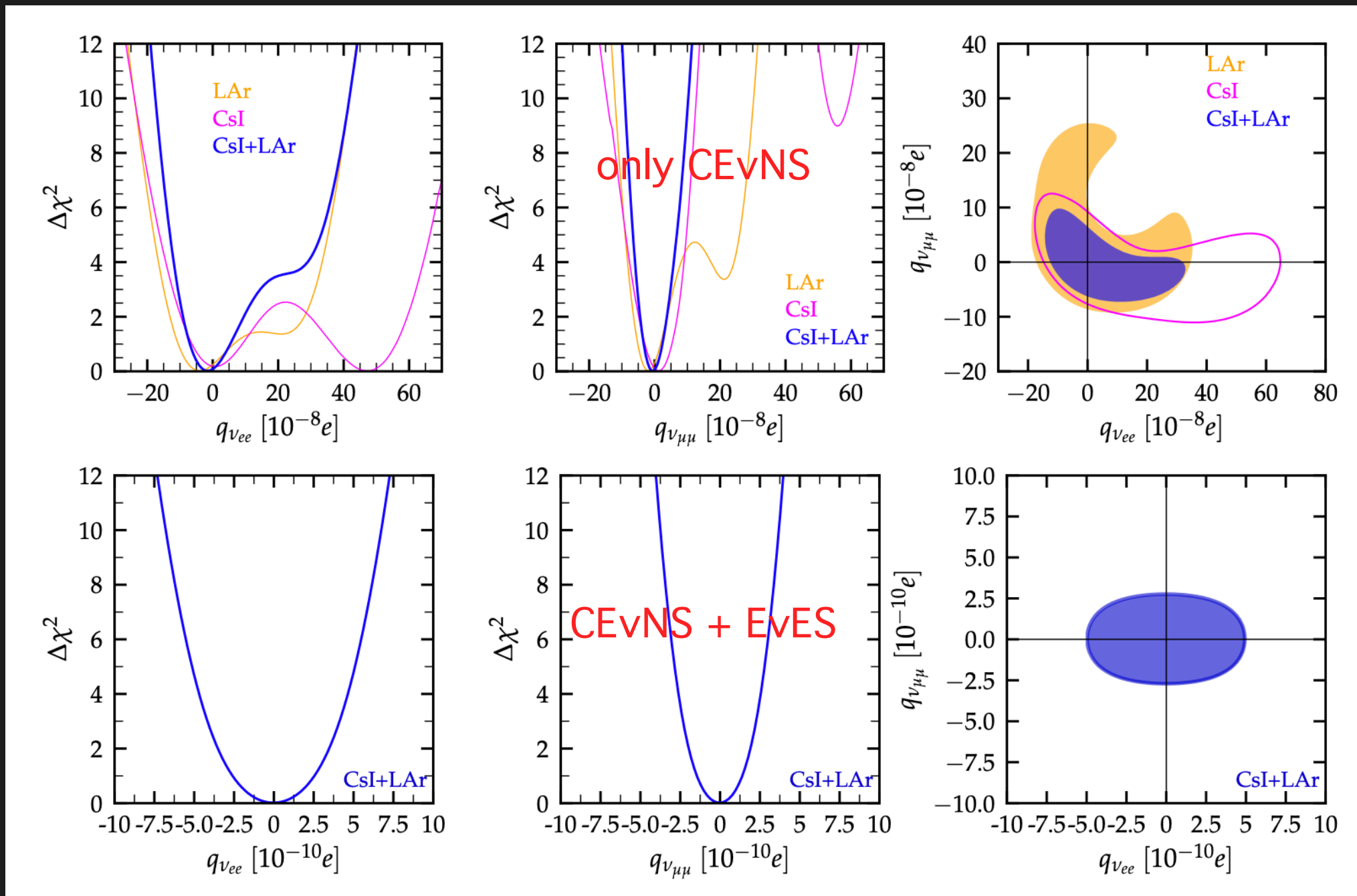
Atzori-Corona+ JHEP 09 (2022) 164

Being the four-momentum $q^2 = -2m_N E_{\text{nr}}$

Interactions with flavor-nondiagonal EC are also possible.

Kouzakov and Studenikin, PRD 95 (2017) 055013

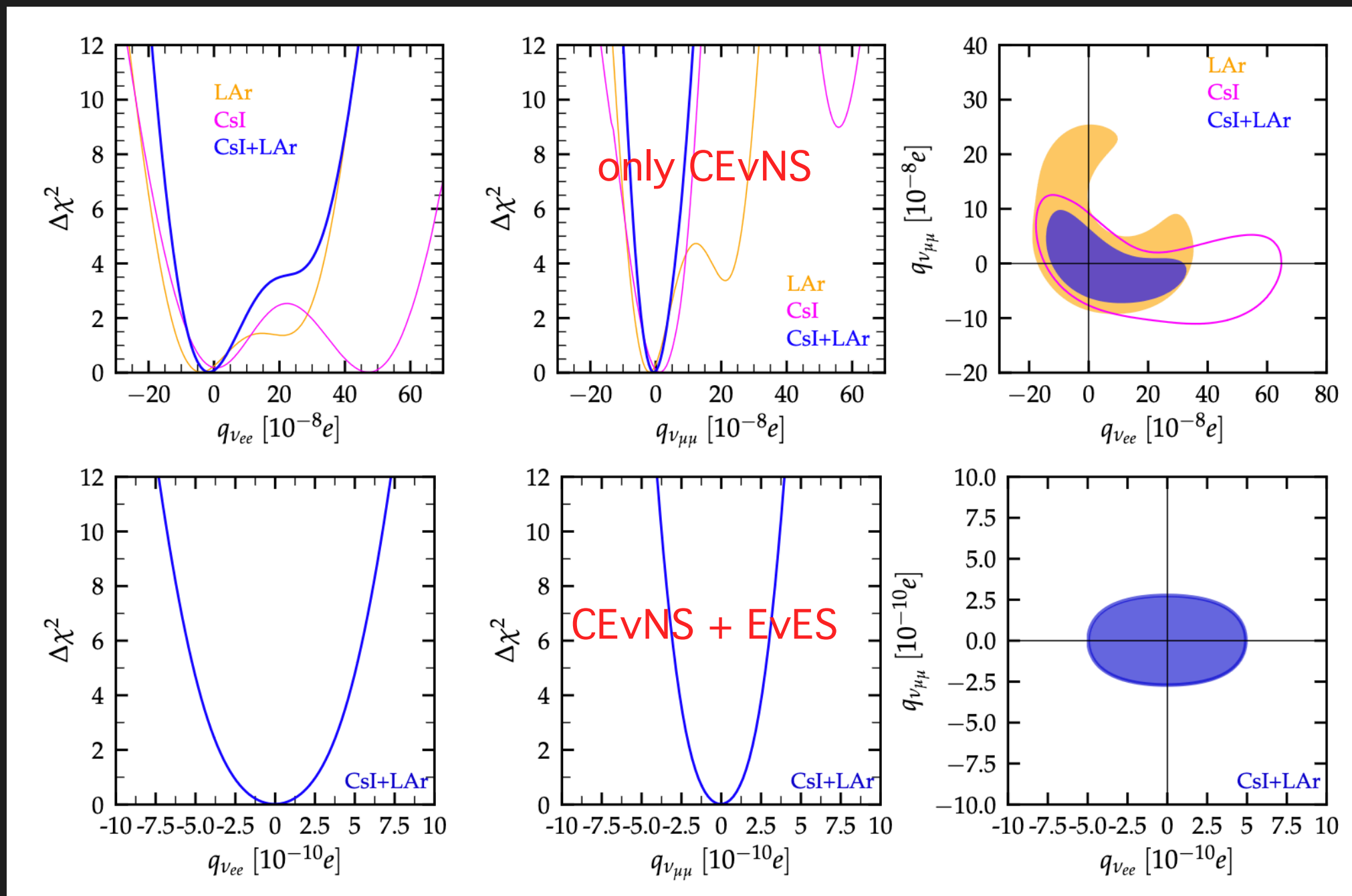
NEUTRINO MILLICHARGE



Including EvES events in the analysis strongly enhances the sensitivity of COHERENT data, because the momentum transferred is much smaller than in CEvNS interactions.

See also Atzori-Corona+ JHEP 05 (2024) 271, Khan Nucl.Phys.B 986 (2023) 116064

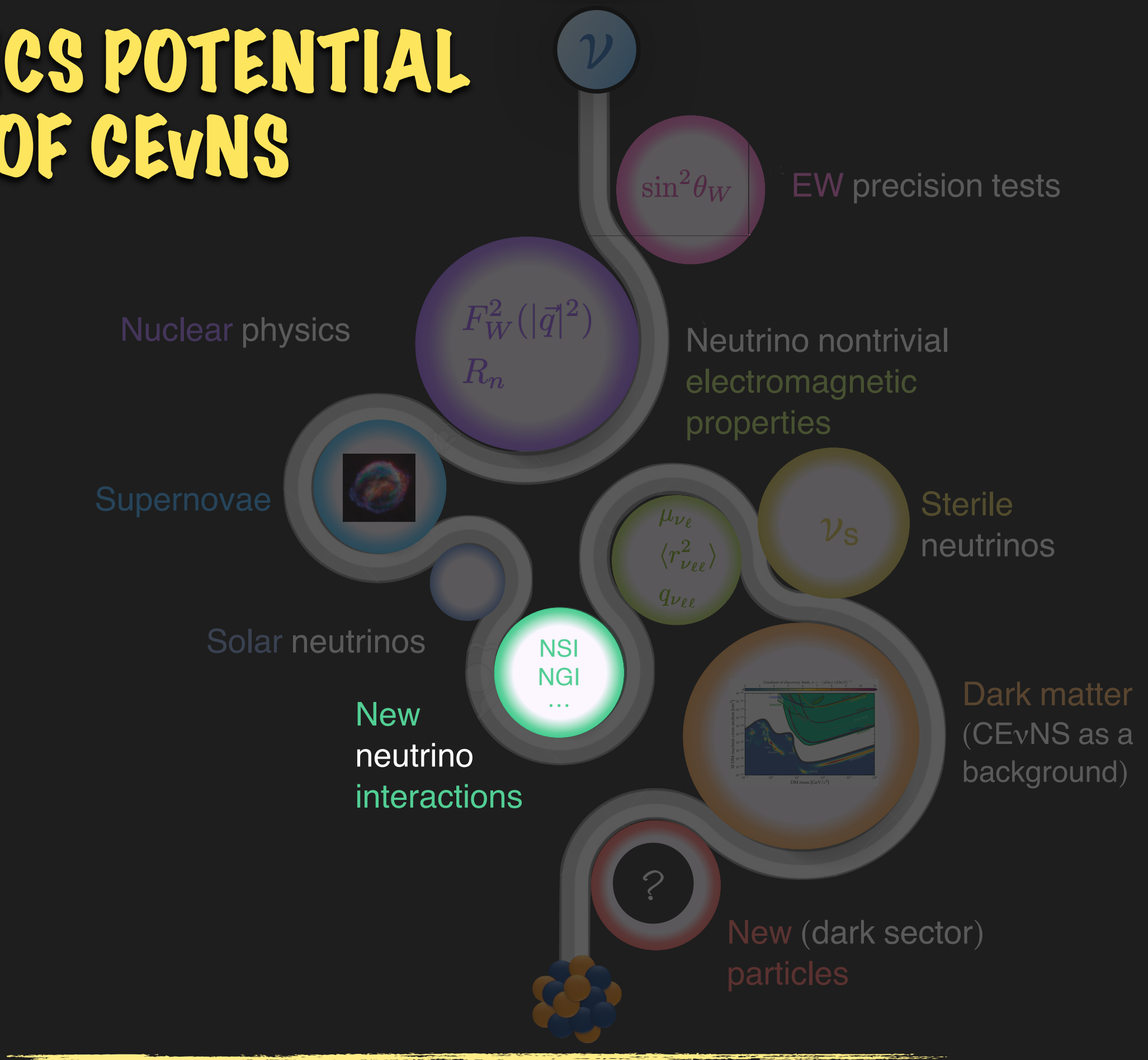
NEUTRINO MILLICHARGE



DM DD and accelerator bounds are stronger.

Gninenko+ Phys.Rev.D 75 (2007) 075014
 Shivasankar+ Physics Letters B 839 (2023) 137742
 Giunti and Ternes Phys.Rev.D 108 (2023) 9, 095044

PHYSICS POTENTIAL OF CEvNS



NEW NEUTRINO INTERACTIONS: NSI

New neutrino interactions BSM appear naturally in most neutrino mass models. Neutrino Non-Standard Interactions (NSI) may be of Charged-Current (CC) or of Neutral-Current (NC) type.

CC-NSI with the matter fields (e, u, d) affect in general the production and detection of neutrinos, while NC-NSI may affect the neutrino propagation in matter.

$$\mathcal{L}_{\text{NSI}}^{\text{CC}} \propto \epsilon_{\alpha\beta}^{ff'X} \left(\bar{\nu}_\alpha \gamma^\mu P_L \ell_\beta \right) \left(\bar{f}' \gamma_\mu P_X f \right)$$

$$\mathcal{L}_{\text{NSI}}^{\text{NC}} \propto \epsilon_{\alpha\beta}^{fX} \left(\bar{\nu}_\alpha \gamma^\mu P_L \nu_\beta \right) \left(\bar{f} \gamma_\mu P_X f \right)$$

These operators are expected to arise generically from the exchange of some mediator assumed to be heavier than the typical momentum transfer of the neutrino interaction.

T. Ohlsson, Rept. Prog. Phys. 76 (2013) 044201
O. Miranda and H. Nunokawa, New J.Phys. 17 (2015) 095002
Farzan and M. Tortola, Front.in Phys. 6 (2018) 10

NEW NEUTRINO INTERACTIONS: NSI

$$\mathcal{L}_{\text{NSI}}^{\text{NC}} \propto \epsilon_{\alpha\beta}^{fX} \left(\bar{\nu}_\alpha \gamma^\mu P_L \nu_\beta \right) \left(\bar{f} \gamma_\mu P_X f \right)$$

When embedded in a complete theory, electroweak gauge invariance generically implies that the NSI-NC parameters are expected to be subject to tight constraints from charged lepton observables.

Gavela+ Phys. Rev. D 79 (2009) 013007
Antusch+ Nucl. Phys. B810 (2009) 036

However, it is possible to build viable models for NSI by invoking an intermediate state of relatively light mass (~ 10 MeV) which has escaped detection so far because of its very small coupling.

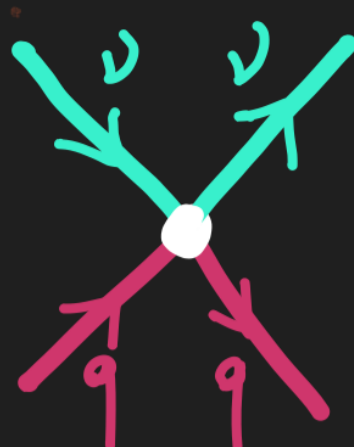
For light mediators bounds from high-energy neutrino scattering experiments such as CHARM and NuTeV do not apply.
NSI-NC generated by light mediators (~ 10 MeV) can only be constrained by their effect in oscillation data and by CEvNS.

Farzan Phys. Lett. B 748 (2015) 311
Farzan and Shoemaker, JHEP 07 (2016) 033
Babu+ JHEP 12 (2017) 096
Denton+ JHEP 07 (2018) 037
Farzan and M. Tortola, Front.in Phys. 6 (2018) 10
Esteban+ JHEP 08 (2018) 180

NEW NEUTRINO INTERACTIONS: NSI

Neutrino NSI can be formulated in terms of the effective (dimension-6) four-fermion Lagrangian:

$$\mathcal{L}_{\text{NC}}^{\text{NSI}} = -2\sqrt{2}G_F \sum_{q,\ell,\ell'} \boxed{\varepsilon_{\ell\ell'}^{qX}} (\bar{\nu}_\ell \gamma^\mu P_L \nu_{\ell'}) (\bar{f} \gamma_\mu P_X f)$$



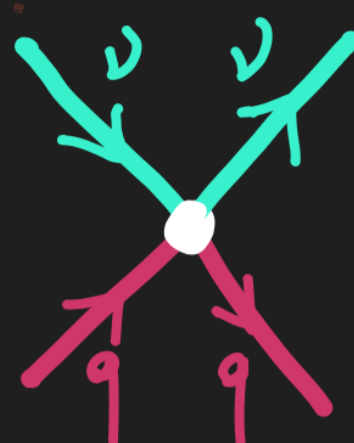
$$Q_V^{\text{NSI}} = [(g_V^p + 2\varepsilon_{\ell\ell}^{uV} + \varepsilon_{\ell\ell}^{dV}) Z + (g_V^n + \varepsilon_{\ell\ell}^{uV} + 2\varepsilon_{\ell\ell}^{dV}) N] \\ + \sum_{\ell,\ell'} [(2\varepsilon_{\ell\ell'}^{uV} + \varepsilon_{\ell\ell'}^{dV}) Z + (\varepsilon_{\ell\ell'}^{uV} + 2\varepsilon_{\ell\ell'}^{dV}) N]$$

The NSI couplings quantify the relative strength of the NSI in terms of G_F and can be either flavour preserving (non-universal) or flavor changing.

NEW NEUTRINO INTERACTIONS: NSI

Neutrino NSI can be formulated in terms of the effective (dimension-6) four-fermion Lagrangian:

$$\mathcal{L}_{\text{NC}}^{\text{NSI}} = -2\sqrt{2}G_F \sum_{q,\ell,\ell'} \boxed{\varepsilon_{\ell\ell'}^{qX}} (\bar{\nu}_\ell \gamma^\mu P_L \nu_{\ell'}) (\bar{f} \gamma_\mu P_X f)$$



$$Q_V^{\text{NSI}} = [(g_V^p + 2\varepsilon_{\ell\ell}^{uV} + \varepsilon_{\ell\ell}^{dV}) Z + (g_V^n + \varepsilon_{\ell\ell}^{uV} + 2\varepsilon_{\ell\ell}^{dV}) N] \\ + \sum_{\ell,\ell'} [(2\varepsilon_{\ell\ell'}^{uV} + \varepsilon_{\ell\ell'}^{dV}) Z + (\varepsilon_{\ell\ell'}^{uV} + 2\varepsilon_{\ell\ell'}^{dV}) N]$$

The NSI couplings quantify the relative strength of the NSI in terms of G_F and can be either flavour preserving (non-universal) or flavor changing.

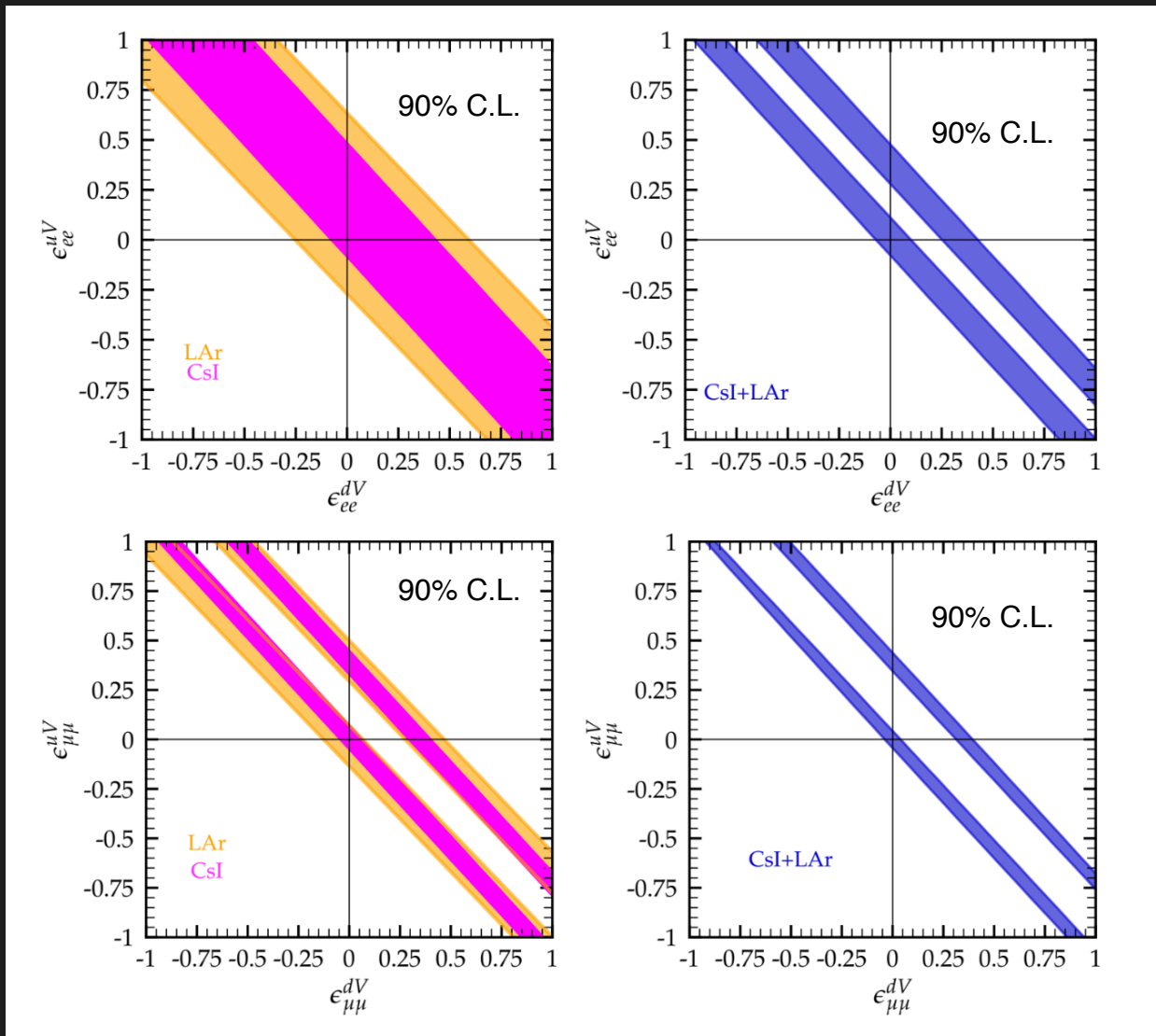
See also: S. Davidson et. al., JHEP 03 (2003) 011 J. Barranco, O.G. Miranda and T.I. Rashba, JHEP 0512 (2005) 021, K. Scholberg, PRD 73 (2006) 033005, Coloma+ Phys. Rev. D 96, 115007 (2017), JHEP 02, 023 (2020), JHEP 05 (2022) 037, Papoulias+ Phys. Rev. D 97, 033003 (2018), Giunti PRD 101, 035039 (2020), Denton+ JHEP 04, 266 (2021), Esteban+ JHEP 08, 180 (2018), COHERENT Colab. arXiv:2110.07730, Coloma+ JHEP 05 (2022) 037, Bresó-Pla+ JHEP 05 (2023) 074, Coloma+ JHEP 08 (2023) 03, Liao+ arXiv:2408.06255 ...

NEW NEUTRINO INTERACTIONS: NSI

Neutrino NSI can be formulated in terms of the effective four-fermion Lagrangian:

$$\mathcal{L}_{\text{NC}}^{\text{NSI}} = -2\sqrt{2}G_F \sum_{q,\ell,\ell'} \boxed{\varepsilon_{\ell\ell'}^{qX}} (\bar{\nu}_\ell \gamma^\mu P_L \nu_{\ell'}) (\bar{f} \gamma_\mu P_X f)$$

COHERENT CsI (2021) + LAr

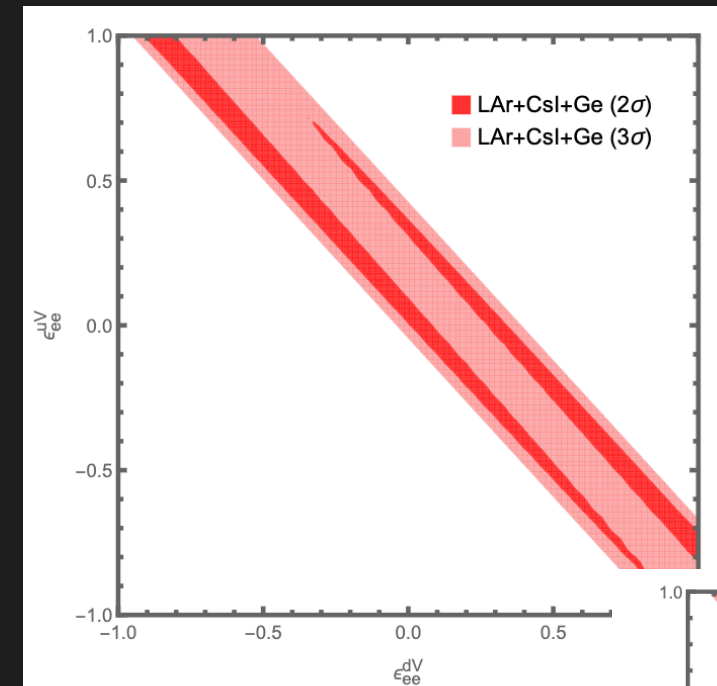
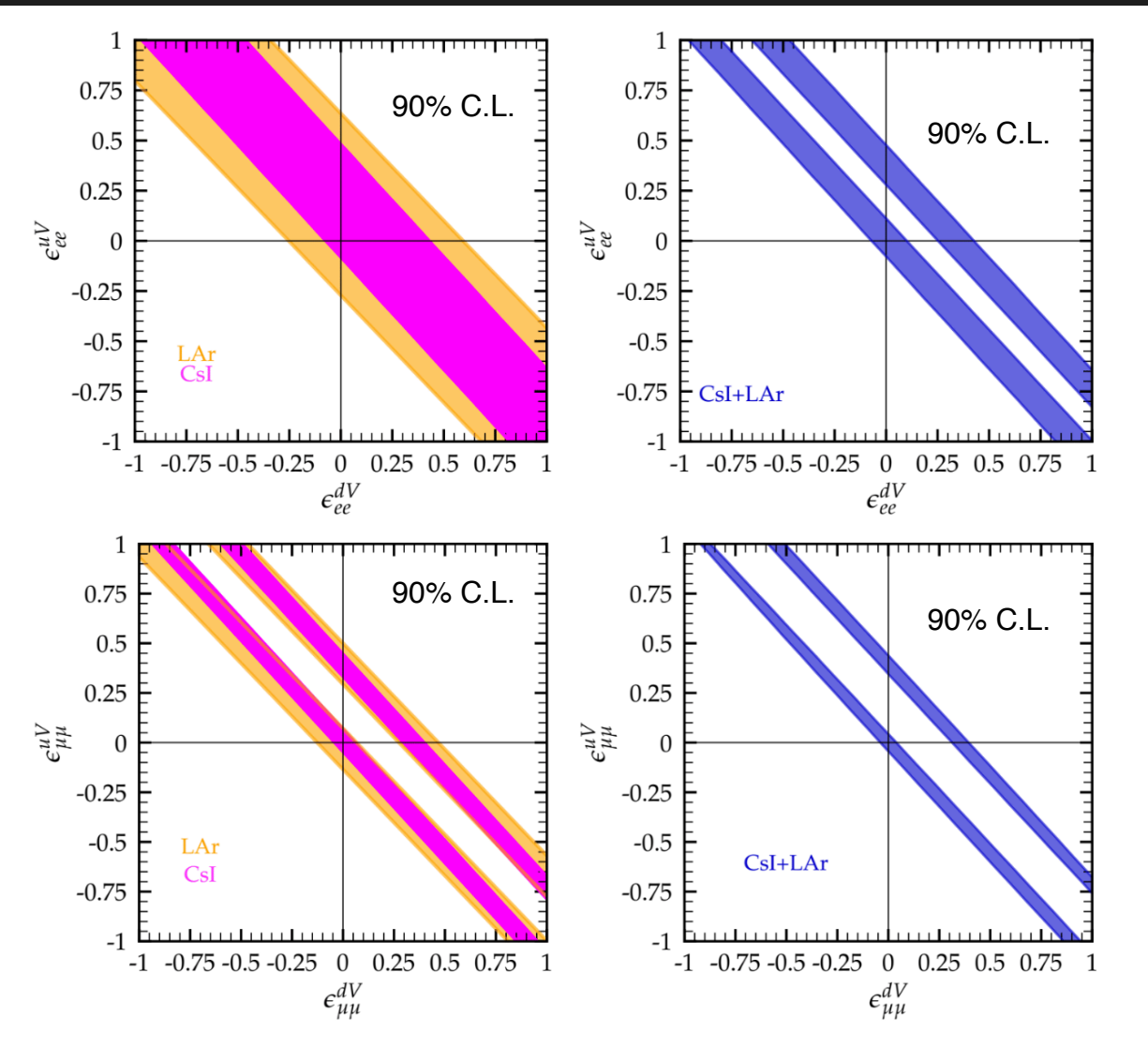


NEW NEUTRINO INTERACTIONS: NSI

Neutrino NSI can be formulated in terms of the effective four-fermion Lagrangian:

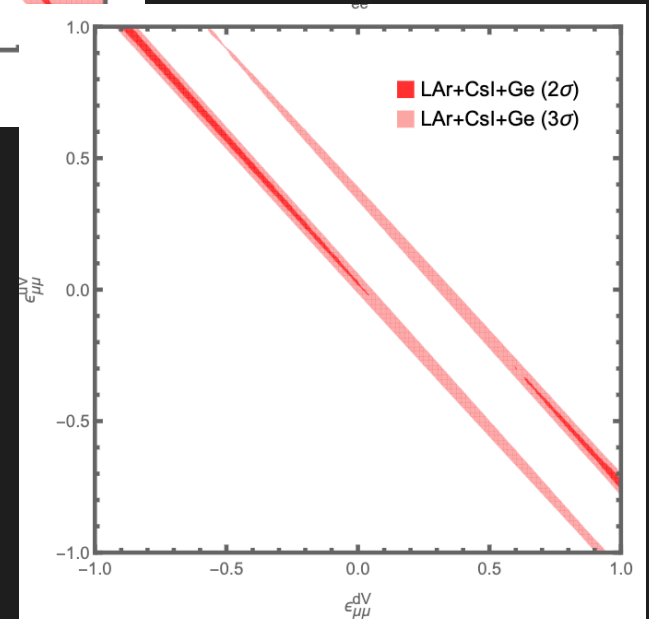
$$\mathcal{L}_{\text{NC}}^{\text{NSI}} = -2\sqrt{2}G_F \sum_{q,\ell,\ell'} \boxed{\varepsilon_{\ell\ell'}^{qX}} (\bar{\nu}_\ell \gamma^\mu P_L \nu_{\ell'}) (\bar{f} \gamma_\mu P_X f)$$

COHERENT CsI (2021) + LAr



COHERENT CsI
(2021) + LAr + Ge

Liao+ arXiv:2408.06255

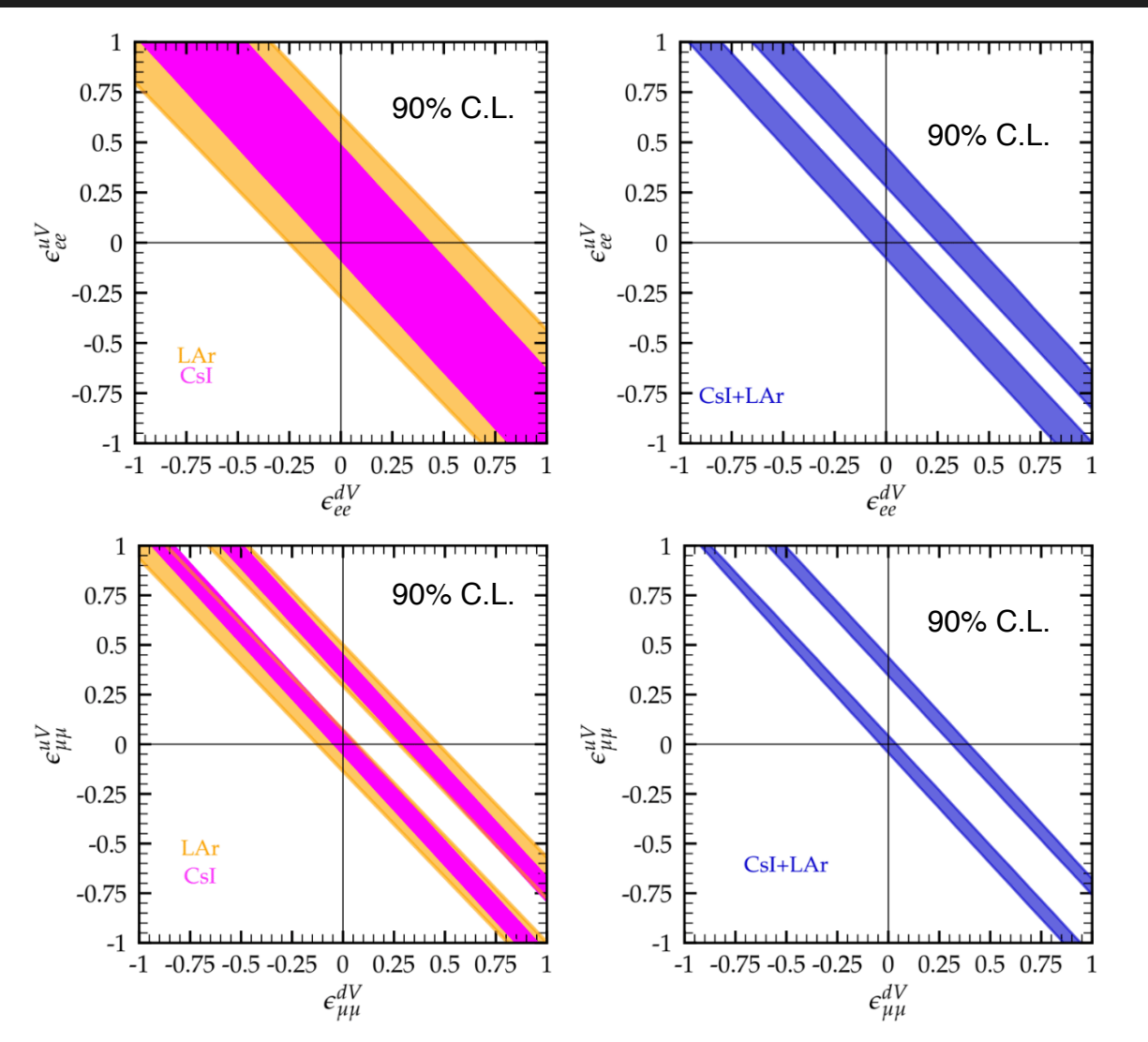


NEW NEUTRINO INTERACTIONS: NSI

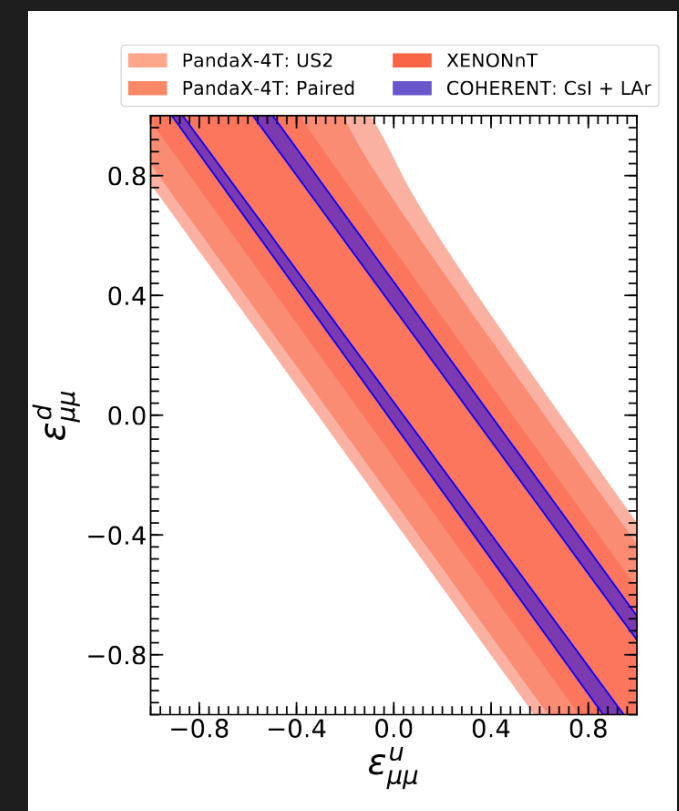
Neutrino NSI can be formulated in terms of the effective four-fermion Lagrangian:

$$\mathcal{L}_{\text{NC}}^{\text{NSI}} = -2\sqrt{2}G_F \sum_{q,\ell,\ell'} \boxed{\varepsilon_{\ell\ell'}^{qX}} (\bar{\nu}_\ell \gamma^\mu P_L \nu_{\ell'}) (\bar{f} \gamma_\mu P_X f)$$

COHERENT CsI (2021) + LAr



COHERENT CsI
(2021) + LAr +
XENONnT +
PANDAX-4T

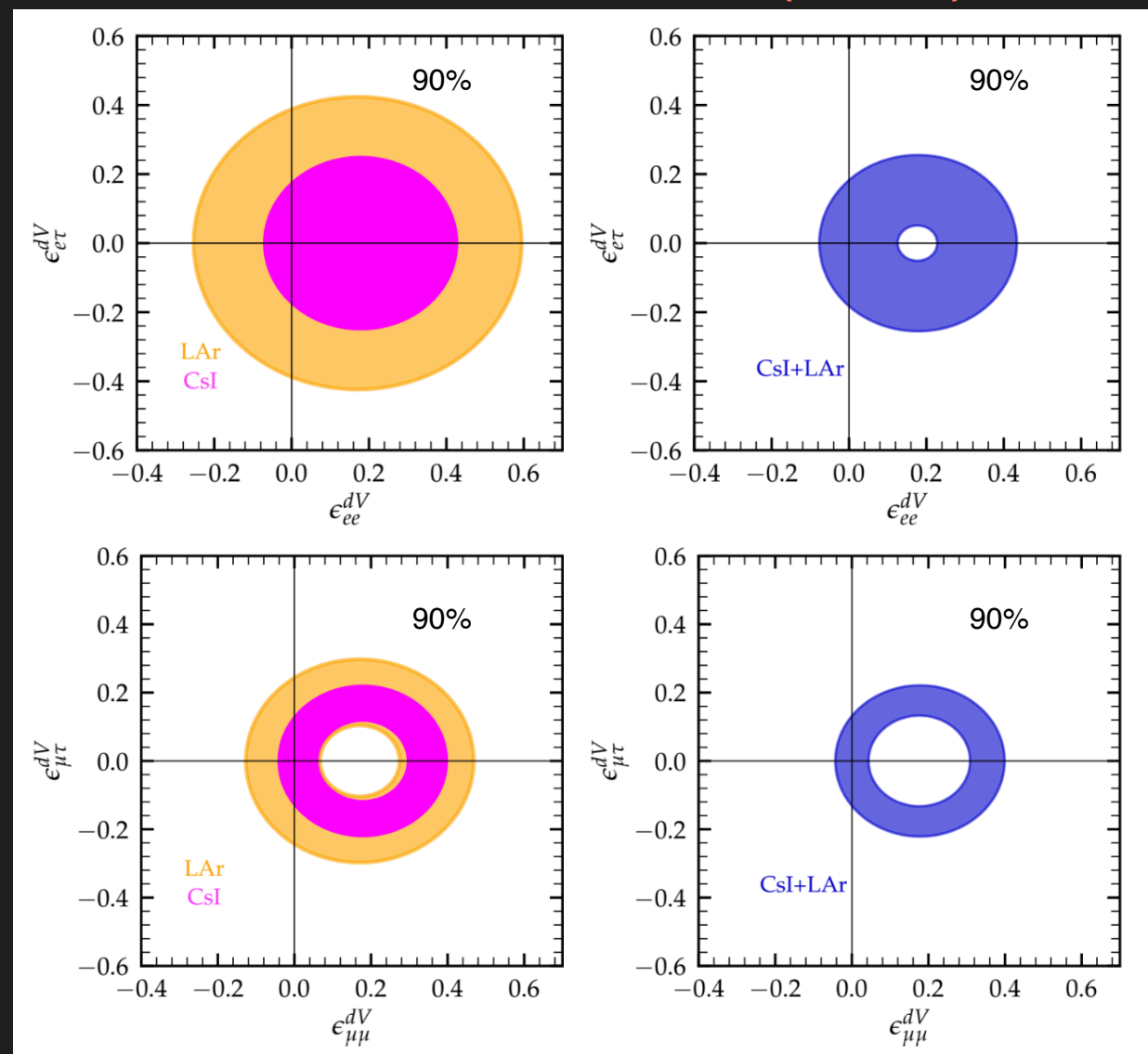


Aristizabal+ arXiv: 2409.02003
See also Li+ 2409.04703

NEW NEUTRINO INTERACTIONS: NSI

$$\mathcal{L}_{\text{NC}}^{\text{NSI}} = -2\sqrt{2}G_F \sum_{q,\ell,\ell'} \boxed{\varepsilon_{\ell\ell'}^{qX}} (\bar{\nu}_\ell \gamma^\mu P_L \nu_{\ell'}) (\bar{f} \gamma_\mu P_X f)$$

COHERENT CsI (2021) + LAr



VDR, Miranda, Papoulias, Sanchez-García, Tórtola and Valle, JHEP 04 (2023) 035

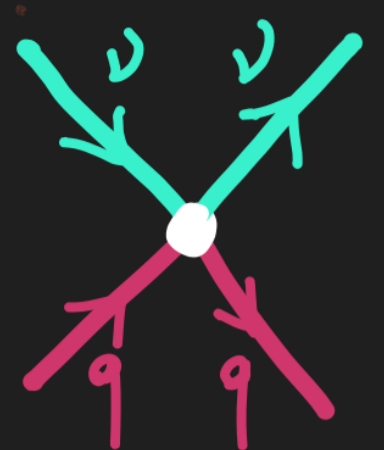
NEW NEUTRINO INTERACTIONS: NGI

Beyond the typical NSI interactions that could arise in gauge extensions of the SM, a more general framework can be considered to accommodate all Lorentz invariant interactions

$$\mathcal{L}_{\text{NC}}^{\text{NGI}} \approx \sum_{X=S,V,T} C_X \bar{\nu} \Gamma_X \nu \bar{\mathcal{N}} \Gamma^X \mathcal{N} + \sum_{(X,Y)=(P,S),(A,V)} D_X \bar{\nu} \Gamma_X \nu \bar{\mathcal{N}} i \Gamma^Y \mathcal{N}$$

$$\Gamma^X = \{ \mathbb{I}, i\gamma^5, \gamma^\mu, \gamma^\mu \gamma^5, \sigma^{\mu\nu} \} \quad \sigma^{\mu\nu} = i[\gamma^\mu, \gamma^\nu]/2$$

C_X , D_X denote the corresponding neutrino-nucleus couplings



Lee and Yang, Phys.Rev. 104 (1956) 254–258
Lindner+ JHEP 03 (2017) 097,
Aristizabal Sierra, VDR, Rojas, Phys.Rev.D 98 (2018) 075018
Flores et al. Phys. Rev. D 105 no. 5, (2022) 05501
...

NEW NEUTRINO INTERACTIONS: NGI

Beyond the typical NSI interactions that could arise in gauge extensions of the SM, a more general framework can be considered to accommodate all Lorentz invariant interactions

$$\mathcal{L}_{\text{NC}}^{\text{NGI}} \approx \sum_{X=S,V,T} C_X \bar{\nu} \Gamma_X \nu \bar{\mathcal{N}} \Gamma^X \mathcal{N} + \sum_{(X,Y)=(P,S),(A,V)} D_X \bar{\nu} \Gamma_X \nu \bar{\mathcal{N}} i \Gamma^Y \mathcal{N}$$

$$\frac{d\sigma}{dE_{\text{nr}}} \Big|_{\text{CE}\nu\text{NS}}^{\text{NGI}} = \frac{G_F^2 m_N}{4\pi} F_W^2 (|\vec{q}|^2) \left\{ C_S^2 \frac{m_N E_{\text{nr}}}{2E_\nu^2} + \boxed{(C_V + 2 Q_V^{\text{SM}})^2} \left(1 - \frac{m_N E_{\text{nr}}}{2E_\nu^2} - \frac{E_{\text{nr}}}{E_\nu} \right) + 8 C_T^2 \left(1 - \frac{m_N E_{\text{nr}}}{4E_\nu^2} - \frac{E_{\text{nr}}}{E_\nu} \right) \boxed{\pm \mathcal{R}} \frac{E_{\text{nr}}}{E_\nu} \right\}$$

Interference
 new vector/SM

Interference
 scalar/tensor
 $R = 2C_S C_T$
 +: antineutrino

Weak charge associated to the new vector boson:

$$C_V = g_{\nu V} \left[(2g_{uV} + g_{dV}) Z + (g_{uV} + 2g_{dV}) N \right]$$

new mediator couplings with neutrinos and quarks

NEW NEUTRINO INTERACTIONS: NGI

Beyond the typical NSI interactions that could arise in gauge extensions of the SM, a more general framework can be considered to accommodate all Lorentz invariant interactions

$$\mathcal{L}_{\text{NC}}^{\text{NGI}} \approx \sum_{X=S,V,T} C_X \bar{\nu} \Gamma_X \nu \bar{\mathcal{N}} \Gamma^X \mathcal{N} + \sum_{(X,Y)=(P,S),(A,V)} D_X \bar{\nu} \Gamma_X \nu \bar{\mathcal{N}} i \Gamma^Y \mathcal{N}$$

$$\frac{d\sigma}{dE_{\text{nr}}} \Big|_{\text{CE}\nu\text{NS}}^{\text{NGI}} = \frac{G_F^2 m_N}{4\pi} F_W^2 (|\vec{q}|^2) \left\{ C_S^2 \frac{m_N E_{\text{nr}}}{2E_\nu^2} + \boxed{(C_V + 2 Q_V^{\text{SM}})^2} \left(1 - \frac{m_N E_{\text{nr}}}{2E_\nu^2} - \frac{E_{\text{nr}}}{E_\nu} \right) + 8 C_T^2 \left(1 - \frac{m_N E_{\text{nr}}}{4E_\nu^2} - \frac{E_{\text{nr}}}{E_\nu} \right) \boxed{\pm \mathcal{R}} \frac{E_{\text{nr}}}{E_\nu} \right\}$$

Interference
new vector/SM

Interference
scalar/tensor
 $R = 2C_S C_T$

+: antineutrino

Weak charge associated to the new scalar boson:

$$C_S = g_{\nu S} \left(Z \sum_q g_{qS} \frac{m_p}{m_q} f_q^p + N \sum_q g_{qS} \frac{m_n}{m_q} f_q^n \right)$$

Cirelli+ JCAP 10 (2013) 019
 Del Nobile arXiv:2104.12785
 Belanger+ Comput. Phys. Commun. 185 (2014) 960–985
 Anselmino+ Nucl. Phys. B Proc. Suppl. 191 (2009) 98–107
 Candela+ 2404.12476

hadronic structure parameters (quark mass contributions to the nucleon)

NEW NEUTRINO INTERACTIONS: NGI

Beyond the typical NSI interactions that could arise in gauge extensions of the SM, a more general framework can be considered to accommodate all Lorentz invariant interactions

$$\mathcal{L}_{\text{NC}}^{\text{NGI}} \approx \sum_{X=S,V,T} C_X \bar{\nu} \Gamma_X \nu \bar{\mathcal{N}} \Gamma^X \mathcal{N} + \sum_{(X,Y)=(P,S),(A,V)} D_X \bar{\nu} \Gamma_X \nu \bar{\mathcal{N}} i \Gamma^Y \mathcal{N}$$

$$\frac{d\sigma}{dE_{\text{nr}}} \Big|_{\text{CE}\nu\text{NS}}^{\text{NGI}} = \frac{G_F^2 m_N}{4\pi} F_W^2 (|\vec{q}|^2) \left\{ C_S^2 \frac{m_N E_{\text{nr}}}{2E_\nu^2} + \boxed{(C_V + 2 Q_V^{\text{SM}})^2} \left(1 - \frac{m_N E_{\text{nr}}}{2E_\nu^2} - \frac{E_{\text{nr}}}{E_\nu} \right) + 8 C_T^2 \left(1 - \frac{m_N E_{\text{nr}}}{4E_\nu^2} - \frac{E_{\text{nr}}}{E_\nu} \right) \boxed{\pm \mathcal{R}} \frac{E_{\text{nr}}}{E_\nu} \right\}$$

Interference
new vector/SM

Interference
scalar/tensor
 $R = 2C_S C_T$

+: antineutrino

Weak charge associated to the tensor interaction:

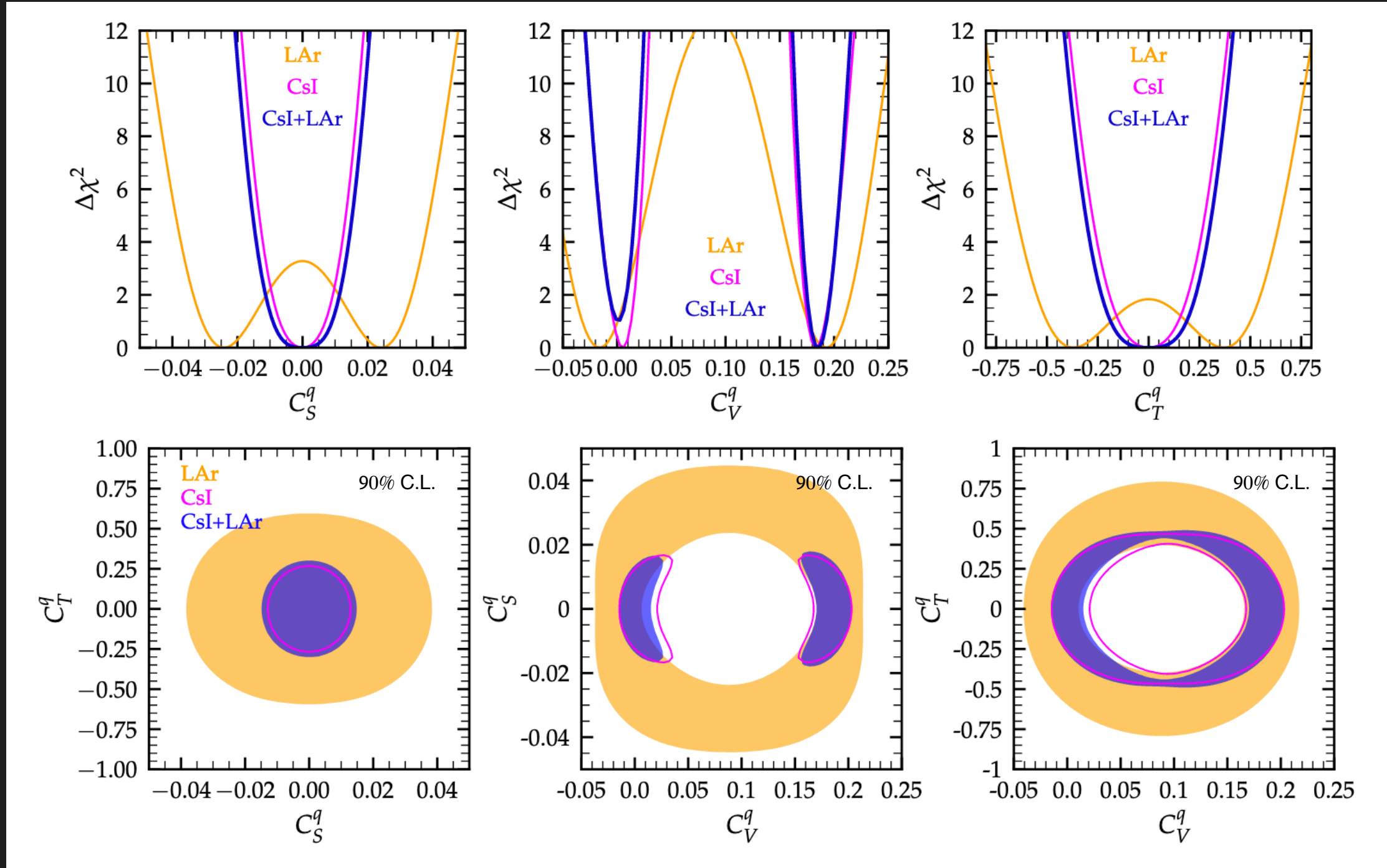
$$C_T = g_{\nu T} \left(Z \sum_q g_{qT} \delta_q^p + N \sum_q g_{qT} \delta_q^n \right)$$

Cirelli+ JCAP 10 (2013) 019
 Del Nobile arXiv:2104.12785
 Belanger+ Comput. Phys. Commun. 185 (2014) 960–985
 Anselmino+ Nucl. Phys. B Proc. Suppl. 191 (2009) 98–107
 Candela+ 2404.12476

tensor charges (difference between the spin of quarks and anti-quarks inside the nucleon)

NEW NEUTRINO INTERACTIONS: NGI

COHERENT CsI (2021) + LAr



VDR, Miranda, Papoulias, Sanchez-García, Tórtola and Valle, JHEP 04 (2023) 035

NEW NEUTRINO INTERACTIONS: LIGHT MEDIATORS

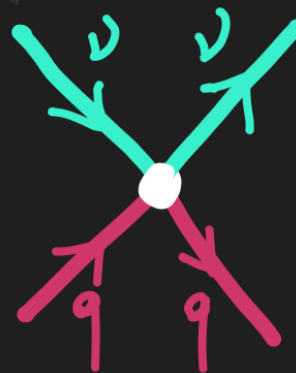
New BSM scenarios might be associated with different types of interactions and mediators. These mediators would contribute to CE ν NS and E ν ES processes leading to detectable distortions of the event rates, especially at low-energy recoils.

Cerdeño+ JHEP 1605 (2016) 118
Bertuzzo+ JHEP 1704 (2017) 073
Farzan+ JHEP 1805 (2018) 066
Denton+ PRD 106 (2022) 015022

Low-energy neutrino experiments are sensitive to interactions involving light mediators, inducing spectral distortions at low recoil energies.

We may consider **light mediators** with a mass comparable to the typical momentum transfer

$$|\mathbf{q}| \approx \sqrt{2m_{\mathcal{N}}E_{\text{nr}}}$$



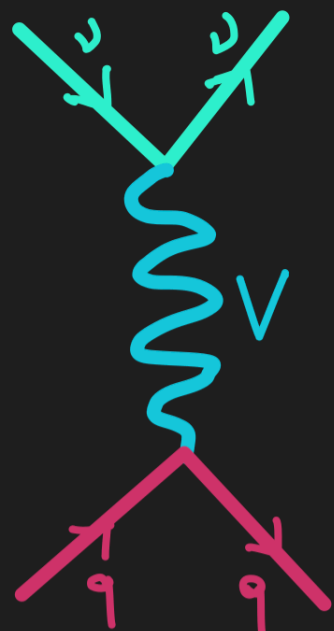
$$G_F^2 |\epsilon_\ell^X|^2 \rightarrow \frac{2g_X^4}{(m_X^2 + |\mathbf{q}|^2)^2}$$



NEW NEUTRINO INTERACTIONS: LV

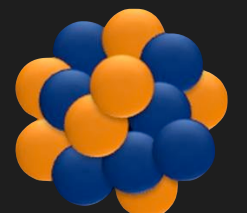
$$\left. \frac{d\sigma}{dE_{\text{nr}}} \right|_{\text{CE}\nu\text{NS}}^{\text{LV}} = \left(1 + \kappa \frac{C_V}{\sqrt{2} G_F Q_W^{\text{SM}} (2m_N E_{\text{nr}} + m_V^2)} \right)^2 \left. \frac{d\sigma}{dE_{\text{nr}}} \right|_{\text{CE}\nu\text{NS}}^{\text{SM}}$$

$$C_V = g_{\nu V} \left[(2g_{uV} + g_{dV}) Z + (g_{uV} + 2g_{dV}) N \right]$$



$\kappa = 1$ for universal couplings
 $\kappa = -1/3$ in the B – L model

$$g_V = \sqrt{g_{\nu V} g_{qV}}$$

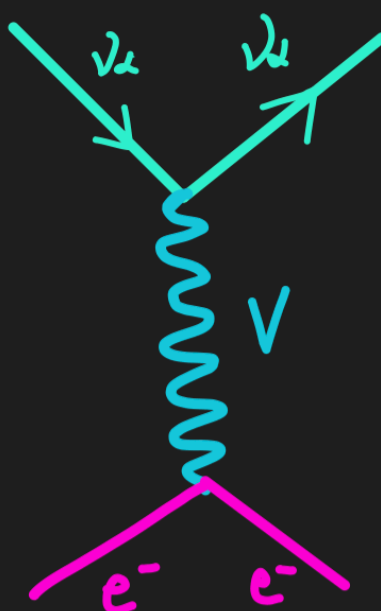


NEW NEUTRINO INTERACTIONS: LV

$$\frac{d\sigma_{\nu_\ell \mathcal{A}}}{dE_{\text{er}}} \Big|_{\text{E}\nu\text{ES}}^{\text{SM}} = Z_{\text{eff}}^{\mathcal{A}}(E_{\text{er}}) \frac{G_F^2 m_e}{2\pi} \left[(g_V^{\nu_\ell} + g_A^{\nu_\ell})^2 + (g_V^{\nu_\ell} - g_A^{\nu_\ell})^2 \left(1 - \frac{E_{\text{er}}}{E_\nu} \right)^2 - \left((g_V^{\nu_\ell})^2 - (g_A^{\nu_\ell})^2 \right) \frac{m_e E_{\text{er}}}{E_\nu^2} \right]$$

effective number of protons
seen by the neutrino for an
energy deposition E_{er}

$$g_V^{\nu_\ell} = g_V^{\nu_\ell} + \kappa \frac{g_{\nu V} \cdot g_{eV}}{2\sqrt{2} G_F (2m_e E_{\text{er}} + m_V^2)}$$



$\kappa = 1$ for universal couplings
 $\kappa = 1$ in the B – L model

$$g_V = \sqrt{g_{\nu V} g_{eV}}$$



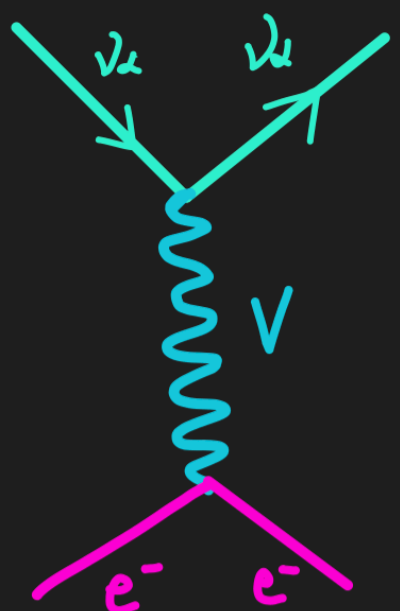
NEW NEUTRINO INTERACTIONS: LV

$$\frac{d\sigma_{\nu_\ell \mathcal{A}}}{dE_{\text{er}}} \Big|_{\text{E}\nu\text{ES}}^{\text{SM}} = Z_{\text{eff}}^{\mathcal{A}}(E_{\text{er}}) \frac{G_F^2 m_e}{2\pi} \left[(g_V^{\nu_\ell} + g_A^{\nu_\ell})^2 + (g_V^{\nu_\ell} - g_A^{\nu_\ell})^2 \left(1 - \frac{E_{\text{er}}}{E_\nu} \right)^2 - \left((g_V^{\nu_\ell})^2 - (g_A^{\nu_\ell})^2 \right) \frac{m_e E_{\text{er}}}{E_\nu^2} \right]$$

effective number of protons
seen by the neutrino for an
energy deposition E_{er}

$$g_V^{\nu_\ell} = g_V^{\nu_\ell} + \kappa \frac{g_{\nu V} \cdot g_{eV}}{2\sqrt{2} G_F (2m_e E_{\text{er}} + m_V^2)}$$

Only relevant for CsI data!
Flavor dependent



$\nu_e - e^-$ Scattering
NC and CC

$$g_V^{\nu_\ell} = 2\sin^2\theta_w + 1/2$$

$$g_A^{\nu_\ell(\bar{\nu}_\ell)} = 1/2 \quad (-1/2)$$

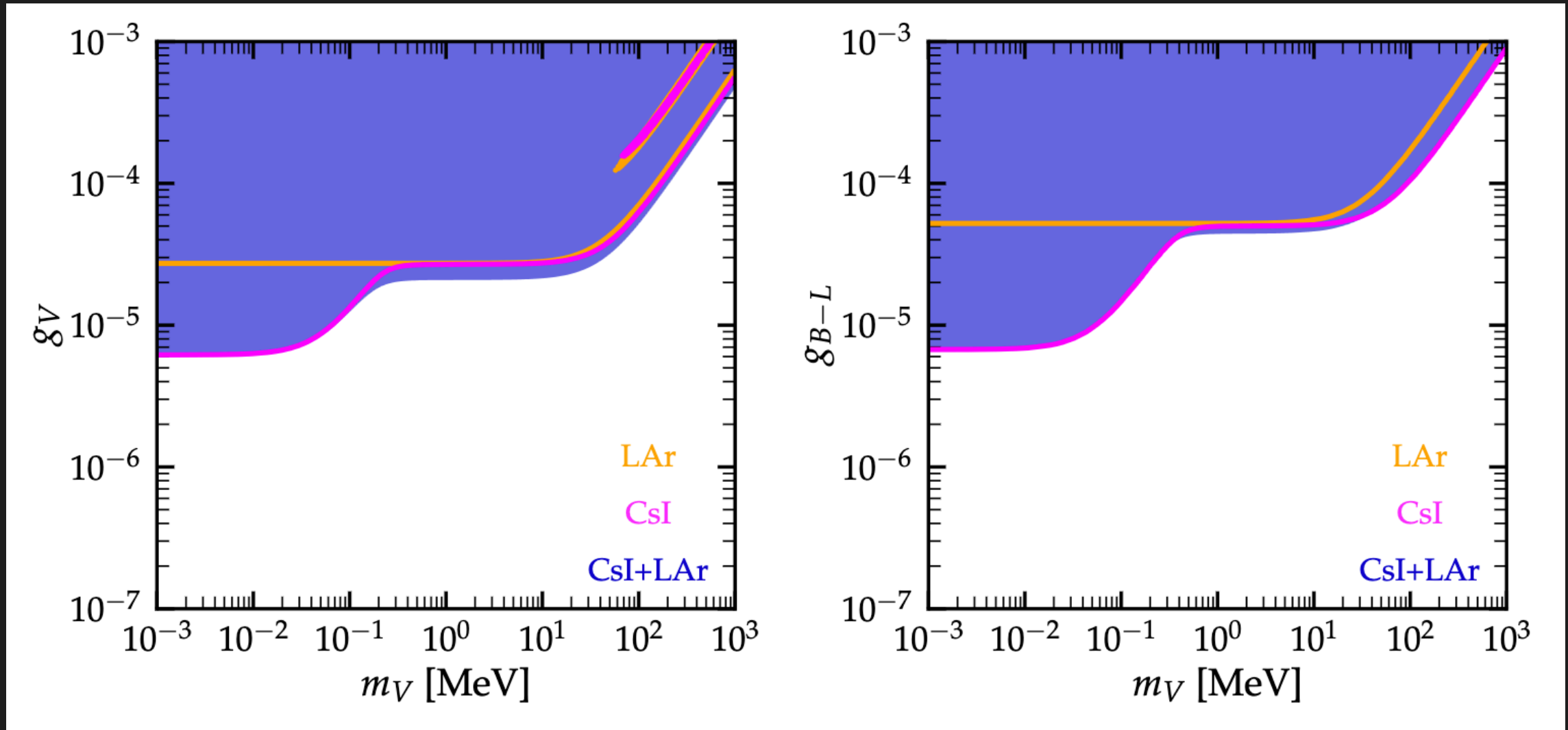
$\nu_{\mu,\tau} - e^-$ Scattering
Only NC

$$g_V^{\nu_\ell} = 2\sin^2\theta_w - 1/2$$

$$g_A^{\nu_\ell(\bar{\nu}_\ell)} = -1/2 \quad (1/2)$$



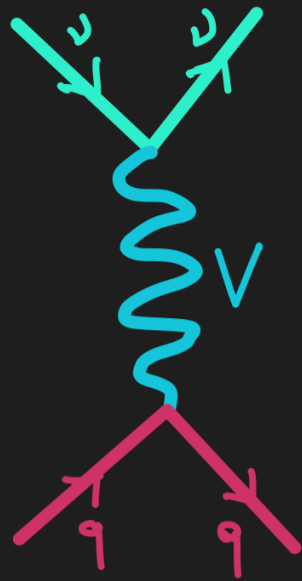
NEW NEUTRINO INTERACTIONS: LV



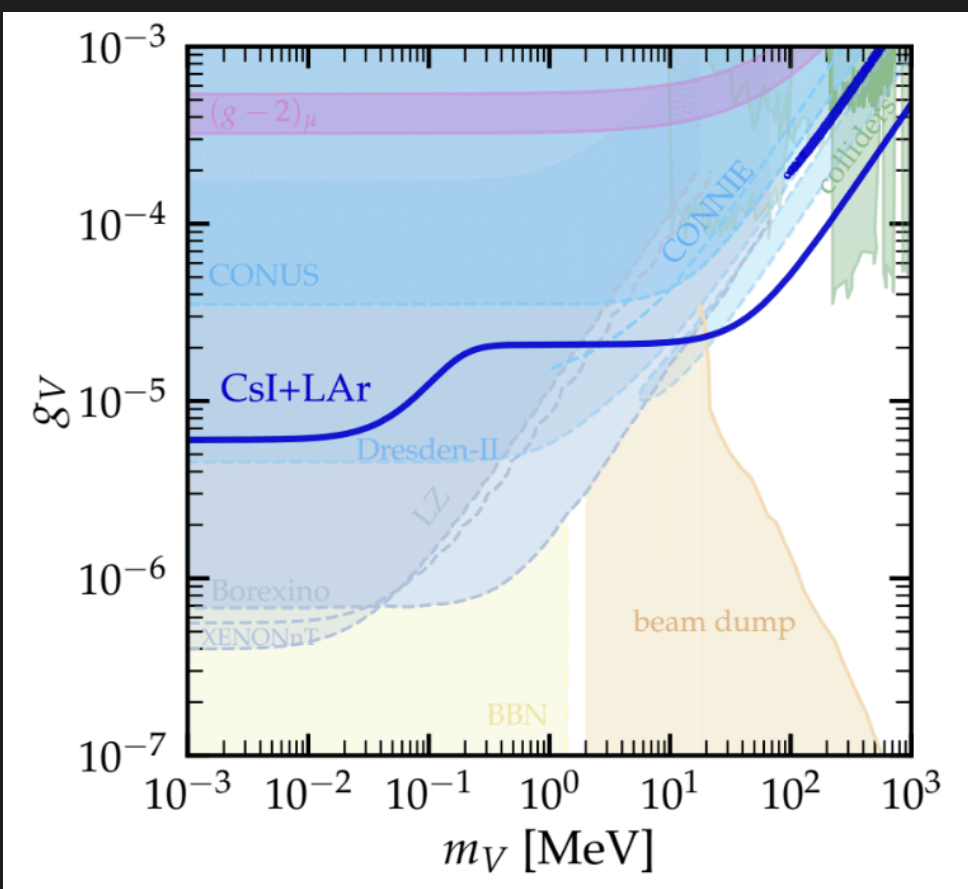
VDR, Miranda, Papoulias, Sanchez-García, Tórtola and Valle, JHEP 04 (2023) 035

- Complementary analyses in: J. Liao, H. Liu, and D. Marfatia, 2202.10622, Coloma et al. 2202.10829, Atzori-Corona et al. 2205.09484, A. Khan 2203.08892, Majumdar+ 2208.13262

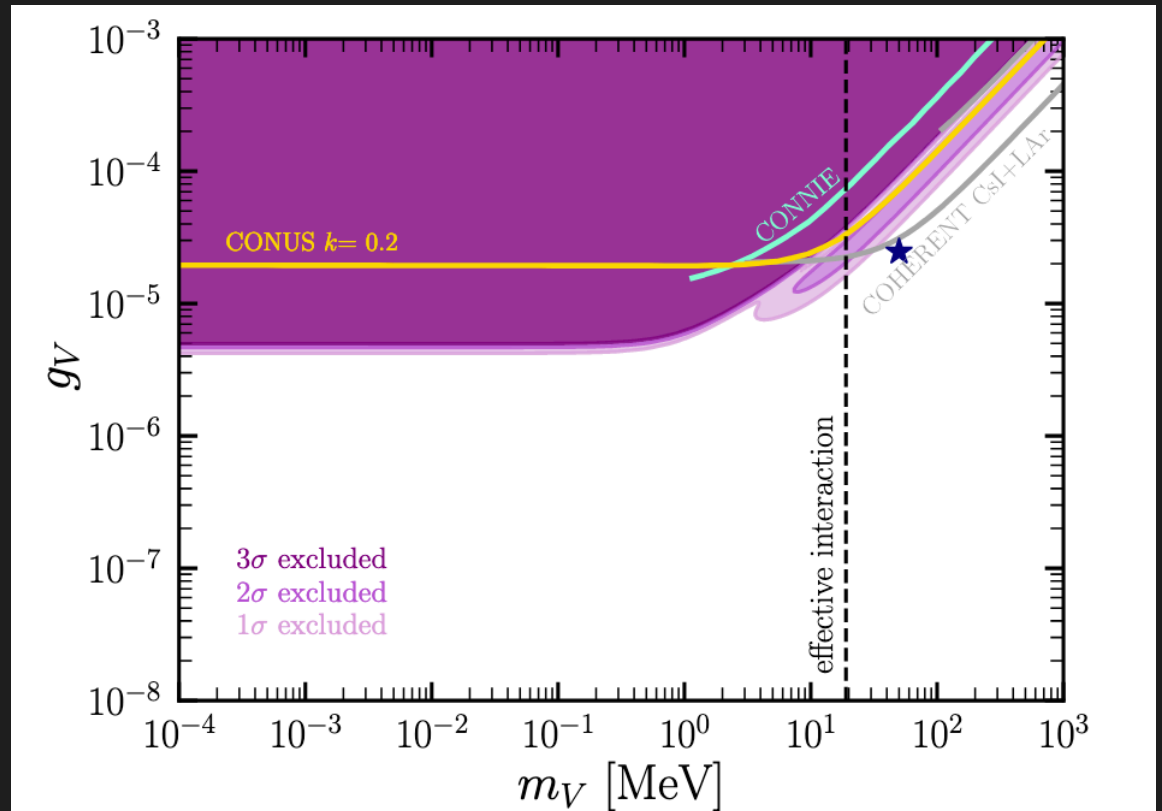
NEW NEUTRINO INTERACTIONS: LV



COHERENT CsI (2021) + LAr



Dresden-II (Ge) - iron filter



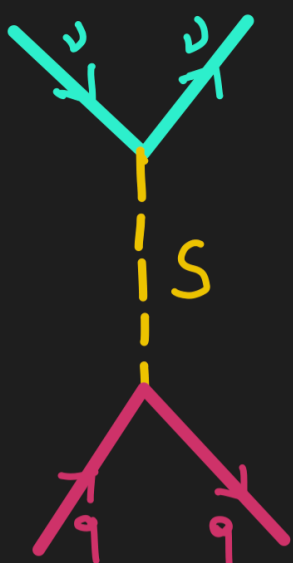
Aristizabal, VDR, Papoulias JHEP 09 (2022) 076

VDR, Miranda, Papoulias, Sanchez-García, Tórtola and Valle, JHEP 04 (2023) 035

- Complementary analyses in: J. Liao, H. Liu, and D. Marfatia, 2202.10622, Coloma et al. 2202.10829, Atzori-Corona et al. 2205.09484, A. Khan 2203.08892, Majumdar+ 2208.13262

NEW NEUTRINO INTERACTIONS: LS

$$\frac{d\sigma_{\nu_\ell \mathcal{N}}}{dE_{\text{nr}}} \Big|_{\text{CE}\nu\text{NS}}^{\text{LS}} = \frac{m_N^2 E_{\text{nr}} C_S^2}{4\pi E_\nu^2 (2m_N E_{\text{nr}} + m_S^2)^2} F_W^2(|\vec{q}|^2)$$



$$C_S = g_{\nu S} \left(Z \sum_q g_{qS} \frac{m_p}{m_q} f_q^p + N \sum_q g_{qS} \frac{m_n}{m_q} f_q^n \right)$$

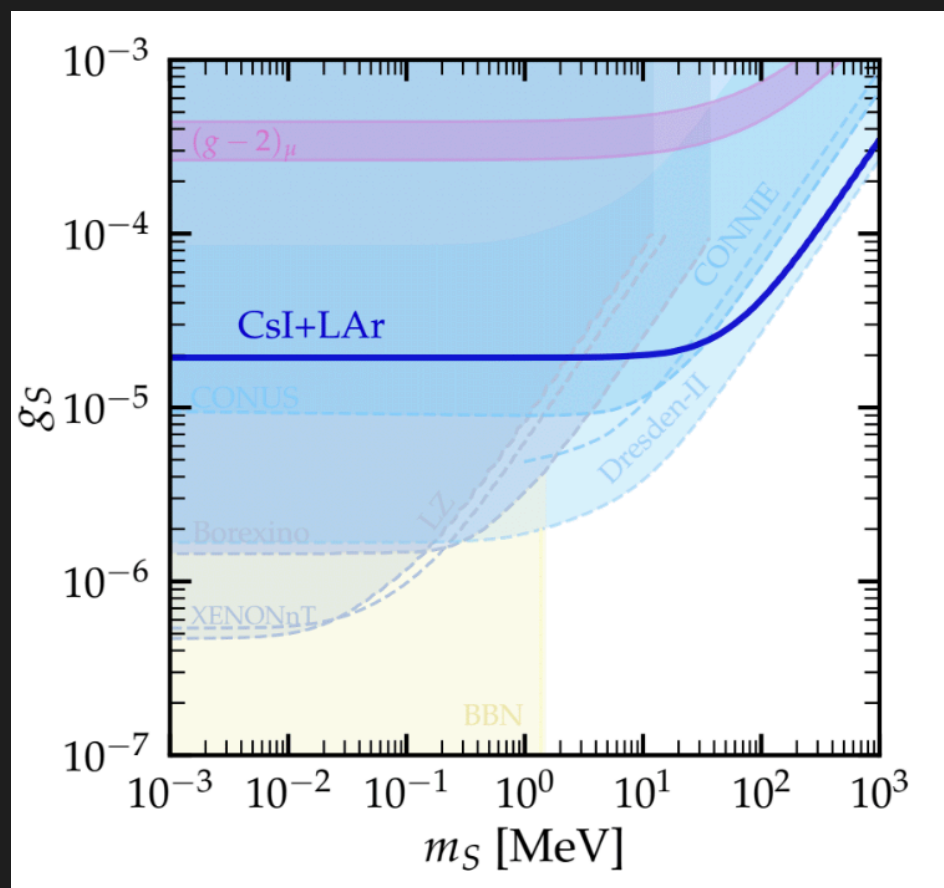
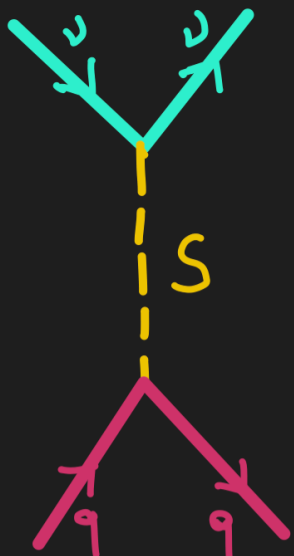
$$g_S = \sqrt{g_{\nu S} g_{qS}}$$

(Scalar-mediated EvES process has no substancial enhancement, the cross section is proportional to $\sim 1/E_{\text{er}}$)



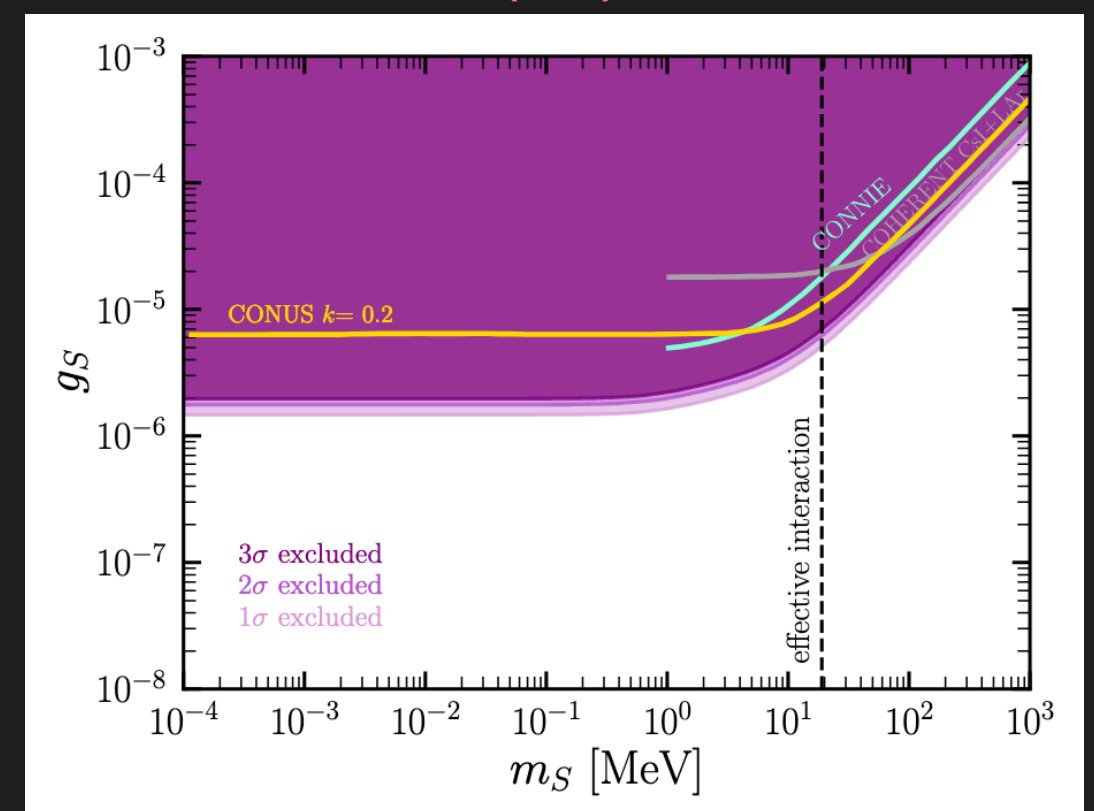
NEW NEUTRINO INTERACTIONS: LS

COHERENT CsI (2021) + LAr



VDR, Miranda, Papoulias, Sanchez-García, Tórtola and Valle, JHEP 04 (2023) 035

Dresden-II (Ge) - iron filter



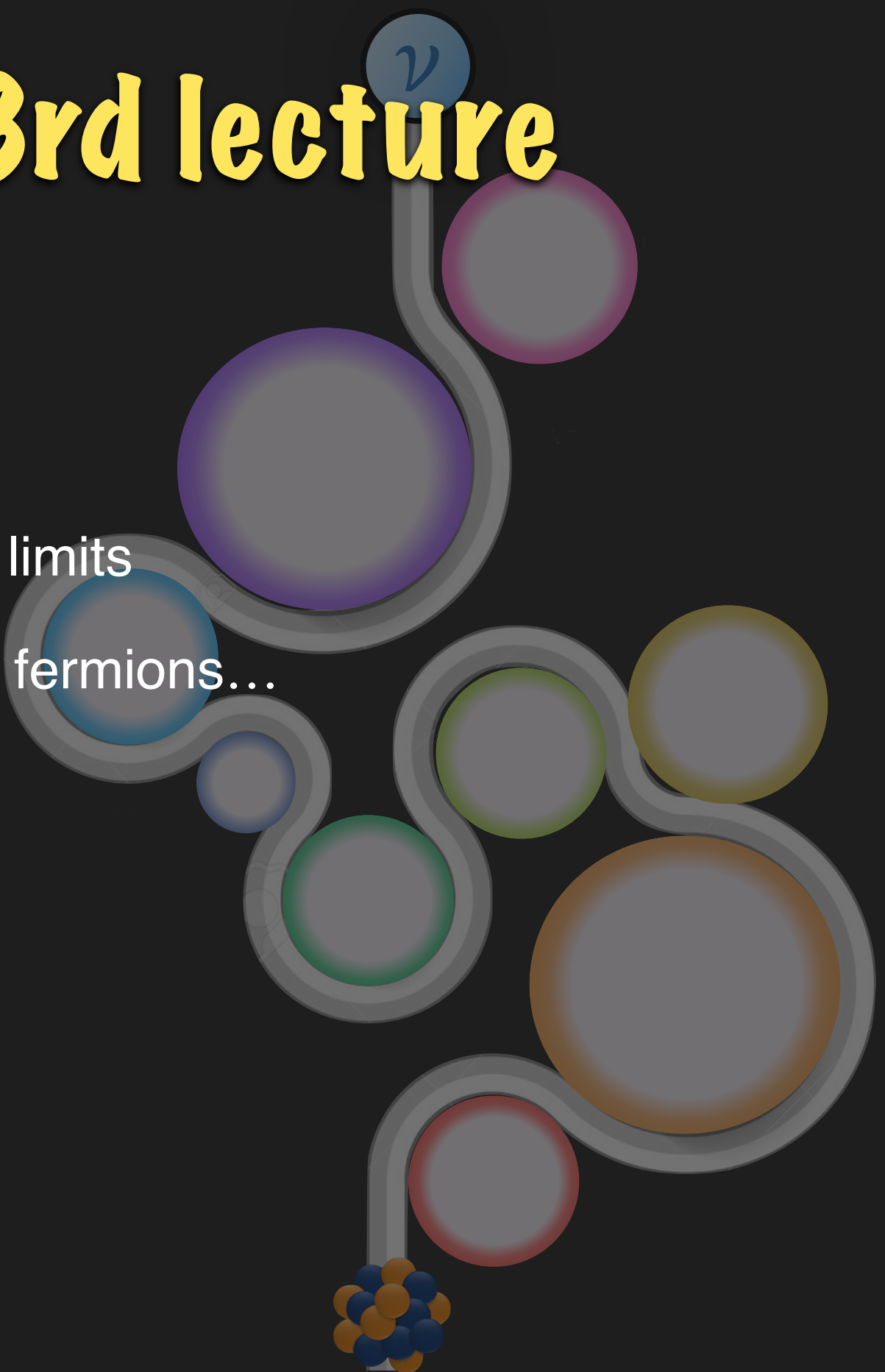
Aristizabal, VDR, Papoulias JHEP 09 (2022) 076

- Complementary analyses in: J. Liao, H. Liu, and D. Marfatia, 2202.10622, Coloma et al. 2202.10829, Atzori-Corona et al. 2205.09484, A. Khan 2203.08892, Majumdar+ 2208.13262

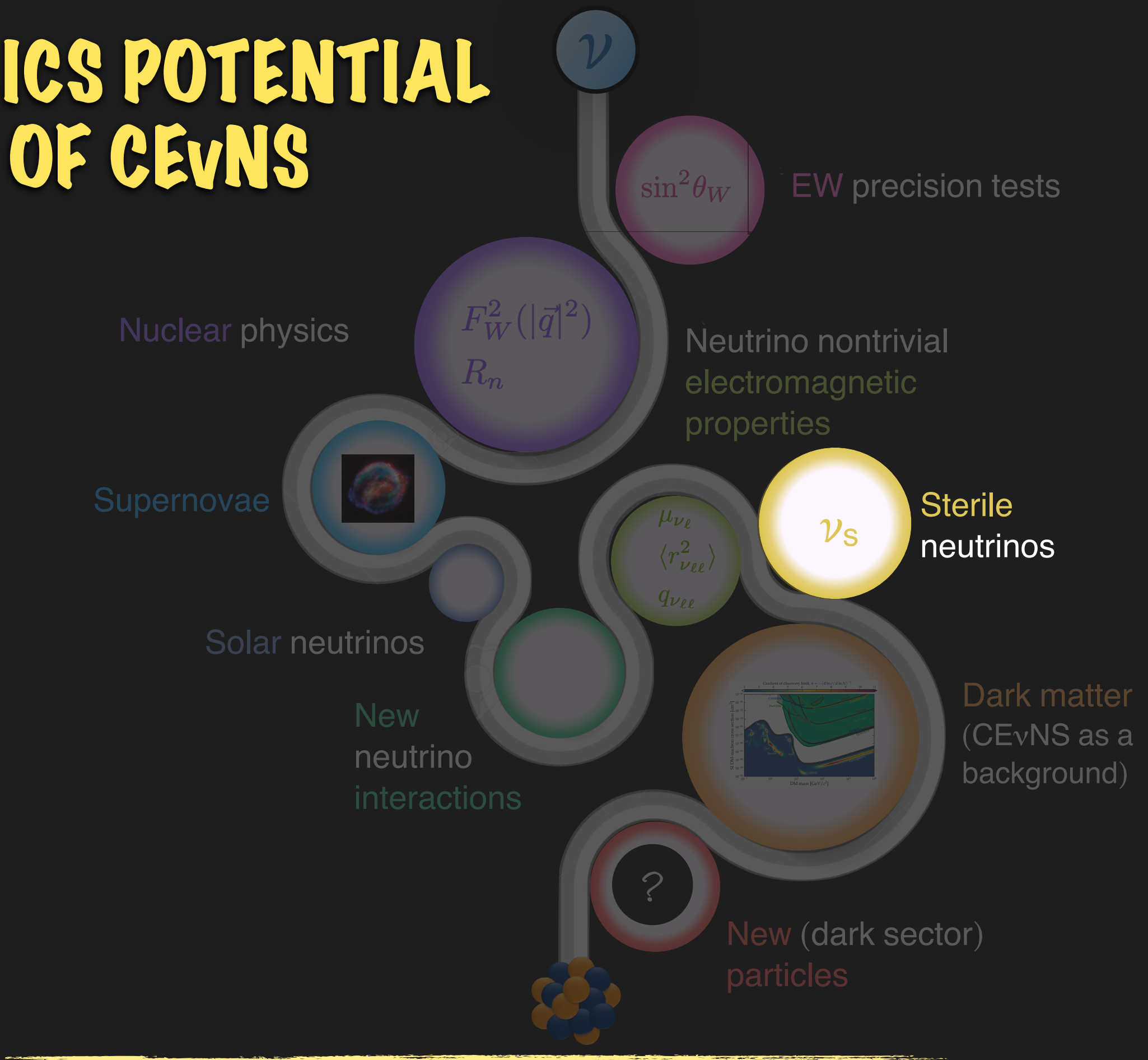
OUTLINE - 3rd lecture

► CEvNS physics potential BSM:

- Sterile neutrinos
- Dark matter detection - discovery limits
- New particles: LDM, ALPs, sterile fermions...



PHYSICS POTENTIAL OF CEvNS



STERILE NEUTRINO DIPOLE PORTAL

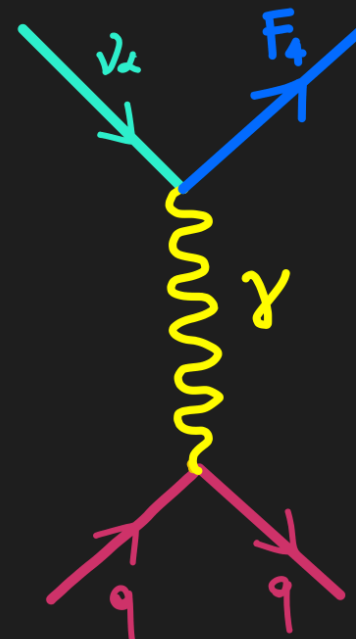
Transition of an active neutrino to a massive sterile state, induced by a magnetic coupling: $\nu_L + N \rightarrow F_4 + N$

McKeen, Pospelov PRD 82 (2010)

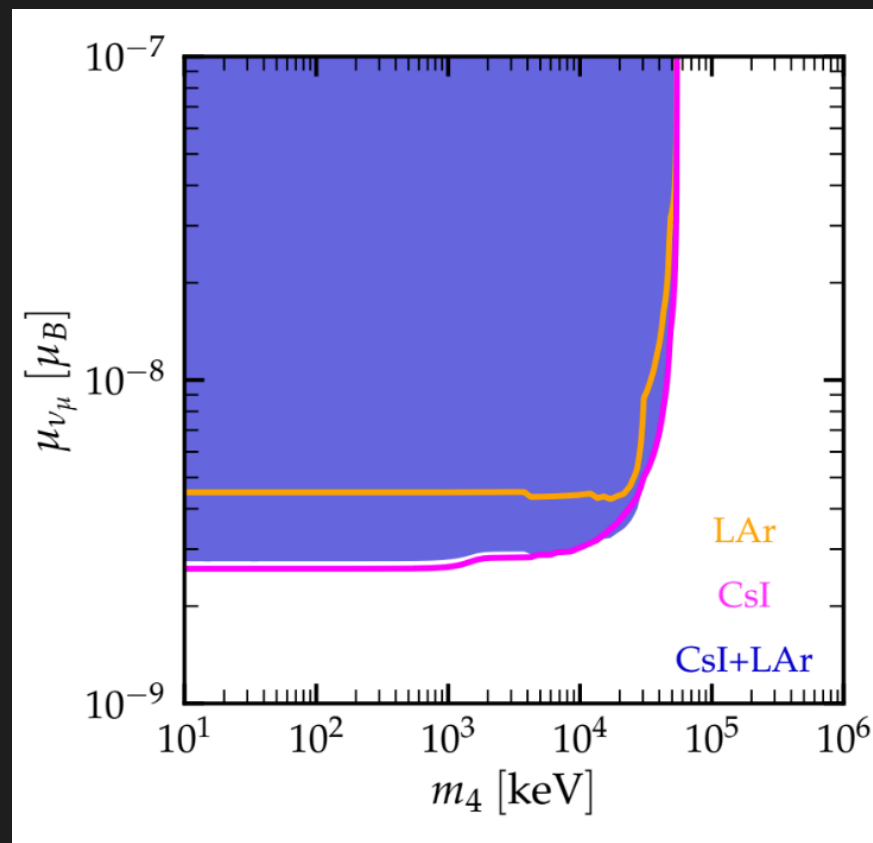
$$\mathcal{L} = \bar{\nu} \sigma_{\mu\nu} \lambda \nu_R F^{\mu\nu} + H.c.$$

$$m_4^2 \lesssim 2m_N E_r \left(\sqrt{\frac{2}{m_N E_r}} E_\nu - 1 \right)$$

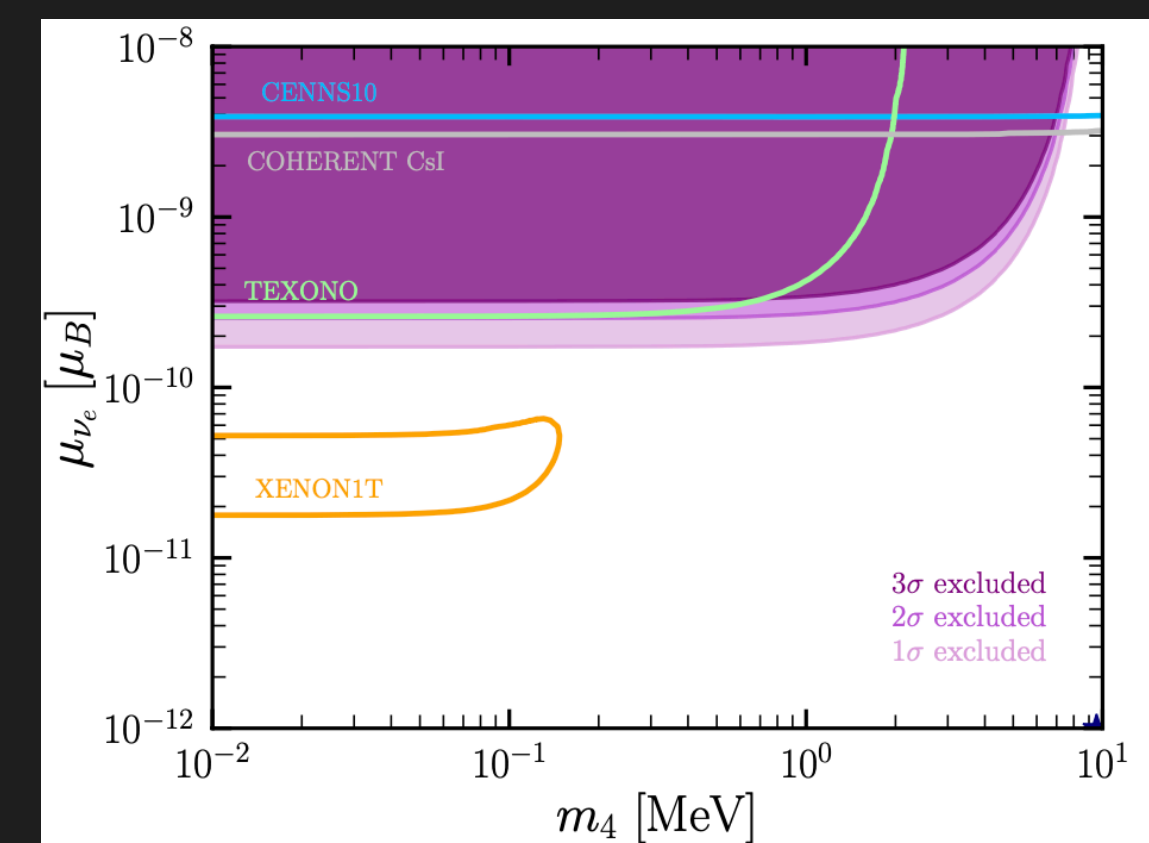
$$\frac{d\sigma}{dE_r} \Big|_{DP} = \alpha_{EM} \mu_{\nu, \text{Eff}}^2 F^2(q^2) Z^2 \left[\frac{1}{E_r} - \frac{1}{E_\nu} - \frac{m_4^2}{2E_\nu E_r m_N} \left(1 - \frac{E_r}{2E_\nu} + \frac{m_N}{2E_\nu} \right) + \frac{m_4^4(E_r - m_N)}{8E_\nu^2 E_r^2 m_N^2} \right]$$



COHERENT CsI (2021) + LAr



Dresden-II (Ge) - iron filter



VDR, Miranda, Papoulias, Sanchez-García, Tórtola and Valle, JHEP 04 (2023) 035

Aristizabal, VDR, Papoulias JHEP 09 (2022) 076

STERILE NEUTRINO OSCILLATIONS

CEvNS' sensitivity to the total active neutrino flux —> search for sterile neutrinos.

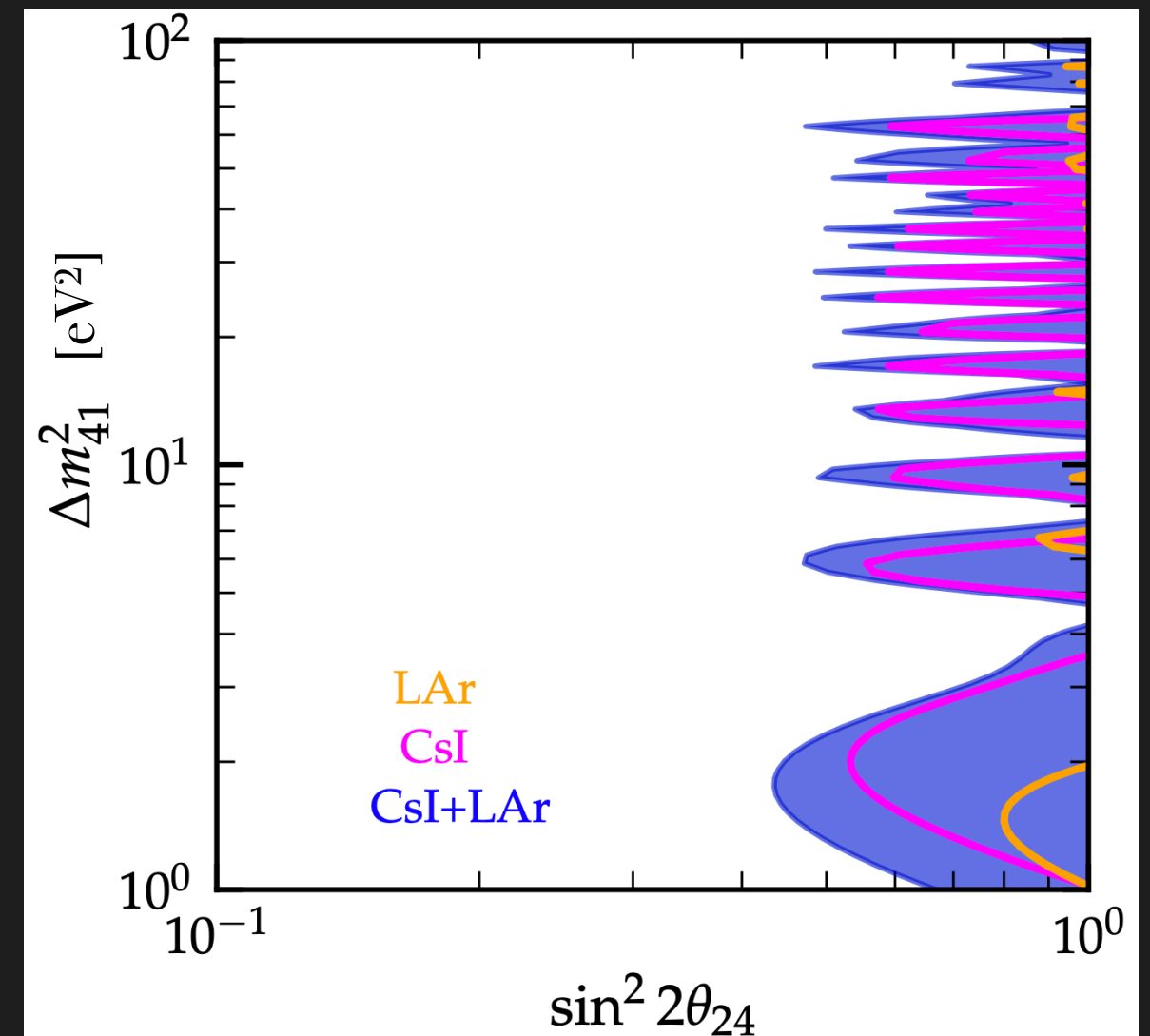
$$P_{\mu\mu}(E_\nu) \simeq 1 - \sin^2 2\theta_{24} \sin^2 \left(\frac{\Delta m_{42}^2 L}{4E_\nu} \right)$$

$$P_{ee}(E_\nu) \simeq 1 - \sin^2 2\theta_{14} \sin^2 \left(\frac{\Delta m_{41}^2 L}{4E_\nu} \right)$$

This scenario leads to a slightly improved fit for the CsI data (compared to the SM), while for LAr it leads to a poorer result.

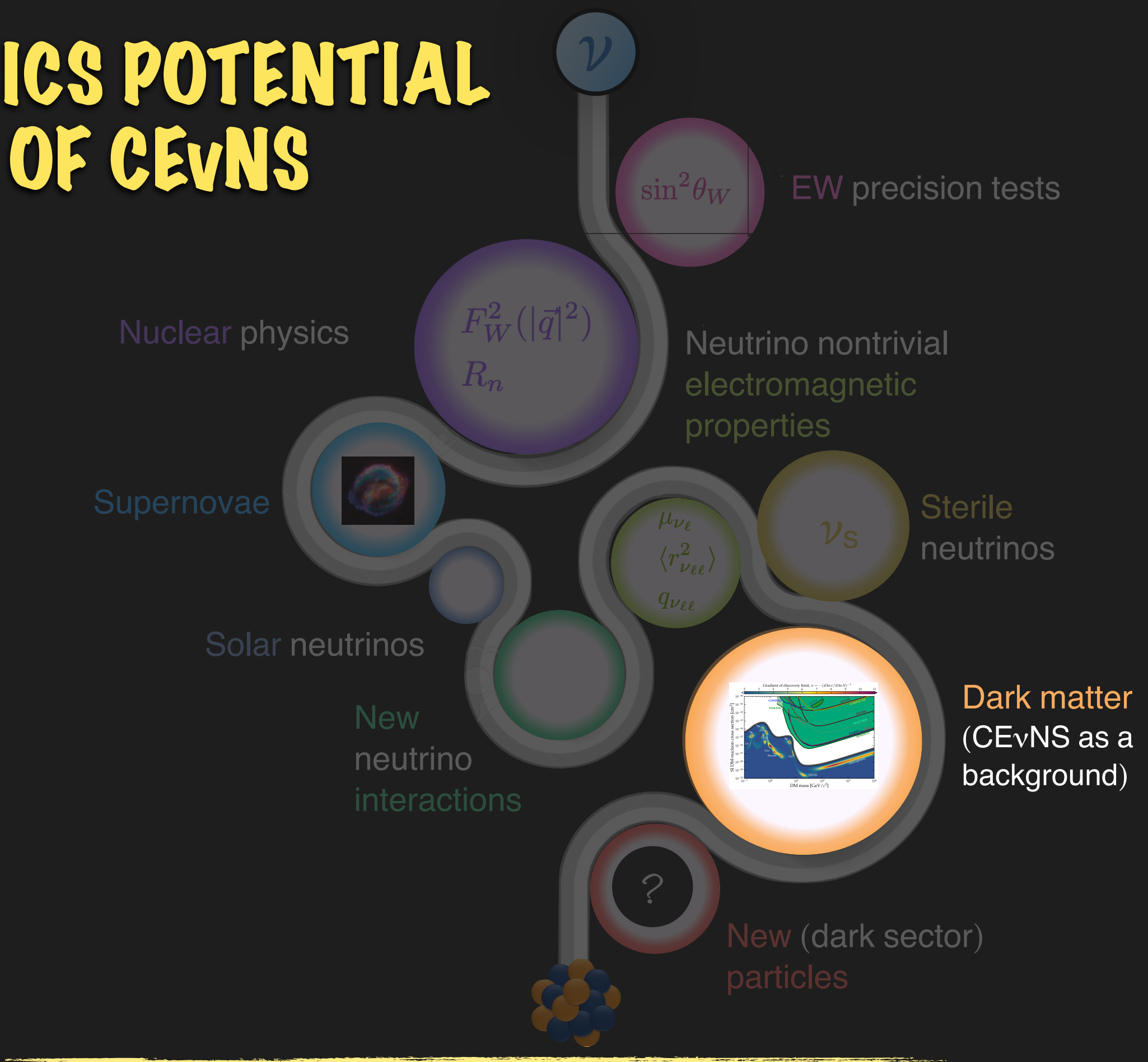
The sensitivity to the new mass splitting and active-sterile mixing angle is rather poor.

COHERENT CsI (2021) + LAr



VDR, Miranda, Papoulias, Sanchez-García, Tórtola and Valle, JHEP 04 (2023) 035

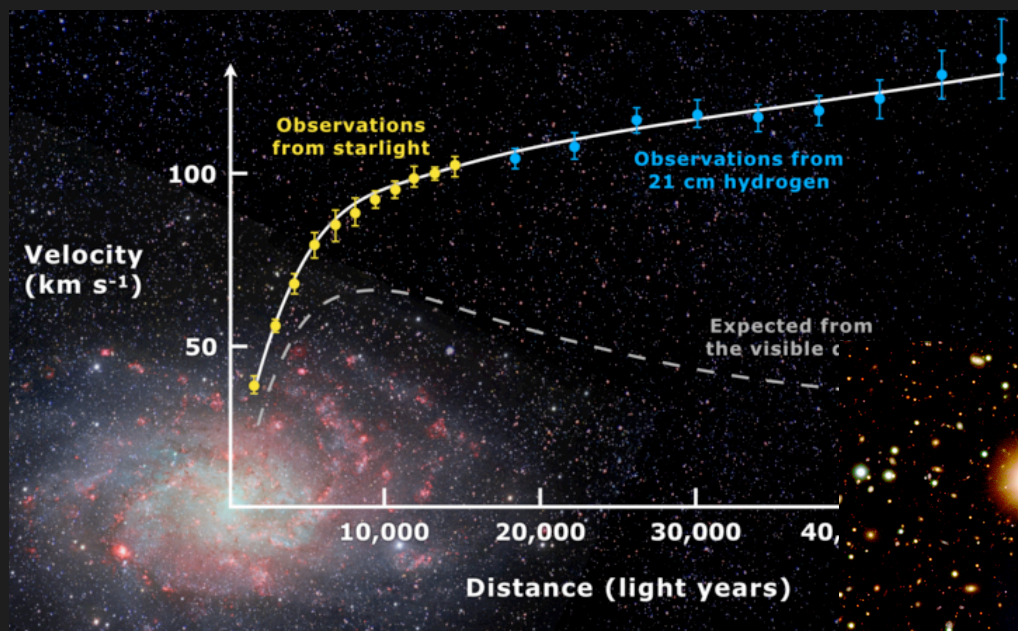
PHYSICS POTENTIAL OF CEvNS



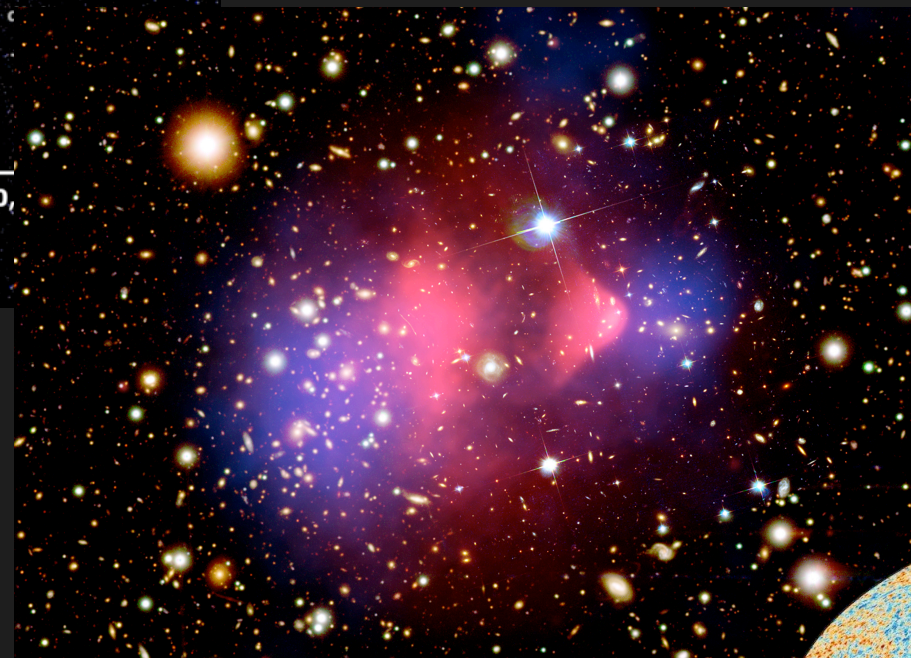
DARK MATTER

Dark Matter is an abundant and necessary component of our Universe.

We have overwhelming (gravitational) evidence for its existence, across many cosmological scales

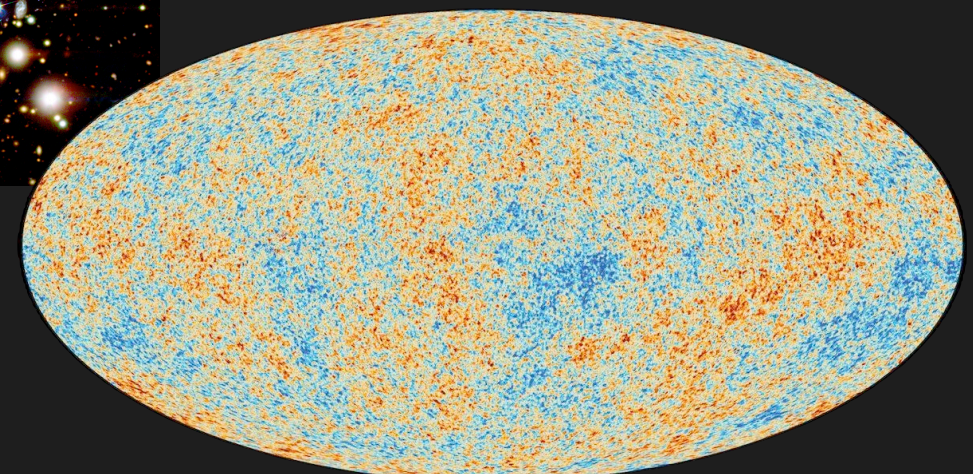


Galaxy rotation curves



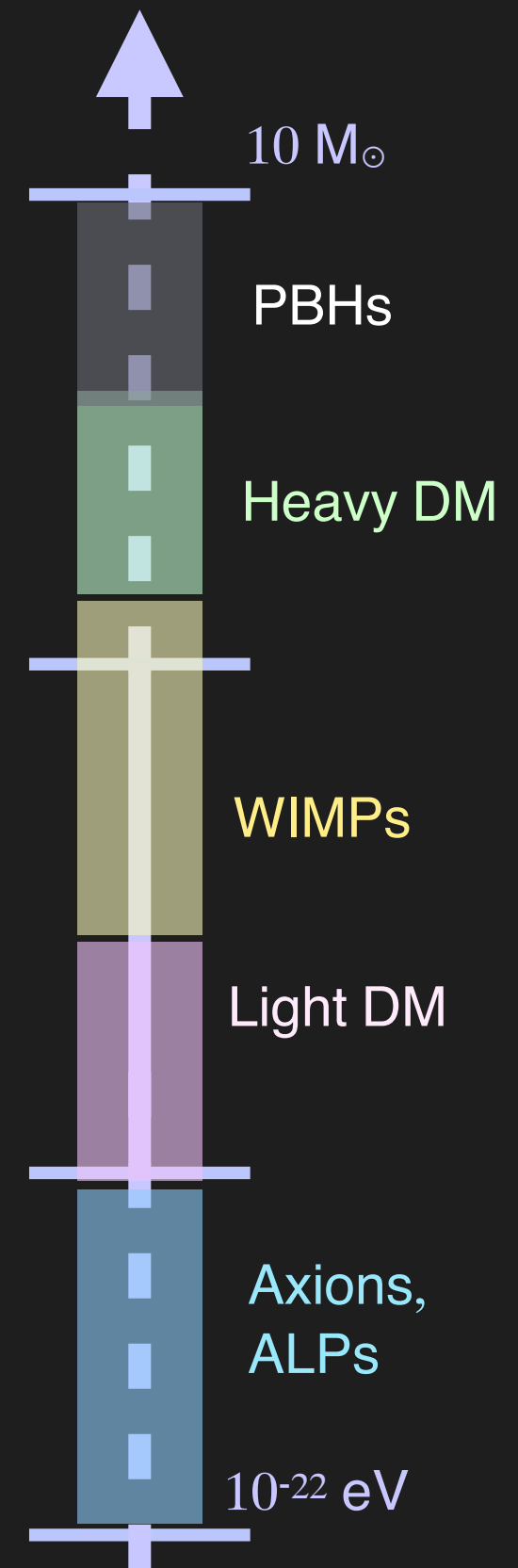
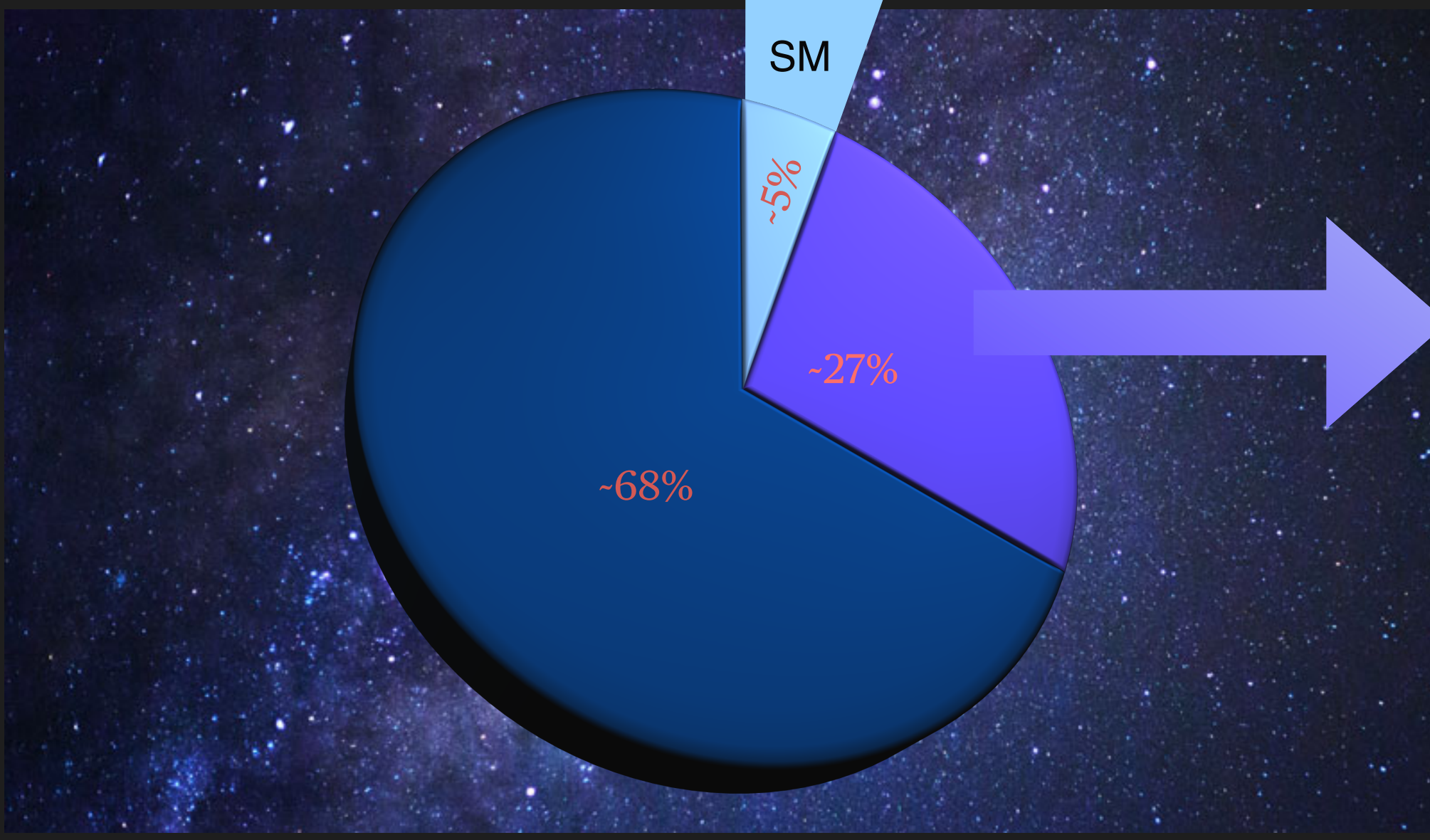
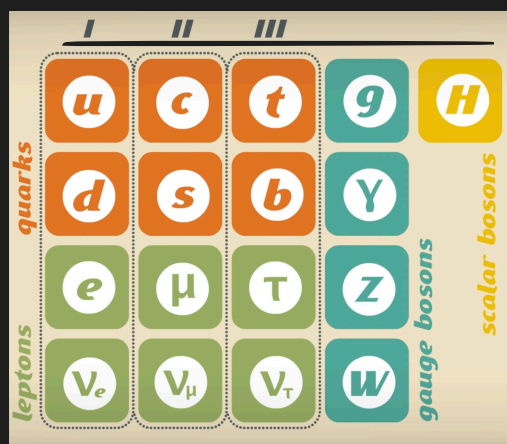
Galaxy clusters

CMB



WHAT IS DARK MATTER?

Its fundamental nature
is still a mystery.



DIRECT WIMP SEARCHES

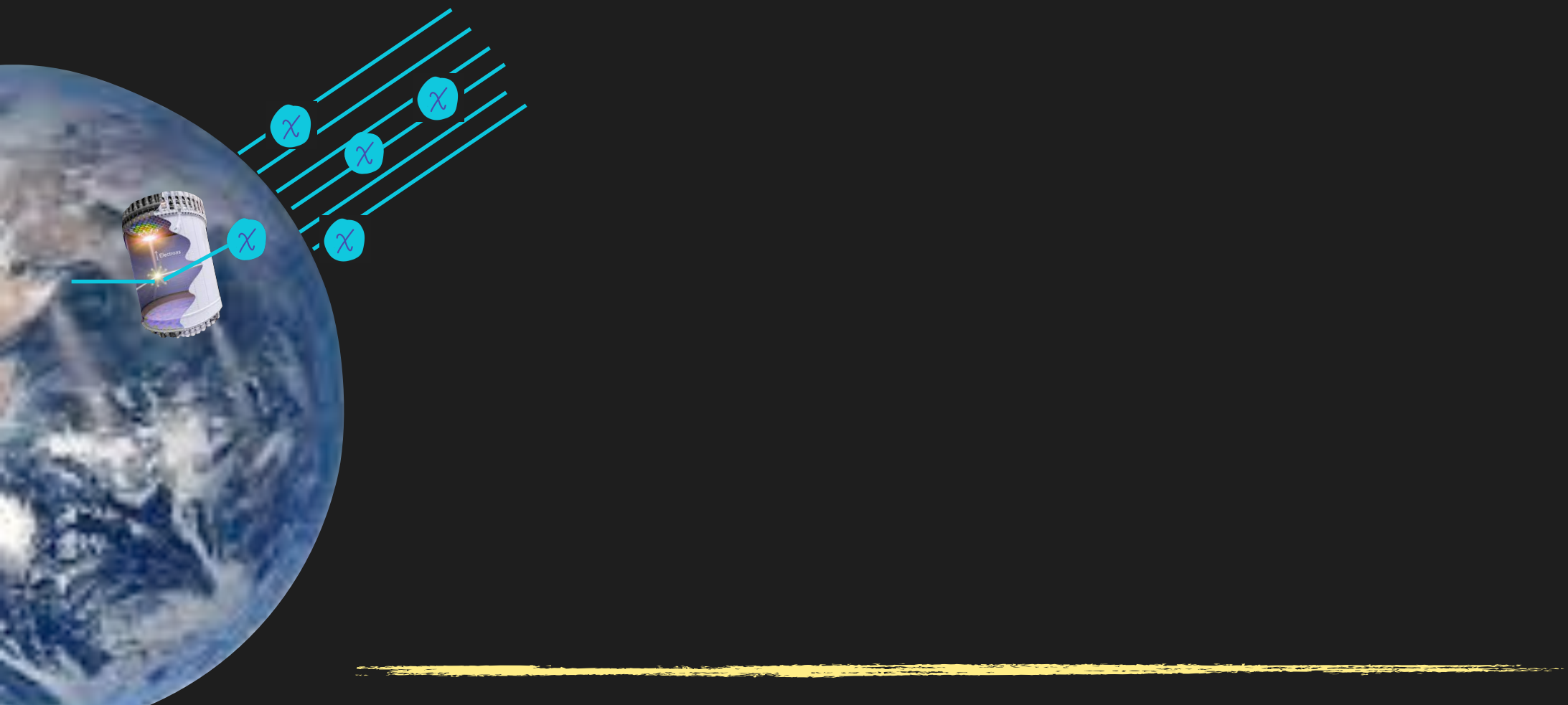
If DM is made of particles that interact among themselves and with SM particles (e.g. WIMPs) we may hope to detect it.

One strategy:



DIRECT DETECTION

Which looks for energy deposited within a detector by the scattering of DM on the target



DIRECT WIMP SEARCHES

If DM is made of particles that interact among themselves and with SM particles (e.g. WIMPs) we may hope to detect it.

One strategy:



DIRECT DETECTION

Which looks for energy deposited within a detector by the scattering of DM on the target



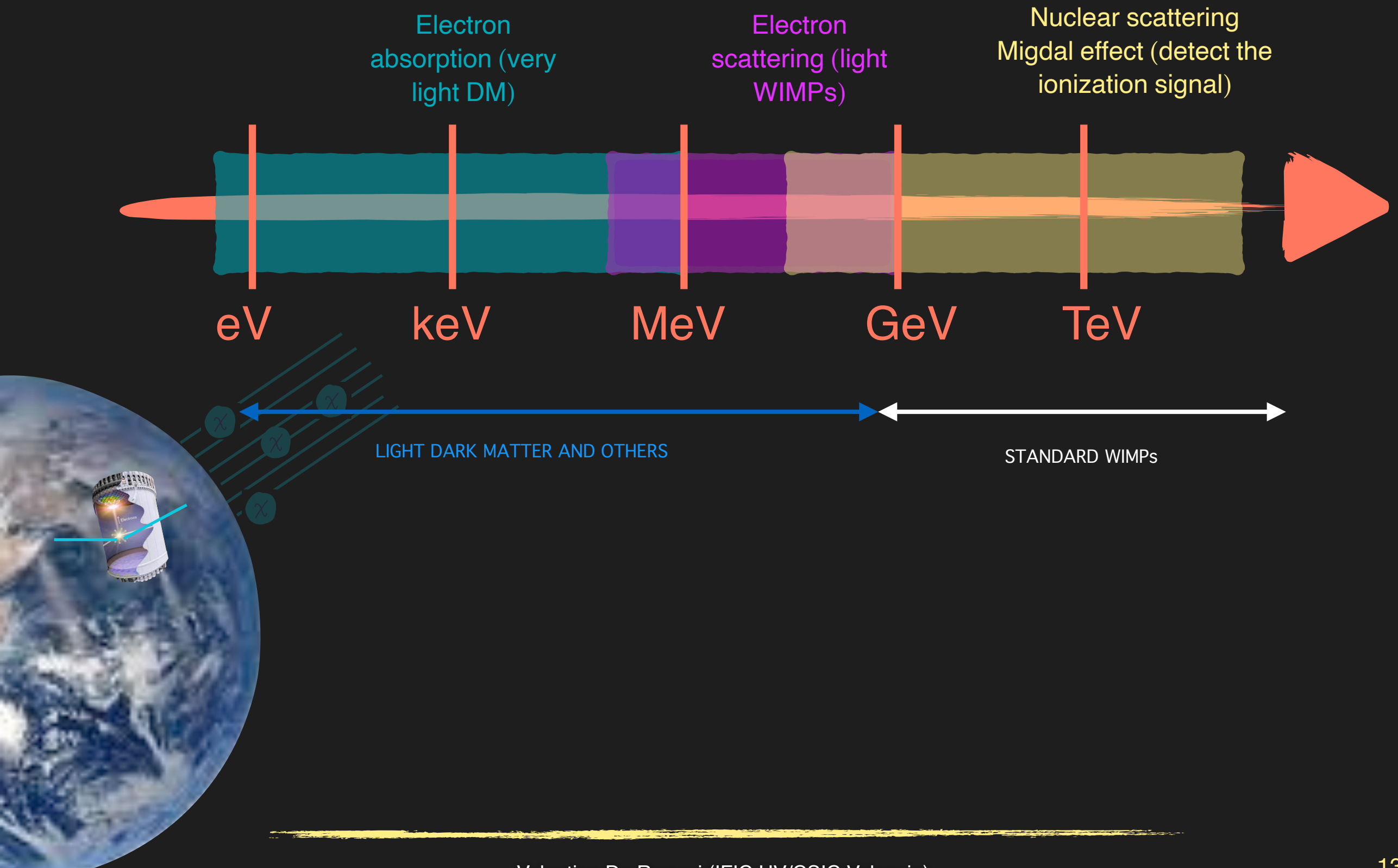
Underground detectors look for “ghostly” particles:

- Neutral (or millicharged)
- Weakly-interacting
- Cosmological or astrophysical origin
- Long-lived enough

Scatterings are infrequent (if any!). Need:

- Excellent background reduction
- Large exposure (time and volume)
- Low energy thresholds

DIRECT WIMP SEARCHES: signals

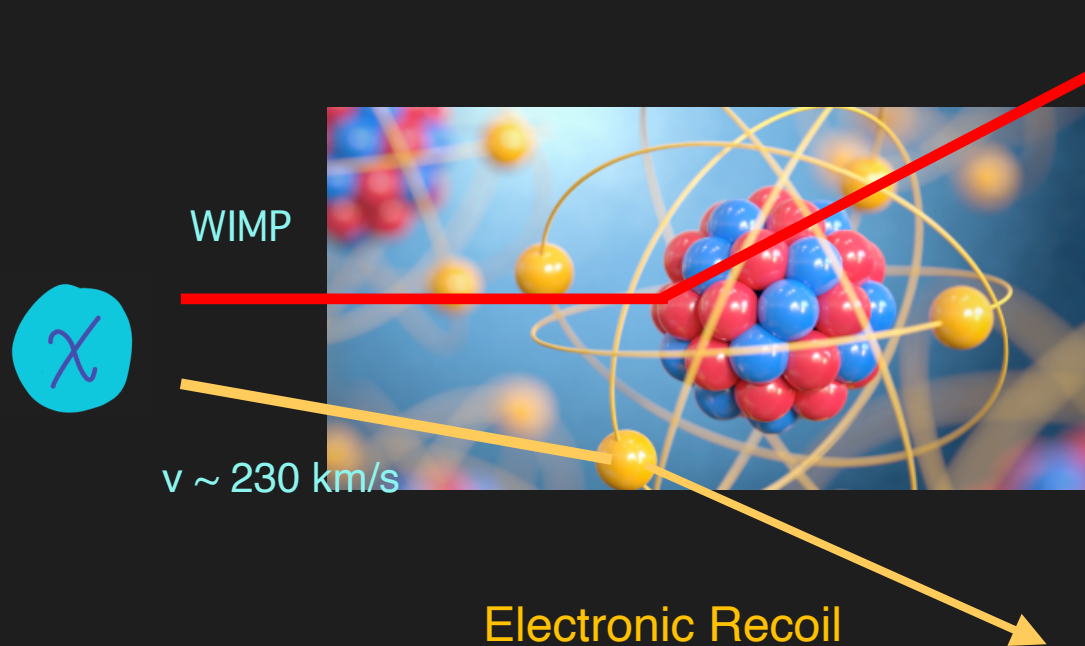


DIRECT WIMP SEARCHES

Detection via elastic scattering off:

nuclei → nuclear recoils

electrons → electronic recoils



Direct detection requires:

- **Astrophysical parameters**
Local dark matter density
Velocity distribution
- **Particle physics parameters**
Dark matter model
Particle mass and cross section
- **Atomic and/or nuclear physics**
Form factors

DIRECT WIMP SEARCHES and CEvNS?

PHYSICAL REVIEW D

VOLUME 9, NUMBER 5

1 MARCH 1974

Coherent effects of a weak neutral current

Daniel Z. Freedman†

National Accelerator Laboratory, Batavia, Illinois 60510

and Institute for Theoretical Physics, State University of New York, Stony Brook, New York 11790

(Received 15 October 1973; revised manuscript received 19 November 1973)

If there is a weak neutral current, then the elastic scattering process $\nu + A \rightarrow \nu + A$ should have a sharp coherent forward peak just as $e + A \rightarrow e + A$ does. Experiments to observe this peak can give important information on the isospin structure of the neutral current. The experiments are very difficult, although the estimated cross sections (about 10^{-38} cm^2 on carbon) are favorable. The coherent cross sections (in contrast to incoherent) are almost energy-independent. Therefore, energies as low as 100 MeV may be suitable. Quasi-coherent nuclear excitation processes $\nu + A \rightarrow \nu + A^*$ provide possible tests of the conservation of the weak neutral current. Because of strong coherent effects at very low energies, the nuclear elastic scattering process may be important in inhibiting cooling by neutrino emission in stellar collapse and neutron stars.

Goodman and Witten pointed out that WIMPs could be searched for using the same detectors proposed by Drukier and Stodolsky for CEvNS measurements.

PRINCIPLES AND APPLICATIONS OF A NEUTRAL CURRENT DETECTOR FOR NEUTRINO PHYSICS AND ASTRONOMY

A. Drukier and L. Stodolsky

Max-Planck-Institut für Physik und Astrophysik
- Werner-Heisenberg-Institut für Physik -
Munich (Fed. Rep. Germany)

Abstract

We study neutrino detection through the elastic scattering of neutrinos on nuclei and identification of the recoil energy. The very large value of the cross section compared to previous methods indicates a detector would be relatively light and suggests the possibility of a true "neutrino observatory". We examine a realization in terms of the superconducting grain idea, which appears in principle feasible through extension and extrapolation of presently known techniques. Such a detector would permit determination of the neutrino spectrum and should be intensive to neutrino oscillations. Various applications and tests are discussed, including spallation sources, reactors, supernovas, solar and terrestrial neutrinos. A supernova would permit a simple determination of the number of neutrinos and their masses, while for solar neutrinos rates of thousands of S.N.U. are theoretically attainable. A preliminary estimate of the most difficult backgrounds is attempted.

PHYSICAL REVIEW D

VOLUME 31, NUMBER 12

15 JUNE 1985

Detectability of certain dark-matter candidates

Mark W. Goodman and Edward Witten

Joseph Henry Laboratories, Princeton University, Princeton, New Jersey 08544

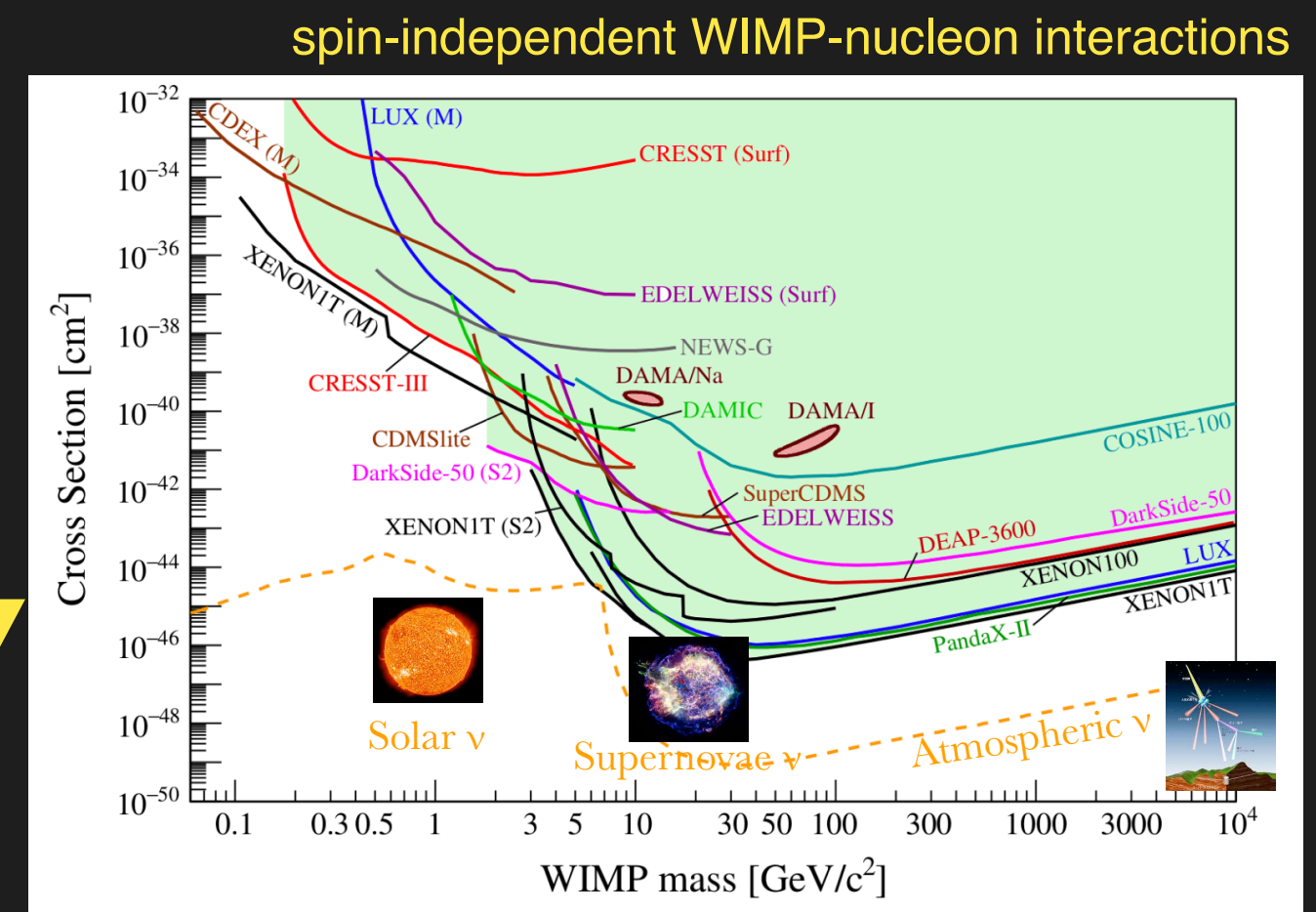
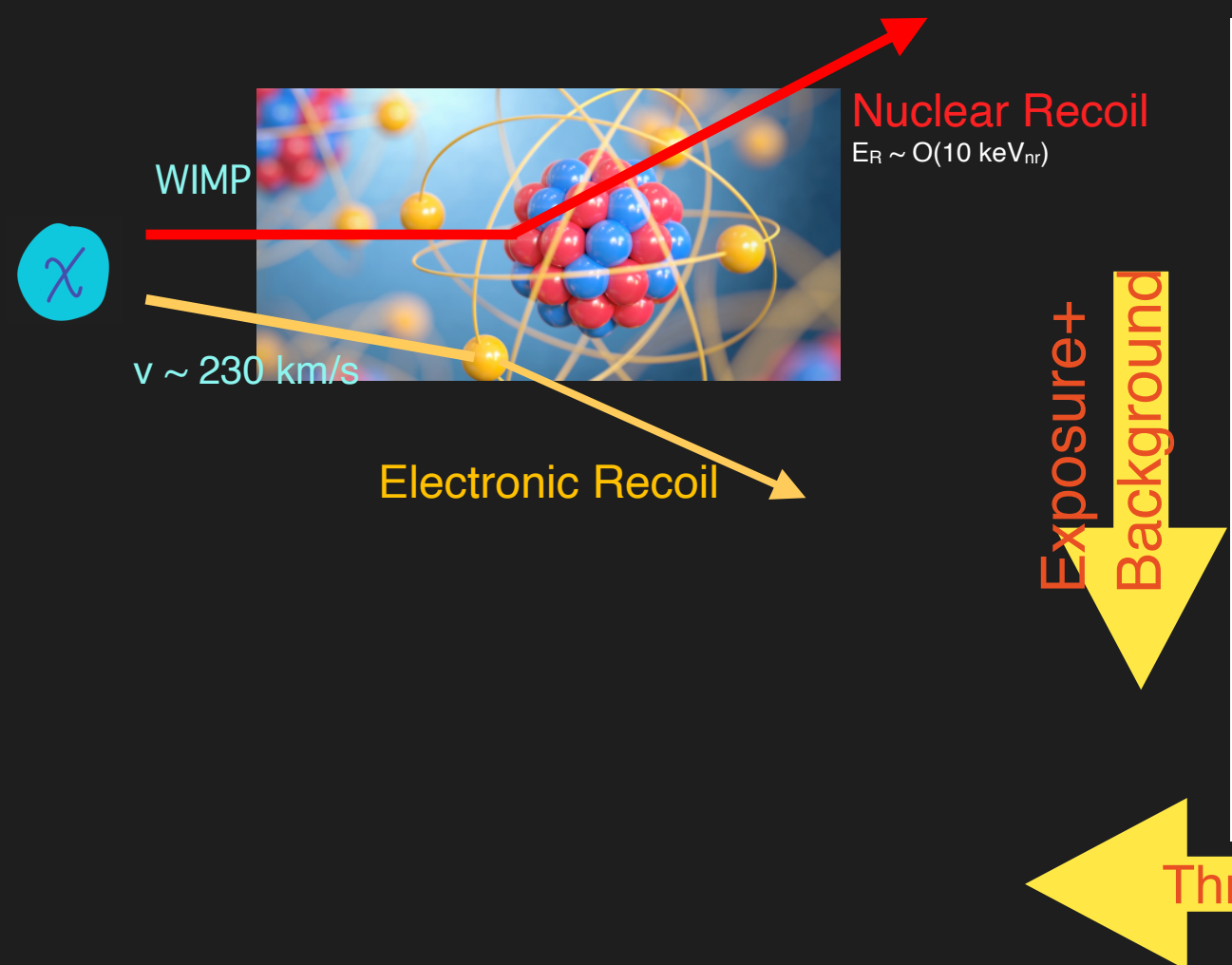
(Received 7 January 1985)

We consider the possibility that the neutral-current neutrino detector recently proposed by Drukier and Stodolsky could be used to detect some possible candidates for the dark matter in galactic halos. This may be feasible if the galactic halos are made of particles with coherent weak interactions and masses $1-10^6 \text{ GeV}$; particles with spin-dependent interactions of typical weak strength and masses $1-10^2 \text{ GeV}$; or strongly interacting particles of masses $1-10^{13} \text{ GeV}$.

Goodman and E. Witten, Phys. Rev. D 31 (1985) 3059
A. Drukier and L. Stodolsky, Phys. Rev. D 30 (1984) 2295
D.Z. Freedman, Phys. Rev. D 9 (1974)

DIRECT WIMP SEARCHES

DM-nuclei scattering:
spin-independent (strong bounds due to coherent enhancement) or spin-dependent (weaker bounds)



Direct Detection of Dark Matter – APPEC Committee Report 2021

NEUTRINO BACKGROUNDS AT DIRECT DARK MATTER DETECTION EXPERIMENTS

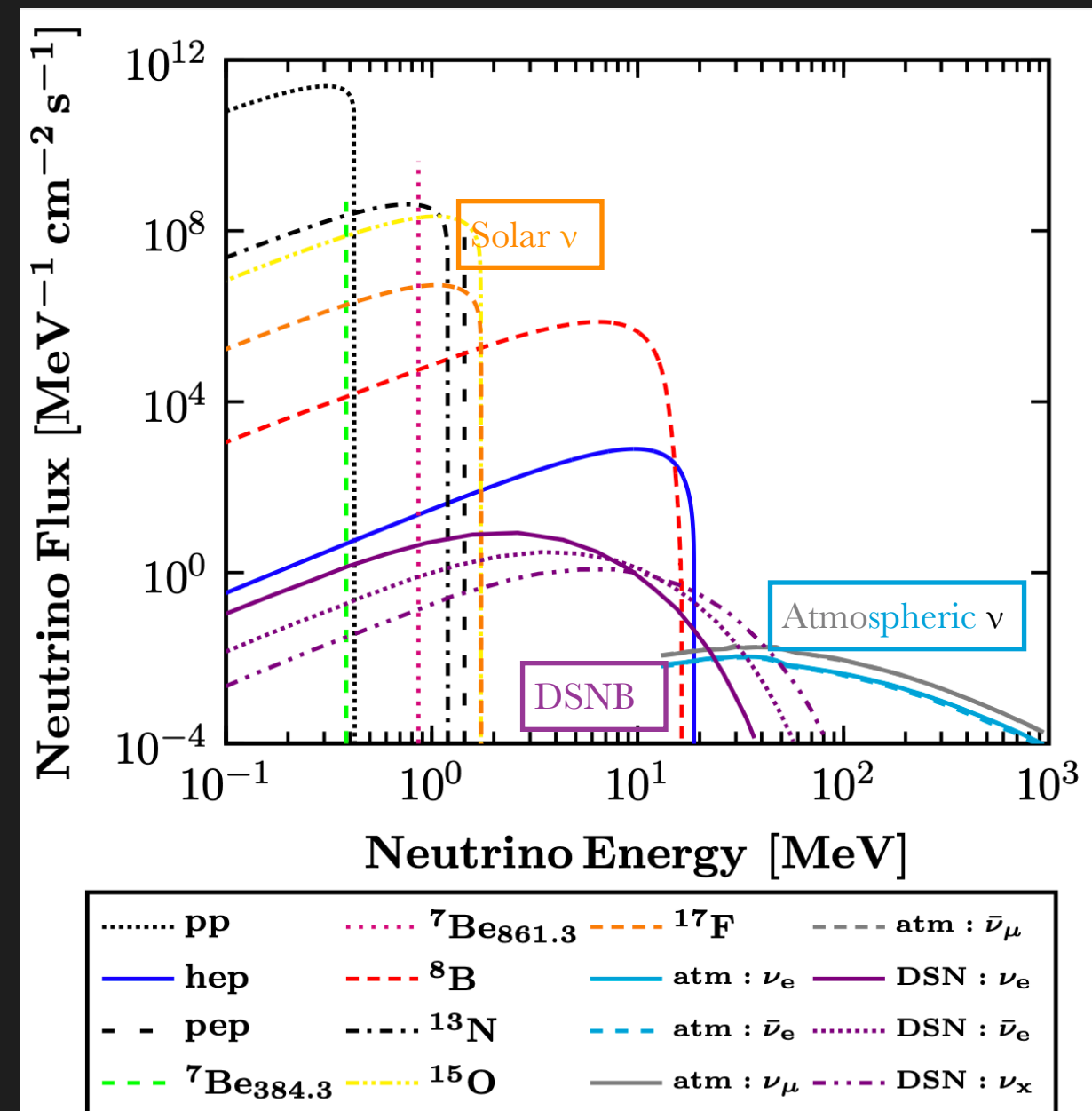
- Solar neutrinos
- Atmospheric neutrinos (FLUKA)
- Diffuse Supernova Neutrinos (DSN)

W. C. Haxton, R. G. Hamish Robertson, and A. M. Serenelli, Ann. Rev. Astron. Astrophys. 51 (2013), 21

G. Battistoni, A. Ferrari, T. Montaruli, and P. R. Sala, Astropart. Phys. 23 (2005) 526

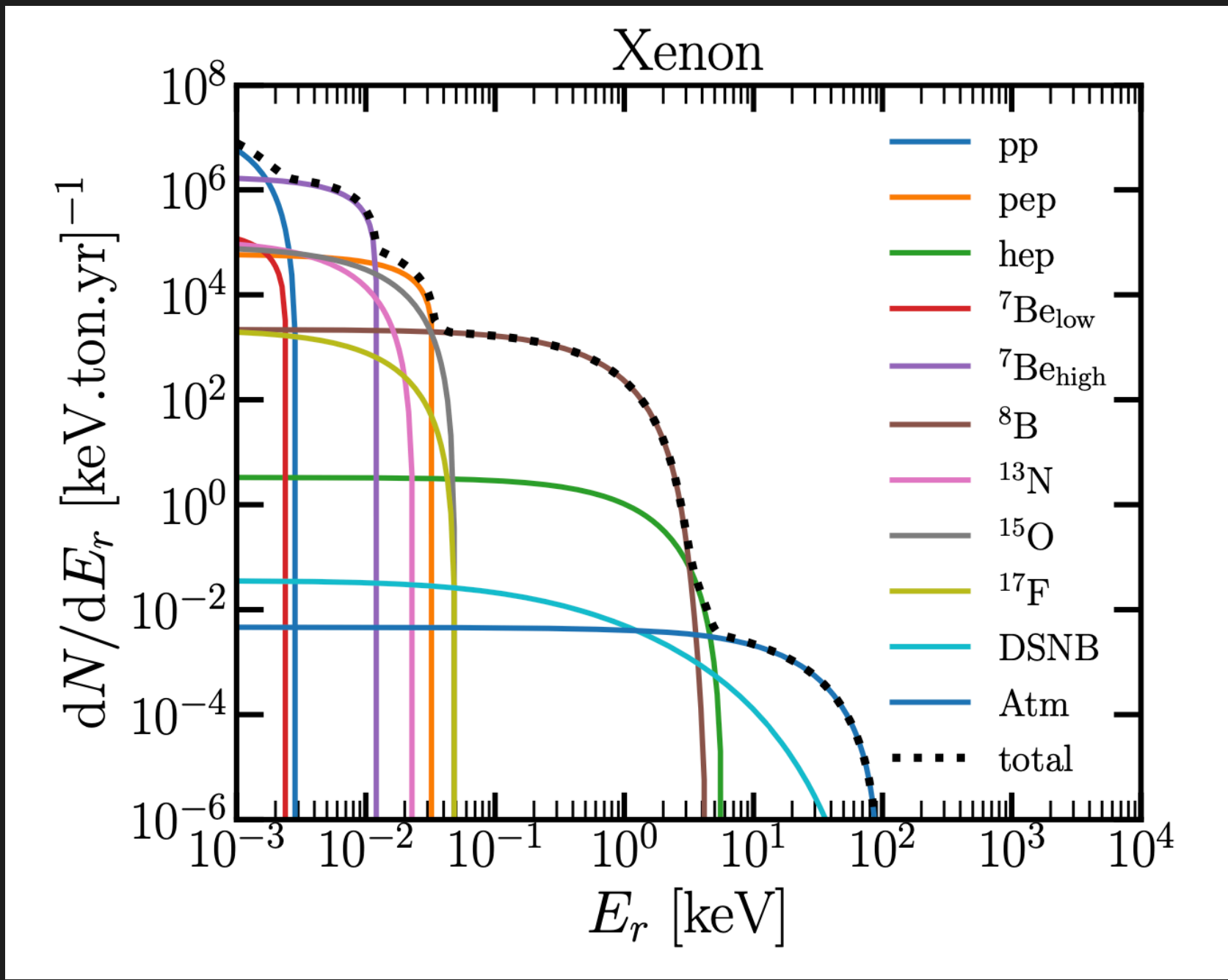
Horiuchi, Beacom, Dwek, PR D79 (2009) 083013

Type	$E_{\nu_{\text{max}}} [\text{MeV}]$	Flux [$\text{cm}^{-2}\text{s}^{-1}$]
<i>pp</i>	0.423	$(5.98 \pm 0.006) \times 10^{10}$
<i>pep</i>	1.440	$(1.44 \pm 0.012) \times 10^8$
<i>hep</i>	18.784	$(8.04 \pm 1.30) \times 10^3$
${}^7\text{Be}_{\text{Below}}$	0.3843	$(4.84 \pm 0.48) \times 10^8$
${}^7\text{Be}_{\text{high}}$	0.8613	$(4.35 \pm 0.35) \times 10^9$
${}^8\text{B}$	16.360	$(5.58 \pm 0.14) \times 10^6$
${}^{13}\text{N}$	1.199	$(2.97 \pm 0.14) \times 10^8$
${}^{15}\text{O}$	1.732	$(2.23 \pm 0.15) \times 10^8$
${}^{17}\text{F}$	1.740	$(5.52 \pm 0.17) \times 10^6$



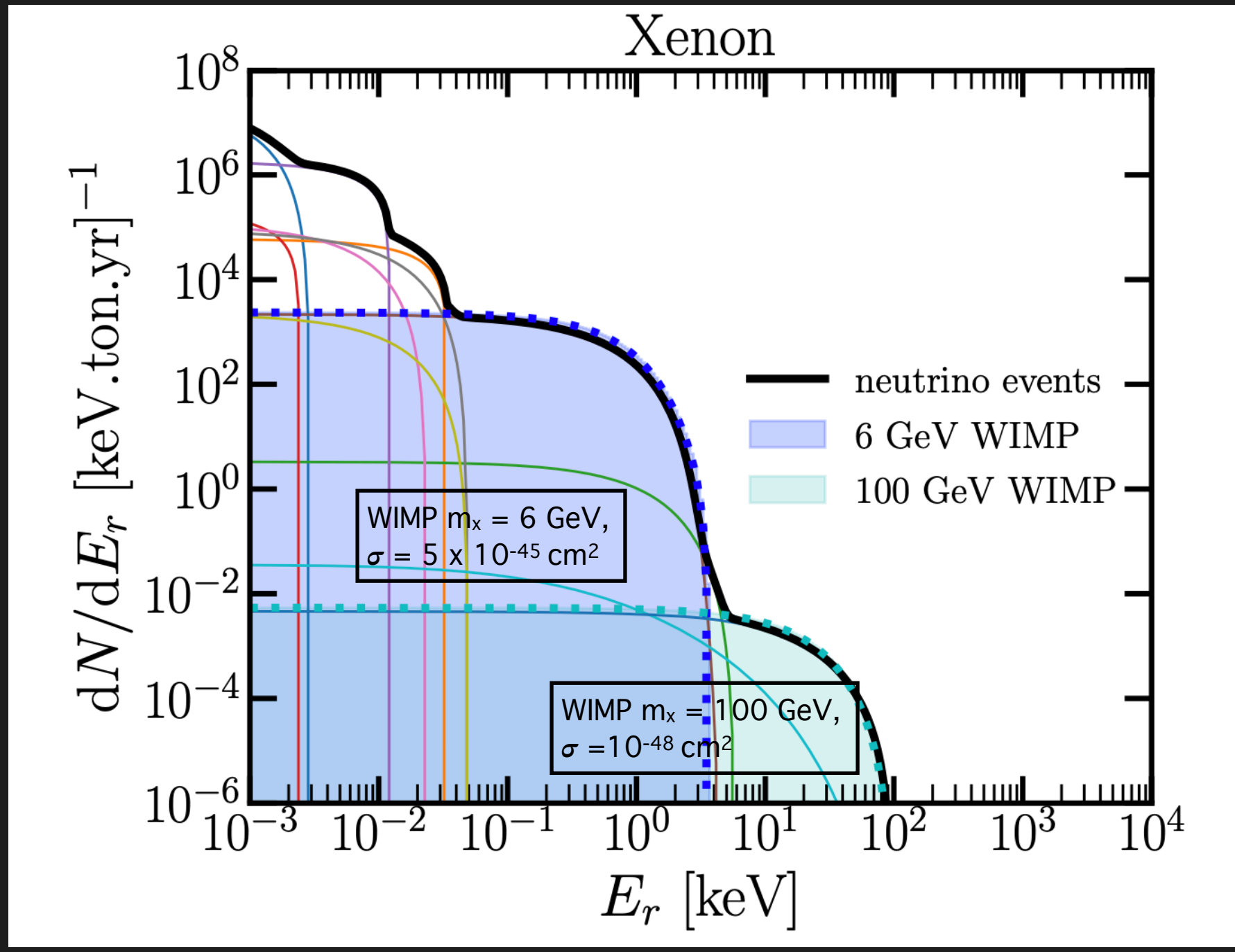
ASTROPHYSICAL NEUTRINOS

Expected recoil rates from coherent neutrino-nucleus scattering on Xenon:



ASTROPHYSICAL NEUTRINOS

Expected recoil rates from coherent neutrino-nucleus scattering on Xenon:



NEUTRINO FLOOR?

- ▶ Neutrino backgrounds induce **coherent elastic-neutrino nucleus scattering** and produce nuclear recoil spectra, which can have a strong degeneracy with those expected from spin-independent WIMP interactions.
- ▶ Increasing exposure does not imply a linear improvement of sensitivities but rather a saturation of its discovery limit, typically referred to as **neutrino floor**.

- ▶ Neutrino floors vary depending on:

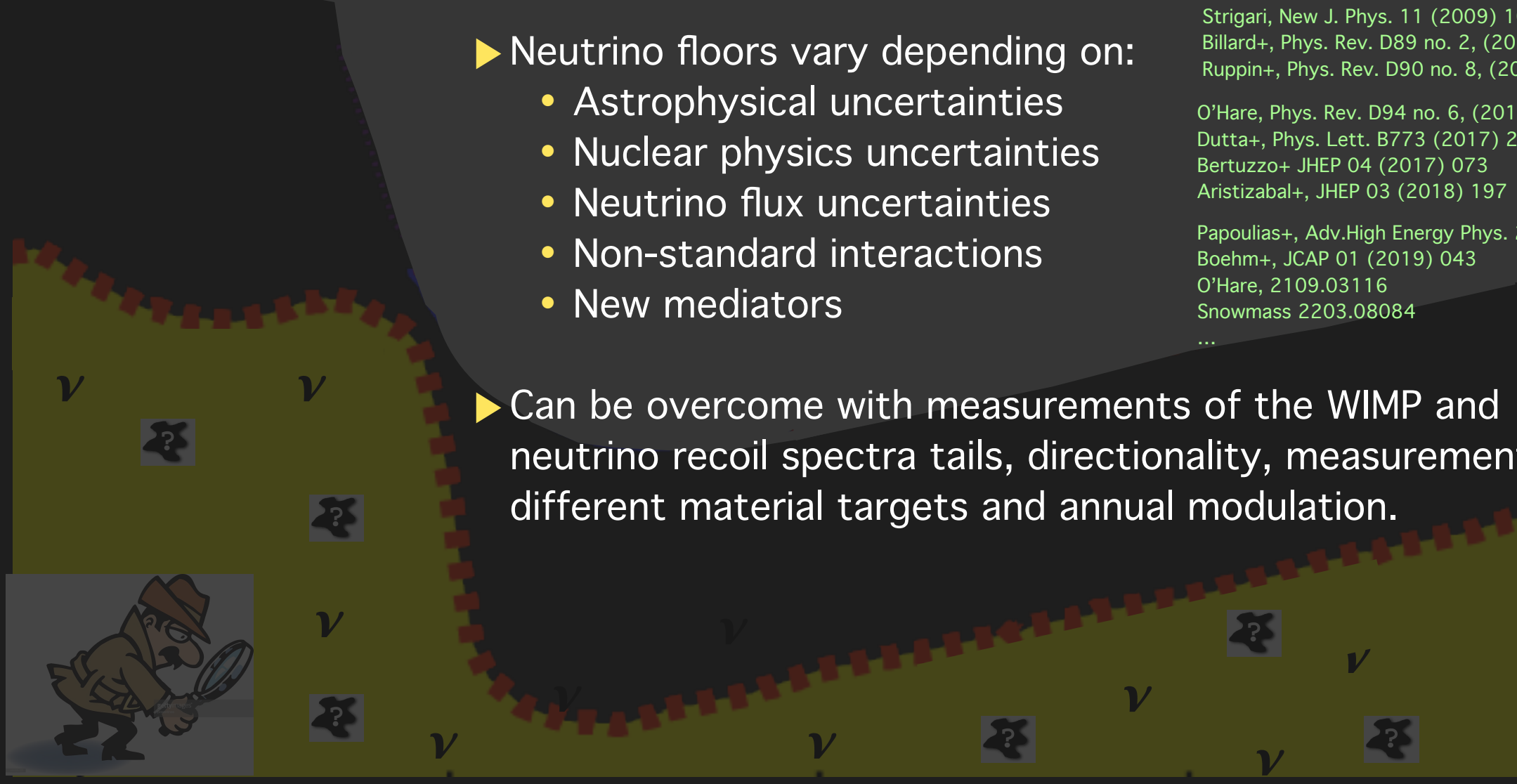
- Astrophysical uncertainties
- Nuclear physics uncertainties
- Neutrino flux uncertainties
- Non-standard interactions
- New mediators

- ▶ Can be overcome with measurements of the WIMP and neutrino recoil spectra tails, directionality, measurements with different material targets and annual modulation.

Strigari, New J. Phys. 11 (2009) 105011
Billard+, Phys. Rev. D89 no. 2, (2014) 023524
Ruppin+, Phys. Rev. D90 no. 8, (2014) 083510

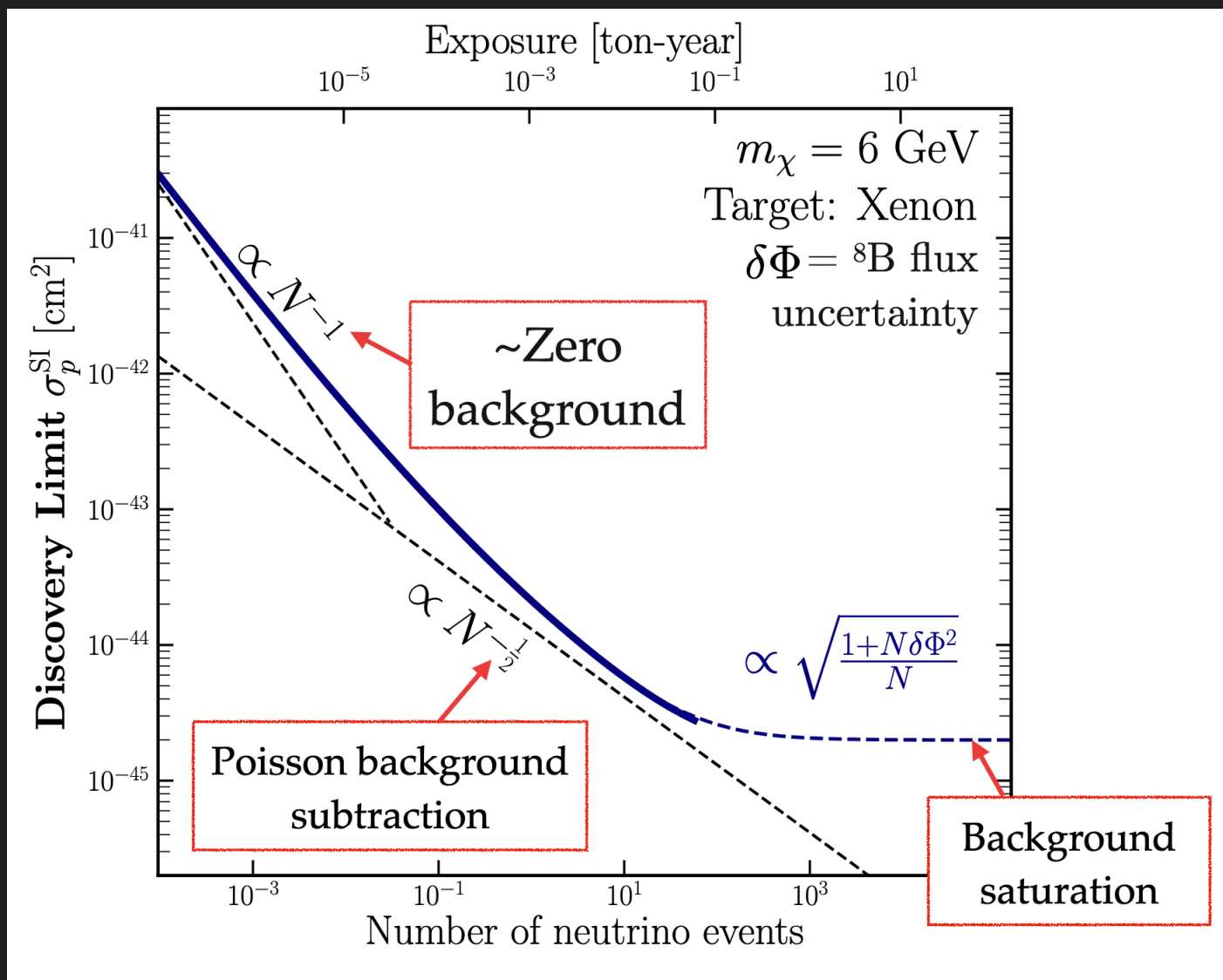
O'Hare, Phys. Rev. D94 no. 6, (2016) 063527
Dutta+, Phys. Lett. B773 (2017) 242–246
Bertuzzo+ JHEP 04 (2017) 073
Aristizabal+, JHEP 03 (2018) 197

Papoulias+, Adv.High Energy Phys. 2018 6031362
Boehm+, JCAP 01 (2019) 043
O'Hare, 2109.03116
Snowmass 2203.08084
...



..OR RATHER FOG

Scaling of sensitivity. If no problematic bckg, would go as Poisson background subtraction.



Experiments cannot probe cross sections smaller than those that generate an excess in events smaller than the expected level of systematic background fluctuations

Billard+, Phys. Rev. D89 no. 2, (2014) 023524

DM/CEvNS signals are not identical!
→ with high statistics, an experiment can disentangle the signal from the background uncertainty using spectral information.
However: absurdly large exposures needed.

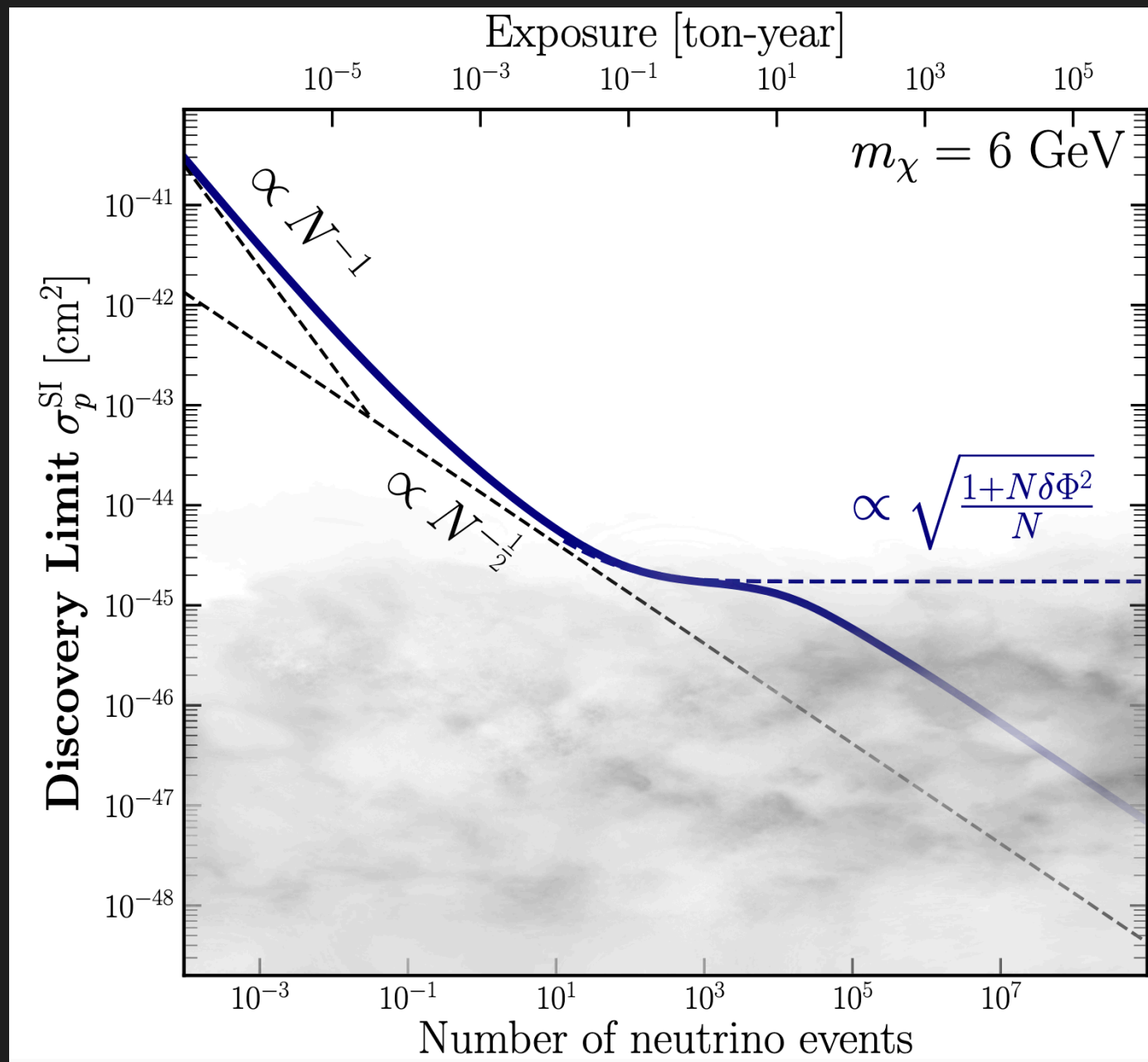
Ruppin+ Phys. Rev. D 90, 083510

O'Hare Phys. Rev. Lett. 127, 251802 (2021)

Adapted from C. O'Hare @Magnificent CEvNS 2024

..OR RATHER FOG

Neutrino “fog” can be quantified by looking at the scaling of sensitivity. Defines how badly the CEvNS background slows progress through DM parameter space.



Neutrino fog opacity:

$$n = -(\frac{d \ln \sigma}{d \ln N})^{-1}$$

$n=2$ Poissonian bckg subtraction
 $n>2$ worse than Poissonian

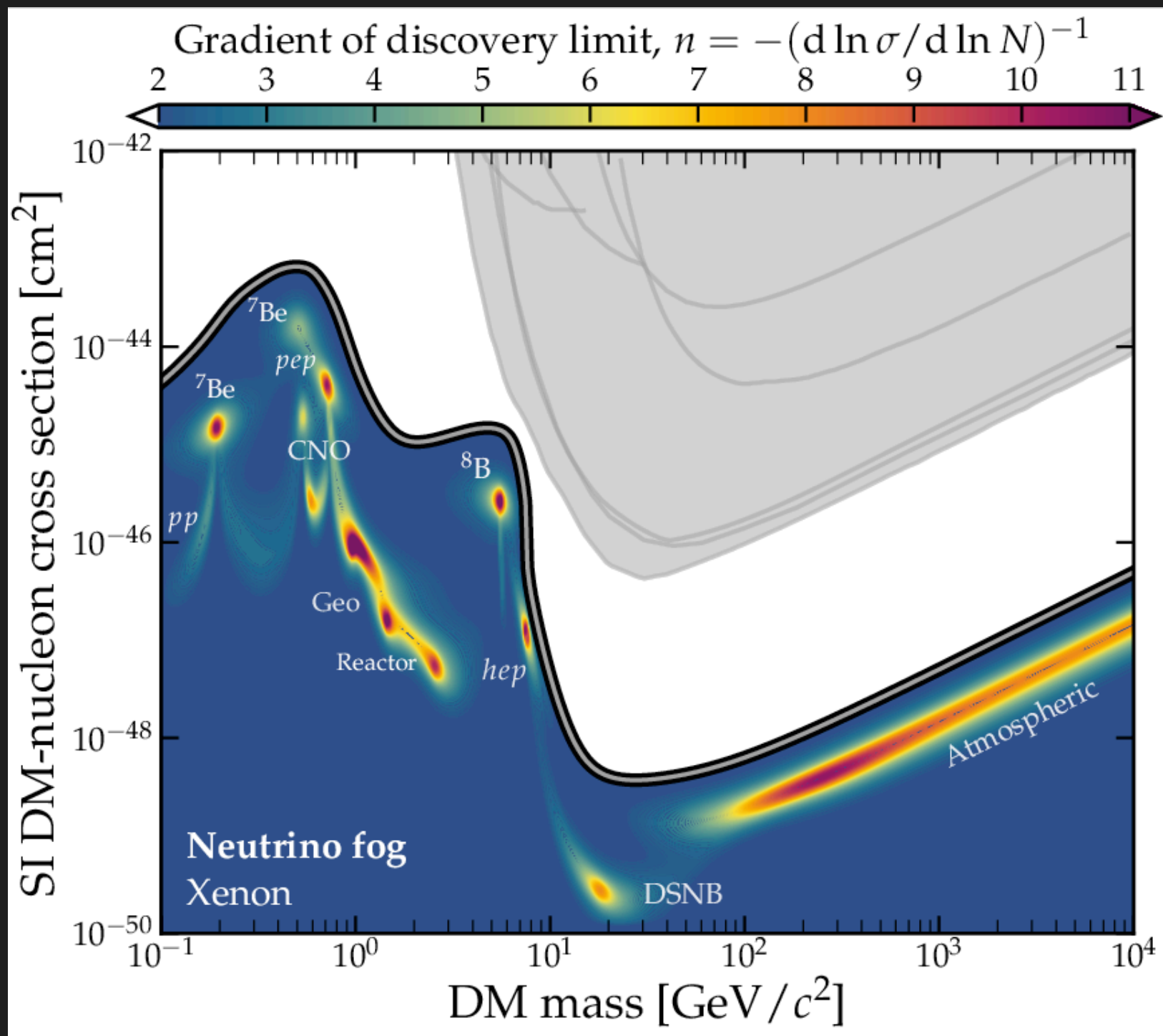
Index n: how fast we can improve upon background

An increase in sensitivity by 10 requires 10^n more exposure.

O'Hare Phys. Rev. Lett. 127, 251802 (2021)

Adapted from C. O'Hare @Magnificent CEvNS 2024

..OR RATHER FOG



O'Hare Phys. Rev. Lett. 127, 251802 (2021)

WIMP DISCOVERY LIMITS

Discovery limit: smallest WIMP cross section for which a given experiment has a 90% probability of detecting a WIMP signal at $\geq 3\sigma$.

$$\mathcal{L}(m_\chi, \sigma_{\chi-n}, \Phi, \mathcal{P}) = \prod_{i=1}^{n_{\text{bins}}} P(N_{\text{Exp}}^i, N_{\text{Obs}}^i) \times \prod_{\alpha=1}^{n_\nu} G(\phi_\alpha, \mu_\alpha, \sigma_\alpha)$$

Billard, Strigari, Figueroa-Feliciano PRD 89(2014)

Follows a frequentist significance test using a likelihood ratio as a test statistic.

The profile likelihood ratio corresponds to a test against the null hypothesis H_0 (CEvNS background only) vs the alternative hypothesis H_1 (WIMP signal + CEvNS background).

- Poisson distribution $P(k, \lambda) = \frac{\lambda^k e^{-\lambda}}{k!}$
- Gauss distribution $G(x, \mu, \sigma^2) = \frac{1}{\sigma\sqrt{2\pi}} e^{-\frac{1}{2}\left(\frac{x-\mu}{\sigma}\right)^2}$
- $N_{\text{Exp}}^i = N_\nu^i(\Phi_\alpha)$
- $N_{\text{Obs}}^i = \sum_\alpha N_\nu^i(\Phi_\alpha) + N_W^i$
- $\lambda(0) = \frac{\mathcal{L}_0}{\mathcal{L}_1}$ where \mathcal{L}_0 is the minimized function
- statistical significance: $\mathcal{Z} = \sqrt{-2 \ln \lambda(0)}$.
e.g. $\mathcal{Z} = 3$ corresponds to 90% C.L.

Neutrino flux components normalizations and uncertainties					
Comp.	Norm. [$\text{cm}^{-2} \cdot \text{s}^{-1}$]	Unc.	Comp.	Norm. [$\text{cm}^{-2} \cdot \text{s}^{-1}$]	Unc.
${}^7\text{Be}$ (0.38 MeV)	4.84×10^8	3%	${}^7\text{Be}$ (0.86 MeV)	4.35×10^9	3%
pep	1.44×10^8	1%	pp	5.98×10^{10}	0.6%
${}^8\text{B}$	5.25×10^6	4%	hep	7.98×10^3	30%
${}^{13}\text{N}$	2.78×10^8	15%	${}^{15}\text{O}$	2.05×10^8	17%
${}^{17}\text{F}$	5.29×10^6	20%	DSNB	86	50%
Atm	10.5	20%	—	—	—

Billard+, PRD 89 n2 (2014) 023524
Ruppin+, Phys. Rev. D90 no. 8, (2014) 083510
O'Hare+, PRD 92 (2015) 063518
O'Hare, Phys. Rev. D94 no. 6, (2016) 063527
Gonzalez-Carcía+, JHEP 07 (2018) 019
....

WIMP DISCOVERY LIMITS

Discovery limit: smallest WIMP cross section for which a given experiment has a 90% probability of detecting a WIMP signal at $\geq 3\sigma$.

$$\mathcal{L}(m_\chi, \sigma_{\chi-n}, \Phi, \mathcal{P}) = \prod_{i=1}^{n_{\text{bins}}} P(N_{\text{Exp}}^i, N_{\text{Obs}}^i) \times G(\mathcal{P}_i, \mu_{\mathcal{P}_i}, \sigma_{\mathcal{P}_i}) \times \prod_{\alpha=1}^{n_\nu} G(\phi_\alpha, \mu_\alpha, \sigma_\alpha)$$

Aristizabal, VDR, Flores, Papoulias JCAP 01 (2022) 01, 055

Follows a frequentist significance test using a likelihood ratio as a test statistic.

The profile likelihood ratio corresponds to a test against the null hypothesis H0 (CEvNS background only) vs the alternative hypothesis H1 (WIMP signal + CEvNS background).

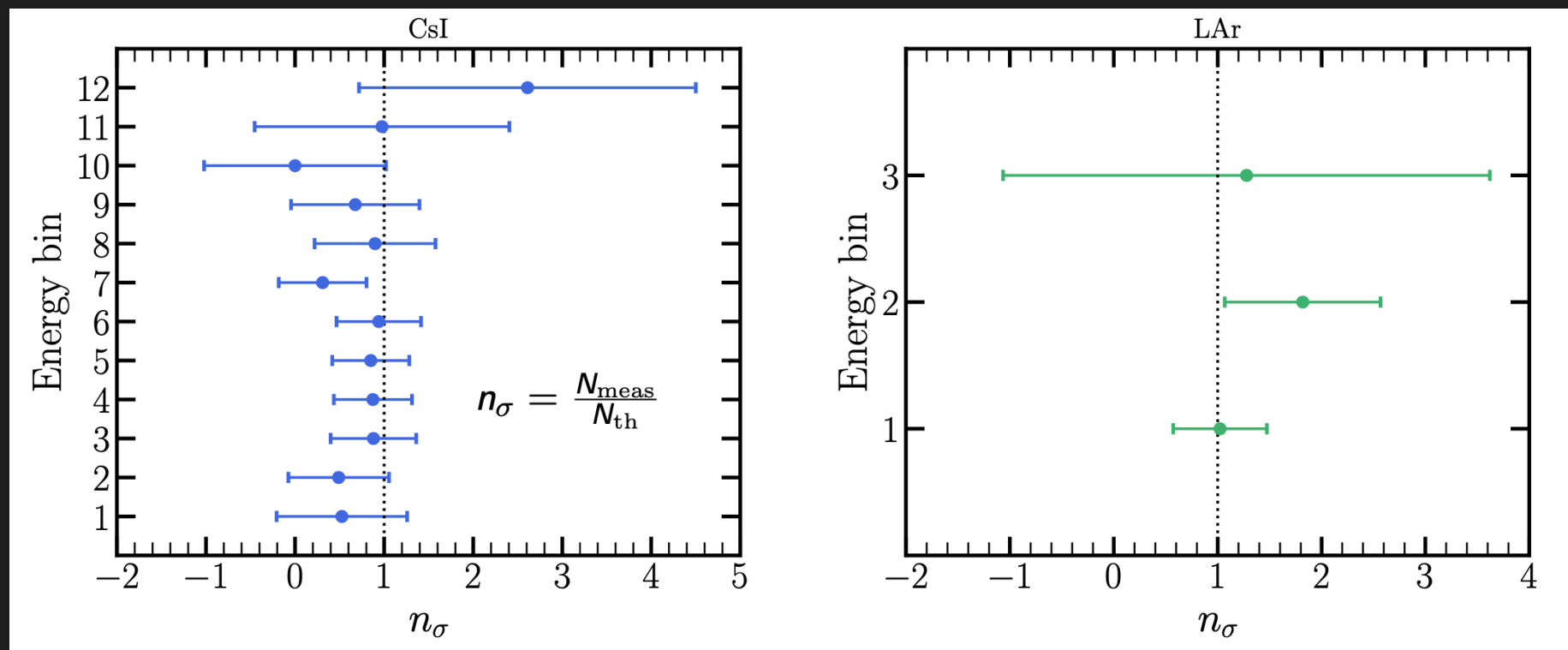
- Poisson distribution $P(k, \lambda) = \frac{\lambda^k e^{-\lambda}}{k!}$
- Gauss distribution $G(x, \mu, \sigma^2) = \frac{1}{\sigma\sqrt{2\pi}} e^{-\frac{1}{2}\left(\frac{x-\mu}{\sigma}\right)^2}$
- $N_{\text{Exp}}^i = N_\nu^i(\Phi_\alpha)$
- $N_{\text{Obs}}^i = \sum_\alpha N_\nu^i(\Phi_\alpha) + N_W^i$
- $\lambda(0) = \frac{\mathcal{L}_0}{\mathcal{L}_1}$ where \mathcal{L}_0 is the minimized function
- **statistical significance:** $\mathcal{Z} = \sqrt{-2 \ln \lambda(0)}$.
e.g. $\mathcal{Z} = 3$ corresponds to 90% C.L.

Parameter (\mathcal{P})	Normalization (μ)	Uncertainty
R_n	4.78 fm	10%
$\sin^2 \theta_W$	0.2387	10%

DATA-DRIVEN ANALYSIS

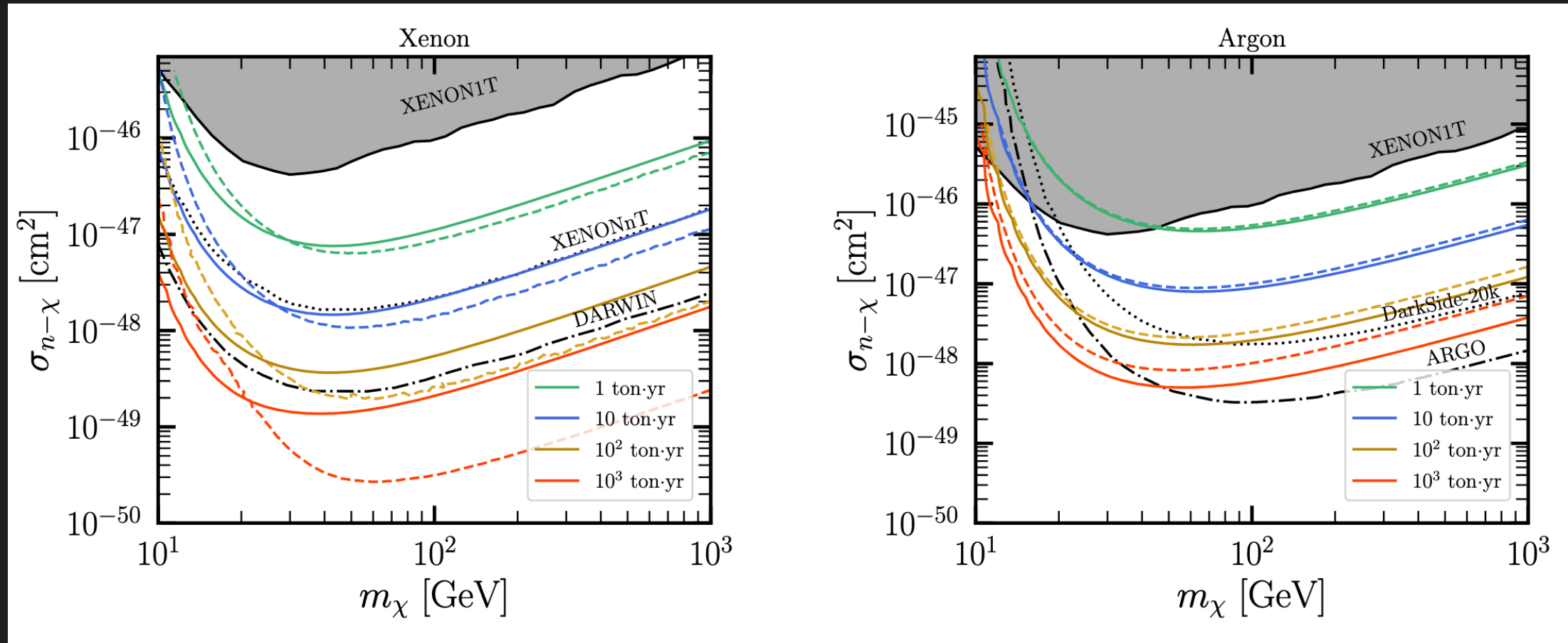
- Use the measured CEvNS cross section with its uncertainty. This approach encodes all possible uncertainties that the cross section can involve, independently of assumptions.
- We extract from the COHERENT CsI and LAr data the CEvNS cross section central values together with their standard deviations.
- We weigh the theoretical SM value of the CEvNS differential cross section with a multiplicative factor n_σ and use a spectral χ^2 test to fit n_σ in each recoil energy bin.

COHERENT CsI (2017) + LAr



Aristizabal, VDR, Flores, Papoulias JCAP 01 (2022) 01, 055

DATA-DRIVEN ANALYSIS



Aristizabal, VDR, Flores, Papoulias JCAP 01 (2022) 01, 055

In the analysis with CsI data, compared with the SM expectation (solid curves), WIMP discovery limits improve. The measured CEvNS cross section (central values) is smaller than the SM expectation, thus resulting in a background depletion.

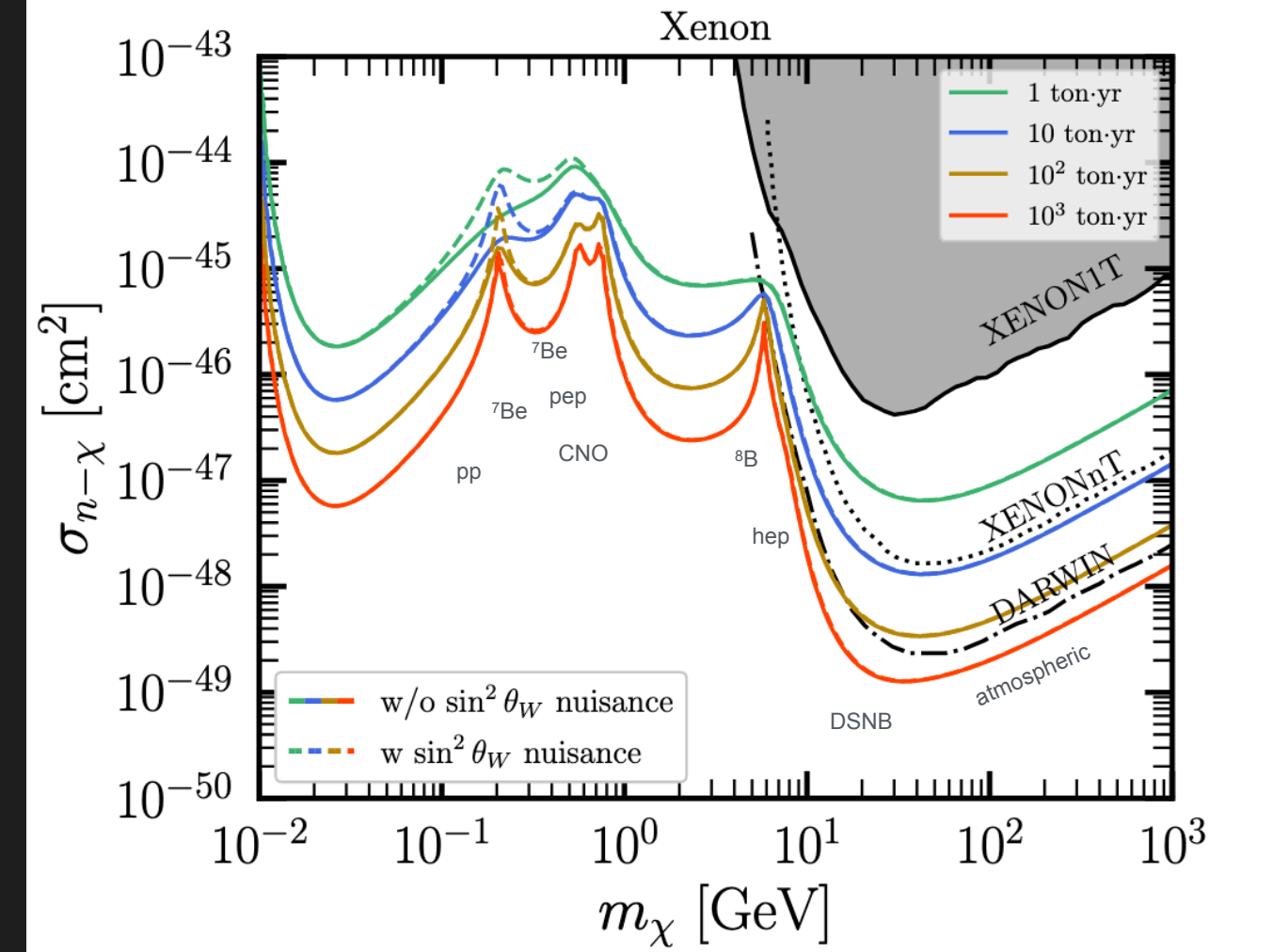
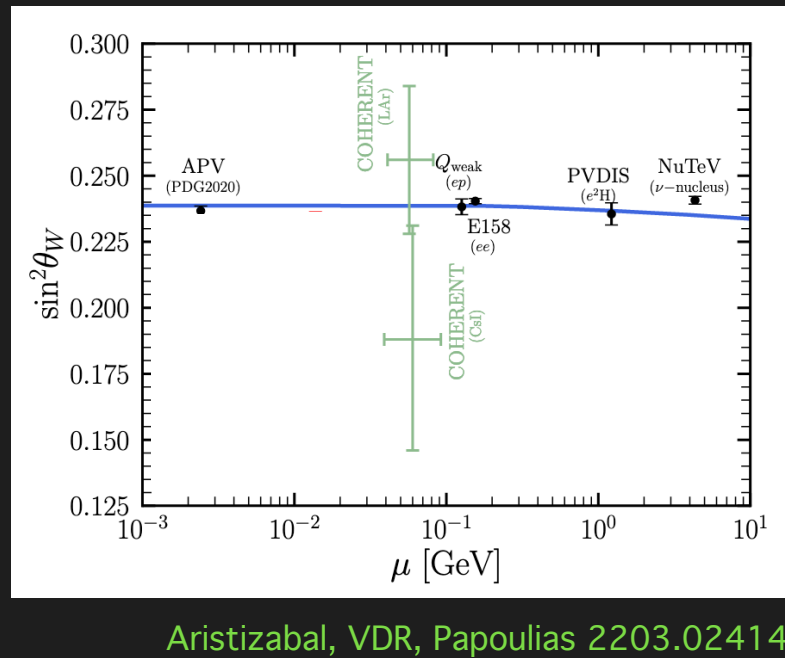
Results derived using the LAr data behave differently.

IMPACT OF WEAK MIXING ANGLE

Effects of **weak mixing angle uncertainties** are expected to be relevant at **low WIMP masses**, where solar neutrino fluxes are more abundant.

- vary around the central value:
 $\sin^2 \theta_W = 0.2387$ (10%)

$$Q_W = (\frac{1}{2} - 2 \sin^2 \theta_W) Z - \frac{1}{2} N$$



As the **weak mixing angle increases**, the **coherent weak charge becomes more negative**.

IMPACT OF NUCLEAR FORM FACTOR

Differences between proton and neutron distributions are expected to be substantial for neutron-rich nuclei → impact on the values of the nuclear form factor.

$$F(q^2) = 3 \frac{j_1(qR_0)}{qR_0} e^{-\frac{1}{2}(qs)^2}$$

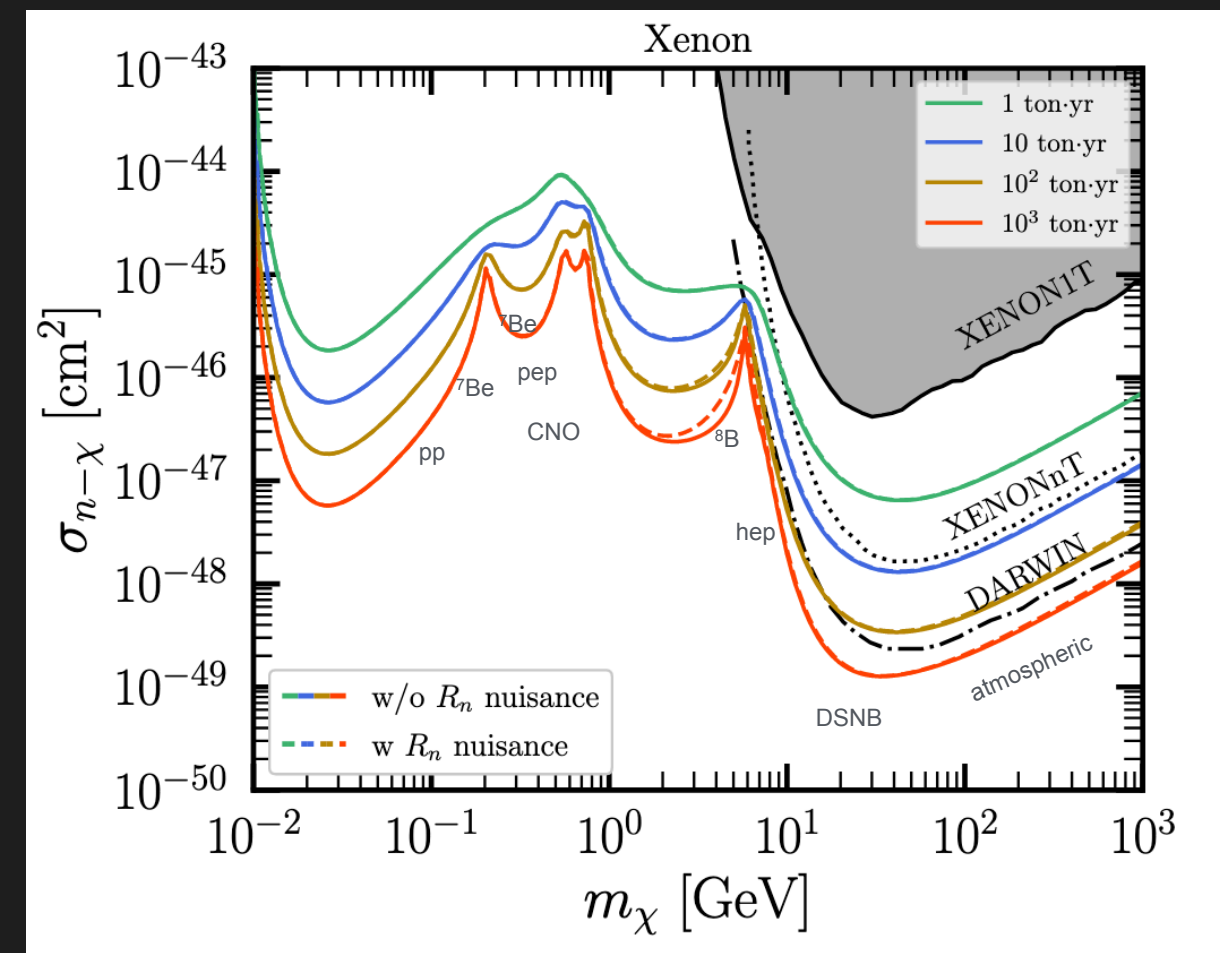
- Rp=4.78 fm (fixed)
- vary around R_n = 4.78 fm (central value)
- assume 10% uncertainty on R_n

Helm parametrization

$$R_0 = \sqrt{\frac{5}{3} (R_X^2 - 3s^2)} \quad (X = p, n)$$

Low WIMP masses and incoming neutrino energies: the zero momentum transfer limit is a good approximation.

With increasing neutron mean-square radius, **nuclear size increases**. The loss of coherence happens for smaller q. As R_n increases, both the neutrino background and the WIMP event rate are (slightly) suppressed.



Aristizabal, VDR, Flores, Papoulias JCAP 01 (2022) 01, 055

LIGHT VECTOR MEDIATOR

$$\frac{d\sigma}{dE_r} = \frac{m_N G_F}{2\pi} Q_V^2 \left(2 - \frac{m_N E_r}{E_\nu^2} \right) F^2(q)$$

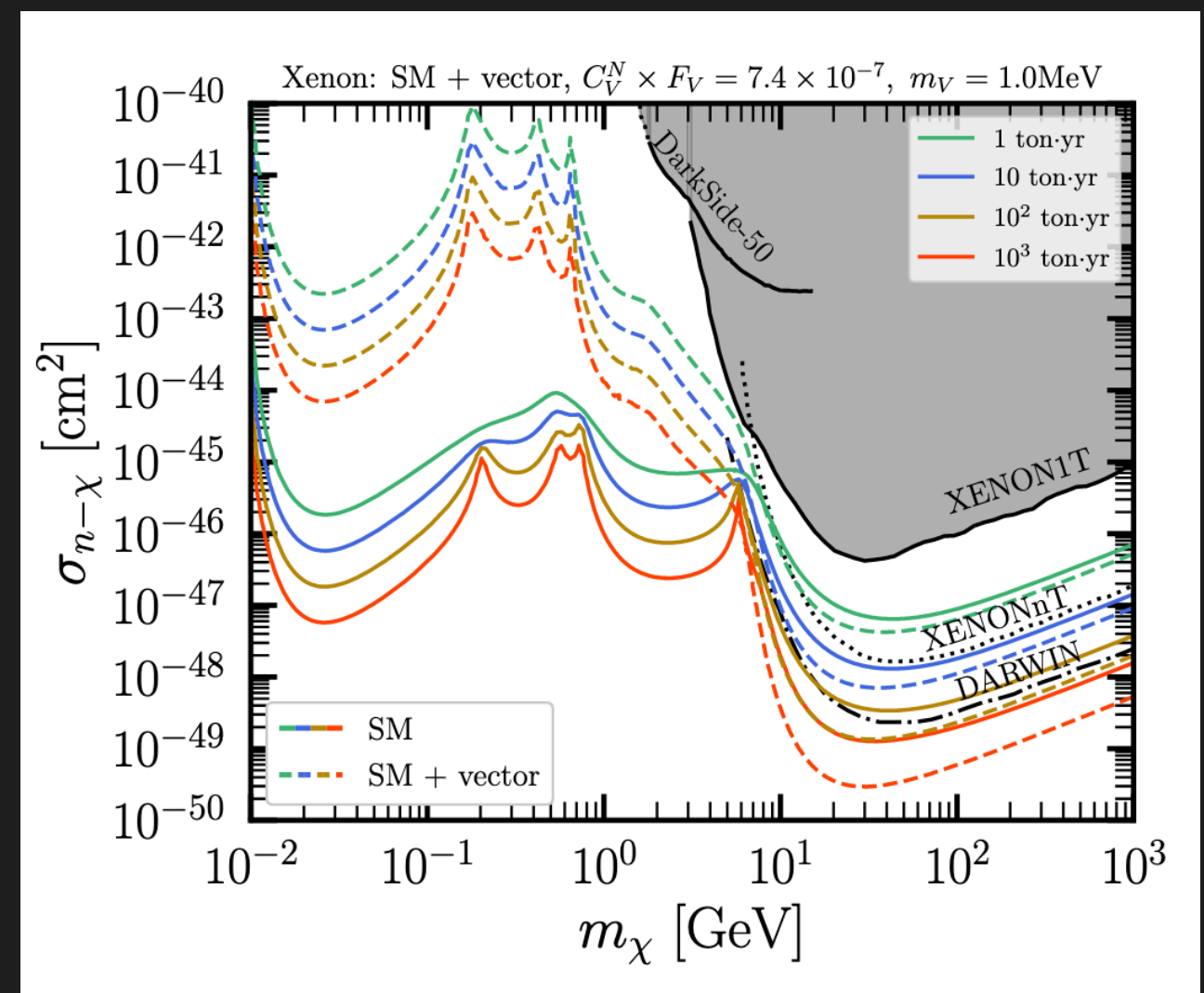
$$Q_V = Q_W + \frac{C_V^N F_V}{\sqrt{2} G_F (2m_N E_r + m_V^2)}$$

Vector coupling to nucleus

Vector coupling to neutrinos

Cerdeño et al. JHEP 05 (2016)

- We fix the product of couplings $C_V^N F_V$ to their maximum allowed value according to COHERENT CsI data.
- Only nuisance parameters are those associated with neutrino flux normalization factors.
- At low momentum transfer the new contribution is enhanced and the neutrino background increases.
- The SM coherent weak charge is negative, while the new contribution is positive. So, as q^2 increases the new contribution becomes less important and destructively interferes with the SM term.

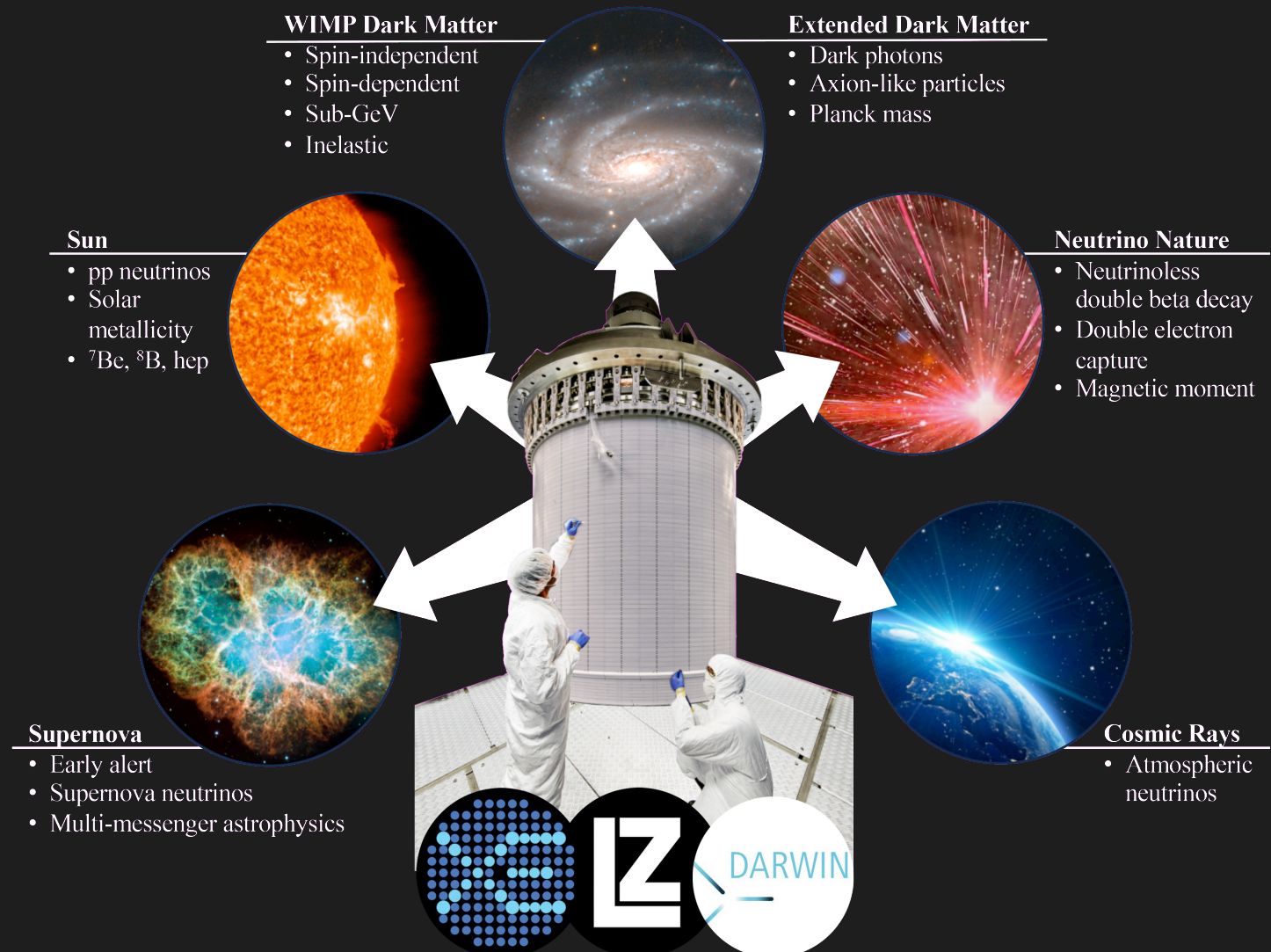
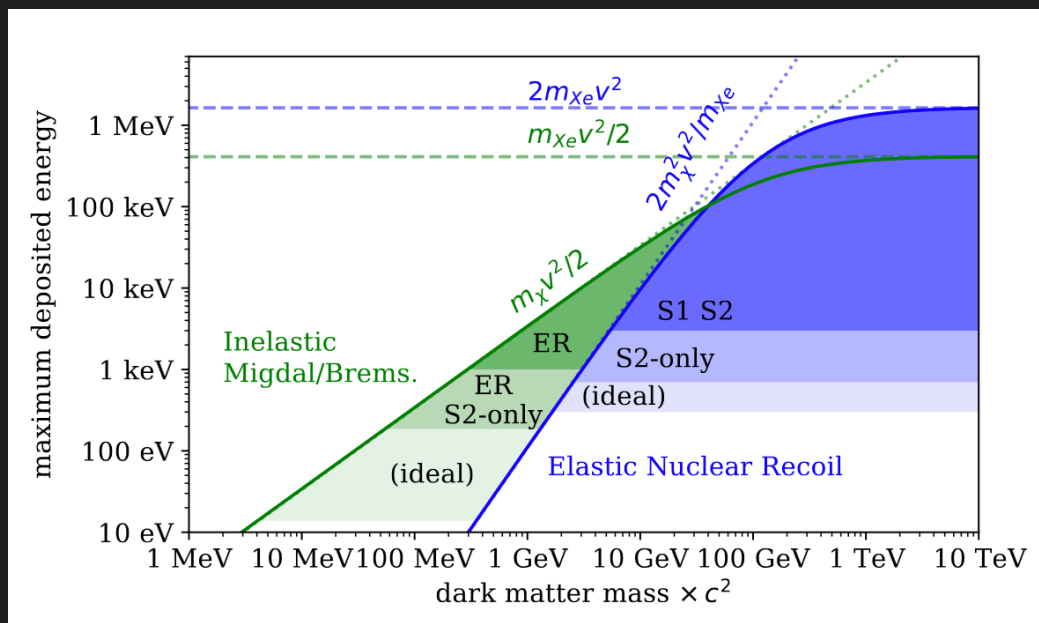


Aristizabal, VDR, Flores, Papoulias JCAP 01 (2022) 01, 055

NEXT-GENERATION LIQUID XENON DETECTORS

A next-generation Xe detector like XLZD will improve in exposure and energy threshold

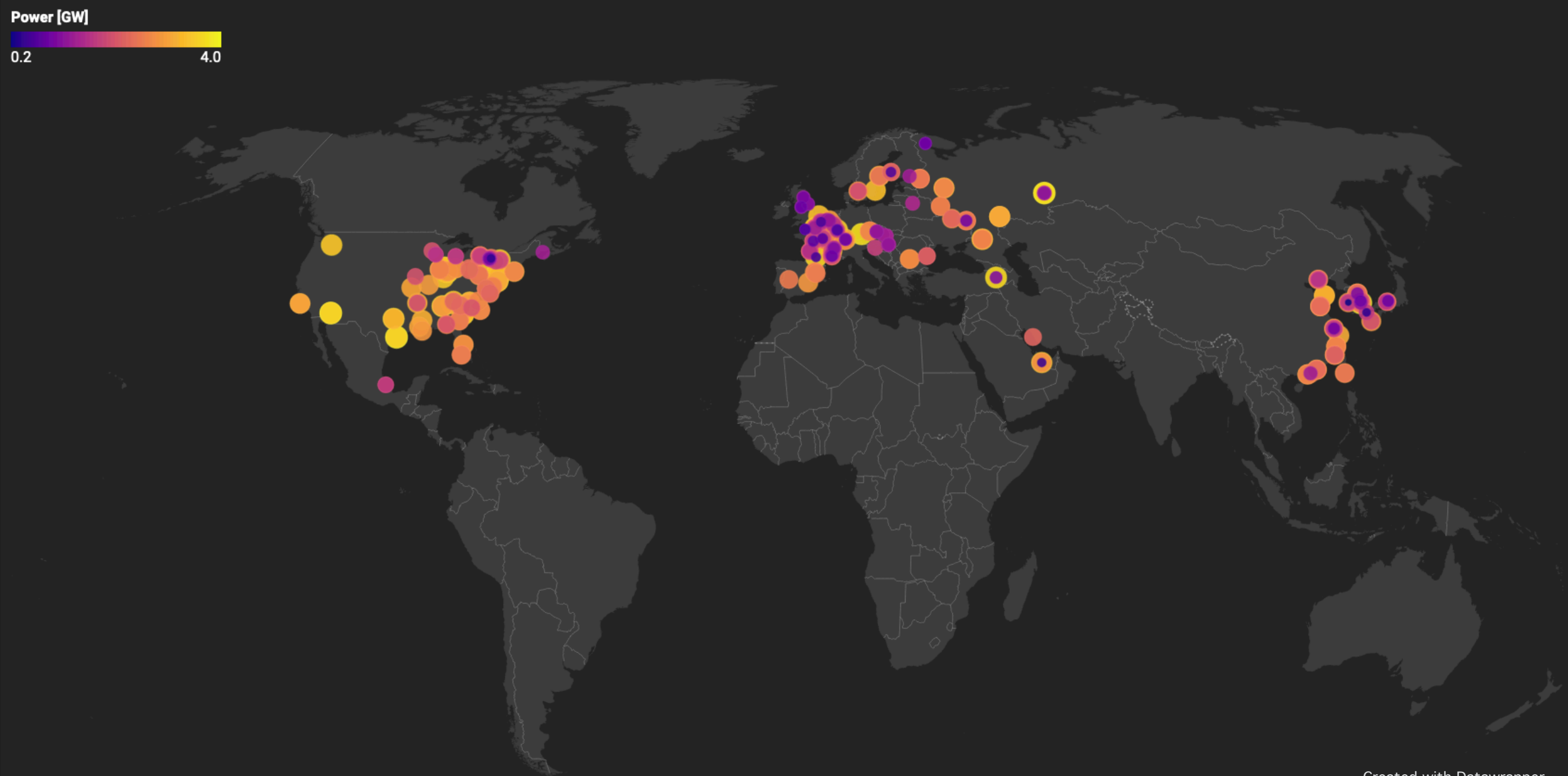
- 40-100 tonnes Xenon
- $E_{\text{thr}} \sim 0.1 - 0.3 \text{ keV}$



<https://xlzd.org/>

XLZD Consortium, Aalbers et al. J. Phys. G: Nucl. Part. Phys. 50 (2023) 01300

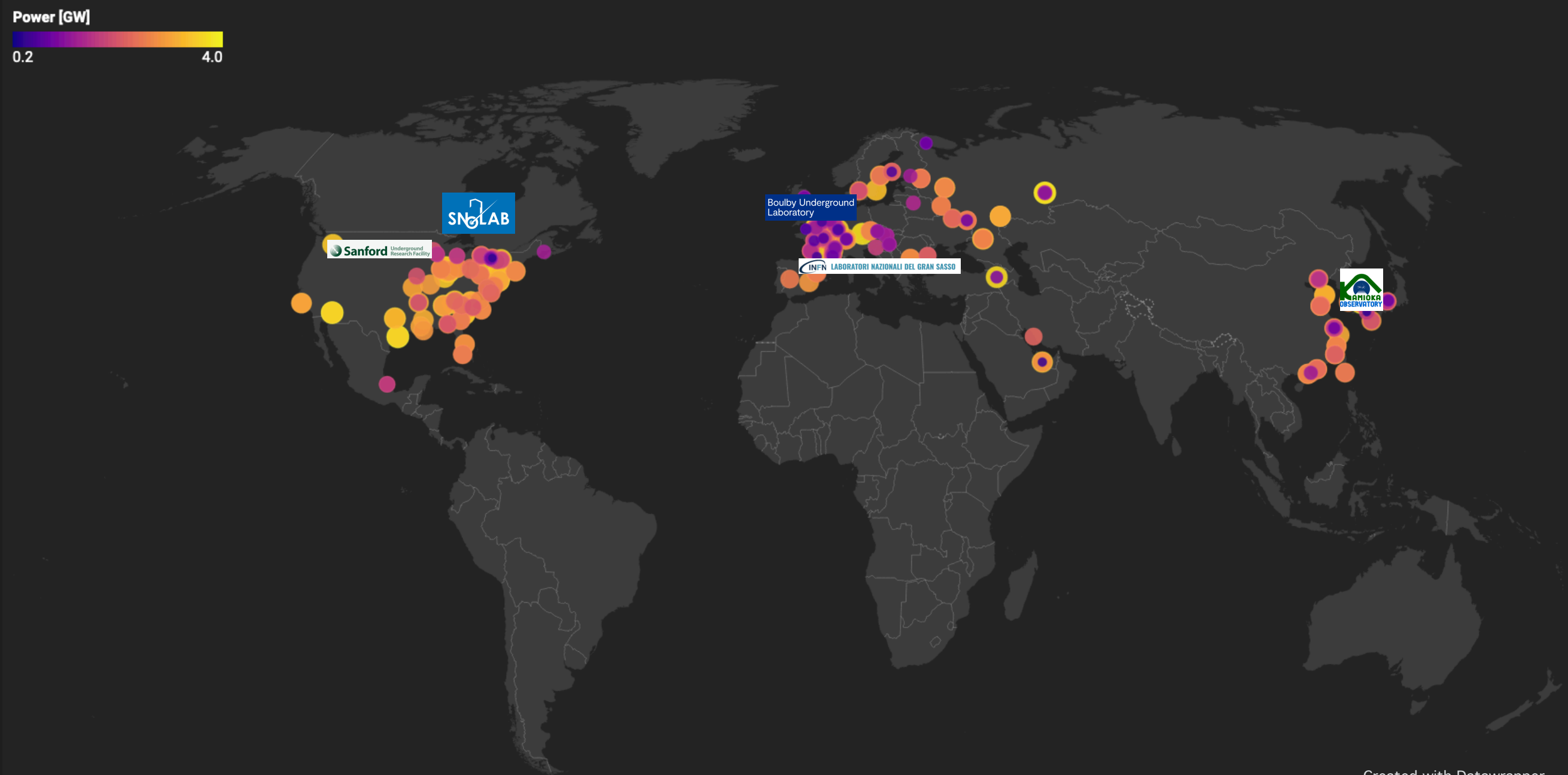
ONLY ASTROPHYSICAL NEUTRINOS?



Created with Datawrapper

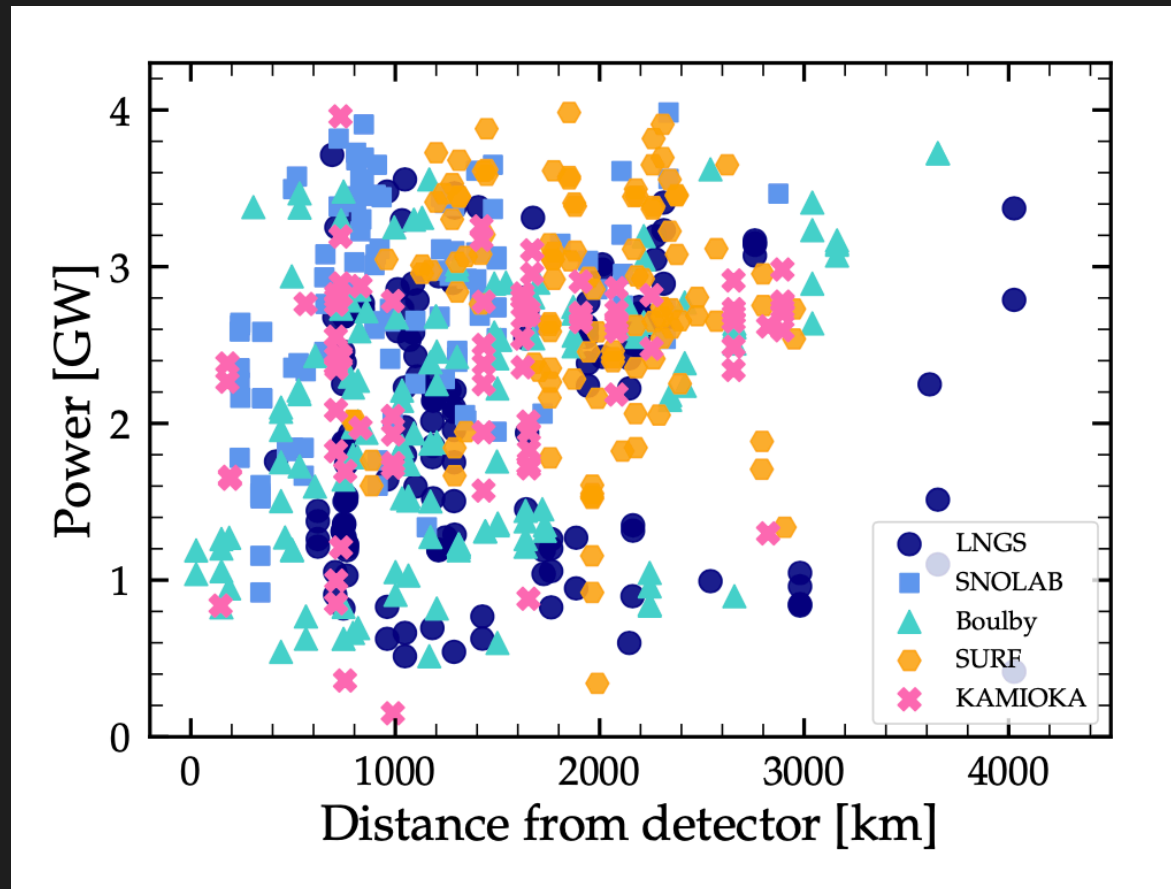
geoneutrinos.org

REACTOR NEUTRINO BACKGROUND



geoneutrinos.org

REACTOR NEUTRINO BACKGROUND



Aristizabal, VDR, Ternes 2402.06416

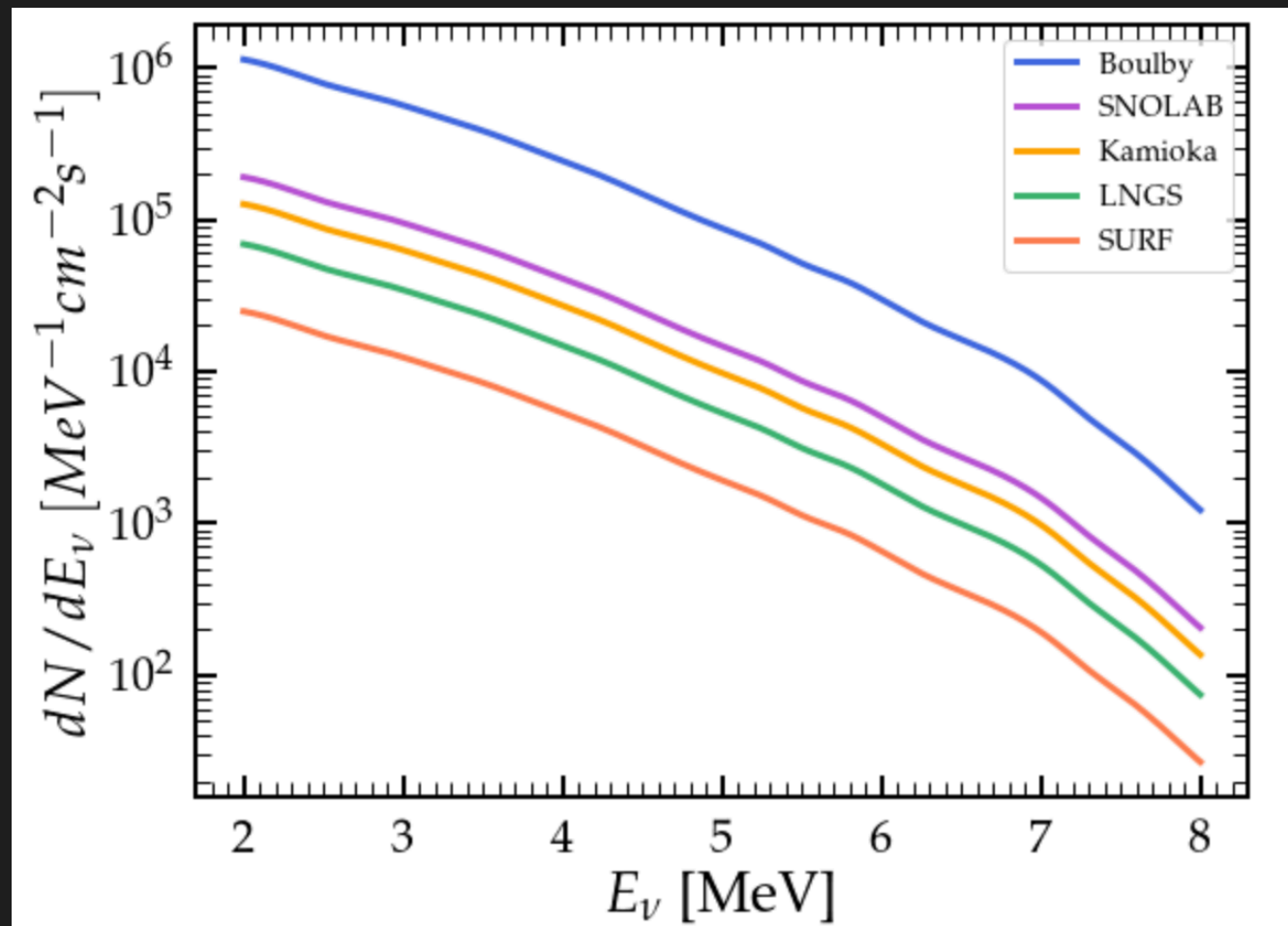
Location	NR	L_{\min} [km]	L_{\max} [km]	P_{\min} [GW]	P_{\max} [GW]
SURF	111	790	2951	0.34	3.9
SNOLAB	104	239	2874	0.92	3.9
Kamioka	86	146	2895	0.15	3.9
LNGS	146	417	4027	0.42	3.7
Boulby	141	26	3654	0.51	3.7

geoneutrinos.org

Only commercial power plants currently operating

Exposure time	Neutrino flux normalisation	CEvNS cross section
$\frac{dR_C}{dE_r} = \frac{m_{\det} N_A \mathcal{T} \eta_C}{m_{\text{mol}}^{\text{Xe}}} \int_{E_{\nu}^{\min}}^{E_{\nu}^{\max}} \frac{d\Phi_{\bar{\nu}_e}}{dE_{\nu}} \frac{d\sigma}{dE_r} F_{\text{H}}^2(E_r) dE_{\nu}$		
Average nuclear mass = 131.4		

REACTOR NEUTRINO FLUX



$$\frac{d\Phi_{\bar{\nu}_e}}{dE_\nu} = \sum_{i=\text{Isotopes}} f_i \frac{d\Phi_{\bar{\nu}_e}^i}{dE_\nu}$$

Kopeikin+ Phys. Rev. D 104 no. 7, (2021) L071301
Huber Phys. Rev. C 84 (2011) 024617

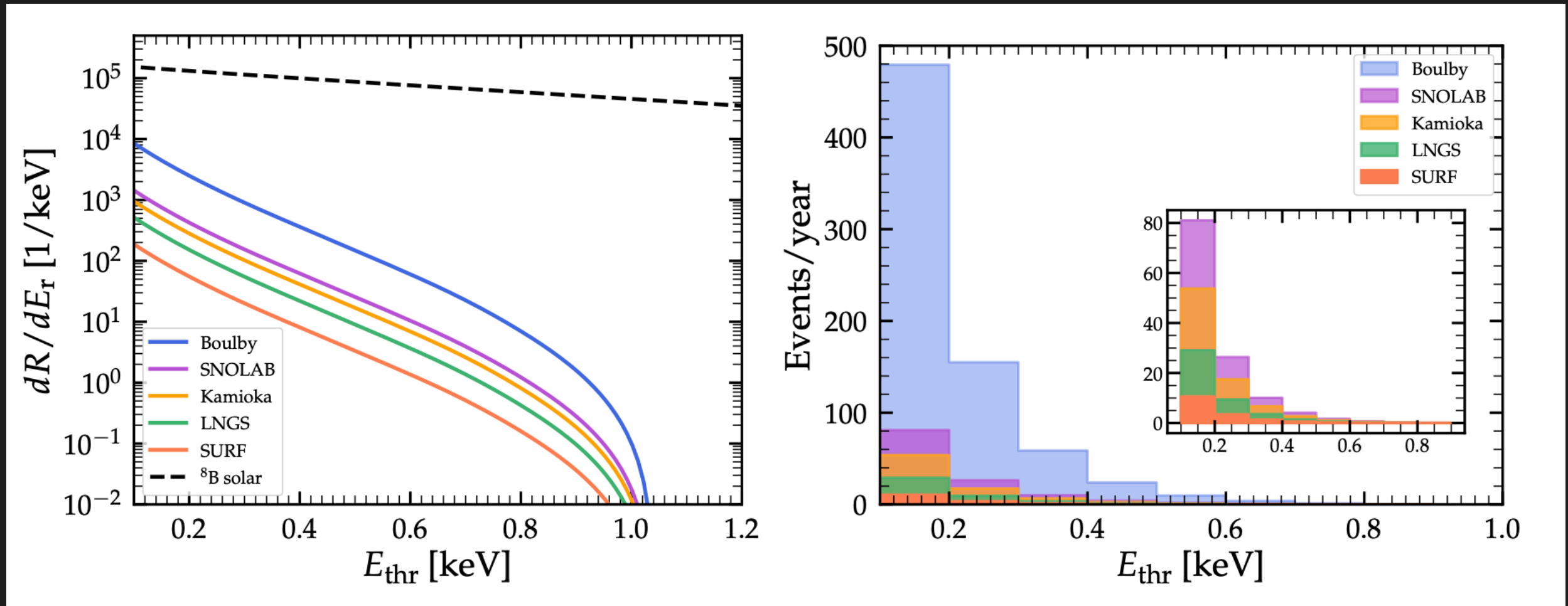
$$f_i = \{f_{^{235}\text{U}}, f_{^{238}\text{U}}, f_{^{239}\text{Pu}}, f_{^{241}\text{Pu}}\} = \{0.55, 0.07, 0.32, 0.06\}$$

Neutrino flux normalizations

Cluster	SURF	SNOLAB	Kamioka	LNGS	Boulby
η_C [cm $^{-2}$ sec $^{-1}$]	20422	156630	103903	56677	932874

REACTOR NEUTRINO BACKGROUND

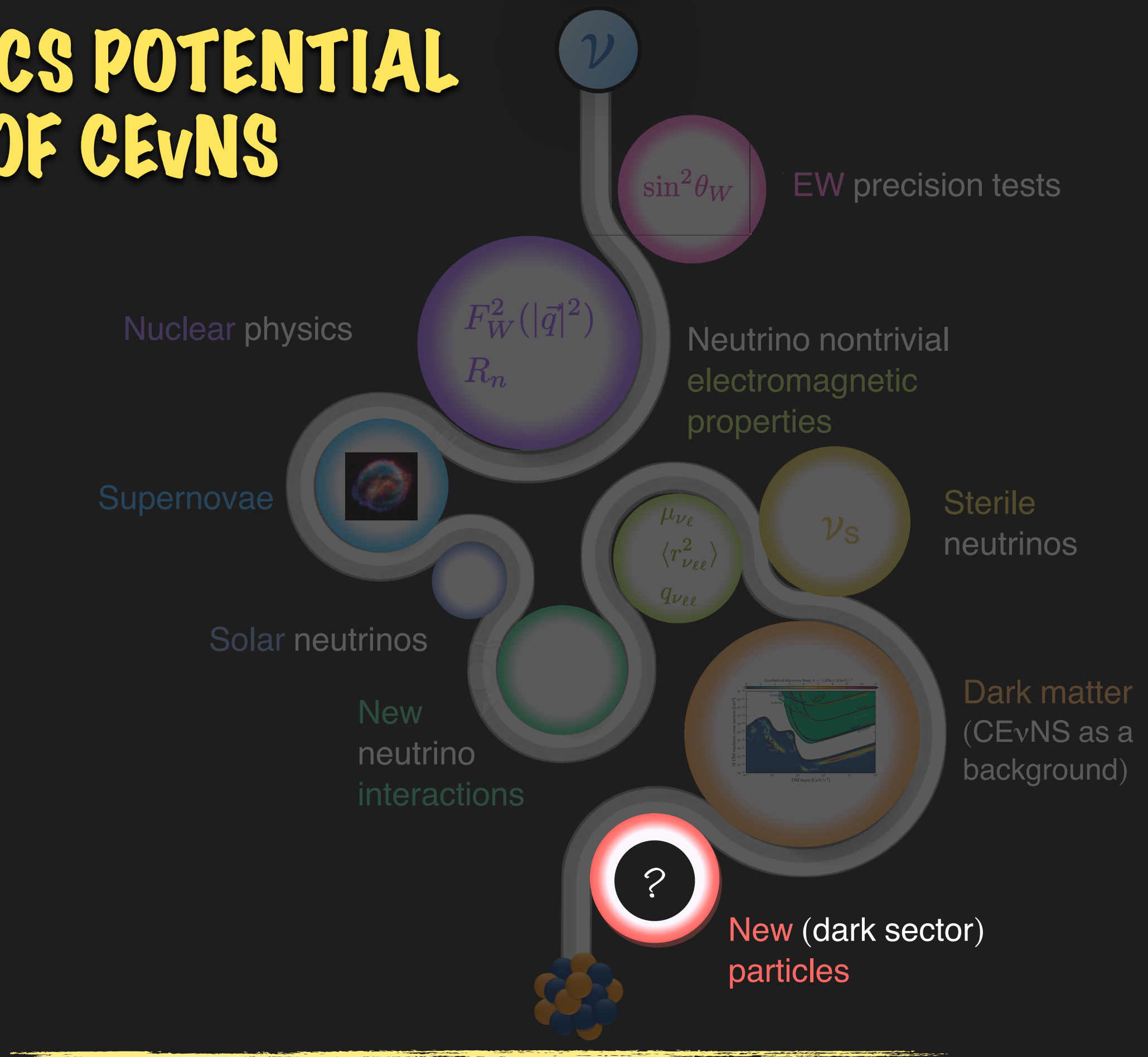
XLZD, 50 ton, $E_{\text{thr}} = 0.1 \text{ keV}$



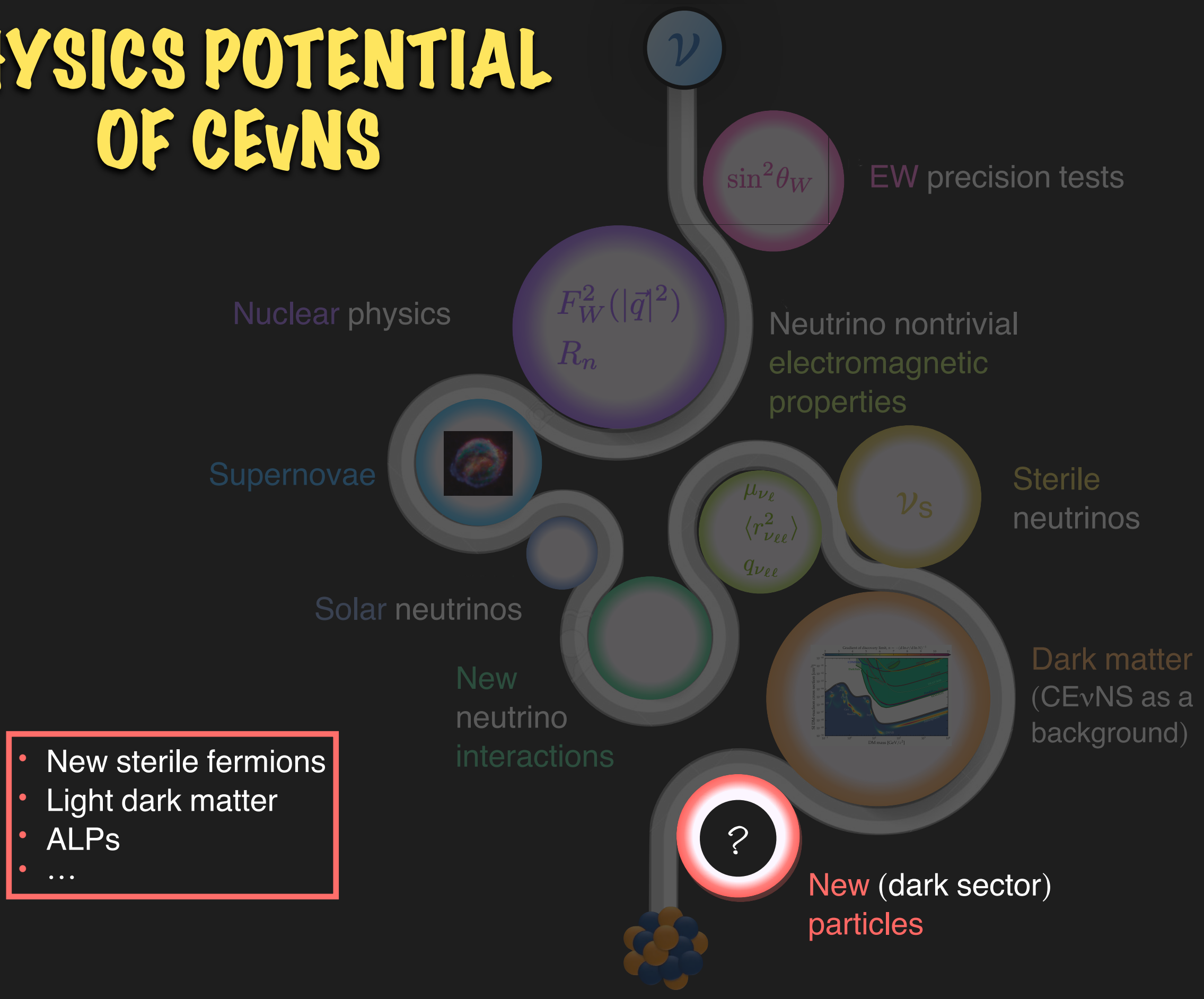
Aristizabal, VDR, Ternes 2402.06416

At 0.1 keV, we find that the neutrino-nucleus event rate per year is: 11 (SURF), 29 (LNGS), 54 (Kamioka), 46.34 (SNOLAB) and 479 (Boulby)

PHYSICS POTENTIAL OF CEvNS

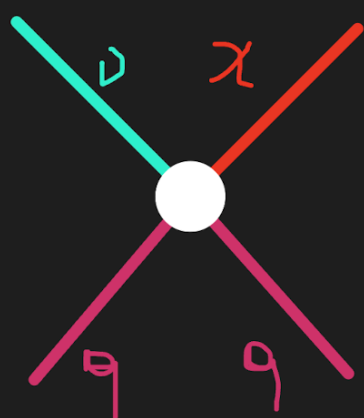


PHYSICS POTENTIAL OF CEvNS



PRODUCTION OF NEW PARTICLES: STERILE FERMION

Possible production of a new MeV-scale fermion through the up-scattering process of neutrinos off the nuclei and the electrons of the detector material through some new scalar (S), pseudoscalar (P), vector (V), axial-vector (A) or tensor (T) interaction.



$$\mathcal{L}_{\text{SF}}^a \supseteq \frac{G_F}{\sqrt{2}} \epsilon_\ell^a (\bar{\chi} \Gamma^a P_L \nu_\ell) (\bar{f} \Gamma_a f) + \text{H.c.}$$

$$\nu_\ell e \rightarrow \chi e, \quad \nu_\ell \mathcal{N} \rightarrow \chi \mathcal{N}$$

See also: Brdar+ JHEP 12 (2018) 024, Chao+ PRD 104 (2021) 095017, Chen+ JHEP 05 (2021) 131, LI & Liao JHEP 02 (2021) 099, Chang & Liao PRD 102 no. 7, (2020) 075004, VDR, Muñoz-Candela, Papoulias Phys.Rev.D 108 (2023) 5, 055001

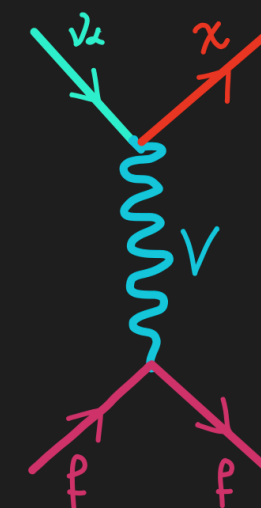
PRODUCTION OF NEW PARTICLES: STERILE FERMION

Consider both effective interactions and light mediators

$$\frac{d\sigma_{\nu_e \mathcal{A}}}{dT_e} \Bigg|_{E\nu\text{ES}}^V = \frac{m_e g_V^4}{2\pi(m_V^2 + 2m_e T_e)^2} Z_{\text{eff}}^{\mathcal{A}}(T_e) \times \left[\left(1 - \frac{m_e T_e}{2E_\nu^2} - \frac{T_e}{E_\nu} + \frac{T_e^2}{2E_\nu^2} \right) - \frac{m_\chi^2}{4E_\nu^2} \left(1 + \frac{2E_\nu}{m_e} - \frac{T_e}{m_e} \right) \right]$$

$$\frac{d\sigma_{\nu_e \mathcal{N}}}{dT_{\mathcal{N}}} \Bigg|_{\text{CE}\nu\text{NS}}^V = \frac{m_{\mathcal{N}} C_V^4}{2\pi(m_V^2 + 2m_{\mathcal{N}} T_{\mathcal{N}})^2} F_W^2(|\mathbf{q}|^2) \times \left[\left(1 - \frac{m_{\mathcal{N}} T_{\mathcal{N}}}{2E_\nu^2} - \frac{T_{\mathcal{N}}}{E_\nu} + \frac{T_{\mathcal{N}}^2}{2E_\nu^2} \right) - \frac{m_\chi^2}{4E_\nu^2} \left(1 + \frac{2E_\nu}{m_{\mathcal{N}}} - \frac{T_{\mathcal{N}}}{m_{\mathcal{N}}} \right) \right]$$

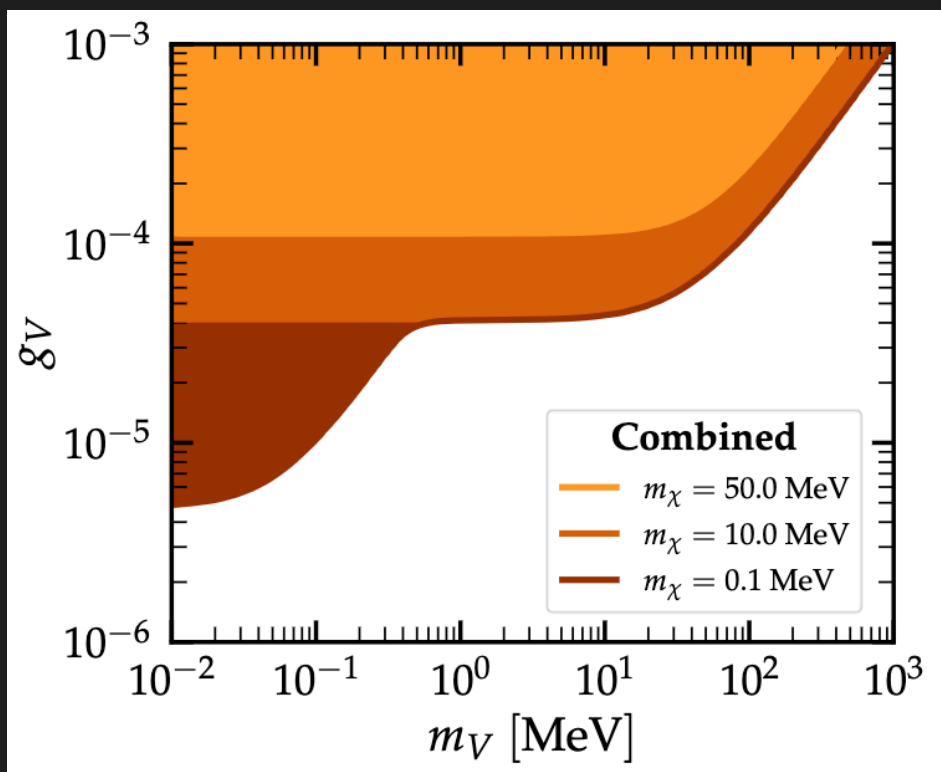
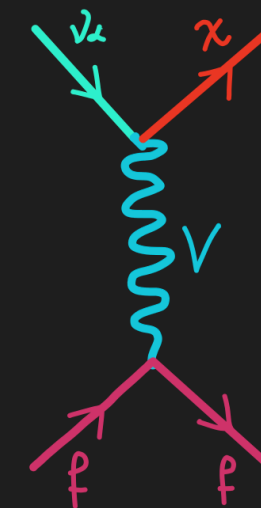
$$C_V^2 \equiv 3A g_V^2$$



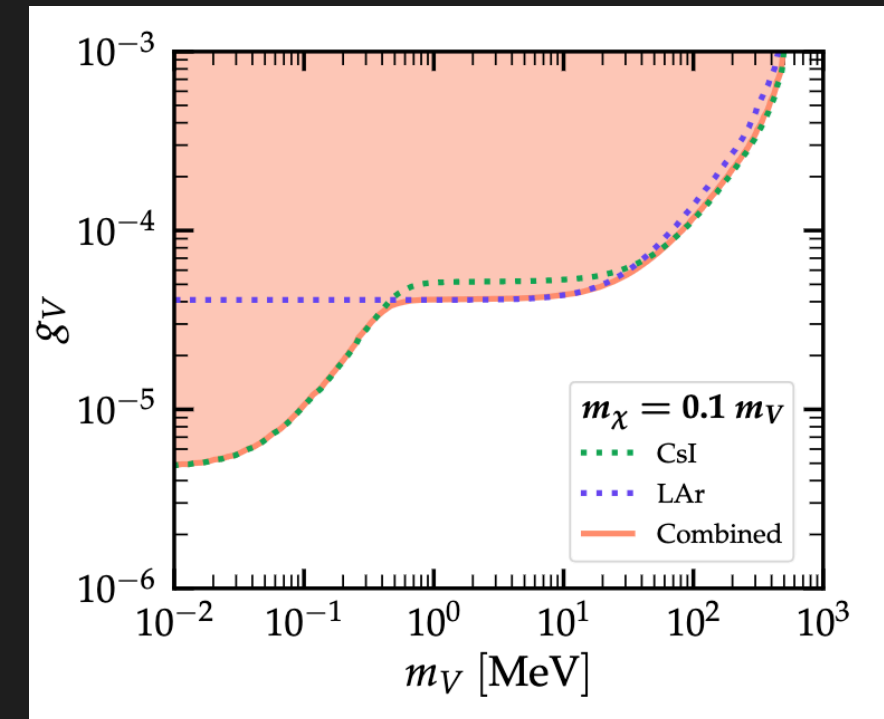
Candela, VDR+ 2404.12476

PRODUCTION OF NEW PARTICLES: STERILE FERMION

Possible production of a new MeV-scale fermion through the **up-scattering process** of neutrinos off the nuclei and the electrons of the detector material, via the exchange of a light vector mediator.



COHERENT CsI (2021) + LAr

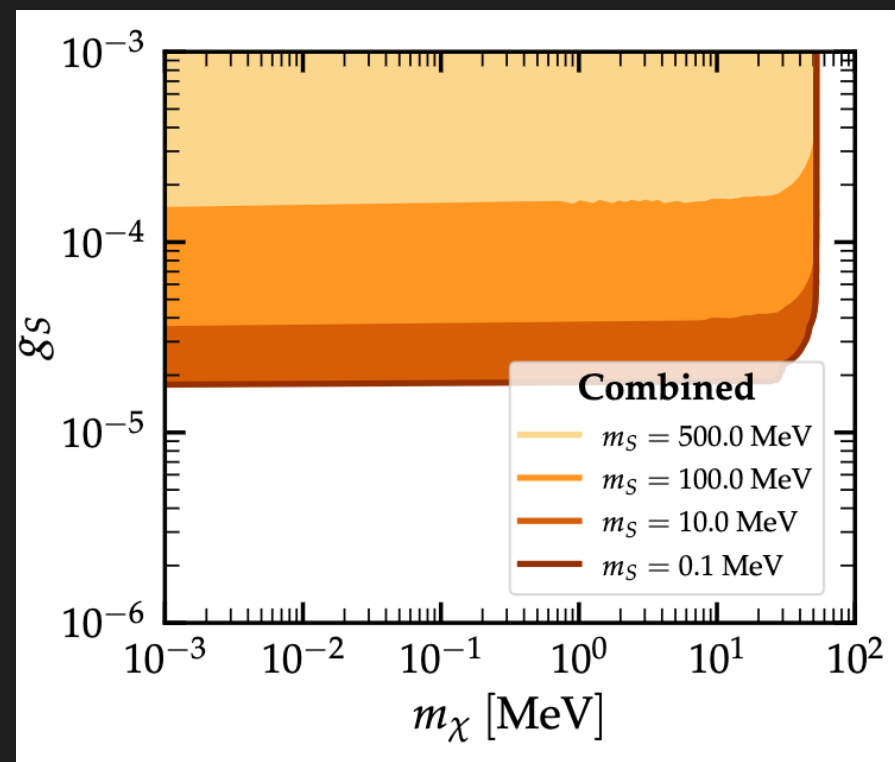
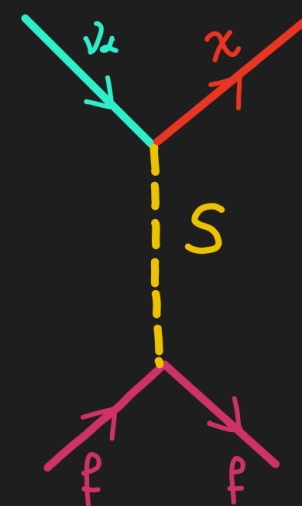


VDR, Muñoz-Candela, Papoulias Phys.Rev.D 108 (2023) 5, 055001

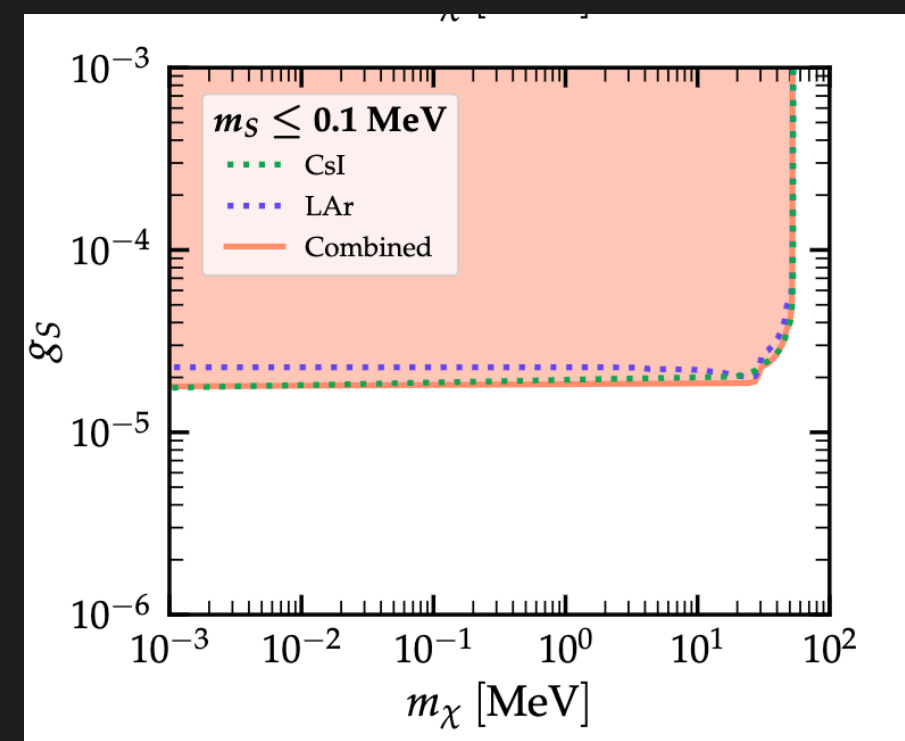
See also: Brdar+ JHEP 12 (2018) 024, Chao+ PRD 104 (2021) 095017, Chen+ JHEP 05 (2021) 131, LI & Liao JHEP 02 (2021) 099, Chang & Liao PRD 102 no. 7, (2020) 075004

PRODUCTION OF NEW PARTICLES: STERILE FERMION

Possible production of a new MeV-scale fermion through the up-scattering process of neutrinos off the nuclei and the electrons of the detector material, via the exchange of a light scalar mediator.



COHERENT CsI (2021) + LAr

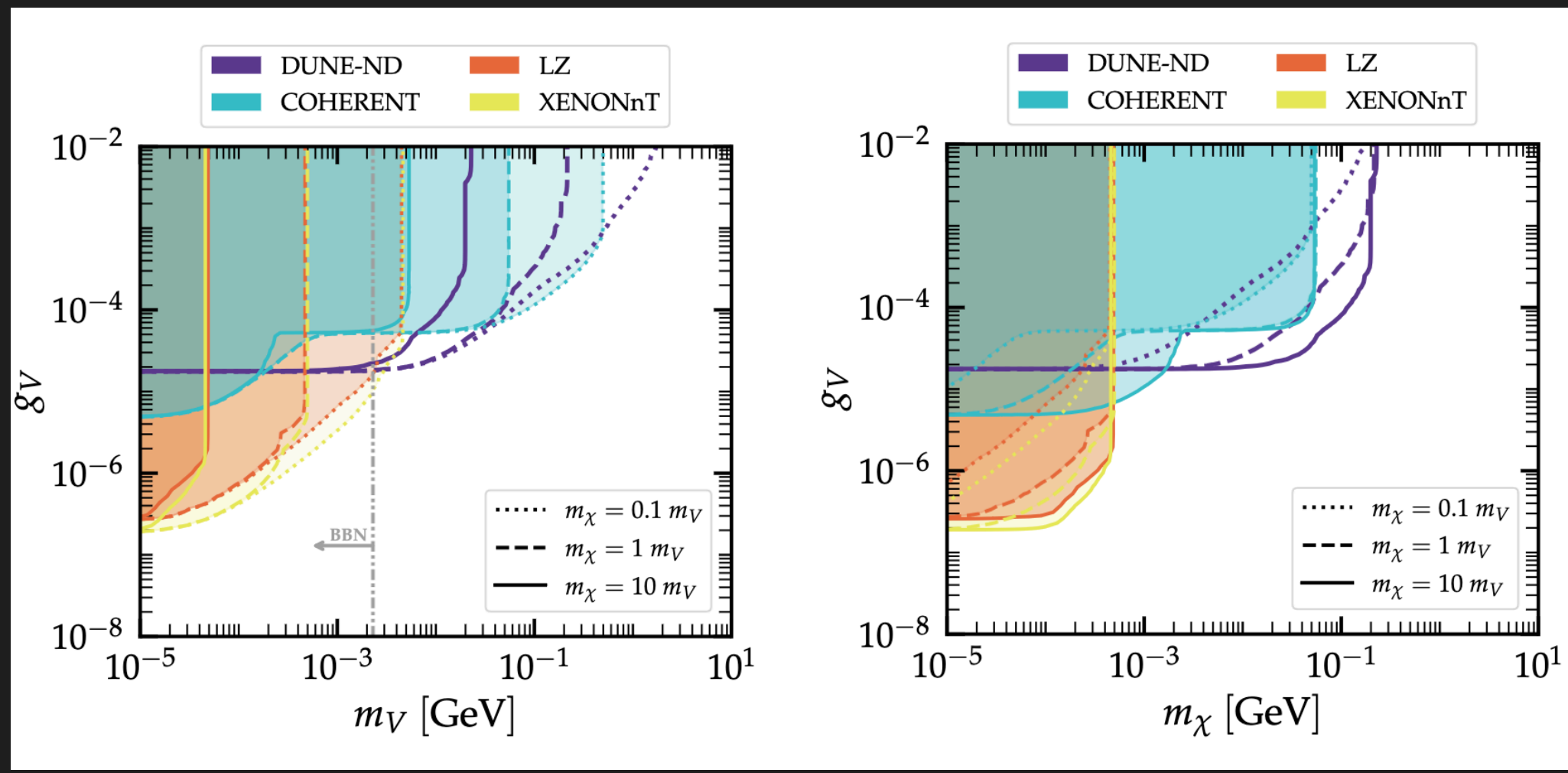


See also: Brdar+ JHEP 12 (2018) 024, Chao+ PRD 104 (2021) 095017, Chen+ JHEP 05 (2021) 131, Li & Liao JHEP 02 (2021) 099, Chang & Liao PRD 102 no. 7, (2020) 075004

VDR, Muñoz-Candela, Papoulias Phys.Rev.D 108 (2023) 5, 055001

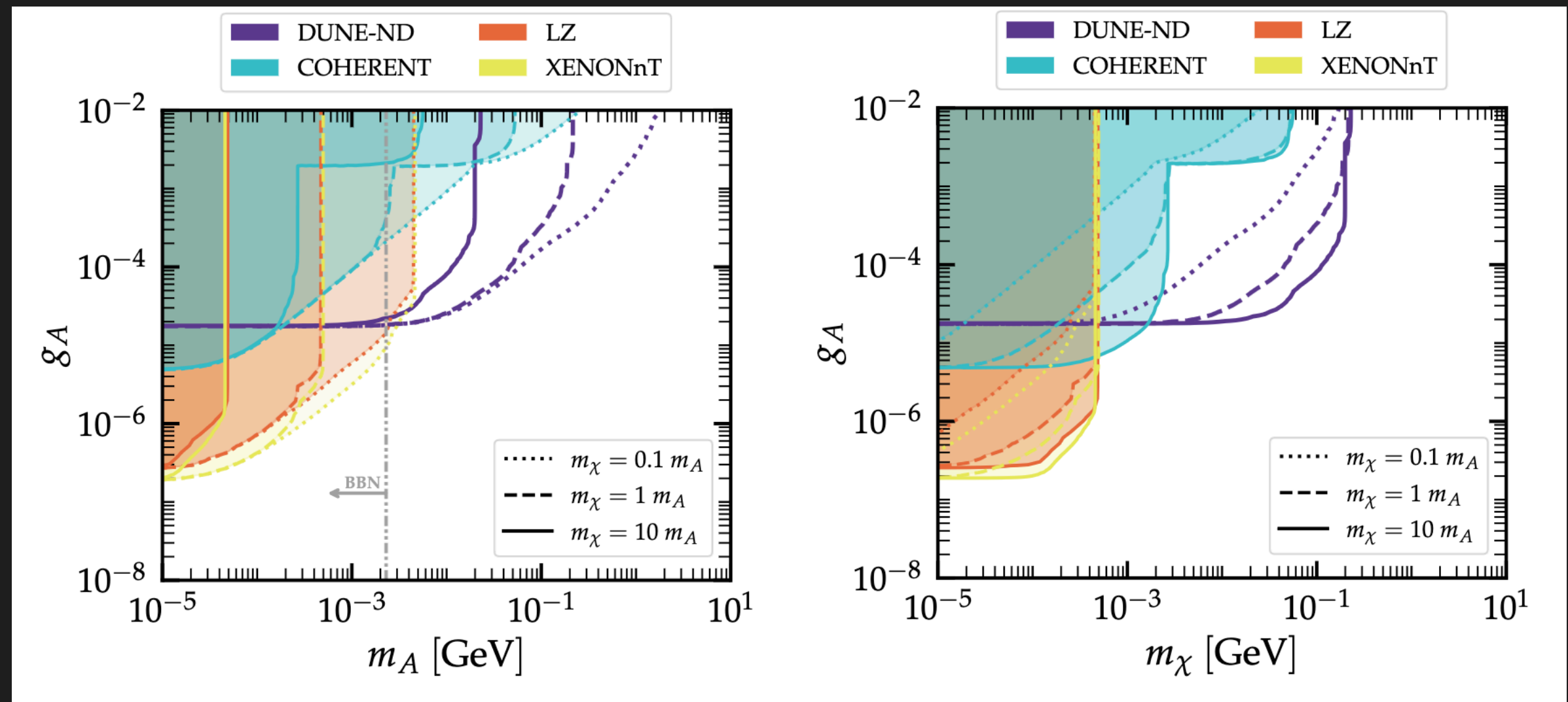
PRODUCTION OF NEW PARTICLES: STERILE FERMION

We analyze elastic neutrino-electron scattering events induced by solar neutrinos in two current DM DD experiments, XENONnT and LZ and from coherent elastic neutrino-nucleus scattering data from the COHERENT (CsI and LAr) experiment. We also explore the sensitivity of the DUNE experiment to this scenario.



Candela, VDR+ [2404.12476](#)

PRODUCTION OF NEW PARTICLES: STERILE FERMION



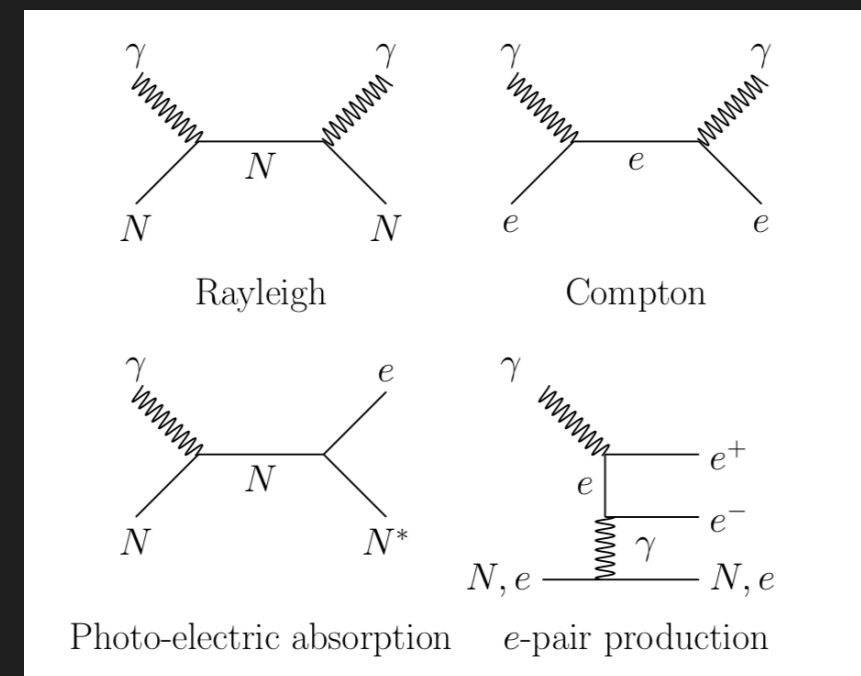
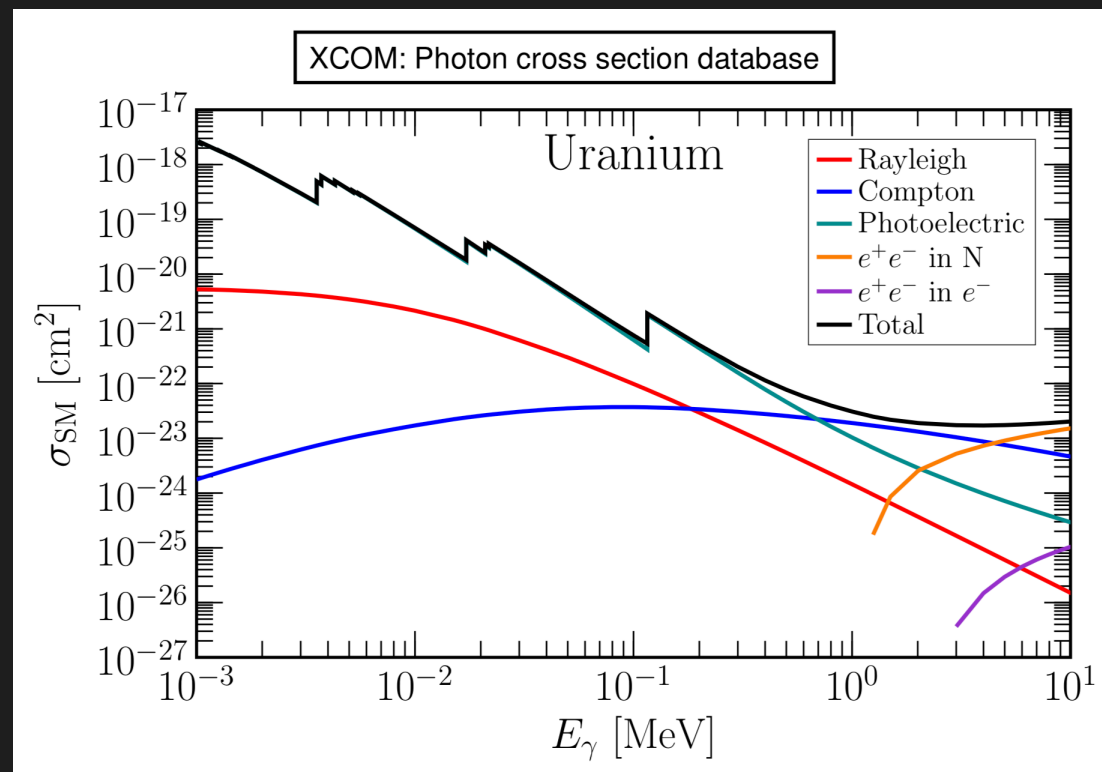
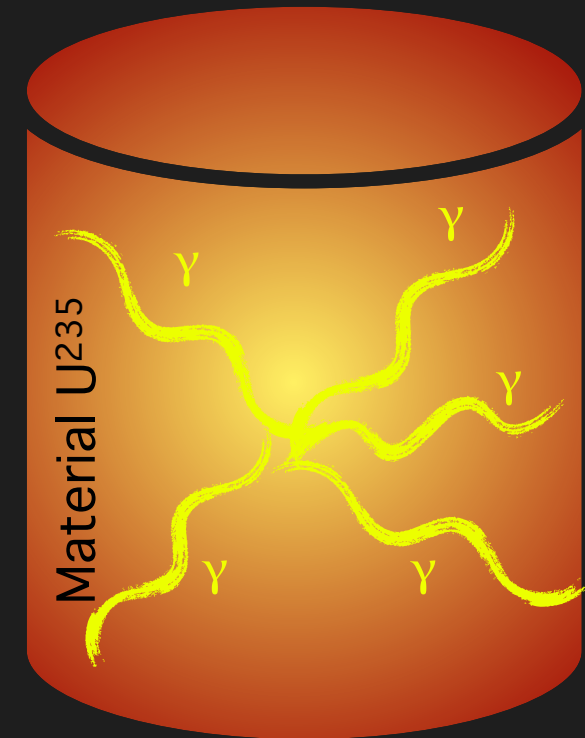
Candela, VDR+ [2404.12476](#)

PHOTON PRODUCTION AT REACTORS

A very large number of photons is produced inside the nuclear reactor core via:

- Prompt fission
- β decay of fission products
- Radiative n capture
- Inelastic n capture

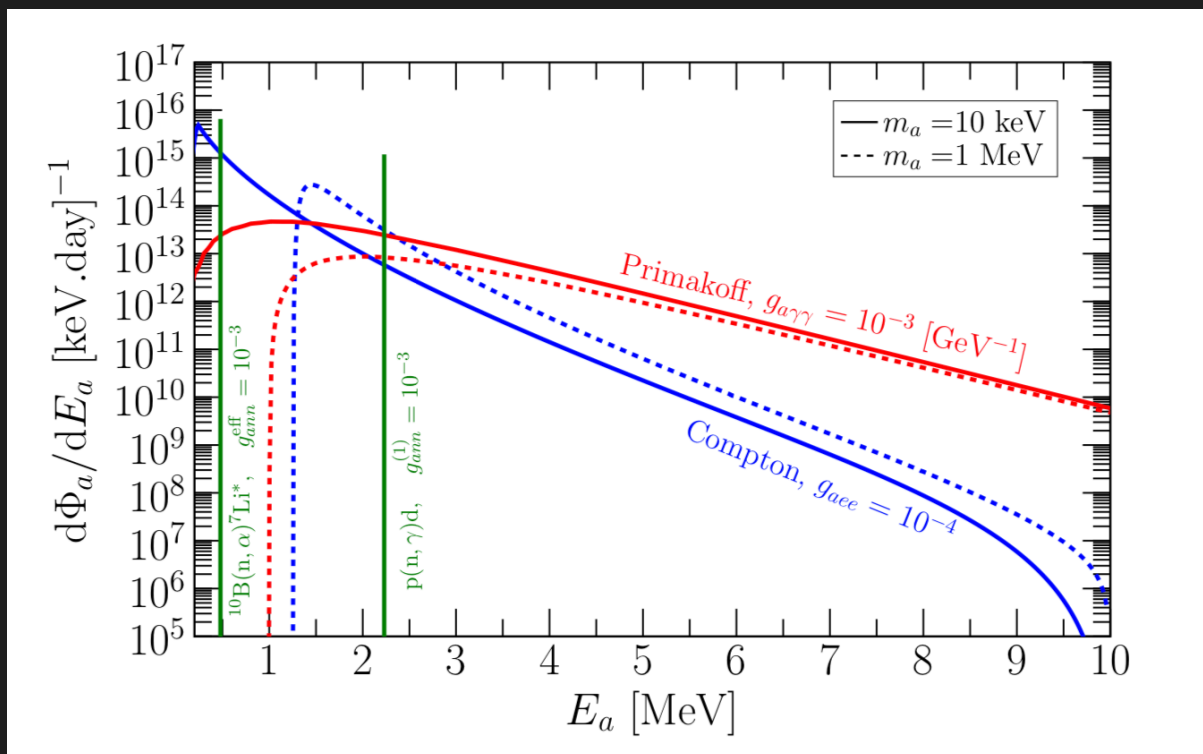
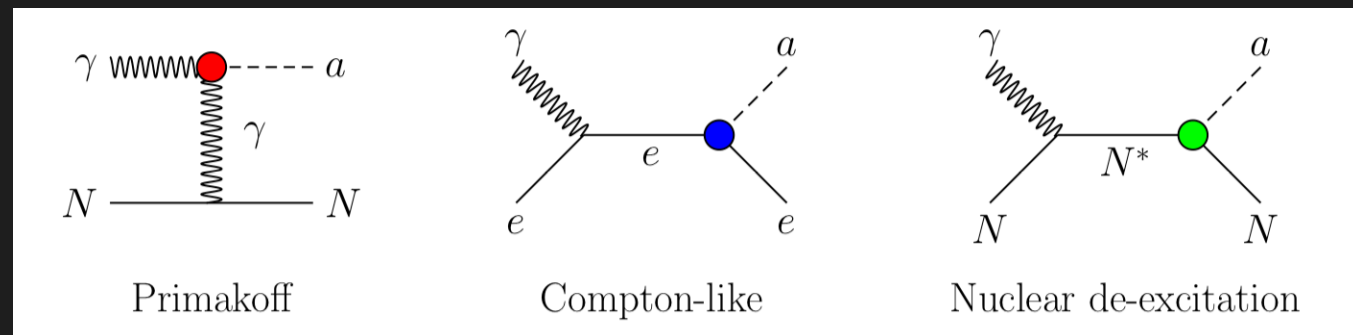
$$\frac{d\Phi_{\gamma'}}{dE_{\gamma'}} = \frac{5.8 \times 10^{17}}{\text{MeV} \cdot \text{sec}} \left(\frac{\text{P}}{\text{MW}} \right) e^{-1.1 E_{\gamma'}/\text{MeV}}$$



Aristizabal, VDR, Flores, Papoulias JHEP 03 (2021) 294

ALP PRODUCTION AT REACTORS

$$\mathcal{L} = \mathcal{L}_a - \frac{1}{4} g_{a\gamma\gamma} a F_{\mu\nu} \tilde{F}^{\mu\nu} - i g_{ae\bar{e}} a \bar{e} \gamma_5 e - i a \bar{n} \gamma_5 \left(g_{ann}^{(0)} + \tau_3 g_{ann}^{(1)} \right) n$$



Typical ALP flux generated in a 4 GW reactor.

See also: Dent+ Phys. Rev. Lett. 124, 211804
 Aguilar-Arevalo (CCM) + Phys. Rev. D 107, 095036
 Batell+ arXiv:2207.06898

Aristizabal, VDR, Flores, Papoulias JHEP 03 (2021) 294

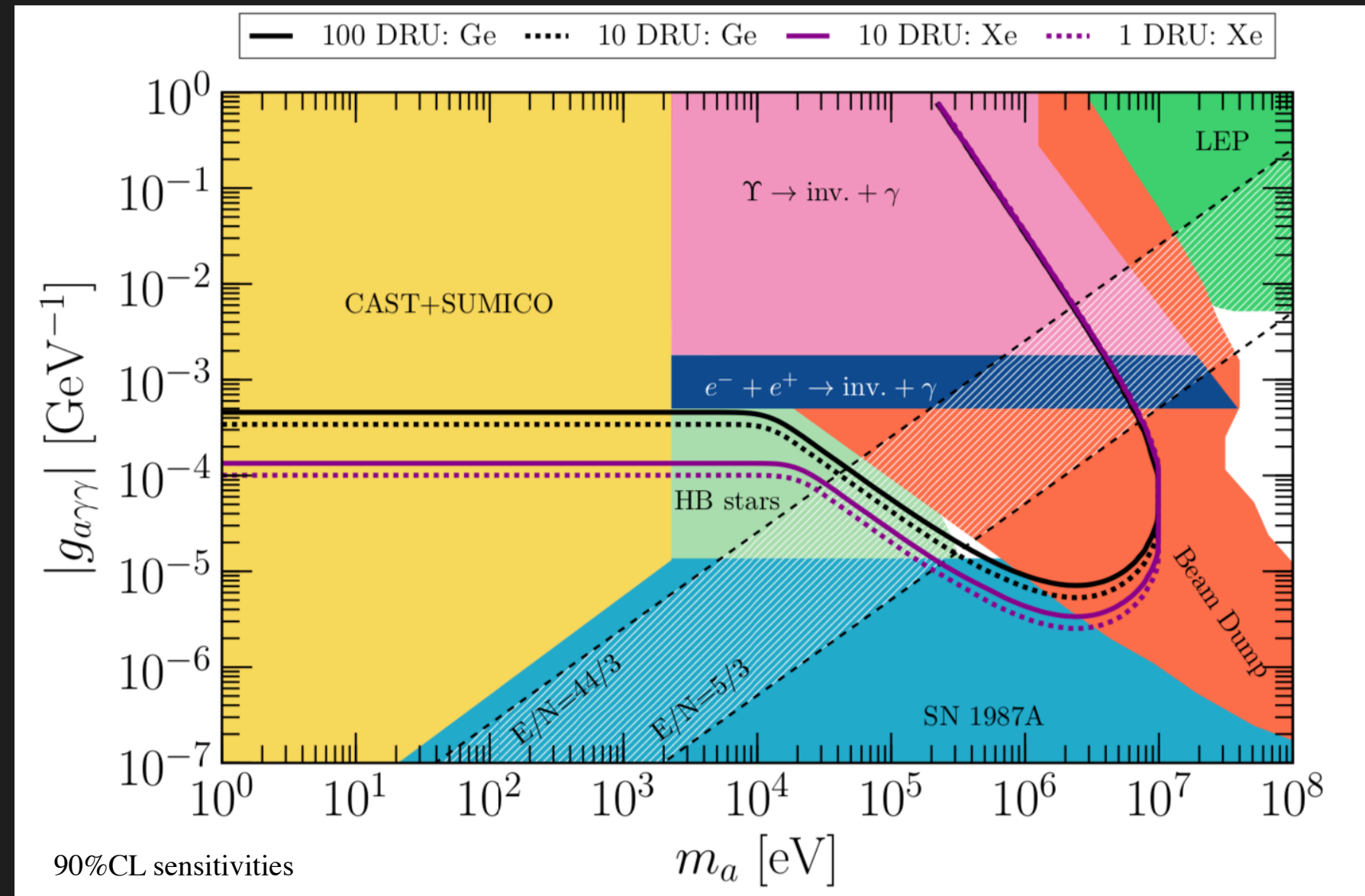
SENSITIVITIES FOR DOMINANT $g_{a\gamma\gamma}$ SCENARIOS

Production:

- $\gamma + N \rightarrow a + N$

Detection:

- $a + N \rightarrow N + \gamma$
- $a \rightarrow \gamma\gamma$



Aristizabal, VDR, Flores, Papoulias JHEP 03 (2021) 294

- Complete coverage of the cosmo triangle (test the Λ CDM hypothesis)
- Test of ALP effects in ν emission (SN 1987A)
- Test of environmental effects

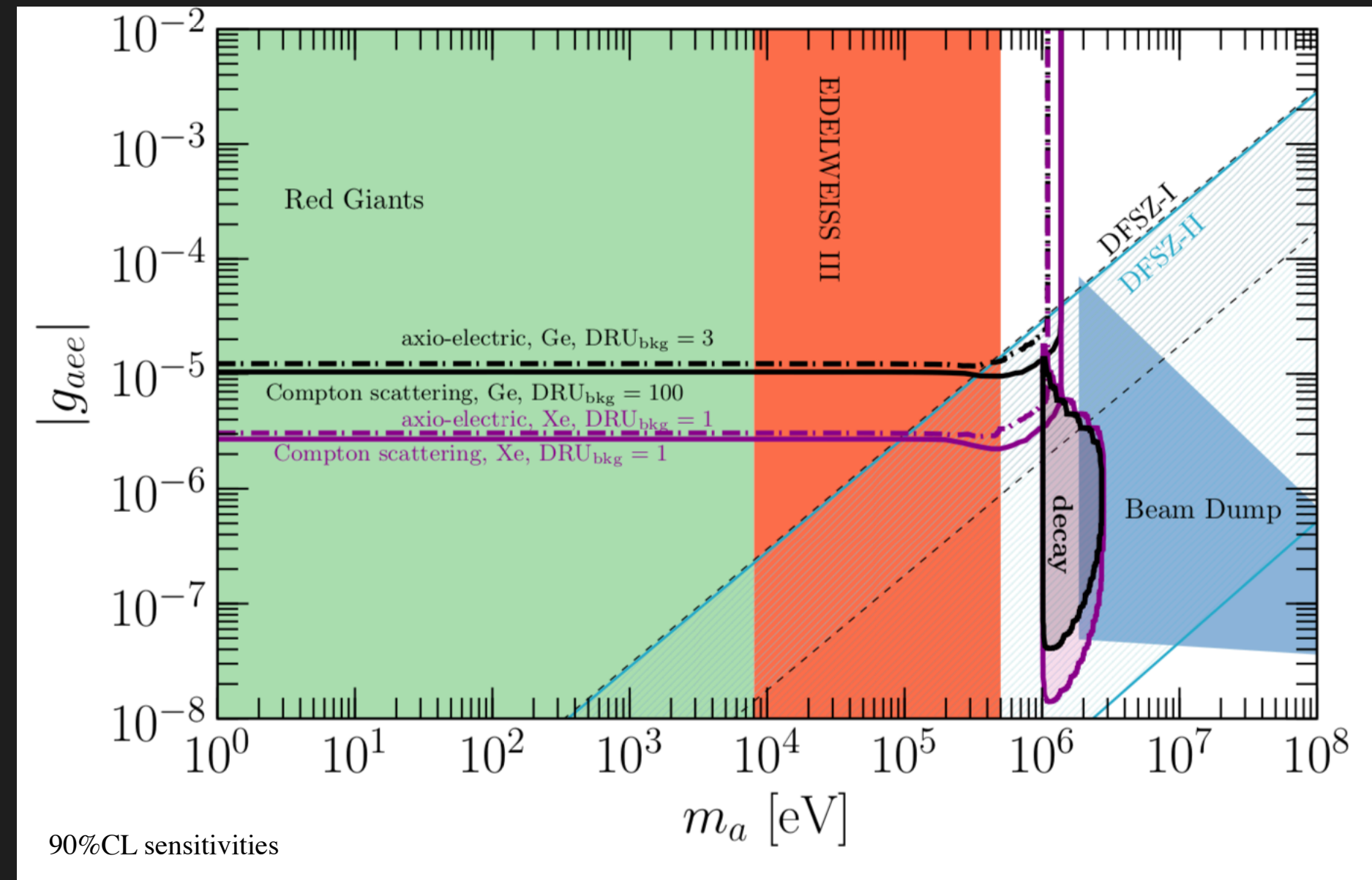
SENSITIVITIES FOR DOMINANT g_{aee} SCENARIOS

Production:

- $\gamma + e \rightarrow a + e$

Detection:

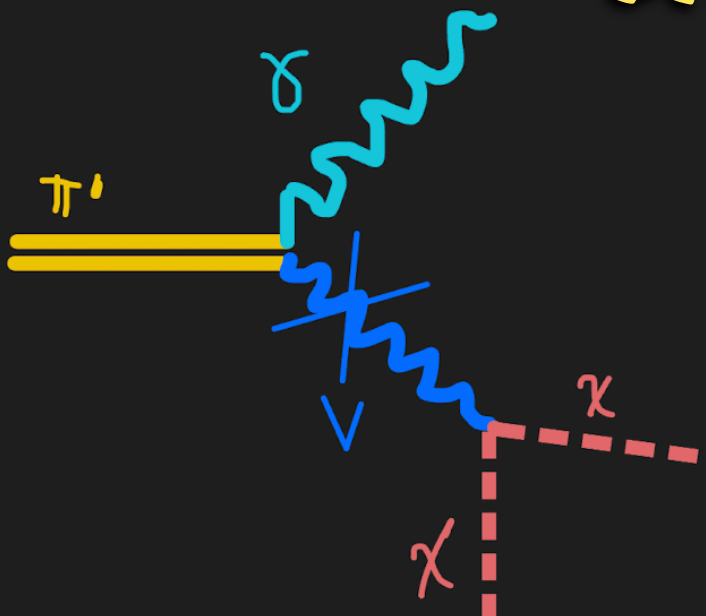
- $a + e \rightarrow e + \gamma$
- $a \rightarrow e^+ e^-$
- $a + e + Z \rightarrow e + Z$



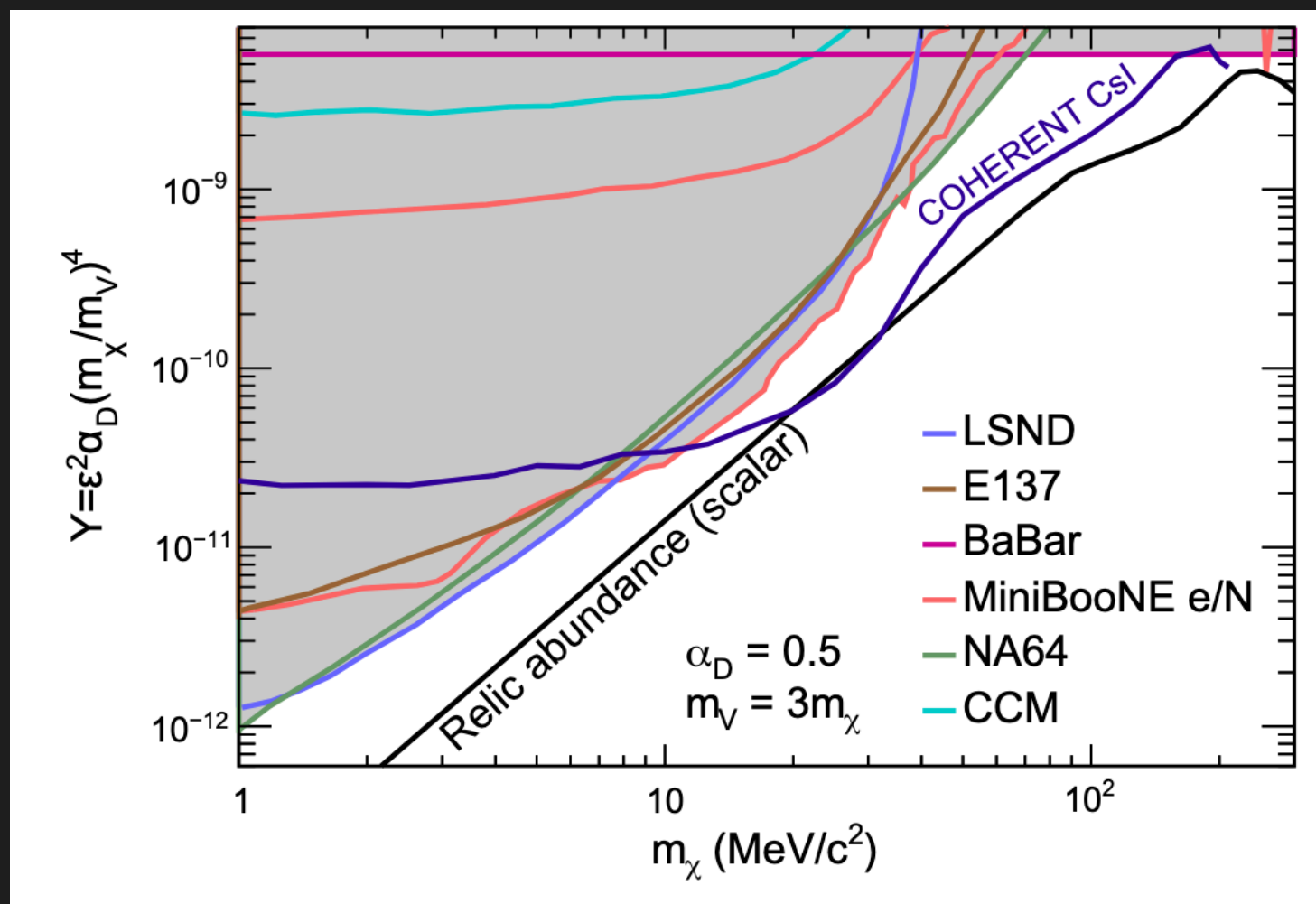
Aristizabal, VDR, Flores, Papoulias JHEP 03 (2021) 294

- Can probe a region of parameter space currently unexplored
- Test of environmental effects in Red Giants

LIGHT DARK MATTER



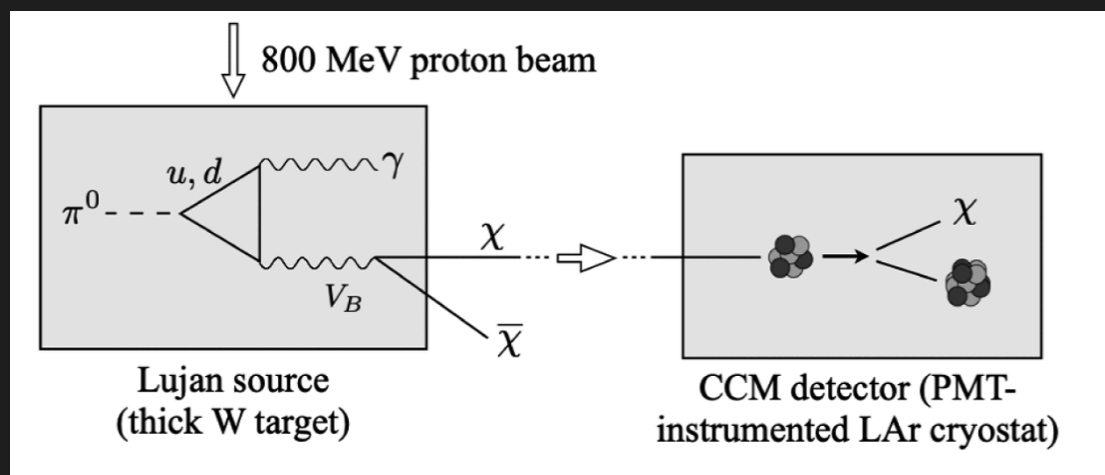
- Dark photon mediator
- Kinetic mixing with SM photon
- Production through π^0 (or η) decay
- Elastic or inelastic scattering off the target nuclei



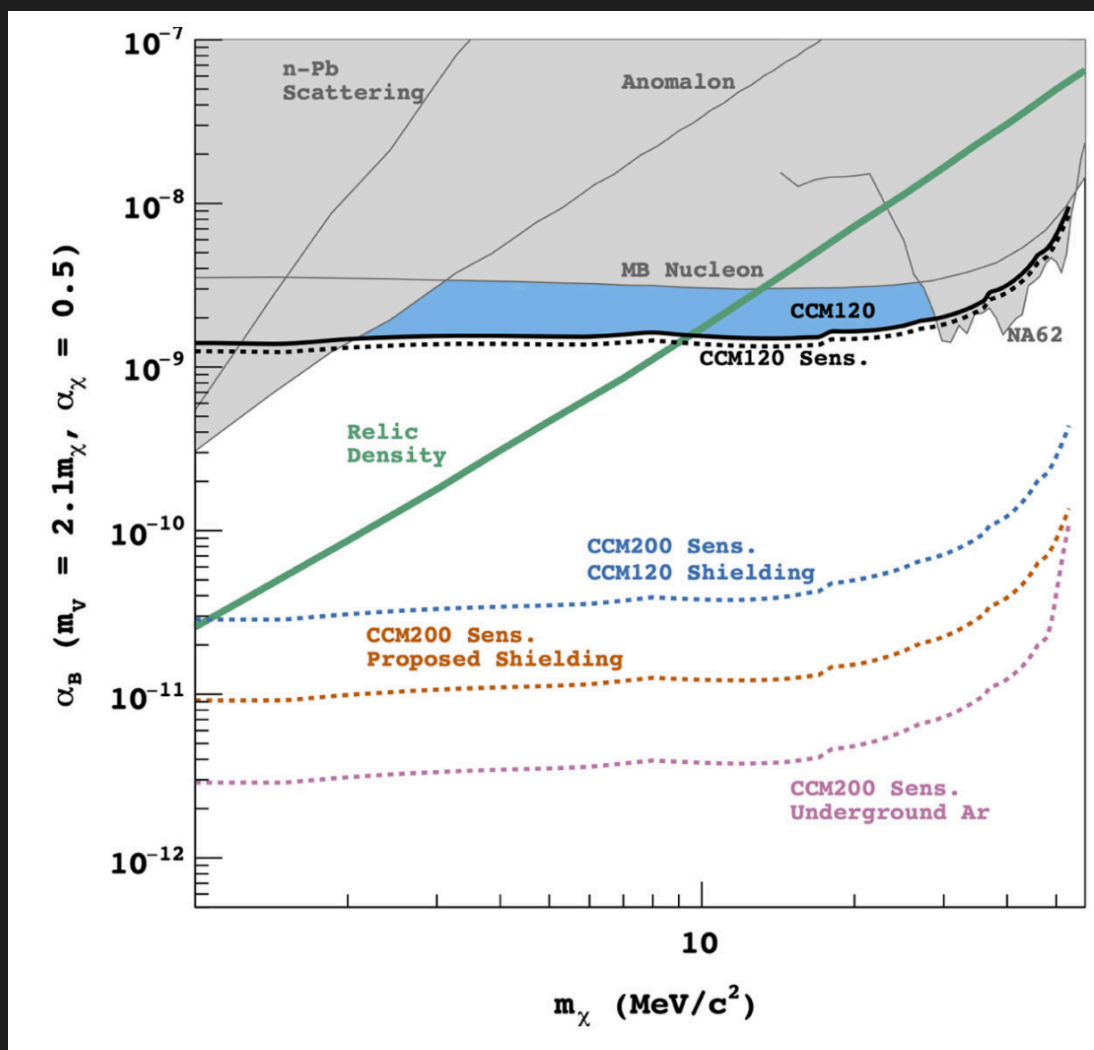
COHERENT Phys.Rev.Lett. 130 (2023) 5, 051803

deNiverville+ Phys. Rev. D 95, 035006 (2017)
 Dutta+ Phys. Rev. Lett. 124, 121802 (2020)
 COHERENT Phys. Rev. D 102, 052007 (2020)
 COHERENT Phys. Rev. Lett. 130 (2023) 5, 051803
 CCM Phys. Rev. D 106, 012001 (2022)
 Dutta+ JHEP 01 (2022) 144
 CCM Phys. Rev. Lett. 129, 021801 (2022)

LIGHT DARK MATTER



- Leptophobic scenario (not anomaly free!)
- scalar DM candidate χ and a vector portal
- gauged baryon number
- Production through π^0 (or η) decay
- Elastic scattering off the target nuclei



deNiverville+ Phys. Rev. D 95, 035006 (2017)
 Dutta+ Phys. Rev. Lett. 124, 121802 (2020)
 COHERENT Phys. Rev. D 102, 052007 (2020)
 COHERENT Phys. Rev. Lett. 130 (2023) 5, 051803
 CCM Phys. Rev. D 106, 012001 (2022)
 Dutta+ JHEP 01 (2022) 144
 CCM Phys. Rev. Lett. 129, 021801 (2022)

Summary

- ▶ CE ν NS process:
 - coherency condition (sources: spallation source, nuclear reactors,...)
 - neutrinos scatter on a nucleus which act as a single particle
 - enhancement of the cross section ($\propto N^2$)
- ▶ CE ν NS experiments and data:
 - COHERENT (CsI, LAr, Ge...)
 - Reactor experiments
 - Now also DM DD experiments!
- ▶ CE ν NS extended physics potential:
 - SM physics (weak mixing angle, nuclear physics)
 - Electromagnetic properties
 - BSM scenarios: NSI, NGI, new light mediators, production of a dark fermion, ALPs, sterile neutrinos...
 - Impact on the neutrino floor/fog
- ▶ Wealth of information from forthcoming data: implications for both precision tests of the Standard Model and for new physics in the neutrino sector!

► **Acknowledgments:**

- CIDEXG/2022/20 (Generalitat Valenciana)
- CNS2023-144124 (MCIN/AEI/ 10.13039/501100011033 and “Next Generation EU”/PRTR)
- PID2020-113775GB-I00 (MCIN/AEI/ 10.13039/501100011033)
- MultiDark Network, ref. RED2022-134411-T
- Severo Ochoa (CEX2023-001292-S)



- Acknowledgments:
- CIDEXG/2022/20 (Generalitat Valenciana)
 - CNS2023-144124 (MCIN/AEI/ 10.13039/50110001105) and “Next Generation EU”/PRTR)
 - PID2020-113775GB-I00 (MCIN/AEI/ 10.13039/50110001105)
 - MultiDark Network, ref. RED2022-13441-T
 - Severo Ochoa (CEX2023-001292-S)

THANK
YOU!